ROYAUME DU MAROC
Université Mohammed V - RABAT -
جامعة محمد الخامس – الرباط –
Faculté des sciences
كلية العلوم
CENTRE D'ETUDES DOCTORALES - SCIENCES ET TECHNOLOGIES

N° d'ordre: 3577

DOCTORAL THESIS

In order to obtain : ***Doctorate***

Research Center: *Pharmaceutical Sciences Research Center, Pole of Competence in Pharmacochemistry*
Research structure: *Heterocyclic Organic Chemistry Laboratory*
Discipline:*Chemistry*
Speciality: *Organic chemistry / Pharmaceutical chemistry*

Date of thesis defense : 25 /12 /2021

WEDAD HASHEM ABDULHAFEDH HASSAN Al-GARADI

Research in 1,4-diazepine and 1,5-benzodiazepine series Synthesis, reactivity and valuation

JURY MEMBERS

Redouane ACHOUR	PES	Faculty of Sciences, Mohammed V University -Rabat	President
Youssef KANDRI RODI	PES	Faculty of Sciences and Techniques, Sidi Mohamed Ben Abdellah University- Fes	Reporter/ Examiner
Noureddine Hamou AHABCHANE	PES	Faculty of Sciences, Mohammed V University -Rabat	Reporter/ Examiner
Youssef RAMLI	PH	Faculty of Medicine and Pharmacy, Mohammed V University - Rabat	Reporter/ Examiner
KARIM FAHSI	PH	Higher Institute of Nursing Professions and Health Technique- Rabat	Examiner
Nada Kheira SEBBAR	PA	Faculty of Applied Sciences AitMelloul, Ibn Zohr University - Agadir	Invited
El Mokhtar ESSASSI	Expert. Pr	Hassan II Academy of Sciences and Technology -Rabat	Co-Supervisor
Lhoussaine El GHAYATI	PH	Faculty of Sciences, Mohammed V University -Rabat	Supervisor

Academic year: 2021-2022

To:

My dear parents,

My brothers and sisters,

My whole family, my friends,

Every dear to my heart,

For their presence at all time,

For the support they have given me,

With all my affection and gratitude

ACKNOWLEDGEMENTS

This work was carried out at the Laboratory of Organic Heterocyclic Chemistry, Faculty of Science, Mohammed V-Agdal University.

First and foremost, I would like to thank Allah, who helped me at all times to complete this piece of work successfully. I am indebted to many colleagues who stood by my side during the completion of this thesis. I would like to express my sincere gratitude to Prof. **Lhoussaine El GHAYATI**, who was my supervisor, for everything he did for me during all the stages of preparing this work.

I would like to express my sincere gratitude to my co-supervisor, **Prof. El Mokhtar ESSASSI**, for his patience, constant support and encouragement. His professionalism, invaluable guidance, and constructive feedback assisted me greatly during the process of my research.

I would like to thank all the members of the faculty of sciences in Rabat. I would also like to extend my gratitude to all the members of the defense jury.

I would like to express my sincere thanks to Mr. **Redouane ACHOUR**, Professor at the Faculty of Sciences, Mohammed V University Rabat, for the honor he has granted me by agreeing to participate in the jury and for his great efforts, support, and encouragement, and his simplicity of dealing is a great honor that I will cherish in my life.

I would like to extend my thanks to **Mr. Youssef KANDRI RODI,** Professor at the Faculty of Science and Technology, Sidi Mohamed Ben Abdallah University, Fes, for his considerable interest in this work and for having spared no attempt to serve on the jury of this thesis.

I would like to thank Mr. **Noureddine HAMOU AHABCHANE**, Professor at the Faculty of Sciences, Mohammed V University, for agreeing to be part of the jury, with my thanks and respect.

I extend my thanks to **Mr. Youssef RAMLI**, Professor at the Faculty of Medicine and Pharmacy, Mohammed V University, Rabat, for his great help and encouragement.

I would like to express my thanks to **Mr. Karim FAHSI**, Professor at the Higher Institute of Nursing Professions and Health Technologies in Rabat, for his great efforts and encouragement.

I would like to offer my thanks to **Mrs. Nada KHEIRA SEBBAR,** Professor at the Faculty of Applied Sciences Ait Melloul, Ibn Zohr University, Agadir.

I would like to extend my sincere thanks to **Mr. Mohammed BENCHIDMI**, Professor in the Laboratory of Organic Chemistry for Heterocyclic Compounds at the Faculty of Sciences, Mohammed V University and I thank him so much for the valuable advice I received from him while working in the laboratory.

I won't forget to thank the professors: **Karim CHKIRATE**, Professor at the Faculty of Science Rabat, and **Mr. Dr. AHMED Moussaif** at the National Center for Energy Sciences and Nuclear Techniques, for their help and for the valuable advice I received from them both scientifically and humanly.

My heartfelt thanks to my dear colleagues for their moral support throughout this journey, who have provided me with constant and indispensable help in completing this work, particularly **Mr. Dr. Youness El BAKRI**, and **Mr. Dr. Mohamed El HAFI**, for all their scientific suggestions and their precious help.

I offer my thanks and respect to my foundation in Yemen, The National Laboratory for Drug Quality Control, for its ongoing quest for the rehabilitation of its members. My special thanks to my colleague **Mrs. Dr. Najla Al-SHAMI** for her permanent cooperation with me.

I would like to express my thanks and appreciation to the center of doctoral studies at the Faculty of Science, Mohammed -V University, and my sincere thanks to **Miss Karima ECHTIOUI**, the doctoral center secretary, for her cooperation and helping me in overcoming all the difficulties during the study period.

I would like to thanks my family for the support that they offered me during the long PhD journey. My heartfelt thanks to my dear parents, my brother **Abduladehm Al GARADI**, and my sisters for their love, confidence, and motivation, which made this dream come true.

Abstract

The presented work concerns the synthesis, the reactivity, the physicochemical, antibacterial and corrosion inhibiting properties of 1,5-benzodiazepin-2-one derivatives. It was shown, in particular, that 1,5-benzodaizepin-2-thiones undergo an interesting rearrangement leading to new benzimidazole derivatives. The formation was explained by a plausible mechanism. The antimicrobial properties of fourteen 1,5-benzodiazepine derivatives and seven benzimidazole derivatives, were evaluated and discussed.

Also, 1,4-diazepin-2-one derivatives were elaborated in order to study their chemical reactivities and also their corrosion inhibiting properties of mild steel in 1M hydrochloric acid solution.

Keywords: Synthesis, Reactivity, Rearrangement, 1,5-benzodiazepines, benzimidazoles, 1,4-diazepines, antibacterials, corrosion.

Résumé

Le travail présenté, concerne la synthèse, la réactivité, les propriétés physicochimiques, antibactériennes et inhibitrices de corrosion de dérivés de la 1,5-benzodiazepin-2-one. Il a été montre, en particulier, que les 1,5-benzodaizepines-2-thiones subissent un intéressant réarrangement conduisant à de nouveaux dérivés du benzimidazole. La formation a été expliquée par un mécanisme plausible. Les propriétés antimicrobiennes de quatorze dérivés du 1,5-benzodiazepines et sept dérivés du benzimidazole, ont été évaluées et discutées.

De même les dérivés de la 1,4-diazepin-2-one ont été élaborés afin d'étudier leurs réactivités chimiques et aussi que leurs propriétés inhibitrices de corrosion de l'acier doux dans une solution 1M de l'acide chlorhydrique

Mots clés : Synthèse, Réactivité, réarrangement, 1,5-benzodiazépines, benzimidazoles, 1,4-diazepines, antibactériens, corrosion.

Résumé détaillé

Les travaux de recherche réalisés au cours de cette thèse s'inscrivent dans le cadre de la stratégie de notre laboratoire qui vise à la recherche de nouvelles molécules hétérocycliques susceptibles de manifester des propriétés biologiques. Nous avons choisi comme thème la synthèse de nouveaux composés hétérocycliques comportant le motif : 1,5-benzodiazépin-2-one, benzimidazole ou 1,4-diazepin-2-one et l'étude de leurs propriétés électrochimiques et biologiques.

Ce travail est composé de deux grandes parties, la première a été consacrée à la synthèse, la réactivité, les propriétés physicochimiques, antibactériennes et inhibitrices de corrosion de dérivés de la 1,5-benzodiazepin-2-one, tandis que la deuxième a été réservée à la recherche en série 1,4-diazepine.

Le premier chapitre de la première partie représente un aperçu bibliographique sur la synthèse et la réactivité des dérivés de la 4-phényl-1,5-benzodiazepin-2-one.

Dans le deuxième chapitre, nous avons préparé, dans une première étape, de nouveaux dérivés de la N-alkyl-4-phényl-1,5-benzodiazepin-2-one via des réactions d'alkylation dans les conditions de la catalyse par transfert de phase liquide-solide avec différents agents alkylants. Dans une deuxième étape, de nouveaux dérivés de la N-alkyl-4-phényl-1,5-benzodiazepin-2-thione via des réactions de sulfuration.

Des résultats originaux ont été obtenus par l'action du chlorhydrate d'hydroxylamine sur les N-alkyl-4-phényl-1,5-benzodiazepin-2-thiones, ces dernières subissent un intéressant réarrangement, conduisant à de nouveaux dérivés du benzimidazole. Les structures des composés synthétisés ont été déterminées par les méthodes spectroscopiques habituelles ^{1}H NMR, ^{13}C NMR et confirmées par des études cristallographiques aux rayons X pour sept produits, montrant notamment que la fonction oxime adopte la configuration E. De même, il nous a été possible de proposer un mécanisme plausible pour expliquer la formation des dérivés du benzimidazoles a partir des 1,5-benzodiazepin-2-thiones, en mettant en évidence un réarrangement original du cycle a sept éléments, en présence du chlorhydrate d'hydroxylamine qui agit comme un réactif bi-nucléophile.

Une étude préliminaire sur la recherche d'une activité antibactérienne de quelques dérivés de la 1,5-benzodiazepin-2-one, 1,5-benzodiazepin-2-thione et benzimidazole préparés a été réalisée et décrite dans le quatrième chapitre.

Les résultats observés se sont révélés être intéressants pour certains composés synthétiques.

Le cinquième chapitre est réservé à la synthèse, caractérisation et étude de la structure cristalline ainsi que d'autres études théoriques de la 4-phényl- decahydro-1H-1, 5-benzodiazépin-2-one.

Dans le dernier chapitre de cette partie, nous avons testé l'effet inhibiteur de la 4-phényl- decahydro-1H-1, 5-benzodiazépin-2-one sur la corrosion de l'acier doux dans la solution d'acide chlorhydrique 1M via différentes méthodes expérimentales: Les courbes de polarisation potentiodynamique, la spectroscopie d'impédance électrochimique.

Les résultats montrent que notre composé évalué est un très bon inhibiteur organique dans l'acide chlorydrique.

Enfin, la deuxième partie, divisée en deux chapitres, concerne la synthèse, analyse de surface de Hirshfeld, l'étude du docking moléculaire et l'évaluation du pouvoir inhibiteur de corrosion de la 7-phényl-2,3,4,5-tétrahydro-1 H -1,4- diazépin-5-one.

Table of contents

ChapterIII: Novel pathways for synthesis benzimidazolederivatives from 4-phenyl-1,5-benzodiazepine-2-thiones derivatives

Chapter IV: Antibacterial activity of new derivatives1,5-benzodiazepin-2-one (thione) and benzimidazole

Abbreviation and symbols

DMF	Dimethylformamide
$CDCl_3$	Deuterated chloroform
DMF- DMA	Dimethylformamid-dimethylacetal
HOBt	1,2,3-benzotriazol-1-ol-monohydrateo1-hydroxybenzotriazole monohydrater
HFI	1,1,1,3,3,3-hexafluoro-2-propyl
EDCI	1-(3-Dimethylaminopropyl)-3-ethylcarbodiimide hydrochloride
Et_3N	Triethylamine
TBAB	Tetrabutylammonium bromide
ESI	Electrospray ionization
NMR	Nuclear magnetic resonance spectroscopy
TEBAC	triethylbenzylammonium chloride
PPA	polyphosphoric acid
THF	Tetrahydrofuran
NBS	N-bromosuccinimid
NCS	N -chlorosuccinimide
R.X	Agent alkylant
DMSO	Dimethyl sulfoxide
PTC	Phase Transfer Catalysis
MIC	Minimum Inhibitory Concentration

BHI	Brain Heart Infusion BHI
MHA	Mueller Hinton Agar MHA
F°	Melting point
ORTEP	OakRidge Thermal Ellipsoid Plot
MW	Mcrowave
Δ	Reflux

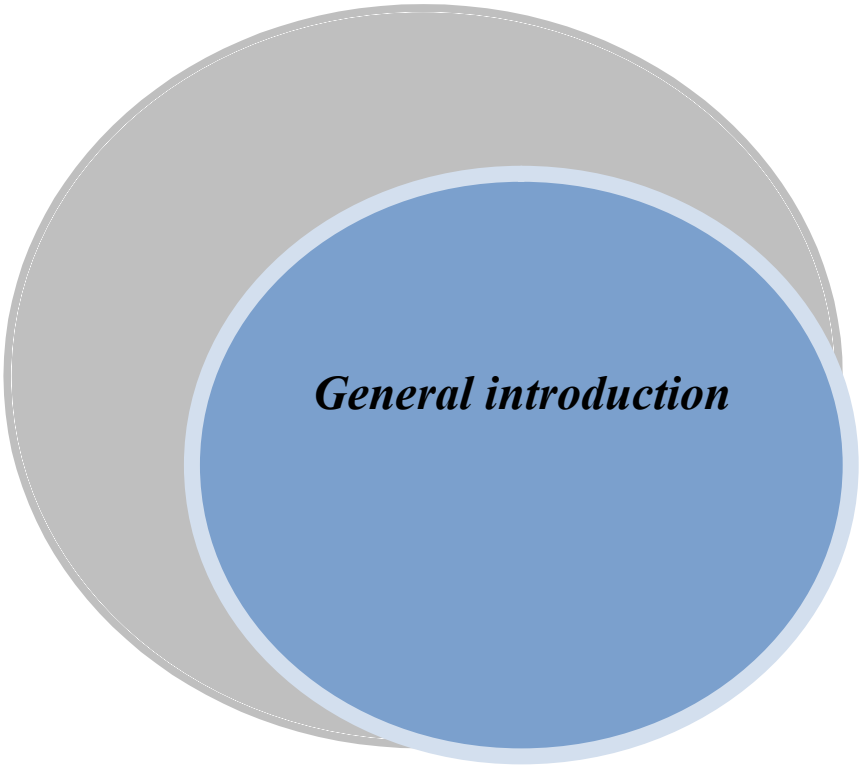
General introduction

General introduction

Interest in molecules containing heterocyclic leads to the fact that these molecules constitute the basic skeleton for a wide variety of compounds of chemical, biological, pharmacological, and industrial importance [1]. It is noted that two-thirds of the organic compounds known in the literature are heterocyclic ring structures containing at least one heteroatom (most often nitrogen, oxygen, or sulfur) [2–4]. Among the heterocyclic entities listed, benzodiazepine derivatives constitute a class of compounds of true medicinal and/or therapeutic importance [5-6]. Nitrogenous heterocyclic are the preferred source of many research topics [7]. Thus, different methods have been developed to access these heterocyclic compounds with nitrogenous rings, such as 1,5-benzodiazepines, benzimidazoles, and 1,4-diazepin-2-one. The latter has been the subject of extensive research in our laboratory [8-13].

Benzodiazepine derivatives are a class of heterocyclic compounds with interesting pharmacological properties. They are widely used for their anxiolytic [14], anticonvulsant [15], antifungal [16], anti-inflammatory [17], and active antitumor [18]. Clobazam [19] (7-chloro-1-methyl-5-phenyl-1,5-benzodiazepine-2,4-dione) ,and lofendazam [20-21] (8-chloro-1-phenyl-1,5-benzodiazepin-2-one) are examples of this important class of therapeutic agents. It has been shown that 7-chloro-1,5-diallyl-1,5-benzodiazepine-2,4-diones has a sedative effect on the central nervous system [22] comparable to that of Clobazam (Figure 1).

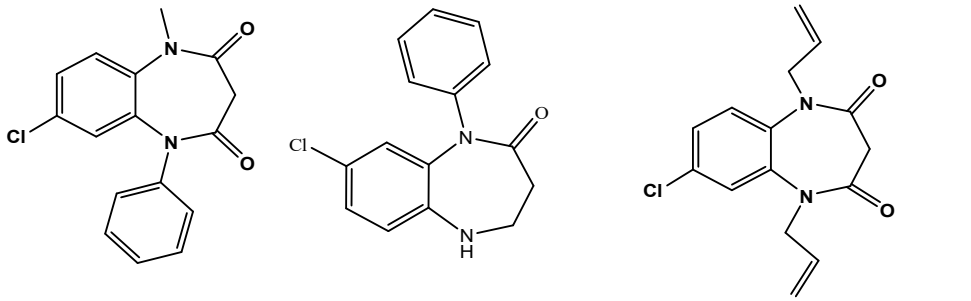

-Figure 1-

1,5-benzodiazepines are interesting precursors for the preparation of other condensed cyclic compounds, such as benzimidazoles. In this family, it has been shown that the pharmacologically important benzimidazoles. We can mention albendazole and flubendazole, which are antiparasitic and deworming drugs (Figure 2).

On the other hand, various research presented by different teams illustrates that certain compounds containing benzimidazole structure have varied biological activities, including neuroprotective [23], antimicrobial [24], anticancer [25], antiviral [26], antioxidant [27], and antimicrobial, anticancer, and anti-tuberculosis activity [28].

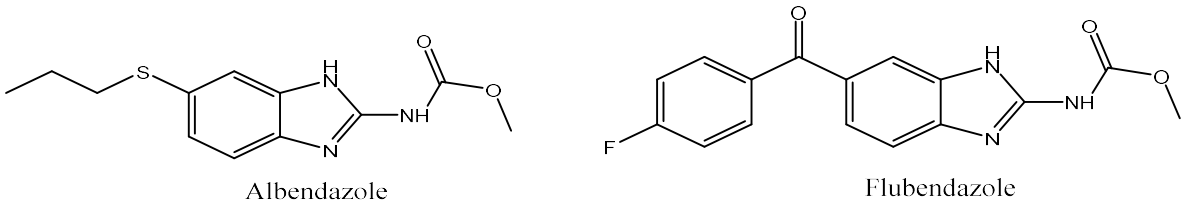

Figure 2: Examples of drugs containing benzimidazole moiety.

The combination of all these interesting properties of benzodiazepine and benzimidazole systems has prompted us to undertake and develop our research in this area. We are interested in the synthesis of new polyfunctional heterocyclic systems derived from benzodiazepine and benzimidazol using condensation, rearrangement, and alkylation reactions.

The results we present in this work will be described in two parts:

Part one will be devoted to the synthesis, reactivity, biological activity, and corrosion inhibition properties of 1, 5-benzodiazepin-2-one derivatives.

The first chapter presents a bibliographic overview of the synthesis and reactivity of 1, 5-benzodiazepin-2-one.

The second chapter explains the reactivity of 4-phenyl-1,5-benzodiazepin-2-one. The result, which is obtained by catalytic (phase transfer catalysis), will undergo sulfurization reactions to give new compounds.

The third chapter presents the synthesis of new heterocyclic systems that regroup the benzimidazole via a new rearrangement of the 1,5-benzodiazepine-2-thiones in the presence of hydroxylamine hydrochloride.

The fourth chapter will focus on the study of the antibacterial activity of new 1,5-benzodiazepine-2-ones (thione) and benzimidazole.

The fifth and sixth chapters cover the subject of synthesis of 4-phenyl-decahydro-1H-1-5-benzodiazepin-2-one as well as its structural study, focusing on the inhibiting capacity.

Part two of this work is devoted to the synthesis and serial reactivity of 1,4-diazepine.

- The first chapter will focus on the synthesis, Hirshfeld surface analysis and molecular docking of 7-phenyl-2,3,4,5-tetrahydro-1H-1,4- diazepin-5-one derivative.

- The second chapter will be devoted to the study and inhibition performance of 7-phenyl-2,3,4,5-tetrahydro-1H-1,4- diazepin-5-one towards mild steel in 1M hydrochloric acid solution with electrochemical techniques.

A general conclusion encompassing all the results obtained is presented at the end of this manuscript.

Part I

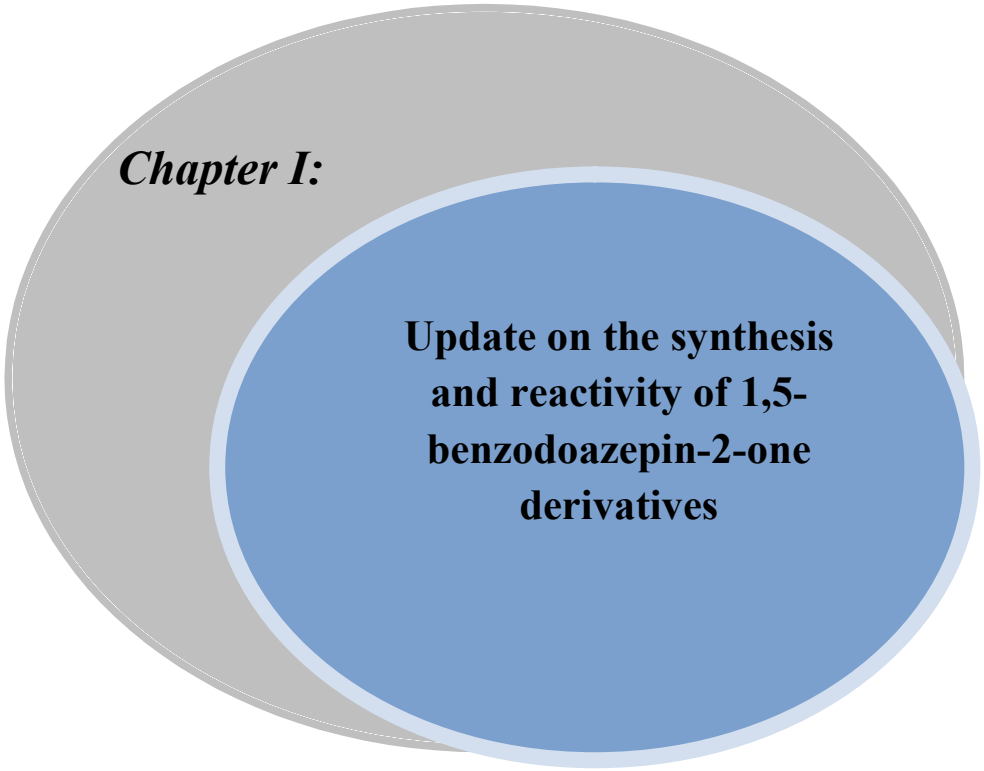
Chapter I:
Update on the synthesis and reactivity of 1,5-benzodoazepin-2-one derivatives

1. INTRODUCTION:

Benzodiazepines are important pharmaceuticals due to their diverse therapeutic properties based on pharmacopoeia information. The 1,5-benzodiazepine ring is a preferred scaffold and is a core structure of drugs and has received much attention in medical research in search of new derivatives with improved pharmacological properties. The structural modification of these heterocyclic allows the development of increasingly active products with an ever-expanding spectrum of therapeutic action. Indeed, the 1,5-benzodiazepine structure is often present in some active ingredients for the treatment of various neurological diseases [29–35]. As a result, before discussing the various steps for synthesizing new 1,5-benzodiazepines with potential pharmaceutical properties, we will present a bibliographic review of the synthesis and reactivity of some heterocyclic 1,5-benzodiazepine derivatives in this chapter.

II- Synthesis of 1,5-benzodiazepin-2-one and its derivatives:

Recently, Mansour *et al.* [36] prepared 4-Amino-3-arylidine-1,5-benzodiazepin-2-one derivatives **4a-e** by reacting, in a first step, ethyl cyanoacetate **1** with aromatic aldehydes in the presence of piperidine in ethanol and then, in a second step, *o*-phenylenediamine **3** with α-ethylcyano-cinnamate derivatives (**2a-e**). However, the action of *o*-phenylenediamine **3** with ethyl cyanoacetate in xylene leads to 4-amino-1,5-benzodiazepin-2-one **5** (Scheme 1).

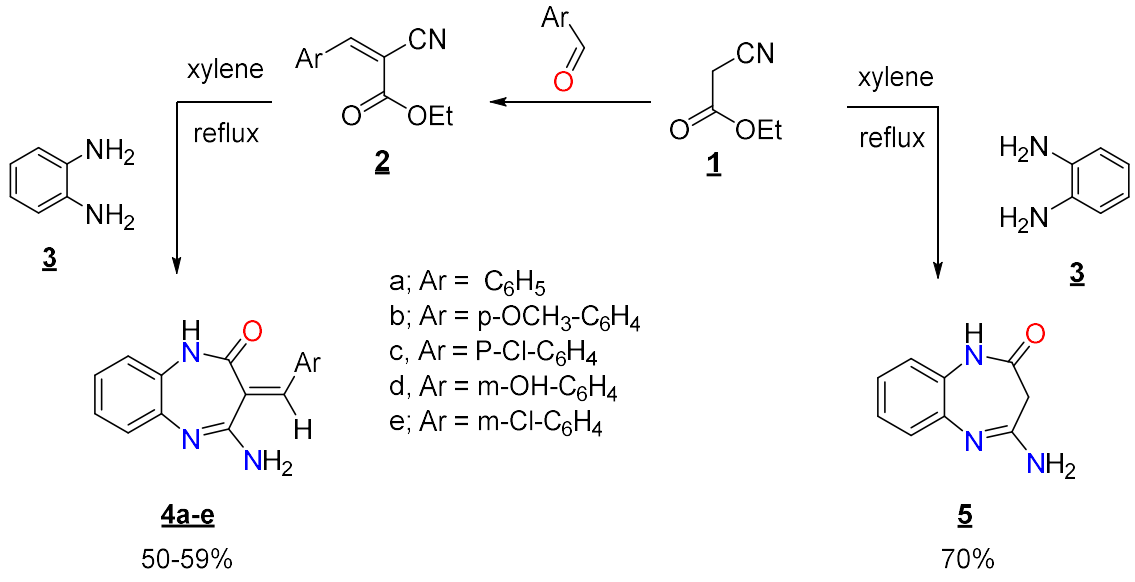

- Scheme 1 -

Obara *et al.* [37] developed two useful methods for the synthesis of 3-amino-1,5-benzodiazepin-2-one derivatives (**9** et **10**). The synthetic methodology includes Michael addition reaction of o-phenylenediamine **6** with dehydroalanine HFI (1,1,1,3,3,3-hexafluoro-2-propyl) or HOBt (HOBt = 1,2,3-benzotriazol-1-ol-monohydrateo1-hydroxybenzotriazole monohydrater) ester derivatives (**7**, **8**), followed by intermolecular cyclization. The scope of HFI ester was explored by condensing various dehydroalanine HFI esters with different *o*-phenylened!!àçiamine in toluene under refluxing conditions. It was observed that various HFI esters bearing Ac, Cbz, and Phth N-substituent 7 reacted smoothly to produce the desired product with good into high yield. The effect of N-substituent on the reactivity of *o*-phenylenediamine and C-3 position on the dehydroalanine reactivity was explored. The authors then investigated the condensation reagent method by employing EDCI=1-(3-Dimethylaminopropyl)-3-ethylcarbodiimide hydrochloride, HOBt, Et_3N and observed that the desired product was obtained in a moderate yield (Scheme 2).

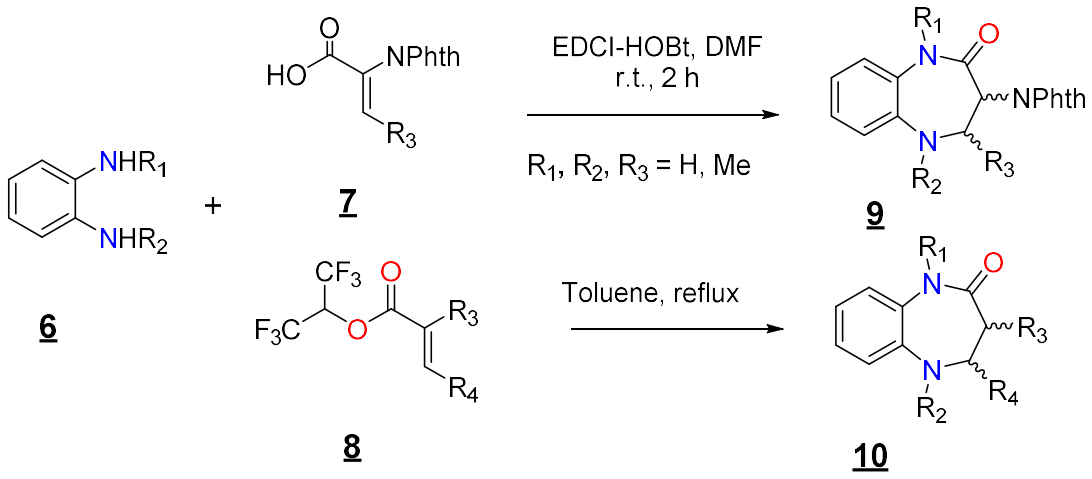

- Scheme 2 -

Wu *et al.* [38] used green chemistry approaches to synthesize two series of rare contractual 1,5-benzodiazepines **12** and **14** via domino condensations (scheme 3). The $CeCl_3$-KI promoted two-component domino reaction of 1,2-phenylenediamines **3a-d** with 1,3-acetonedicarboxylate **11** in ethanol gave rise to the novel 1,5-benzodiazepin-2-one **12a-d** (Scheme 3, strategy I). A rapid approach to 1,5-benzodiazepines **14aa-dk** was also developed via a three-component process. A rapid approach to 1,5-benzodiazepines **14aa-dk** was also developed via three-component domino reactions using 1,2-phenylenediamines **3a-d**, 1,3-acetonedicarboxylate **11** and aldehydes **13a-k** in the presence of magnetic nanoparticles (γ-Fe_2O_3@SiO_2/$CeCl_3$) in ethanol at room temperature (Scheme 3, Strategy II).

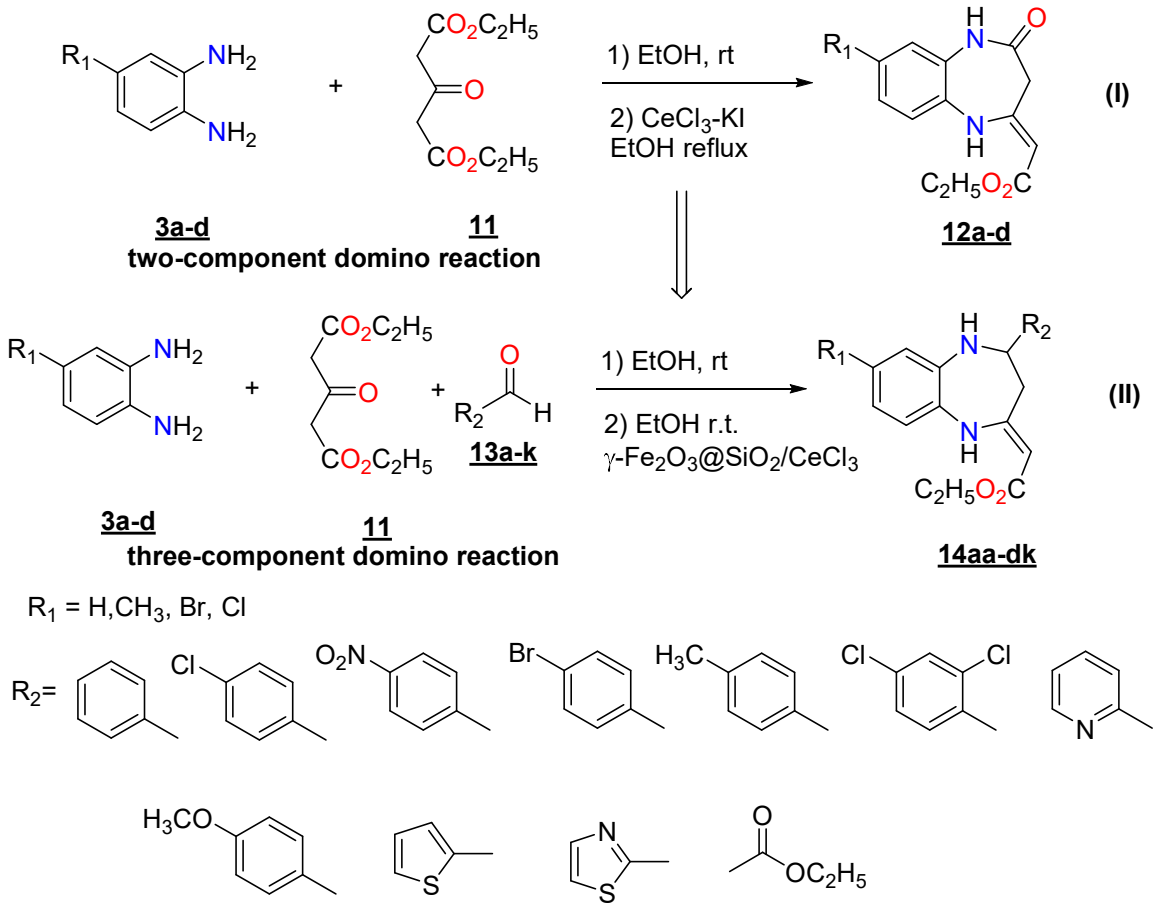

-Rare construction of seven membered ring
-Domino reactions
-Mild conditions and fast reaction
-Green-chemistry approaches
-An intramolecular 1,5-hydride transfer

- Scheme 3 –

Qomi *et al*. [39] described the synthesis of a series of novel tricyclic pyrimidine clubbed 1,5-benzodiazepine derivatives **18** through the successful use of an enaminone-based approach in the three-step synthesis methodology. In the first step, the required intermediate 1,5-benzodiazepine-2,4-diones **16** was synthesized by reacting benzene-1,2-diamines **15** with 1,3-propanedioic acid in the presence of HCl at 80 °C. The β-enaminonamide intermediates **17** were then prepared by refluxing the benzodiazepine **16** with DMF-DMA in dry p-xylene and/or toluene or under solvent-free conditions. The functionalized intermediates **17** were then condensed with substituted guanidine and thiourea in a solution of sodium ethoxide and absolute ethanol followed by mild acid treatment to give the final compounds **18** in 70-94% yield (Scheme 4). The main strengths of the developed methodology were its versatility, simplicity, minimal steps, mild reaction conditions and excellent yield of the final product.

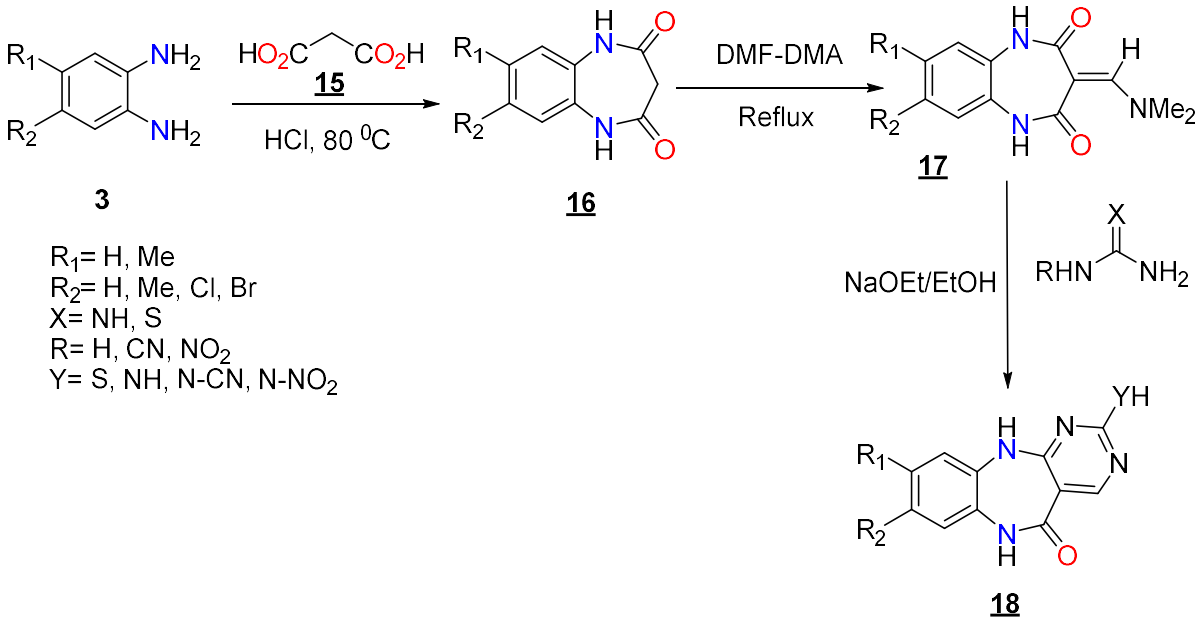

- Scheme 4 –

Lyubimov *et al.* [40] synthesized 1,5-benzodiazepin-2-one derivatives **20 a-b** by condensation of 1,2-phenylenediamine **3** with ethyl- 3-oxopropanoate **19a-b** (Scheme 5). The authors also prepared 7-methylsubstituted substrate **23** in satisfactory yield, *in-situ* generation of diketene from acetyl chloride **21** followed by addition of 4-methyl-*o*-phenylenediamine **3b** was found to be more efficient (Scheme5)

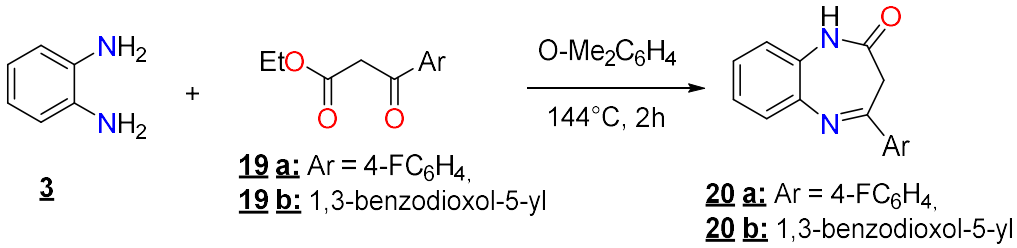

- Scheme 5 –

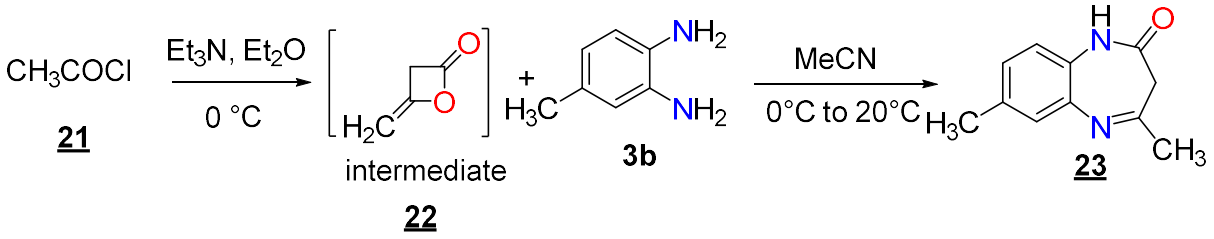

Scheme5–

Jaafar *et al.* [41] used 4-hydroxycoumarin **24** and 1,2-phenylenediamine **3** as starting materials in xylene to synthesize 4-(2-hydroxyphenyl)-3H-1,5-benzodiazepin-2-ones **25**. Also, Chniti *et al.* [42] succeeded in developing a new strategy for the re-synthesize of

tetracyclic 1,5-benzodiazepin-2-one derivatives **27,** from 1,5-benzodiazepin-2-one **25**, which reacted with DMF-DMA in toluene at 100 ^{0}C for 2 h (Scheme6).

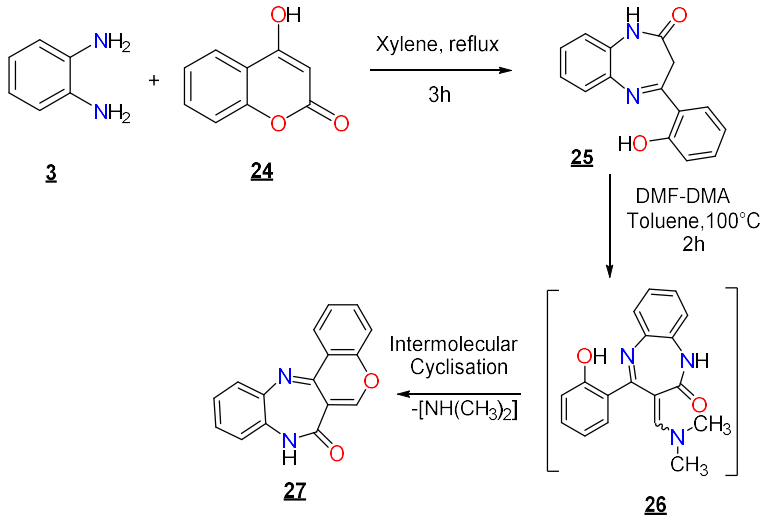

- Scheme 6 –

Chander *et al.* [43-44] synthesized in two steps a series of 5-benzoyl-4-methyl-1,3,4,5-tetrahydro-2H-1,5-benzodiazepin-2-one derivatives **30a-n** according to the reaction condition indicated below (scheme 8). The first step involved the reaction of *o*-phenylenediamine **3** with crotonic acid **28** in refluxing in toluene for 10 hours to give the intermediate **29**. In the second step, intermediate **29** was converted to the desired products **30a-n** from moderate to excellent yield by reacting it with suitable acid chlorides in the presence of triethylamine as base and anhydrous tetrahydrofuran as solvent (Scheme7).

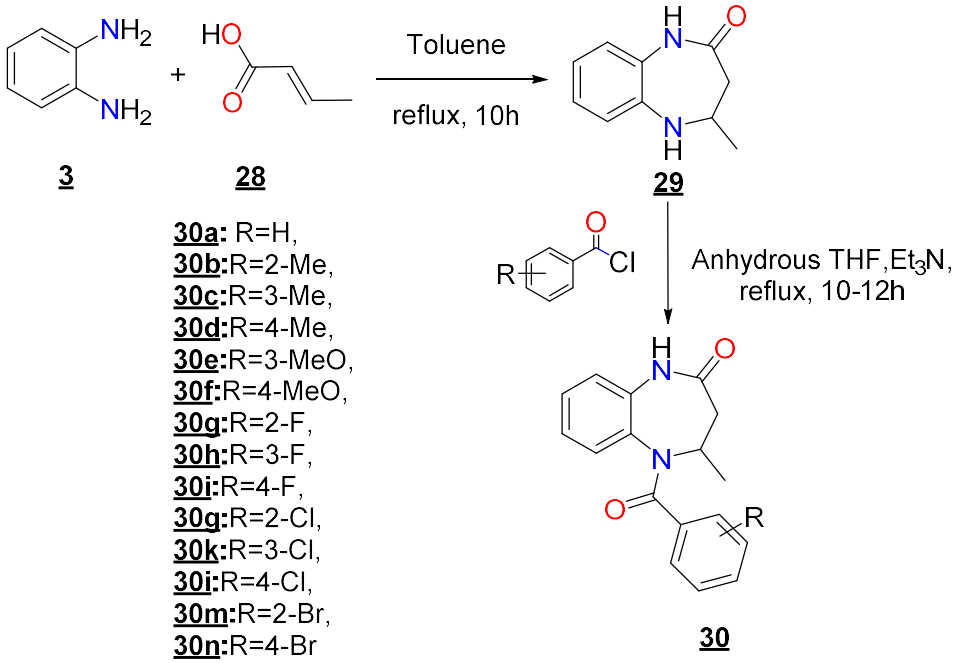

- Scheme7–

Castillo *et al.* [45] reported that tricyclic and 1,3-dihydro-2H-1,5-benzodiazepin-2-ones **33** or **34** could be obtained from *o*-phenylenediamine **3** and α-oxo-ketenes **A** and **B** derived from diazo compounds **31** or **32**. In practice, microwave irradiation of a **1**:**1** mixture of compounds **31** or **32** and **3** provided the desired 1,5-benzodiazepin-2-one **33** or **34** in good yield by a domino reaction without the need for additives (Scheme 8).

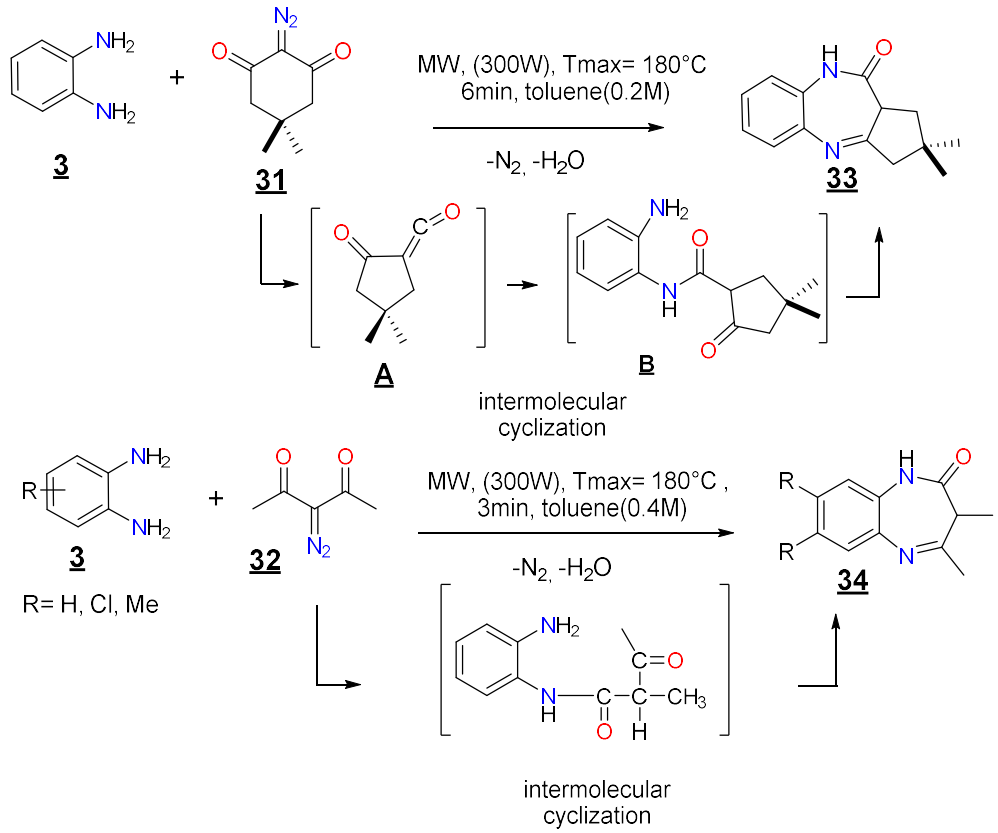

- Scheme 8 –

Rao *et al*. [46] carried out the reaction of 3-aryl -5(4H)-isoxazolones **35** with 4-methyl-1,2-benzenediamine **3** in acetic acid in a water bath at 90°C, to give two products, which were characterized 4-aryl-7-methyl-1H-1,5-benzodiazepin-2(3H)-ones **36 a-e** major and a minor product 2,5 (or 6) dimethylbenzimidazole **37 f-g** (scheme9).

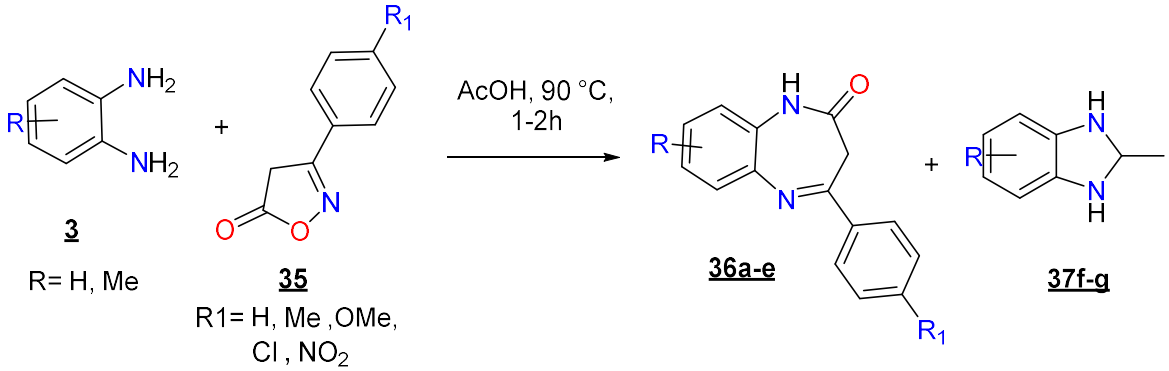

- Scheme 9 -

Misra *et al.* [47] developed a new synthetic strategy, which, in addition to being highly innovative, is simple to implement and in operation, requires low-cost materials, and is applicable to a wide range of functionalized substrates. For the synthesis of quinazoline-condensed 1,5-benzodizepine derivatives (**41**, **45**) with widely explored chemotherapeutic activities and a broad spectrum of biological properties. The strategy is employed based on the use of a nitrile as a coupling partner with an activated benzanilide (whose activation is achieved by its reaction with Tf_2O and then with 2-chloropyridine) [48]. The resulting nitrilium ion will set the stage for its cyclocondensation with the π-electron system with the vinyl or arene part of the benzamide to deliver the quinazoline ring in one step [49]. Schemes (10-11) show the synthesis of analogues quinazoline of 1,5-benzodiazepines (**41**, **45**) and corresponding nitrile derivatives.

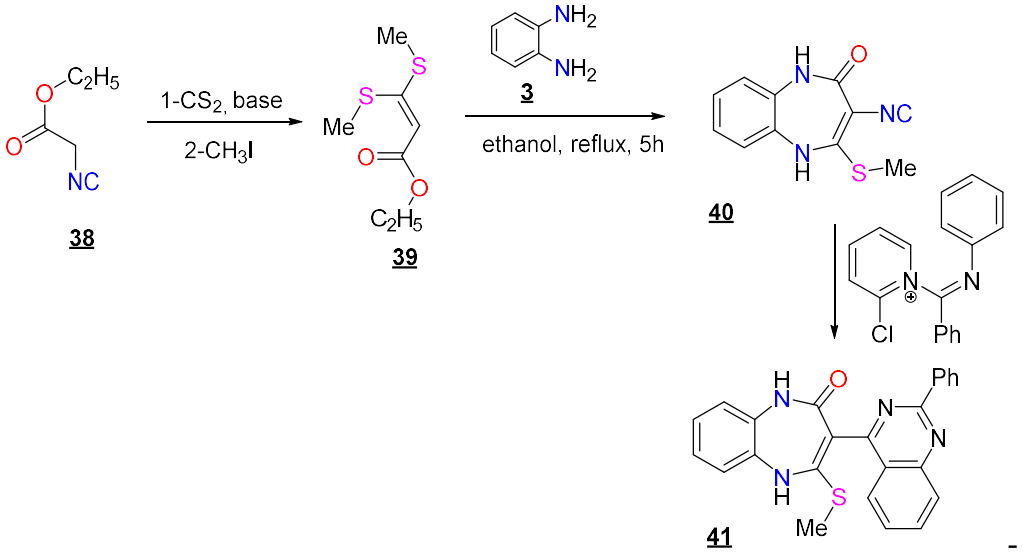

Scheme 10 –

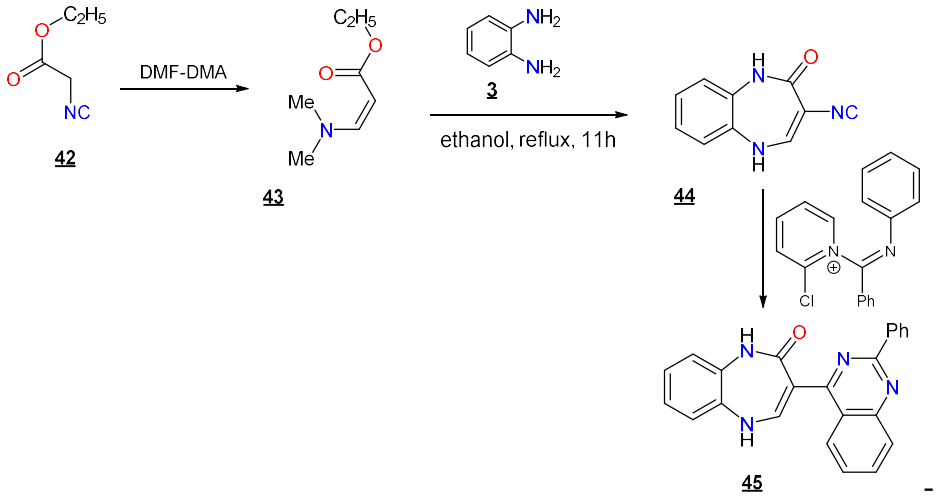

Scheme 11-

Fang *et al.* [50] hypothesized that it may be possible to achieve a formal [3+4] annulation of α,β-unsaturated acylazoliums with readily available substituted aryl 1,2-diamines for the direct synthesis of N-H-free enantioenriched 1,5-benzodiazepin-2-ones **48** that can easily undergo subsequent N-functionalization (Scheme 12). However, there are two competing reaction routes when 2-bromoenals **46** [51, 52] and aryl 1,2-diamines **3** are used as substrates with NHC catalysis. In addition to the desired pathway (path a) via intermediate **II**, another pathway (path b) could also take place to form **III** as end products or as intermediates which can then undergo intermolecular conjugate addition to give the undesired racemic products **48'**.Therefore, Fang *et al.* [50] challenge to achieve a highly chemo-selective and enantioselective [3+4] annulation in this process. Fortunately, the desired 1,5-benzodiazepine-2-ones **48** were obtained in moderate to high yields with high chemo-selectivity and enantioselectivity when the reactions were carried out in the presence of a chiral NHC precursor. Herein, report an unprecedented asymmetric formal [3+4] annulation of aryl 1,2-diamines with α,β-unsaturated acylazoliums derived from 2-bromoenals (Scheme12).

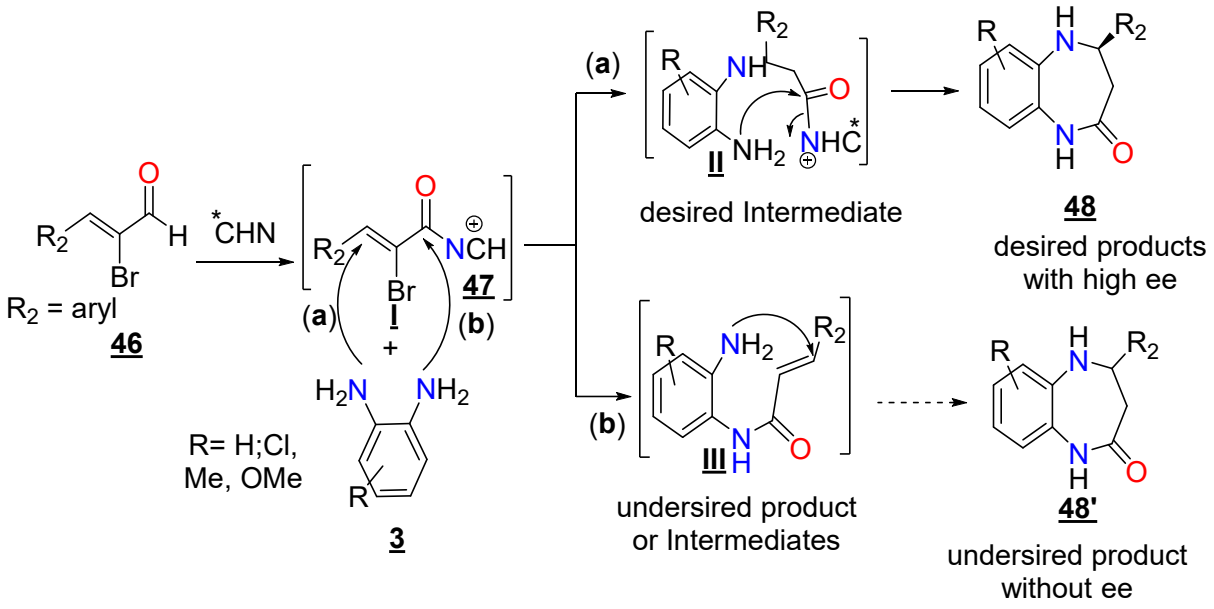

- Scheme 12 –

On the other hand, El Abbassi *et al.* [53] synthesized benzodiazepine derivatives **51a** or **51b** in appreciable yields (70-90%) by the reacting two moles of o-phenylenediamine **3** with one mole of pyran-2-ones **49** or **50** in various alcohols (MeOH, EtOH, PrOH, iPrOH, n-BuOH) for 12-18 h, yielding a mixture of four products (**51a** or **51b**, **52** or **53**), that could be separated by silica column chromatography, when the same reaction is carried out in xylene at reflux, the authors isolated the three compounds **51b**, **52** or **53** (Scheme 13).

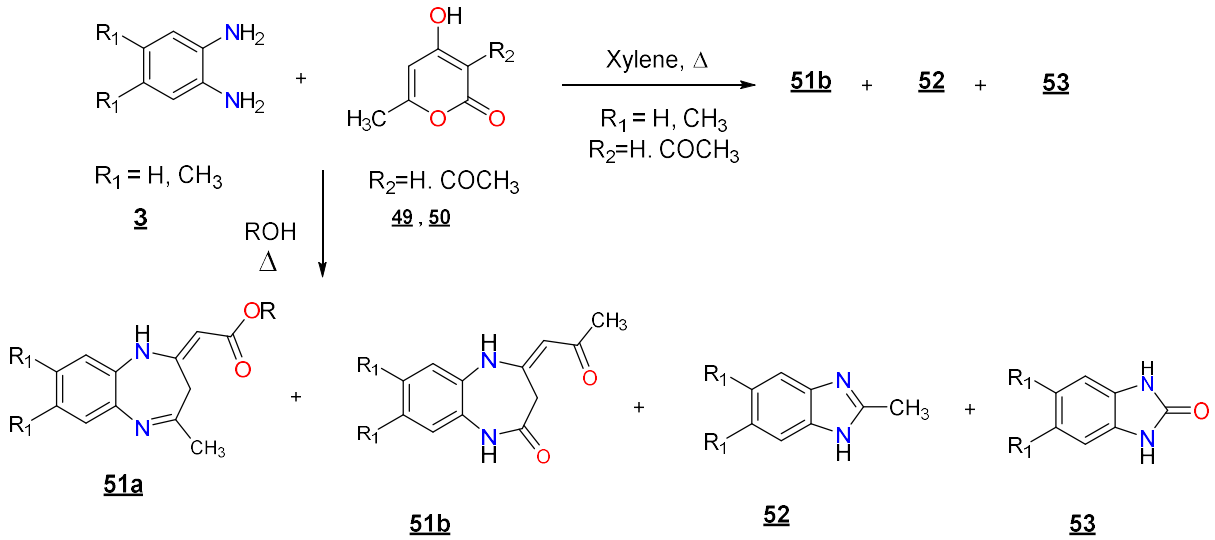

- Scheme 13-

Wang *et al.* [54] synthesized 1,5-benzodiazepin-2-one derivatives **58**-**61** by solvent less reaction of *o*-phenylenediamine **3** with β-ketoesters under microwave irradiation is summarized (scheme 14). The reaction of *o*-phenylenediamine with β-keteesters (R = Bu^t or Ph) gave 1,5-benzodiazepin-2-one derivatives **58** and **59**, respectively. A similar reaction with methyl cyclohexanonecarboxylate produced the corresponding 1,5-benzodiazepin-2-one derivative **60**, while with methyl cyclopentanonecarboxylate gave compound **61** (scheme14).

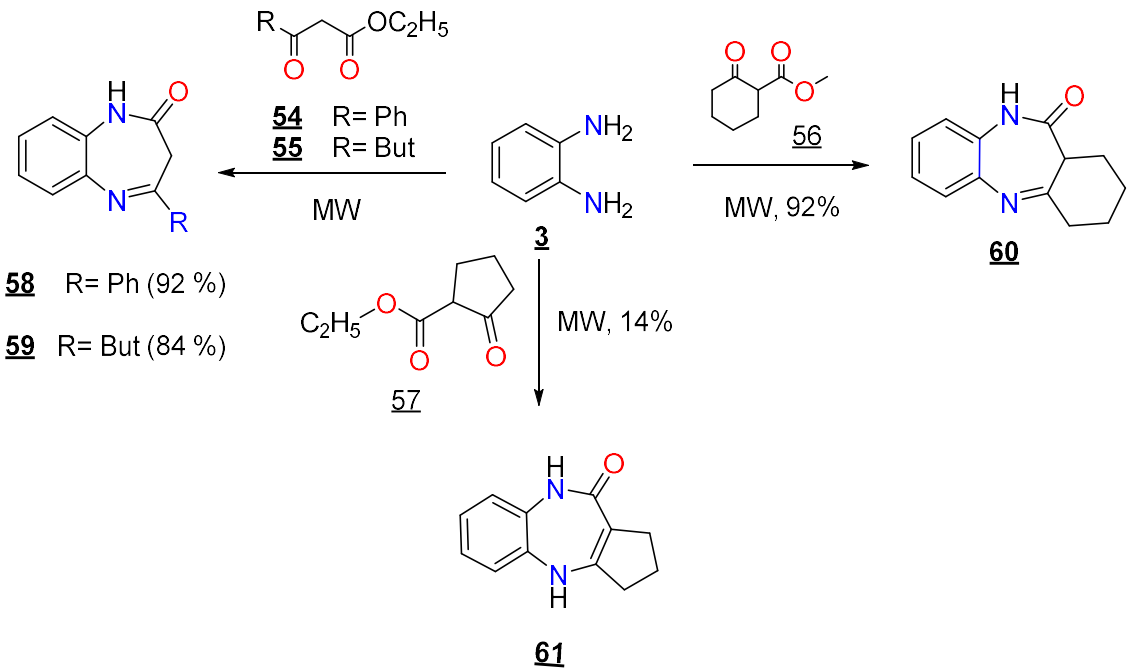

- Scheme 14 -

Bougrin *et al.* [55] haves synthesized 1,5-benzodiazepin-2-one derivatives **58 and 63,** by condensation of ethyl acetoacetate **62** or ethyl benzoyl acetate **54** with *o*-phenylenediamine **3** derivatives in xylene under microwave irradiation (Scheme 15).

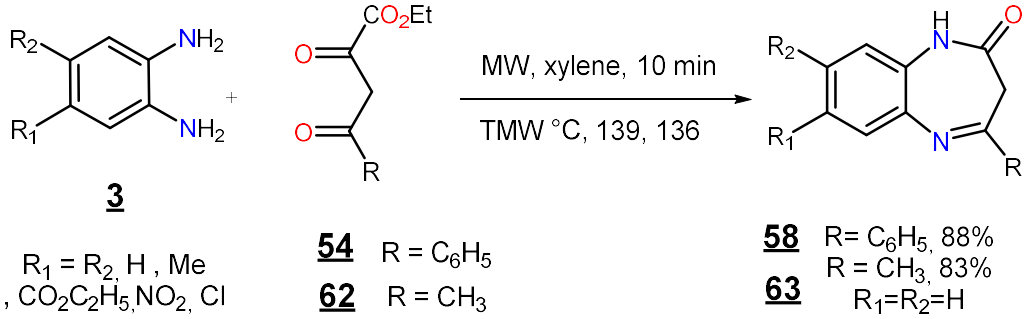

- Scheme 15 -

In the same context, other researchers [56-57] synthesized 4-methyl-1H-1,5-benzodiazepin-2(3H)-one **63** by condensation of *o*-phenylenediamine **3** and ethyl acetoacetate **62,** which were heated in xylene under reflux for 1 hour to give a crystal of this compound **63** in 90% yield (scheme 16).

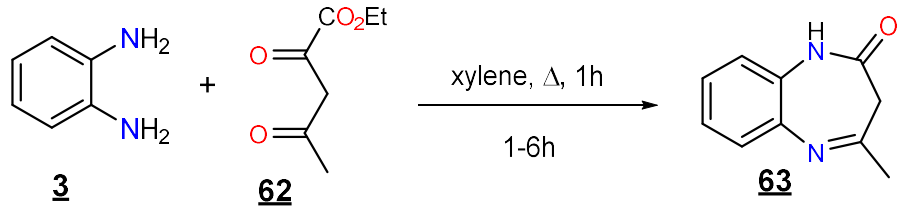

- Scheme 16 -

Essassi *et al.* [58] prepared 4-cyclopropyl-l,5-benzodiazepine-2-ones **65a-c** by the action of *o*-phenylenediamine **3** on ethyl 3-cyclopropyl-3-oxopropanoate **64** in refluxing xylene as solvent (Scheme 17).

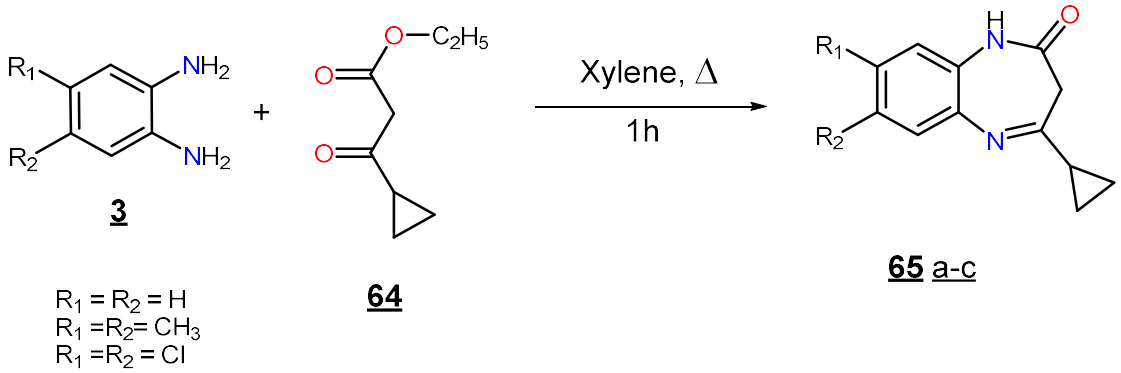

- Scheme 17 –

Similarly, under the same conditions, Achour *et al.* [59] prepared adamantylated compounds by condensation between 1,2-phenylenediamine **3** and a β-keto-ester containing

an adamantyl group **66**, under reflux in xylene to give 4-adamantyl-1,5-benzodiazepin-2-one **67** in 65% yield (Scheme 18).

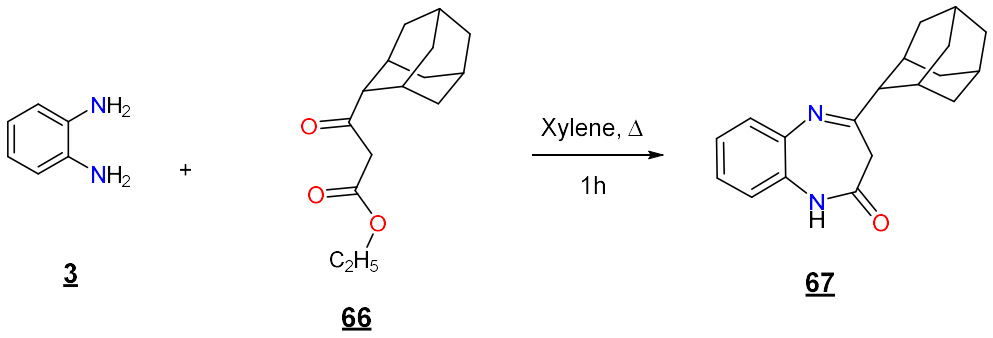

3 **66** **67**

- Scheme 18 –

Tabata *et al*. [60] synthesized 3-methyl-2,3,4,5-tetrahydro-1H-1,5-benzodiazepin-2-one **70a** in 51% yield and **70b** in 86% yield from the condensation of 2-nitroaniline **68** with methacrylic acid **69** in sulfuric acid at 80 ^{0}C (scheme 19).

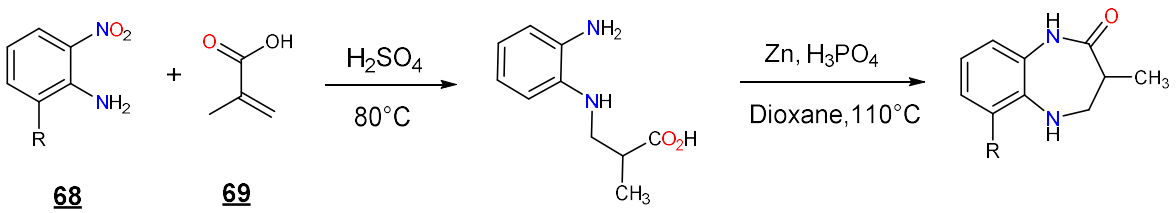

68 **69** **70a,b**

R= H, Me

- Scheme19-

Kanyonga *et al*. [61] prepared 4-phenyl-l, 5-benzodiazepin-2-one **58** by the action of *o*-phenylenediamine **3** on the β-ketoester **54** in refluxing xylene (scheme 20).

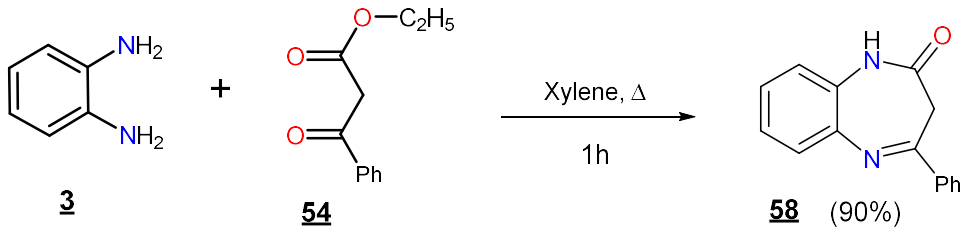

3 **54** **58** (90%)

- Scheme 20 -

II- Reactivity of 1, 5-benzodiazepin-2-one

II-1 Alkylation reactions

1,5-benzodiazepine and its derivatives possess a wide variety of reactivation sites: methylene groups, carbonyl groups, or imine groups, and the carbon atom of the fused benzinc ring. Therefore, the compounds that are synthesized have high reactivity, which allows them to participate in condensation, alkylation, sulfurization, and 1,3-dipolar cycloaddition reactions.

Ansari *et al.* [62] studied the action of 4-(2-hydroxyphenyl)-3H-1,5-benzodiazepin-2-one **25** with 2-diazopropane (DAP) in anhydrous dichloromethane. The reaction mixture was stirred at 0°Cfor 12h to give a mixture of 2-isopropylether of 4-(2-hydroxyphenyl)-3H-1, 5-benzodiazepine **71** (43%) and 1-isopropyl-4-(2-hydroxyphenyl)- 3H-1,5-benzodiazepine-2-one **72** (28%) (Scheme21).

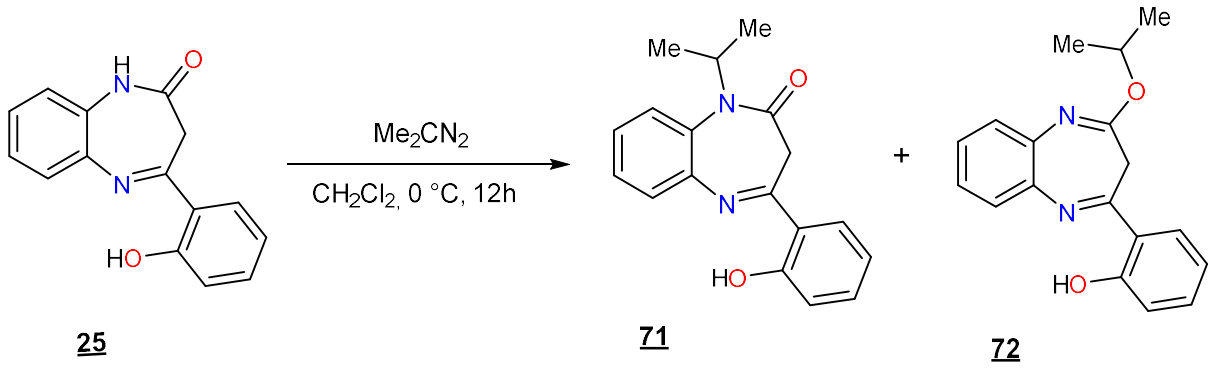

25 **71** **72**

- Scheme 21 -

Rida *et al*. [63] studied the alkylation reaction of 3-hydroxy-4-phenyl-1,5-benzodiazepin-2-one **73a-b** trans by different alkylating agents: methyl iodide, allyl bromide, benzyl chloride, ethyl bromoacetate, and ethyl bromide under the conditions of liquid/liquid phase transfer catalysis in benzene in the presence of sodium hydroxide as a base and triethylbenzylammonium chloride (TEBAC) as a catalyst. They isolated 1,5-benzodiazepine **74c-k** derivatives in good yield scheme 22.

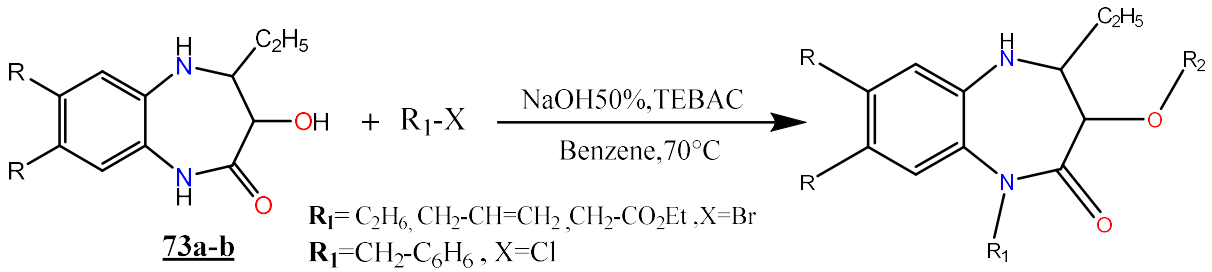

73a-b

a:R= H

b:R= CH_3

$\mathbf{R_1}$= C_2H_6, CH_2-CH=CH_2 ,CH_2-CO_2Et ,X=Br
$\mathbf{R_1}$=CH_2-C_6H_6 , X=Cl
$\mathbf{R_1}$= CH_3 ,X=I

74c-k

c:R= CH_3,R_1=C_2H_5, R_2=H
d:R=H=R_2 , R_1=CH_2-C_6H_5 ,
e:R= CH_3,R_1= C_2H_5=R_2

f:R= H ,R_1= C_2H_5=R_2
g:R=H=R_2 , R_1=CH_2-CO_2Et ,
h:R=H=R_2 , R_1=CH_2=CH-CH_2
k:R=H=R_2 , R_1=CH_2-C_6H_5 ,

- Scheme 22 -

Miraoui *et al.* [64] reported the alkylation and acylation reactions of 4-(2-hydroxy-phenyl)-1,5-benzodiazpin-2-ones **25**. The showed that the alkylation occurred specifically on the

amide moiety, while the acylation reaction took place only on the hydroxyl group, giving respectively to compounds **75a-c** and **76** (scheme 23).

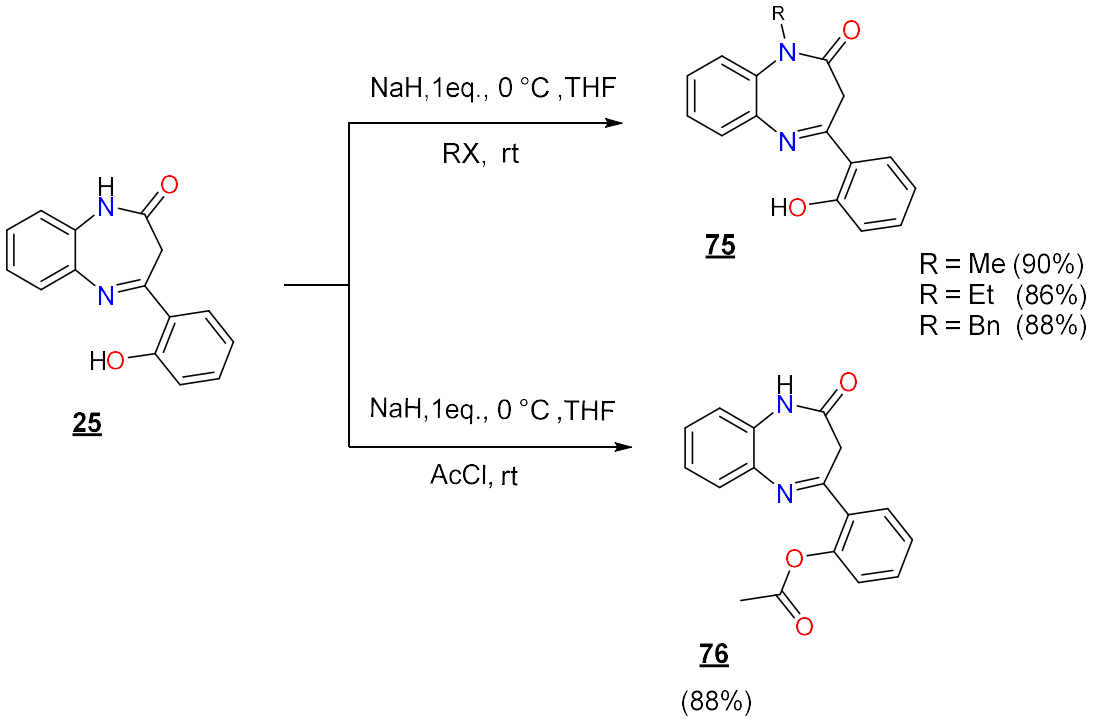

- Scheme 23 –

Recently, El Foujji *et al*. [65] studied the alkylation of (4Z)-4-(2-oxopropylidene)-2,3,4,5-tetrahydro-1,5-benzodiazepin-2-one **51b** using the liquid-solid phase transfer catalysis method. Thus, the action of ethyl iodide on 1,5-benzodiazepin-2-one **51b** for 10 hours at room temperature, allowed the preparation of mainly (3R,4Z)-1,3-diethyl-4-(2-oxopropylidene)-2,3,4,5-tetrahydro-1H-1,5-benzodiazepin-2-one **77** in good yield (scheme 24).

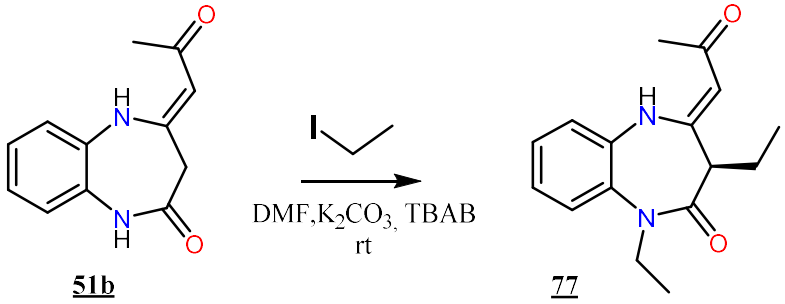

- Scheme 24 -

In 2016, Sebhaoui *et al*. [66] performed the alkylation reaction of (4Z)-2-oxopropylidene-1,5-benzodiazepin-2-one **51b** with dodecane bromide under the conditions of liquid-solid phase transfer catalysis. They were able to isolate the N-alkyl compounds **78** in good yield (scheme 25).

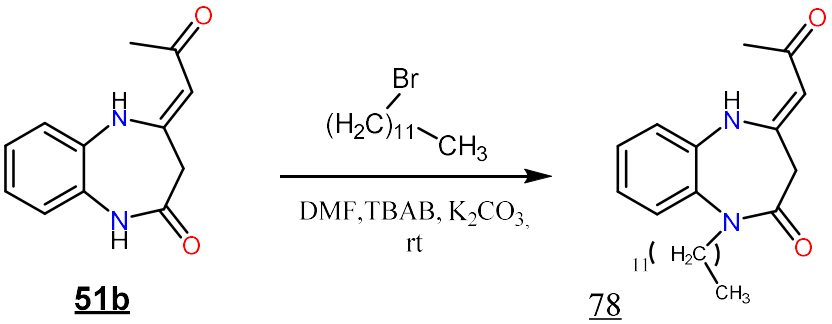

51b 78

- Scheme 25–

II-2 Sulfurization reactions

Ballo *et al.* [67] proposed a simple method for the synthesis of the substituted compound 1,5-benzodiazepine-2-thione **81** by reacting phosphorus pentasulphide with 1-benzyl-4-phenyl-1,5-benzodiazepin-2-one **79** in refluxing leading to the corresponding sulfurazal compound 80 namely1-benzyl-4-phenyl-1,5-benzodiazepin-2-thione was subjected to the action of DMF-DMA at 110 °C for 12 hours to afforded the benzodiazepine **81** .The authors showed showed that the methylene group at position 3 of the diazepine ring was affected (scheme 26).

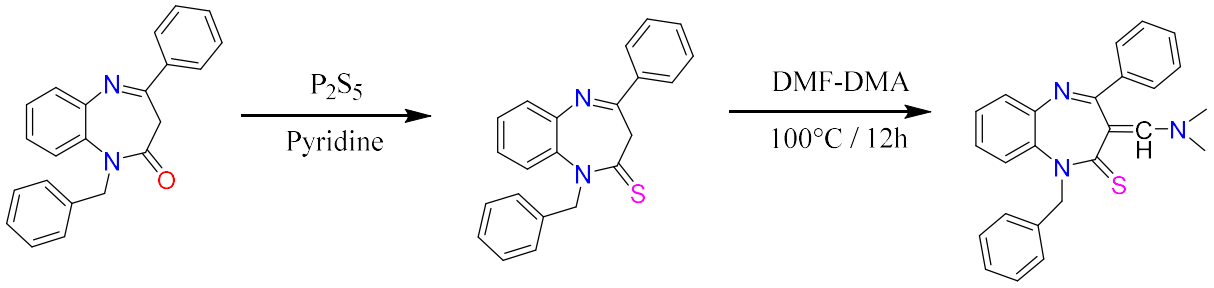

79 **80** **81**

- Scheme 26-

In 2017, El Ghayati *et al.* [68] isolated 1-ethyl-4-phenyl-1,5-benzodiazepine-2-thione 83 by reacting 1-ethyl-4-phenyl-1,5-benzodiazepin-2-one 82 with phosphorus pentasulfide in refluxing pyridine for 4 h (scheme 27).

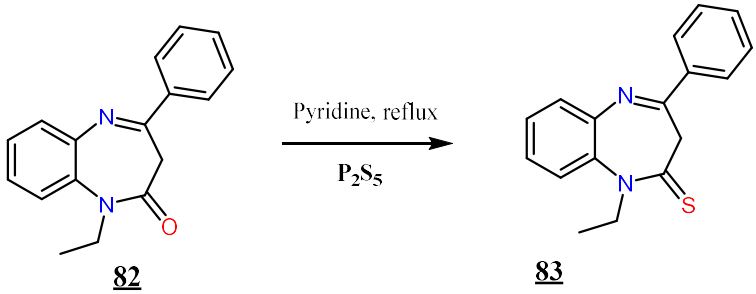

82 **83**

- Scheme 27-

II- 3 1,3-dipolar cycloaddition

Alaoui, I. C. *et al*. [69] synthesized new polycyclic compounds **85** and **87** by condensing *p*-chlorobenzonitriloxide with 1,5-diallyl (dipropargyl)-1,5-benzodiazepine-2,4-diones **84** and **86** (scheme 28 and 29).

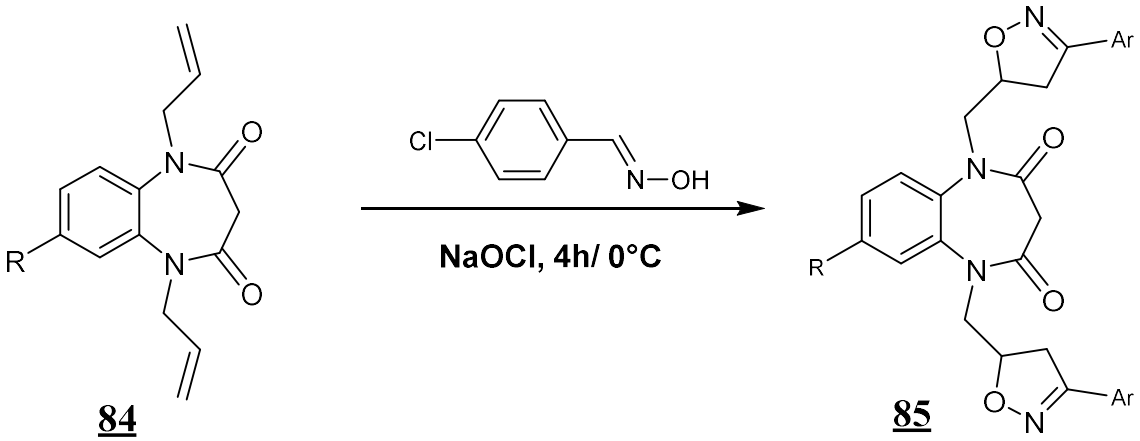

84 **85**

- Scheme 28-

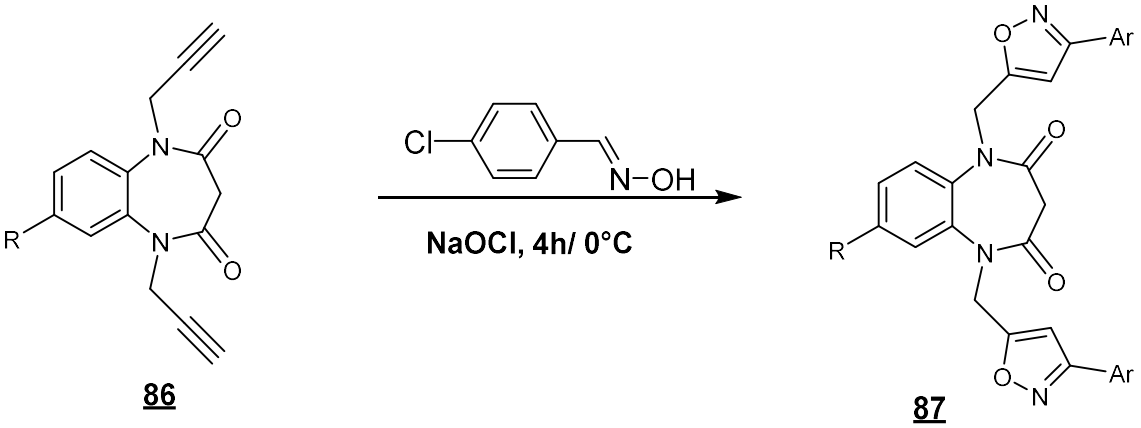

86 **87**

- Scheme 29-

In the same context, Ahabchane *et al*. [70] have synthesized new 1,5-benzodiazepine-2-ones substituted in position 1 by chains containing different heterocyclic, such as pyrazole, isoxazole, and 1,2,3-triazole (scheme 30).

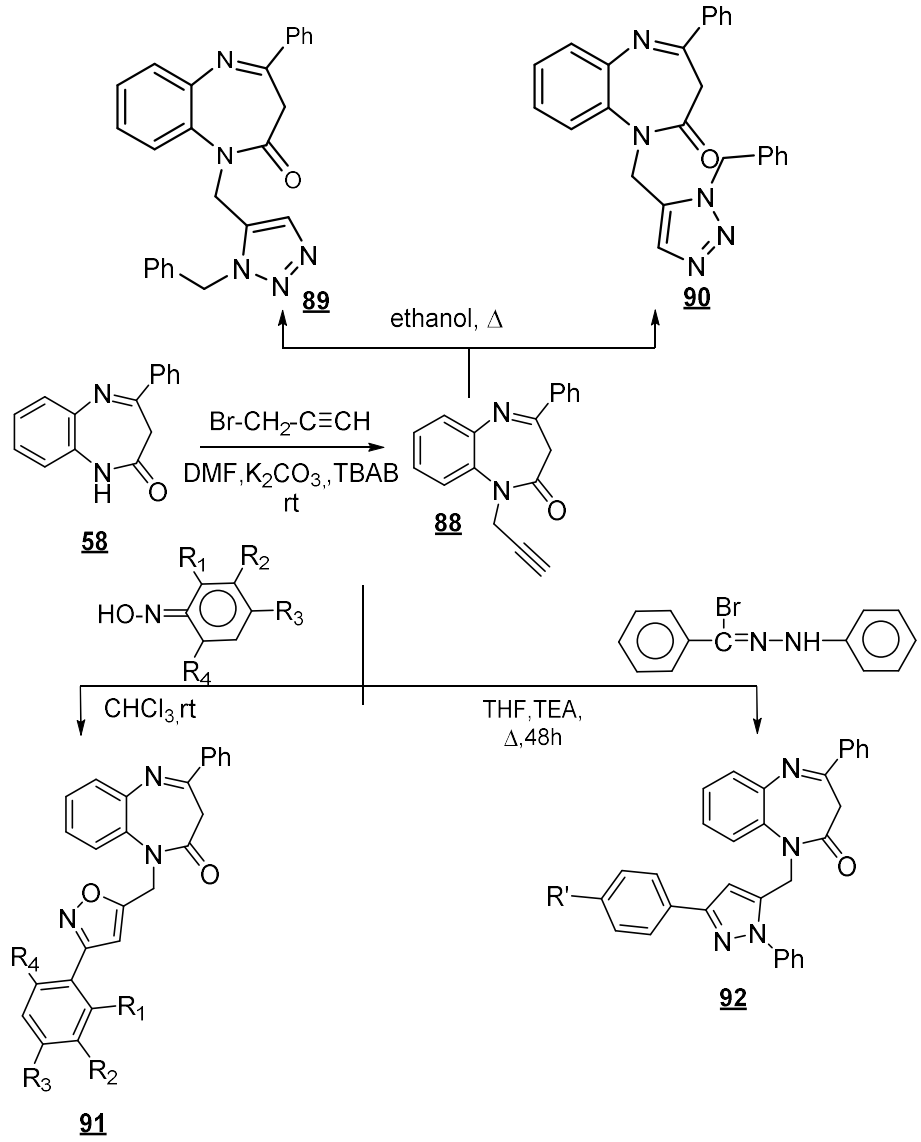

- Scheme 30-

II- 4 Reaction with aromatic aldehydes:

Solomko *et al.* [71a] prepared 4-styryl-l,5-benzodiazepin-2-one **93a-g** derivatives by condensation of aromatic aldehydes with 4-methyl-2,3-dihydro-1H-l,5-benzodiazepin-2-ones **63 a-d** in refluxing benzene or alcohol in the presence of piperidine as a base (scheme 31).

Ei-Shafei *et al*. [71b], reported that according to chemical transformations, compounds **94e-g** are 3-arylidene derivatives **93'**. However, the authors did not prove the structure of the resulting compounds. The authors showed that the compounds **93'** are used as durable dyes for nitrone [71c], have a tranquilizing effect [7d], and are also employed for the treatment of asthma as well as complexing agents [71e].

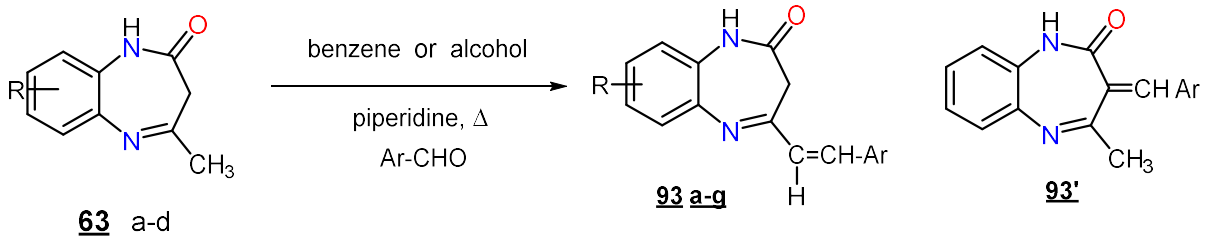

63 a-d

93 **a-g**

93'

63: a- R=H, b R=8-Cl, r R=8-CH_3O, d -R=7-NO_2

93 a- R=H, Ar=C_6H_5, b- R=8-Cl, Ar=C_5H_6, e-R=8-CH_3O, Ar=C_5H_6, d-R=7-NO_2, At=C_5H_6, e-R=H, Ar=4-NO_2--C_6H_4, f- R=H, Ar=3-NO_2H_4, g -R=H, Ar=4-$(CH_3)_2N$-C_6H_4

- Scheme 31 -

Other researchers, [72] prepared the corresponding arylidene derivative alkyl- 4-methyl-l,5-benzodiazepin-2-one **93'a-c** by condensation of the aromatic aldehydes with 1-alkyl- 4-methyl-l,5-benz1diazepin-2-one **94a-c** in refluxing ethanol in the presence of piperidine. The authors showed that the methylene group **93' a-c** **in** position 3 of the diazepine ring constitutes the seat of the reactions (scheme 32).

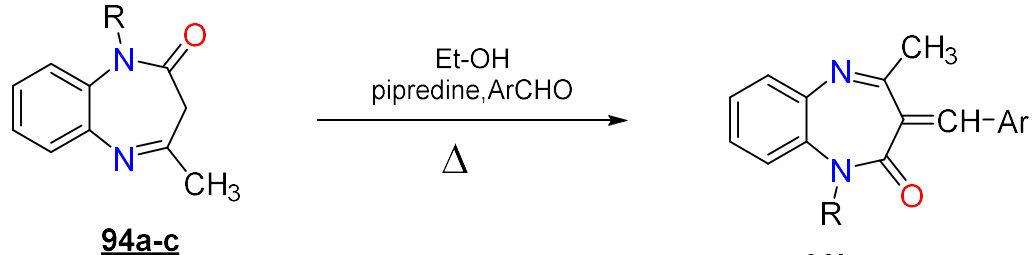

94a-c

R = H , CH_3, C_2H_5

93'a-c

Ar = p-$N(CH_3)_2C_6H_4$;
Ar= P.$NO_2C_6H_4$

- Scheme 32 -

II- 5 Reactions with halogens (Br_2, Cl_2):

Avramenko *et al.* [73] studied the halogenations reactions of 4-(*p*-methoxyphenyl)-2,3-dihydro-IH-l,5-benzodiazepin-2-one **95** with various halogenating agents. They found that bromination with an equimolar amount or an excess of N-bromosuccinimide (NBS) in carbon tetrachloride in the presence of benzoyl peroxide gives, as in the case of unsubstituted diazepinone 3-bromo-4-(*p*-methoxyphenyl)-2,3-dihydro-1H-l, 5-benzodiazepin-2-one **96** (scheme 33).

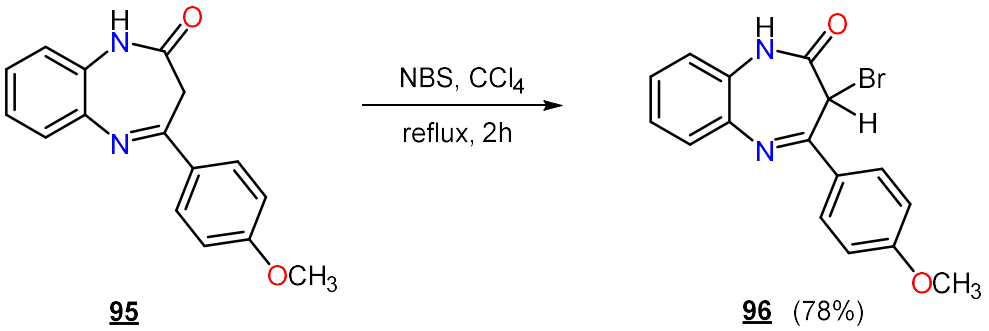

95 **96** (78%)

- Scheme 33 –

Bozhanov *et al.* [74] prepared derivatives of 3-bromo-4-pyridyl-1,5-benzodiazepine-2-one **98a-b** (scheme 34). Bromination of benzodiazepin-2-one with molecular bromine or N-bromosuccinimide occurred regioselectively at the 3-position of the heterocyclic to give the 3-bromo derivatives **98a-b**, characterized by ^{1}H NMR spectra highlighted a singlet signal of the methine proton in the range 6.00-6.20 ppm, while the signals of the methylene protons have disappeared.

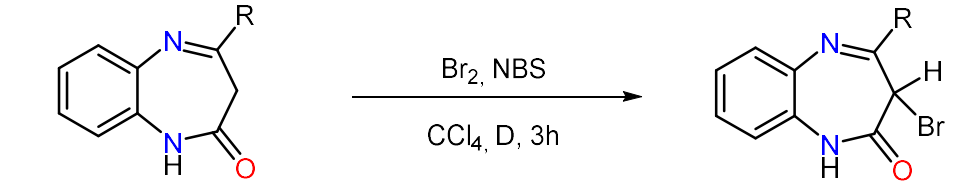

R = 3-pyridyl, 4-pyridyl

97 **98a-b**

- Scheme 34 -

Similarly, Abronin *et al.* [75] showed that chlorination reactions of 4-methyl-8-methoxy-I,5-benzodiazepin-2-one **99** with 2 moles of N-chlorosuccinimide in CCl_4 lead to the mixture of 3-chloro- and 3,3-dichloro-4-methyl-8-methoxy-1,5-benzodiazepin-2-ones **100** and **100'** (scheme 35).

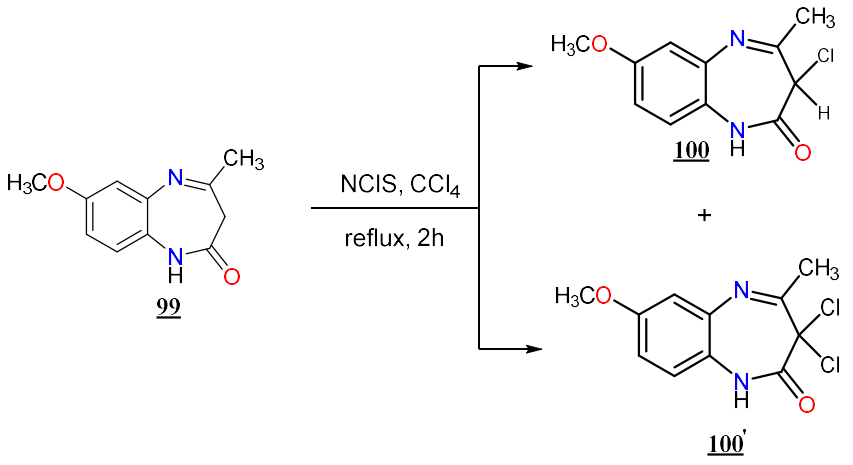

99 **100** **100'**

- Scheme 35 -

Other researchers [76-77] treated 1,5-benzodiazepin-2-one **54** and **62** with an equimolar amount of bromine in chloroform as solvent and isolated 3-bromo and 3,3-dibromo-1,5-benzodiazepin-2-one derivatives (**101 a-b)** or (**101' a-b)** (scheme 36).

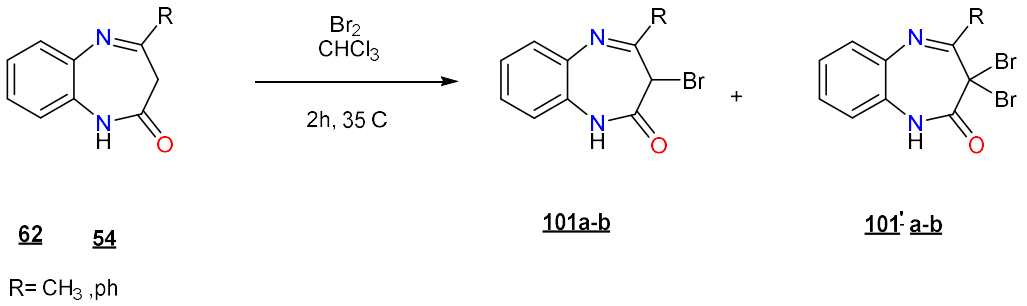

62 54

R= CH_3 ,ph

101a-b 101' a-b

- Scheme 36 -

II- 6- Hydrogenation:

Lyubimov *et al*. [78] performed hydrogenation of 1,5-benzodiazepin-2-ones using mixed-ligands catalytic systems from phosphoramidite or phosphite with different solvents to show higher enantioselectivity leading to 1,5-benzodiazepin-2-one **102** and **103** (scheme 37).

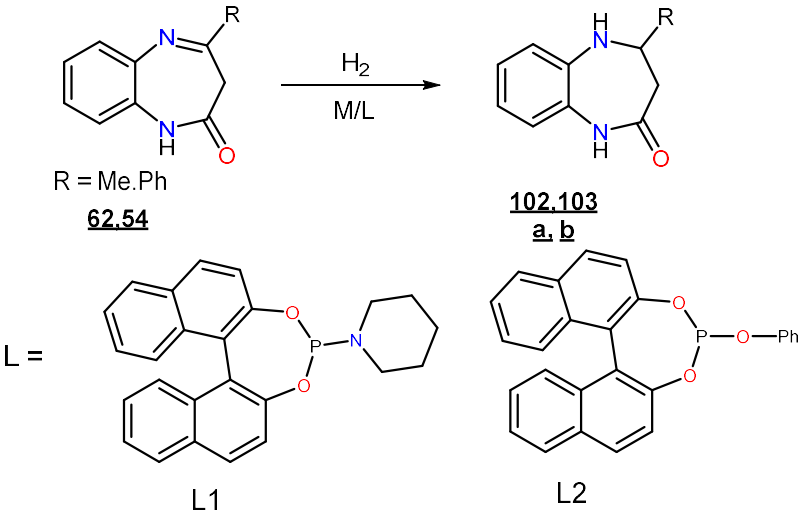

- Scheme 37 –

Other researchers [79] studied the catalyzed hydrogenation of 4-phenyl-1,3-dihydro-2H-1,5-benzodiazepin-2-one **95a-c** in dichloromethane (Scheme 38), and showed that use of the ligands resulted in quantitative conversion, but the enantioselectivity did not exceed 8%. The replacement of the solvent by ethanol markedly increased the reaction selectivity, and L1 proved to be the best ligand. Moreover, the use of methanol produces some increase in the asymmetric induction, whereas trifluoroethanol (TFE) and propan-2-ol lead conversely to a pronounced decrease in the enantioselectivity.

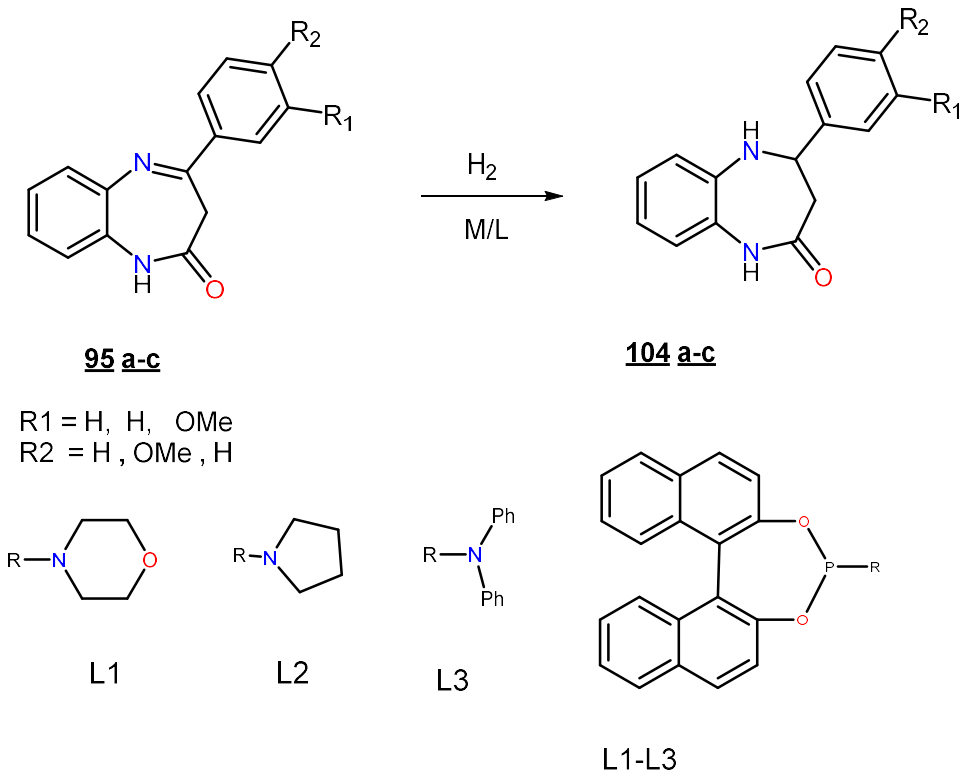

- Scheme 38 –

Also, Yang et al. [80] developed a method for the hydrogenation reaction of 4-substituted 1.5-benzodiazepin-2-one derivatives **105 a-c**, providing a facile methodology for the synthesis of heterocyclic compounds that have importance in pharmaceuticals applications. The reaction conditions were described, allowing for moderate enantioselectivities (scheme 39).

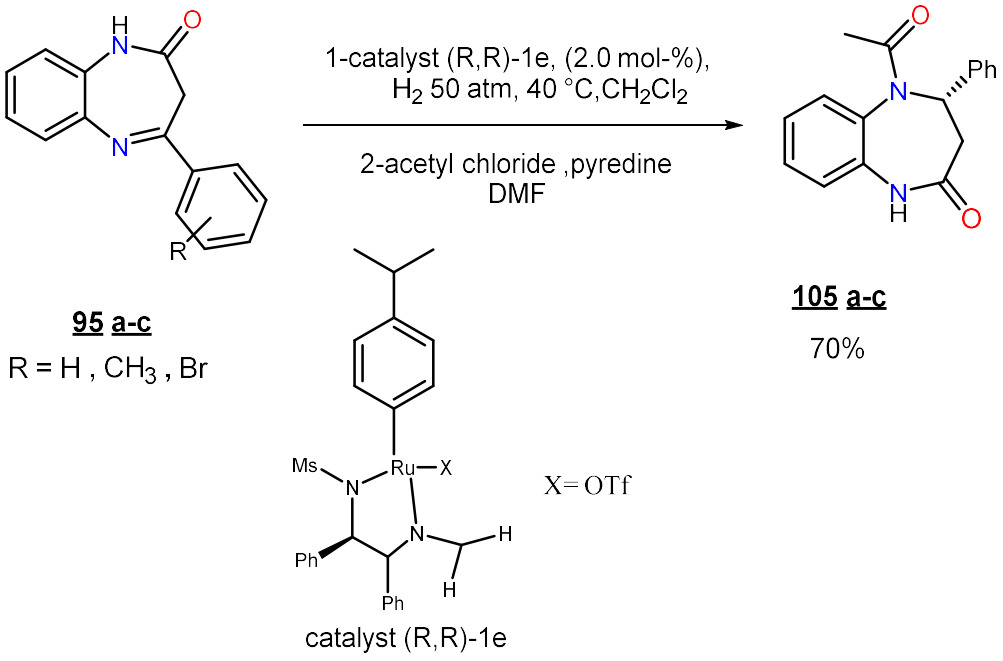

Scheme39

Essassi, E. M. *et al*. [81], reported the catalytic hydrogenation of the 1-alkyl-4-phenyl-1,5-benzodiazepin-2-ones and observed which an opening of the seven-membered ring involving of the imine group of the diazepine ring to obtain the amidic compounds (scheme 40).

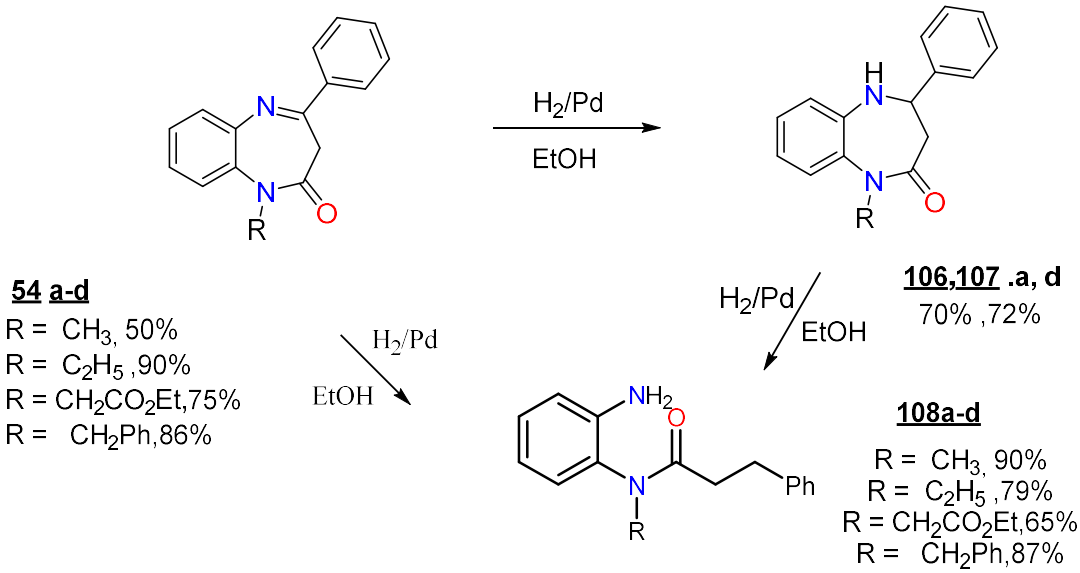

- Scheme 40 –

Conclusion:

Derivatives of 1,5-benzodiazepine occupy an important place in several fields, especially in the pharmaceutical field. A great variety of synthetic approaches have been used to prepare new 1,5-benzodiazepine derivatives. As starting materials, the authors employed generally substituted *o*-phenylenediamines and electrophonic insatured compounds in conventional conditions or under microwave irradiation. A multicomponent reaction (MCR) has also been achieved. However, the modifications of the basic structure of 1,5-benzodiazepine allowed the production of new derivatives presenting a broad spectrum of biological activities. The 1,5-benzodiazepine derivatives are very rich due to the presence of different reactive sites involved in several reactions, such as alkylation, halogenation, sulfurization, hydrogenation reactions, and 1,3-dipolarcycloaddition.

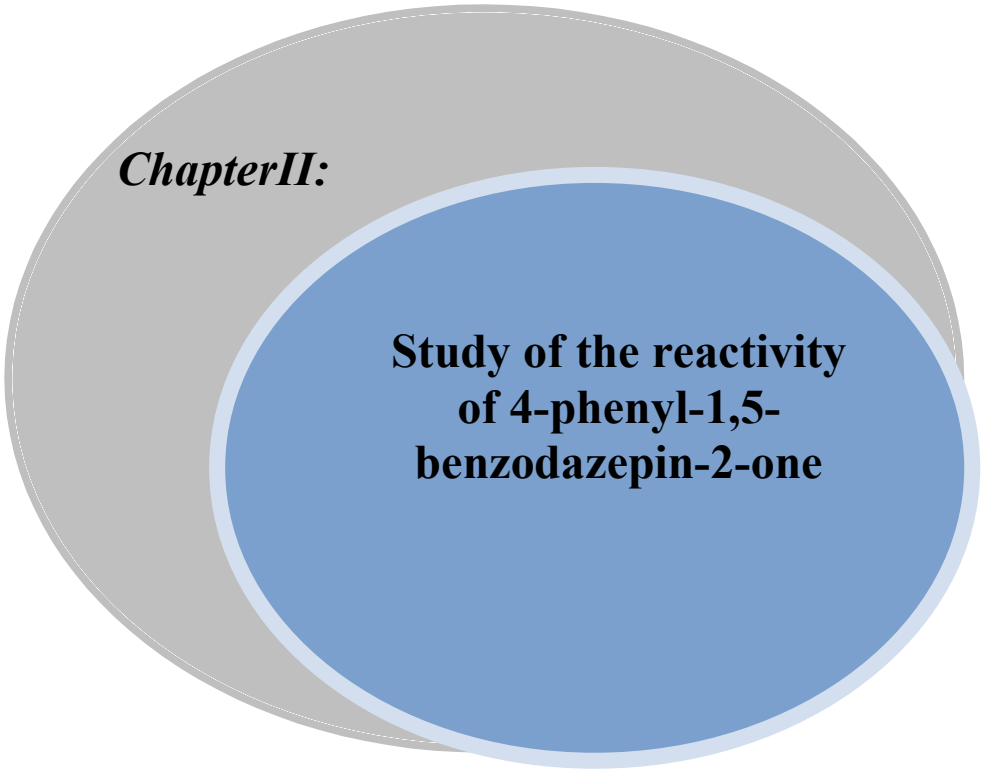
ChapterII:
Study of the reactivity of 4-phenyl-1,5-benzodazepin-2-one

I- Introduction

The 1,5-benzodiazepine scaffold constituted a highly reactive heterocyclic unit that has been part of many organic synthesis reactions. The 1,5-benzodiazepines are known for their various therapeutic properties, including anti-proliferative activity, antimicrobial activity, neuropharmacological activities, antioxydant activity, and lipid peroxidation inhibition [82-85]. In order to synthesize new derivatives of N-alkyl-1,5-benzodiazepin-2-one (2-thione) that may present interesting biological properties or products that would serve as starting reagents in a large number of reactions, we studied the alkylation and sulfurization reactions of 4-phenyl-1,5-benzodiazepin-2-one.

II- Preparation of 4-phenyl-1,5-benzodiazepin-2-one:

The Synthesis of 4-phenyl-1,5-benzodiazepin-2-one **58** is carried out by condensation of *o*-phenylenediamine **3** with ethyl benzoyl acetate **54** [61] in refluxing xylene for 3 hours (Scheme 41).

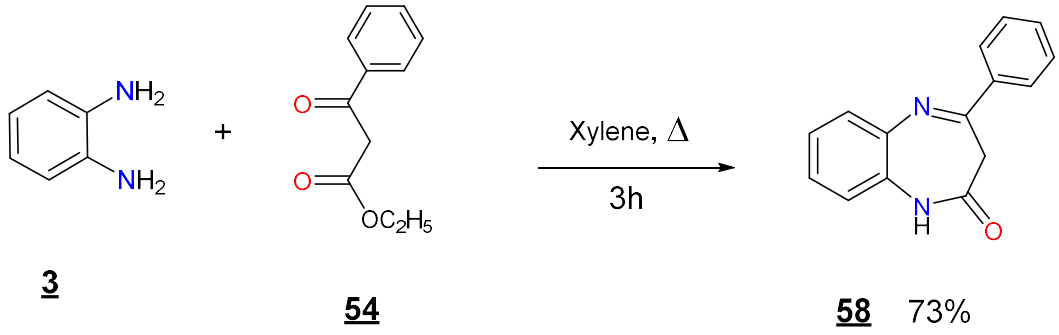

3 **54** **58** 73%

- Scheme 41 -

The structure of compound **58** has been elucidated based on its ^{1}H, ^{13}C NMR and MS spectral analysis, and by comparison with previously reported data [61].

Indeed, the examination of the RMN^{1}H spectrum of compound **58** reveals, in addition to the signals corresponding to the aromatic protons, which appear in the form of a massif between 7.20-7.90 ppm, a singlet centered at 3.40 ppm, corresponding to the two-methylene protons in position 3. We also note a signal at 9.37ppm attributable to the NH group.

The spectrum of ^{13}C NMR highlights, in particular, the signal relating to the methylene group in position 3 at 39.79 ppm. The most deshielding carbon atom was attributed to the lactam carbonyl group at 167.80 ppm.

III- Reactivity of 4-phenyl-1, 5-benzodiazepin-2-one:

Prepared of 4-phenyl-1,5-benzodiazepin-2-one **58** presents several reactive sites; the nitrogen in position 1, the diazepine double bond, and the methylene group in position 3 of the seven-membered ring. The presence of all these reactive sites gives it a high reactivity allowing it to be used in several types of reactions.

III-1 Alkylation

Conventional alkylation techniques use strong bases (NaOH) in liquid ammonia or dimethylformamide [86-87] or weak bases (e.g. K_2CO_3) in acetone. These techniques have a number of drawbacks: they are expensive, which leads to a loss of yield, and it is difficult to produce a pure product.

Faced with all these difficulties, the researchers developed another very effective alkylation method: Phase Transfer Catalysis (PTC) [88].

In summary, this method has several advantages:

- Energy gain (reaction at room temperature)
- Good yield
- Ease of use

Depending on the nature of the base, we can distinguish:

- Liquid-Liquid PTC: the base used is a soda solution in an aprotic solvent such as dichloromethane, benzene or toluene.
- Solid-Liquid PTC: it uses a less strong base, potassium carbonate in DMF, in the presence of a catalyst, tetrabutylammonium bromide (TBAB).

To prepare new mono-substituted 1,5-benzodiazepin-2-one which may also be used as substrates for the synthesis of new heterocyclic, N-alkylation reactions seemed to be the most effective way of synthesis. For this purpose, we have chosen solid-liquid phase transfer catalysis as the synthesis method.

III-2 Preparations of N-alkyl-4-phenyl-1,5-benzodiazepine-2-ones:

The literature reviews several studies involving reagents halogenated long-carbon chains as alkylating systems. For example, this work was described by Chebabe *et al.* [89], and led to synthesize new S-alkylated surfactant molecules (figure 3).

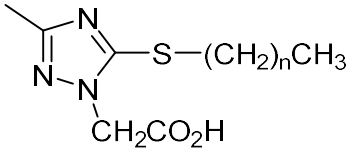

109

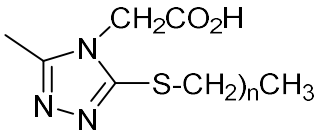

110

Figure 3

Chkirate *et al.* [90] studied the alkylation of benzodiazepine **51b** with alkyl bromides under liquid-liquid phase transfer catalysis conditions showing that potassium hydroxide provided, on the one hand, deportation of NH nitrogen to form N-alkyl products **111** and, on the other hand, the engagement of DCM as a alkylating reagent to give bis-benzodiazepines **112** (Scheme 42).

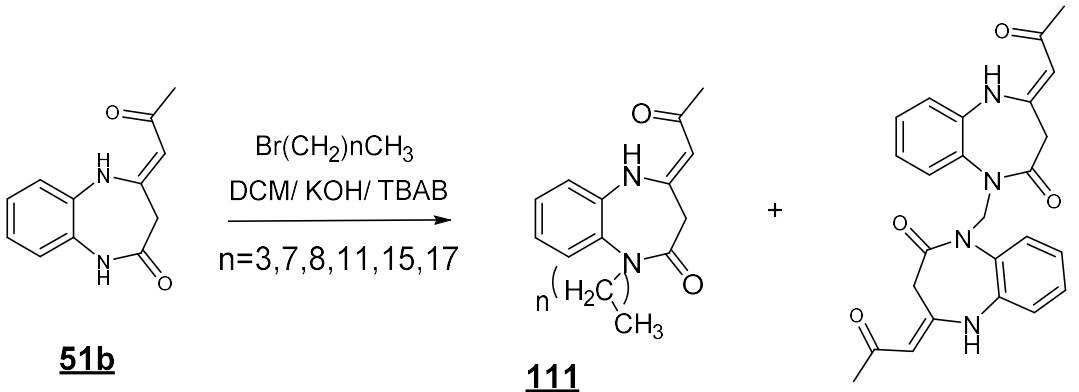

51b **111** **112**

- Scheme 42-

N. Ongone, *et al*. [91] studied the alkylation of 4-phenyl-1,5-benzodoazepin-2-one **58** with four long carbon chain derivatives and showed that the alkyl products **113**-**116** have good analgesic activity (Scheme 43)

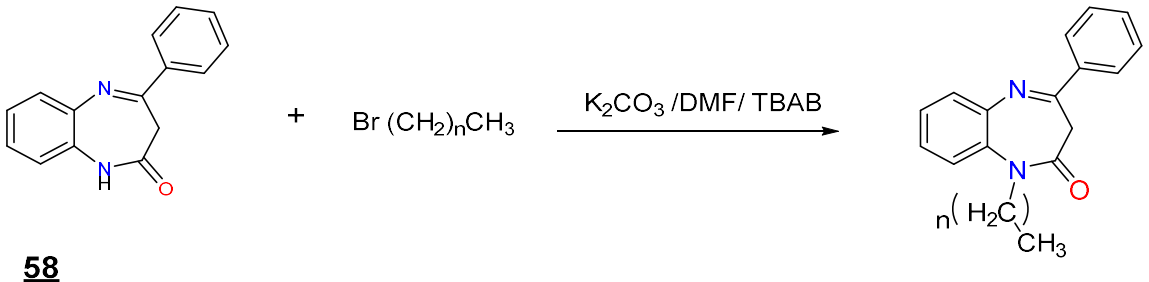

58

n=7 : **113** , n= 9 : **115**
n=8 : **114** , n=11: **116**

- Scheme 43 -

For our part, we have prepared a large number of N-alkylated 4-phenyl-1,5-benzodiazepin-2-one compounds by condensation of 4-phenyl-1,5-benzodiazepin-2-one **58** with the alkyl halide. The reactions led to the normally expected products **113**-**121** in good yields (Scheme 44).

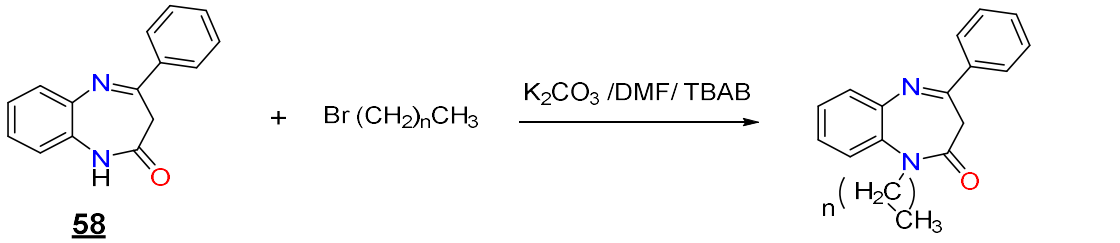

- Scheme 44 -

Structures of compounds **113-121** are perfectly characterized by the usual spectral methods (^{1}H, ^{13}C NMR, and MS), as well as in some cases by X-ray diffraction crystallographic study.

III.2.1. Spectral characterization of the compound 117:

On the $^{1}HNMR$ spectrum, taken in $CDCl_3$ of compound **117** (figure 4), we noted, in particular, a multiplet between 1.08-1.15 ppm due to the protons of the chain, the absence of the signal corresponding to the N-H proton which attests to its involvement in the alkylation reaction, as well as the presence of a central AB system at 4.08 ppm attributable to the protons of the methylene group at position 3.

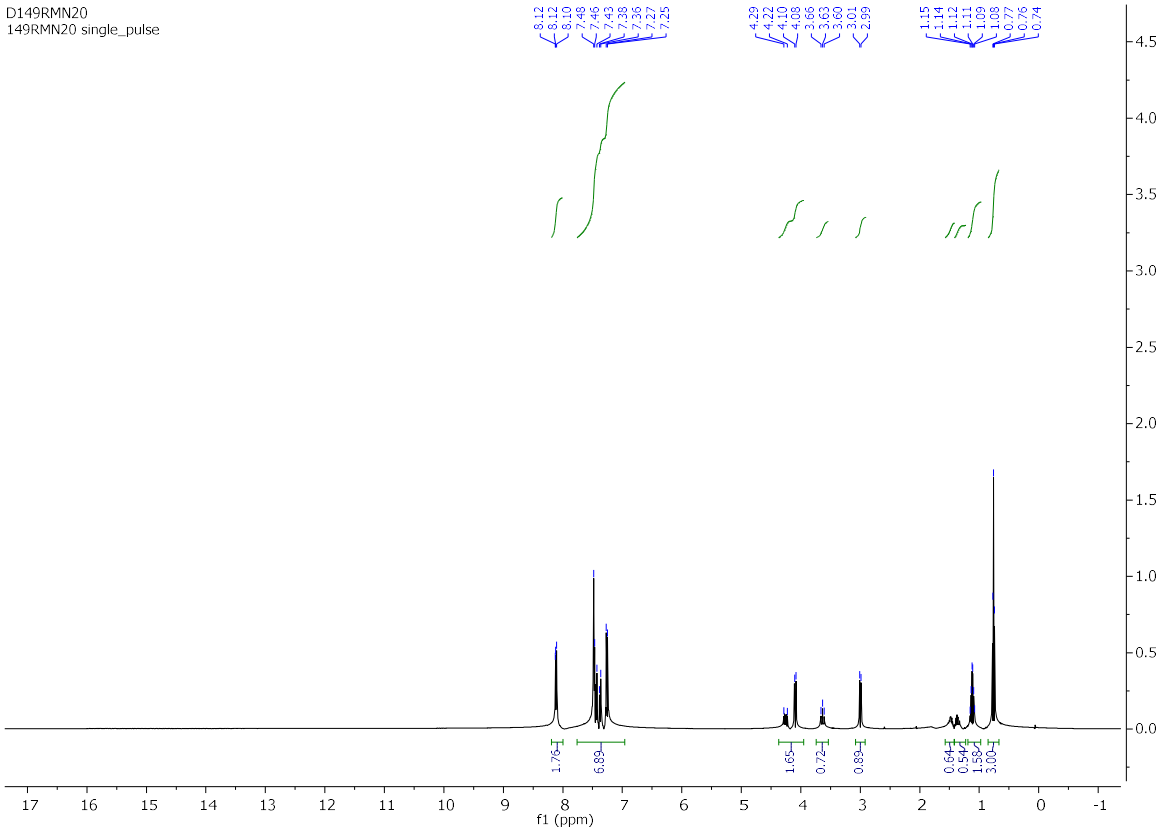

Figure 4:^{1}H NMR spectrum of compound **117** ($CDCl_3$, 500 MHz)

The ^{13}CNMR spectrum (figure 5) of the same compound, taken in $CDCl_3$, shows, in particular, a signal at 13.69 ppm due to the methyl group of the carbon chain, signals at 19.46, 30.10, 40.14 and 47.04 ppm corresponding to the three CH_2 groups of the carbon chain, and a signal at 165.84 ppm attributed to the lactam group C=O.

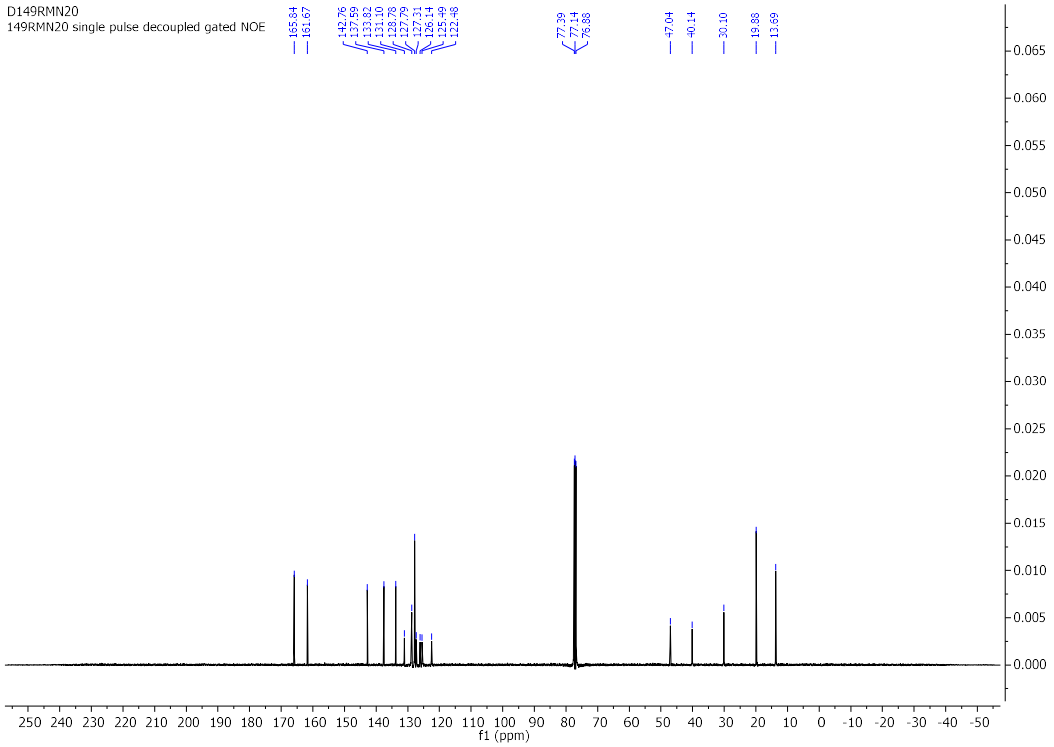

Figure 5:^{13}C NMR spectrum of compound **117** ($CDCL_3$, 125MHz)

The mass spectrum (ESI) (figure 6) shows a peak for the protonated molecular ion $[M + H]^+$ at m/z= 293.16.

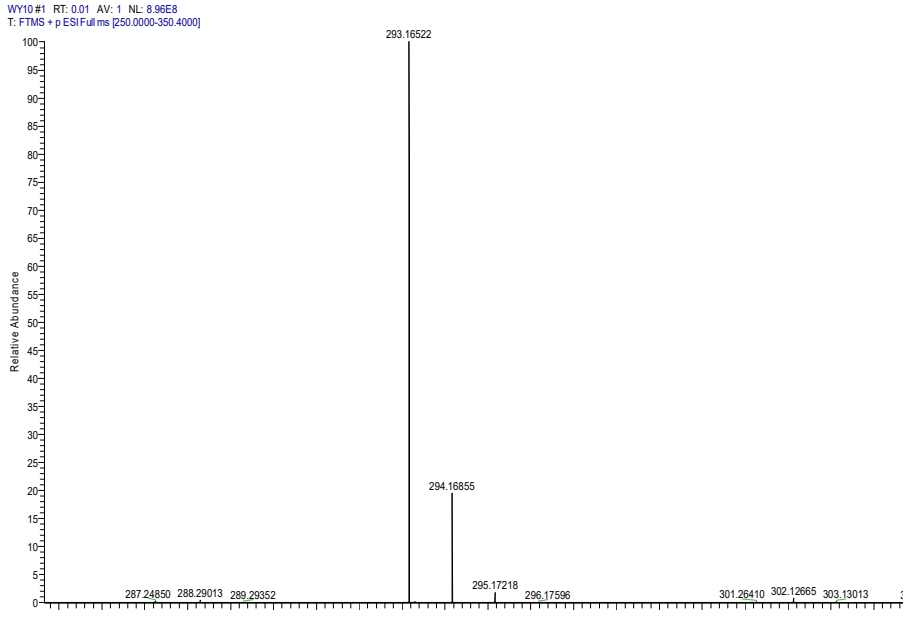

Figure 6: Mass spectrometry (ESI) of the compound **117**

Figure 7 shows the infrared spectrum of compound **117**. A fine band of the C=O group was observed at about 1707 cm^{-1}, the CH_2 groups of the long chain appeared at about 2856 and 2973 cm^{-1}.

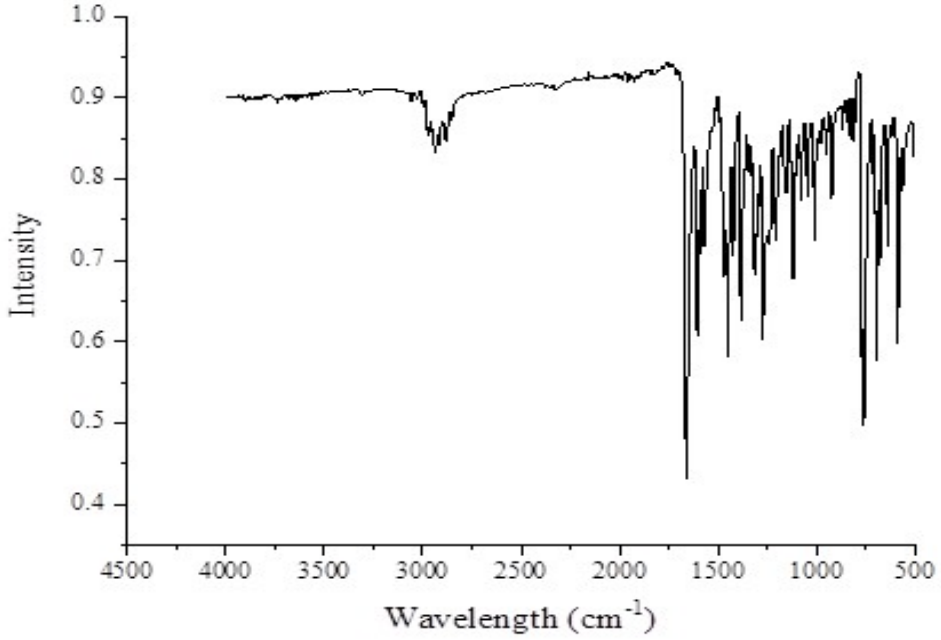

Figure 7: IR spectrum of the compound **117**

III.2.2. Crystallographic study of the compound 117

The crystal used for the crystallographic study was obtained by evaporating the solution of the compound in ethanol at room temperature. They are in the form of colorless needles.

X-ray diffraction analysis of a single crystal allowed us to determine the complete structure of this benzodiazepine derivative. It crystallizes in the orthorhombic system. The determination and refinement of the structure were conducted in the Orthorhombic, Pbca

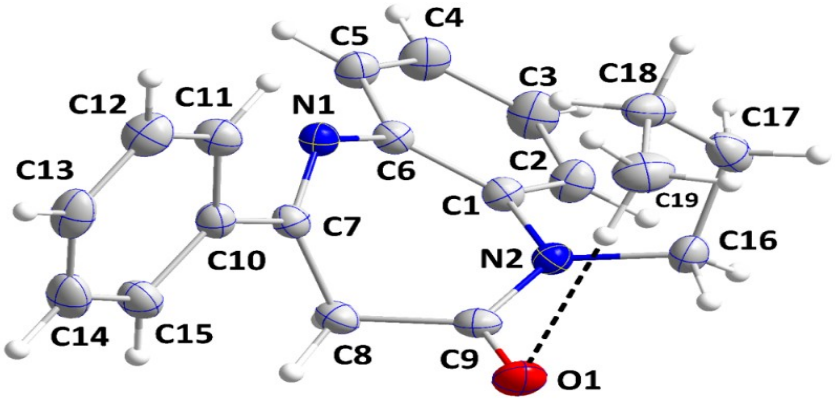

Figure 8: ORTEP of compound **117** with atom numbering

In molecule **117** the 7-membered ring adopts a flattened boat conformation, and the orientation of the butyl group is partially determined by an intermolecular C—H···O

hydrogen bond. In this crystal, C—H···O hydrogen bonds form inversion dimers which are connected into layers by additional C—H···O hydrogen bonds with the layers linked by C—H···π (ring) interactions.

The details of the crystal data and structure refinement are given in **table 1**.

Table 1: Crystal data and structure refinement details

Chemical formula	$C_{19}H_{20}N_2O$
Mr	292.37 g/mol
Crystal system, space group	Orthorhombic, Pbca
Temperature (K)	170
a, b, c (Å)	16.1382 (3), 10.5138 (2), 18.4153 (4)
V ($Å^3$)	3124.59 (11)
Z	8
Radiation type	Mo Kα
Crystal size (mm)	0.218 x 0.242 x 0.410 mm
Data collection	
Diffractometer	Bruker D8 QUEST PHOTON 3 diffractometer
Absorption correction	Numerical
Tmax, Tmin	0.9830 and 0.9690
Reflections collected	148742
Independent reflections	4758 [R(int) = 0.0490]
Refinement	
R[F2 > 2σ(F2)], wR(F2), S	0.041, 0.118, 1.04
R.M.S. deviation from mean	0.040 $eÅ^{-3}$
Data / restraints / parameters	4758 / 0 / 200

III.2.3. Spectral characterization of the compound 118:

The ^1H NMR spectrum (figure 9) of compound, taken in ($CDCl_3$ 500MHz), shows in particular, a triplet at 0.73 ppm corresponding to the CH_3 of the aliphatic chain, a multiplet between 1.08- 1.50 ppm attributable to the CH_2 protons of the aliphatic chain.

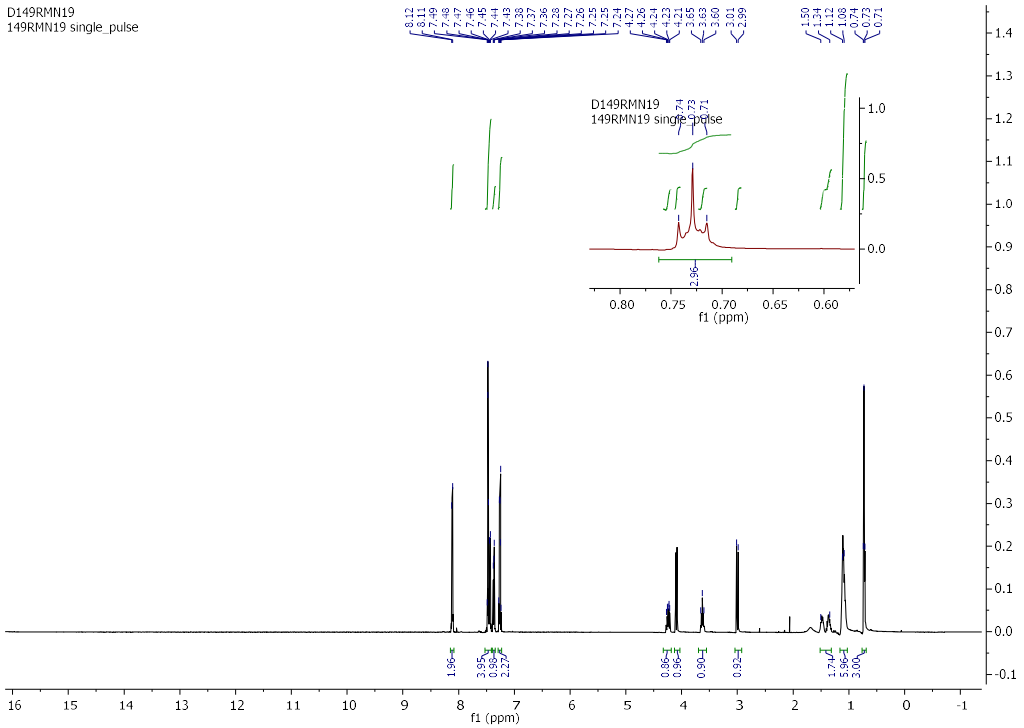

Figure 9: ^{1}H NMR spectrum of compound **118** ($CDCL_3$, 500 MHz)

The ^{13}C NMR spectrum taken in $CDCl_3$ of product **118** is shown in figure 10. The analysis of the spectral data shows the signals of 6 carbons of the long chain from the 13.92 ppm up to 40.11 ppm. signal of the CH_2 carbon of diazepine around 47.21 ppm. The signal from the lactamic C=O group appeared at about 165.96 ppm.

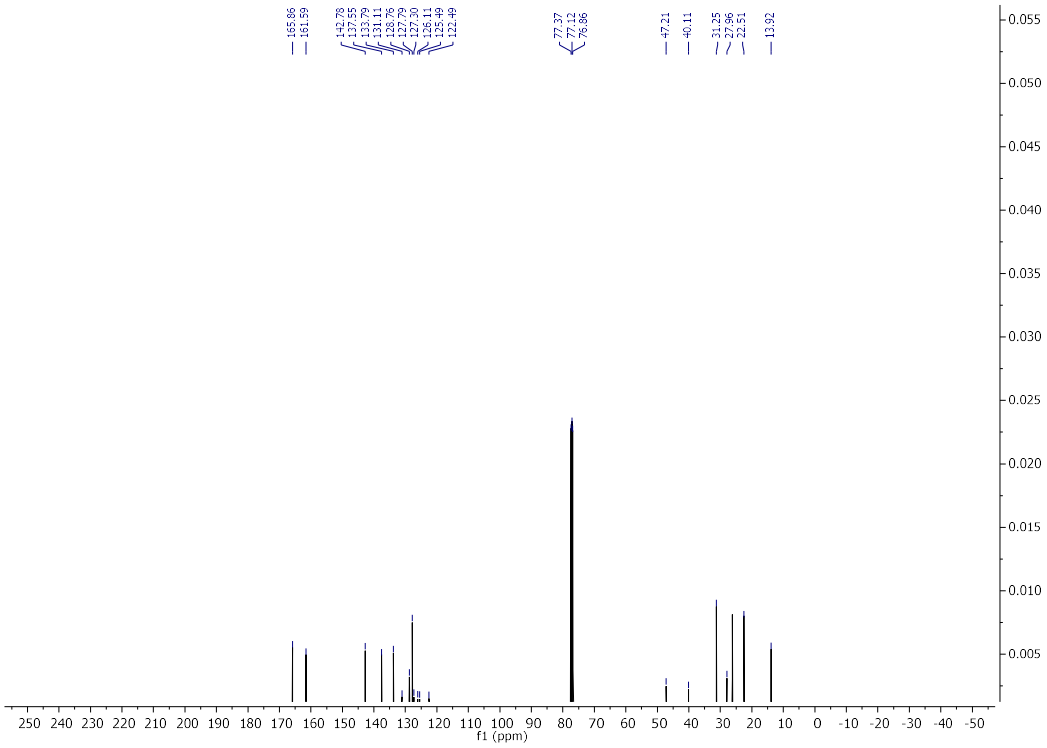

Figure 10:^{13}C NMR spectrum of compound **118** ($CDCL_3$, 125 MHz)

The mass spectrum (ESI) figure 11 shows a peak related to the protonated molecular ion $[M + H]^+$ at m/z= 321.19 confirming the proposed structure.

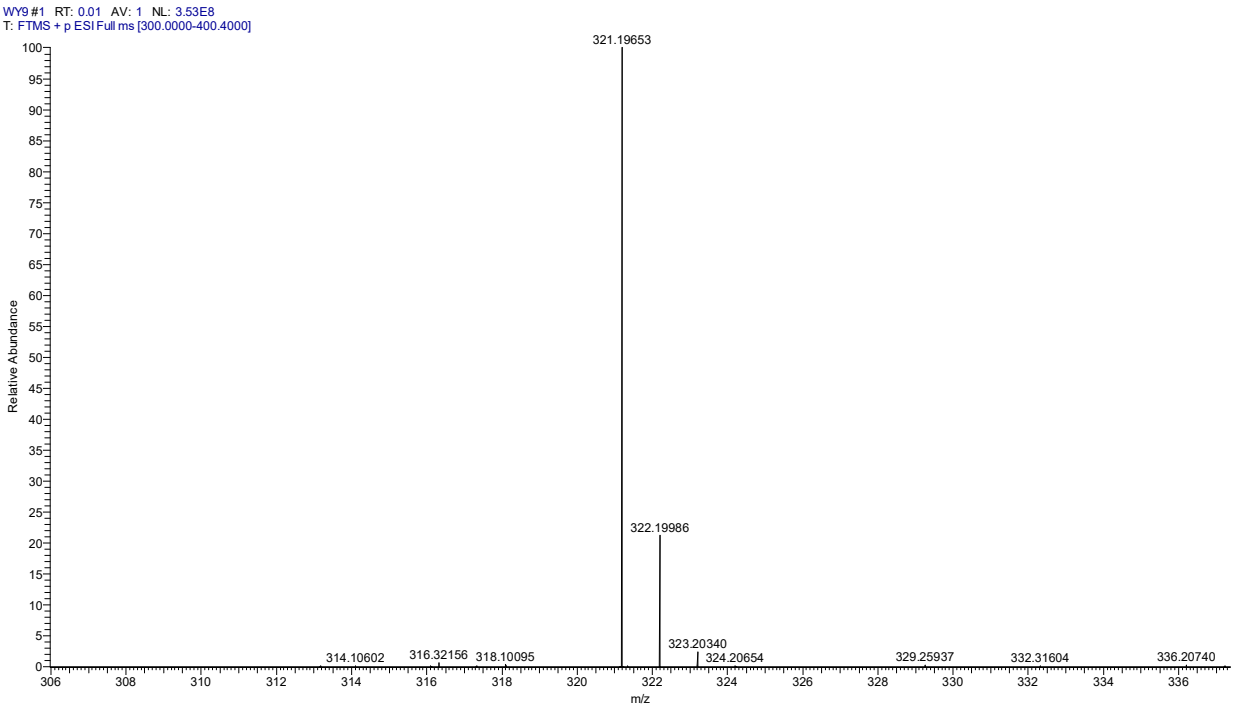

Figure 11: Mass spectrum (ESI) of the compound **118**

IR spectrum figure 12 taken directly without potassium bromide showed an absorption band at 1675 cm^{-1} due to the presence of the carbonyl function. The CH_2 groups of the long carbon chain appeared at 2856 and 2973 cm^{-1}.

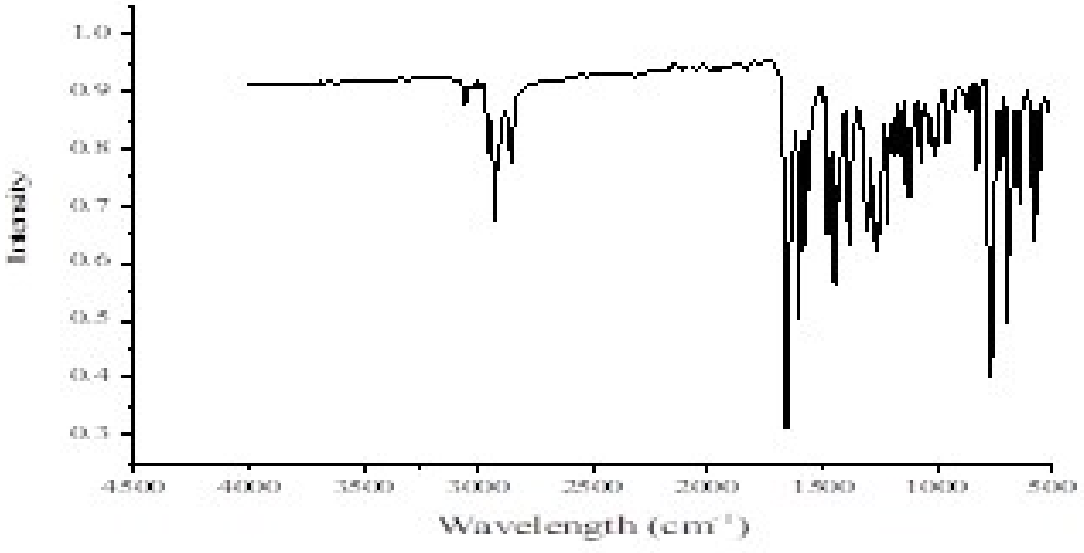

Figure 12: IR spectrum of the compound **118**

III.2.4. Crystallographic study of the compound 118

The crystal used for the crystallographic study was obtained by evaporating the solution of the compound in ethanol at room temperature.

They are in the form of colorless needles.X-ray diffraction analysis of a single crystal allowed us to determine the complete structure of this benzodiazepine derivative. It crystallizes in the monoclinic system.

The determination and refinement of the structure were conducted in the Monoclinic, $P2_1/n$.

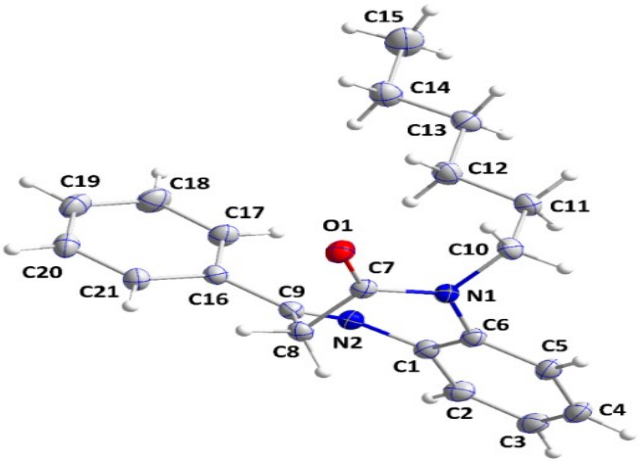

Figure 13: ORTEP of compound **118** with atom numbering

In molecule **118** ($C_{21}H_{24}N_2O$), the 7-membered ring adopts a boat conformation. In the crystal, C—H···O hydrogen bonds and C —H···π (ring) interactions form corrugated sheets of molecules parallel to (101), which pack with interdigitation of the hexyl groups.

The details of the crystal data and structure refinement are given in **table 2.**

Table 2: Crystallographic data of compound **118**

Chemical formula	$C_{21}H_{24}N_2O$
Mr	320.42 g/mol
Crystal system, space group	Monoclinic, $P2_1/n$
Temperature (K)	150
a, b, c (Å)	14.0633 (14), 8.8298 (9), 14.1479 (15)
β (°)	91.259 (4)
V (Å^3)	1756.4 (3)
Z	4
Radiation type	Mo Kα
Crystal size (mm)	0.220 x 0.387 x 0.390 mm
Data collection	
Diffractometer	Bruker D8 QUEST PHOTON 3 diffractometer
Absorption correction	Numerical
Tmax, Tmin	0.9840 and 0.9710
independent reflections	5324 [R(int) = 0.0357]
Reflections collected	71412
Refinement	
Data / restraints / parameters	5324 / 0 / 218
R.M.S. deviation from mean	0.041 eÅ^{-3}

III.2.5. Spectral characterization of the compound 115

The ^{1}H NMR spectrum figure 14 of compound **115** taken in ($CDCl_3$ 500MHz); presents in particular a triplet at 0.86 ppm corresponding to the CH_3 of the aliphatic chain, a multiplet between 1.04 -1.38 ppm attributable to the protons of the CH_2 of the aliphatic chain.

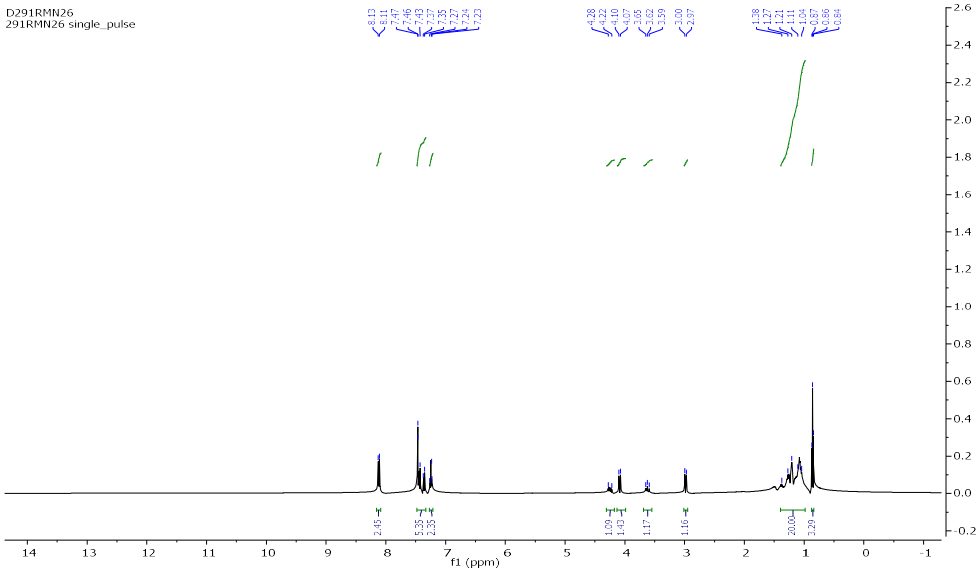

Figure 14 .^{1}H NMR spectrums of compound **115** ($CDCL_3$, 500 MHz)

The examination of the spectrum of carbon 13 and the use of techniques known as DEPT-135 (figures 15 and 16) of compound **115**, allowed us to assign practically and without ambiguity all the signals to the corresponding carbons.

The DEPT spectrum of compound **115** shows the existence of 11 signals between 20.08 and 40.08 ppm attributed respectively to CH_2 groups and a signal at 47.15 ppm of the methylene group of diazepine ring.

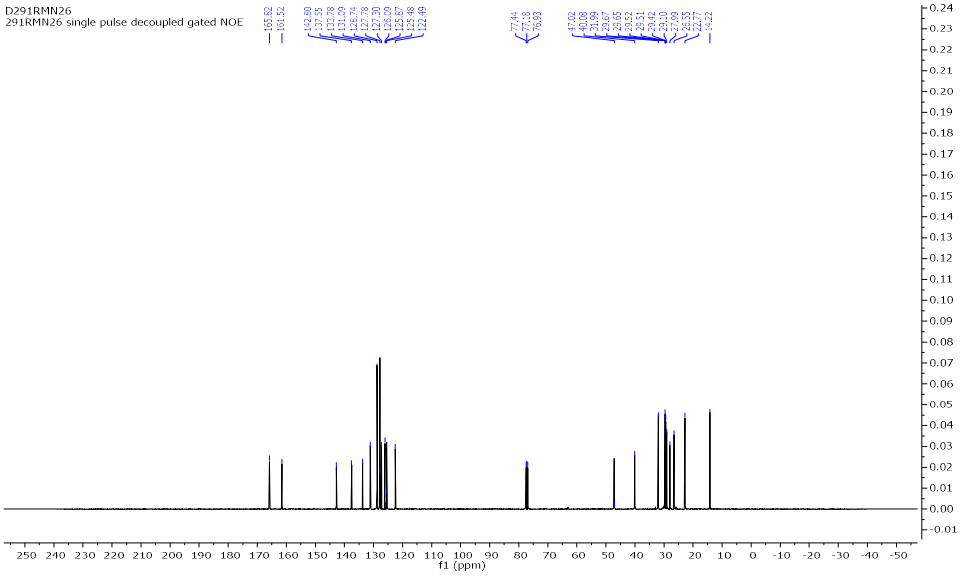

Figure 15:^{13}C NMR spectrum of compound **115** ($CDCL_3$, 125 MHz)

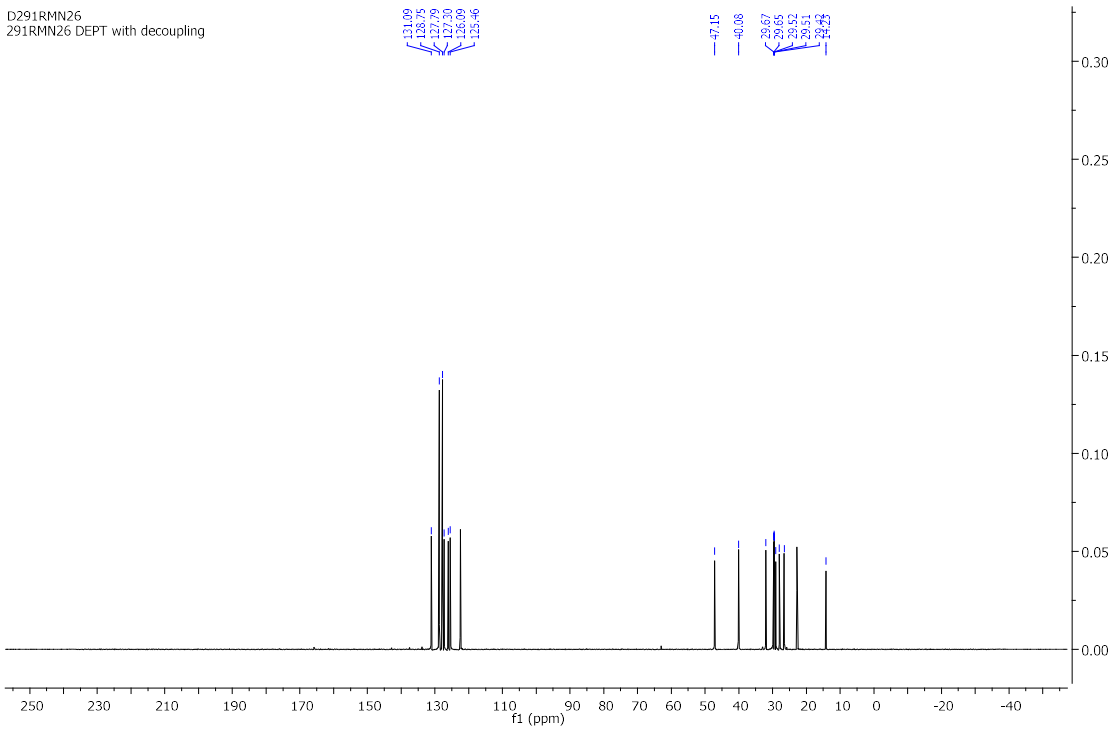

Figure 16: DEPT-90 NMR spectrum of compound **115** ($CDCl_3$, 125MHz)

IV- Action of benzyl chloride:

The action of benzyl chloride **122** on 4-phenyl-1,5-benzodiazepin-2-one **58** in DMF for 24 hours at a temperature of 60 °C under the conditions of phase transfer catalysis (PTC) using (TBAB) as a catalyst and K_2CO_3 as a base, allows the alkylation of the amide nitrogen and subsequently leads to the formation of the product **79** in good yield (Scheme 45).

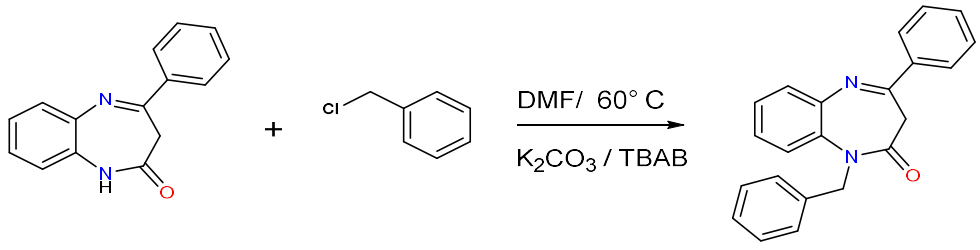

58 **122** **79**

- Scheme 45 -

The structure of compound **79** has been identified by a physical comparison of a sample already prepared in our laboratory [47].

V- Sulfurization reaction:

The literature reports several works on the thionation of benzodiazepines. This reaction can be carried out in acetonitrile as well as in pyridine. After synthesizing N-alkyl-4-phenyl-1,5-benzodiazepin-2-one **113-121 and 79**, these are treated with phosphorus pentasulfide

(P_2S_5) under pyridine reflux for 4 hours, allowing us to access the products **123-132** with good yields (Scheme 46)

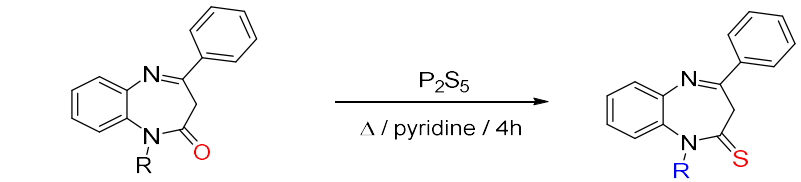

113: R= $(CH_2)_7CH_3$
114 : R= $(CH_2)_9CH_3$
115: R= $(CH_2)_{11}CH_3$
116 : R= $(CH_2)CH_3$
117 : R= $(CH_2)_3CH_3$
118 : R= $(CH_2)_5CH_3$
119: R= $(CH_2)_{13}CH_3$
120 : R= $(CH_2)_{15}CH_3$
121 : R= $(CH_2)_{17}CH_3$
79 : R= CH_2-Ph
123 : R= $(CH_2)CH_3$
124 : R= $(CH_2)_3CH_3$
125 : R= $(CH_2)_5CH_3$
126 : R= $(CH_2)_7CH_3$
127 : R= $(CH_2)_9CH_3$
128: R= $(CH_2)_{11}CH_3$
129 : R= $(CH_2)_{13}CH_3$
130 : R= $(CH_2)_{15}CH_3$
131: R= $(CH_2)_{17}CH_3$
132: R= CH_2-Ph

- Scheme 46

All the structures of the isolated products have been confirmed by spectral data of ^1H, ^{13}C NMR, and mass spectrometry. The overall results of the ^1H, ^{13}C NMR Spectrum of **123-132** products are reported in tables 3 and 4.

Table 3: ^1H NMR spectral data of compounds 124-131.

Products	N-CH_2	-(CH_2)n	CH_3	$H_{Aromatic}$
124	4.80 (t, 2H, NCH_2)	1.12-1.63 (m, 4H, CH_2)	0.79 (t, 3H, CH_3)	7.24-8.30 (m, 9H, H_{ar}).
126	4.88 (t, 2H, NCH_2)	1.12-1.65 (m, 12H, CH_2)	0.81 (t, 3H, CH_3)	7.23-8.34 (m, 9H, H_{ar}).
127	4.81(t, 2H, NCH_2)	1.18-1.72 (m,16H, CH_2)	0.90 (t, 3H, CH_3)	7.29-8.40 (m, 9H, H_{ar}).
128	4.82(t, 2H, NCH_2))	1.14-1.63(m, 20H, CH_2)	0.87 (t, 3H, CH_3)	7.23-8.35 (m, 9H, H_{ar}).
129	4.91(t, 2H, NCH_2)	1.18-1.64 (m,24H, CH_2)	0.91 (t, 3H, CH_3)	7.28-8.39 (m, 9H, H_{ar}).
130	4.92 (t, 2H, NCH_2)	1.13-1.60 (m,28H, CH_2)	0.88 (t, 3H, CH_3)	7.29-8.35 (m, 9H, H_{ar}).
131	4.85 (t, 2H, NCH_2)	1.17-1.63(m,32HCH_2)	0.89 (t, 3H, CH_3)	7.27-8.39 (m, 9H, H_{ar}).

Table 4: ^{13}C NMR spectral data of compounds 124-131

Products	C=S	N-CH_2	-(CH_2)n	$CH_{Aromatic}$
124	194.10	55.10	19.90-48.73	122.43-131.42
126	194.12	55.24	22.53-48.74	122.39-131.42
127	194.07	55.14	22.60 -48.63	122.35-131.32
128	194.08	55.27	22.70- 48.64	12235-131.33
129	193.86	55.35	22.87- 48.65	122.35-131.33
130	193.03	55.21	22.73- 48.64	122.36-131.36
131	194.04	55.21	22.73- 48.64	122.36-131.36

V.1. Spectral characterization of the compound <u>127</u>:

The ^{1}H NMR spectrum taken in $CDCl_3$ of compound **<u>127</u>** figure 17 highlights in particular; a triplet at (0.88-0.90) ppm, characteristic of the methyl group of the C10 carbon chain, two multiplet between (1.18-1.69) ppm due to the protons of the CH_2 groups of the chain, a triplet at 3.35ppm of the CH_2 of the chain linked to the nitrogen a poorly resolved AB system at 4.06 ppm due to the diazepinic CH_2.

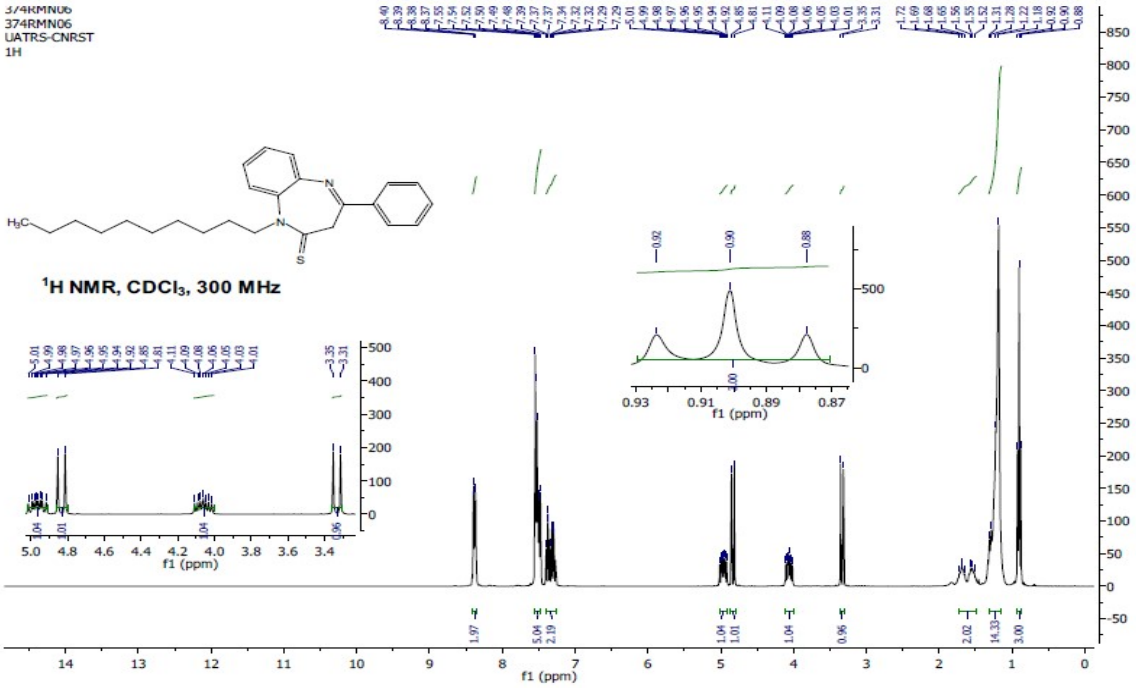

Figure 17 ^{1}H NMR spectrum of product **<u>127</u>** ($CDCl_3$, 300 MHz)

The ^{13}C NMR spectrum taken in $CDCl_3$ of product **<u>127</u>** is shown in figure 17, the analysis of the spectral data shows the first signal at 14.13 due to the CH_3 group, followed by the signals of three carbons of the long-chain from 22.60 ppm to 48.63 ppm, and the signal at 55.14 ppm of CH_2 carbons of diazepine ring at position 3. Finally, the signal from the C=S group appeared at 194.07 ppm.

The DEPT-135 spectrum further confirms the proposed structure since we observe, depending on the technique adopted, the inversion of the signals of the methylene carbons of the chain figure 19.

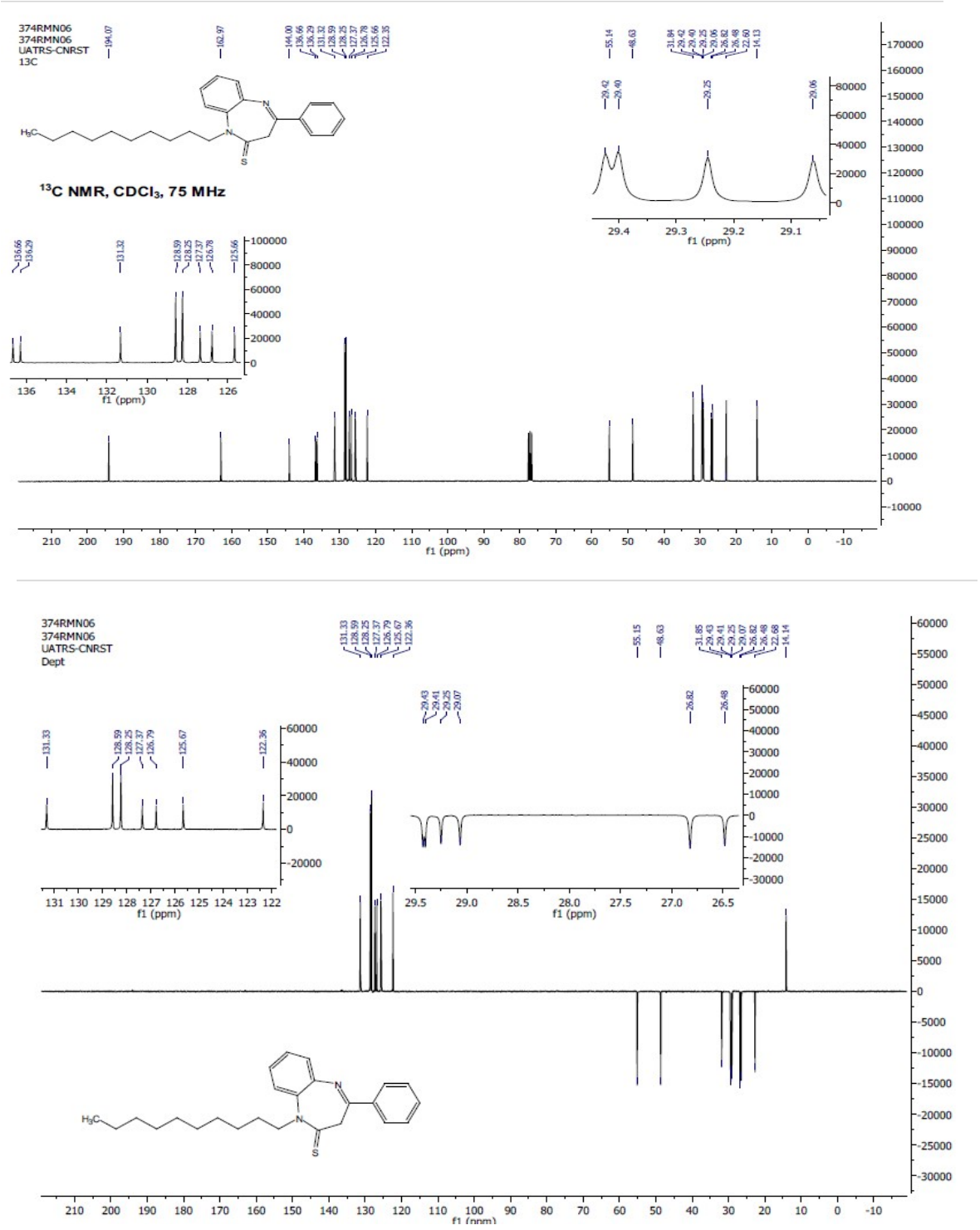

Figure 19: DEPT-135 spectrum of compound **127** ($CDCl_3$, 75 MHz)

The analysis of the mass spectrum (figure 20) using ESI as ionization technique highlights the presence of the peak related to the protonated molecular ion (MH^+ = 392.23), thus confirming the proposed structure.

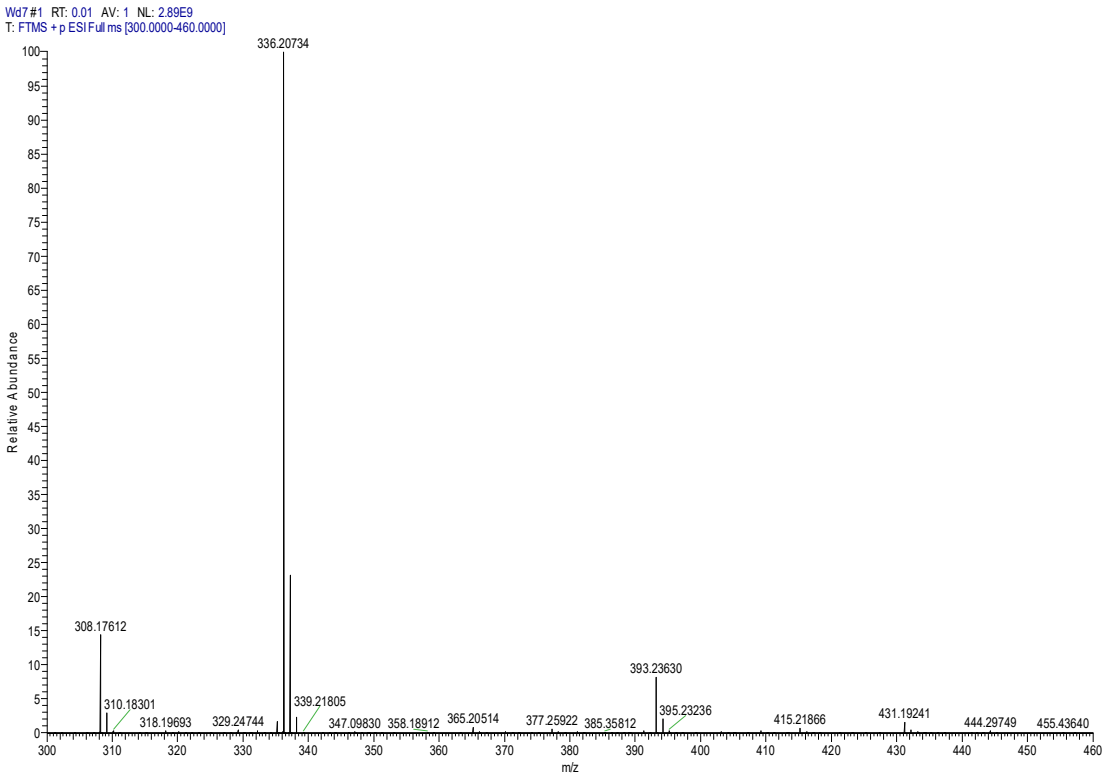

Figure 20: Mass spectrometry (ESI) of the compound **127**

Conclusion:

In this chapter, this work focused on studying the alkylation of the 4-phenyl-1,5-benzodiazepin-2-one by various alkylating reagents such as long-chain bromoalkanes, benzyl chloride through liquid-solid phase transfer catalysis conditions, in the presence of potassium carbonate, and tetrabutylammoium bromide (TBAB), N,N-dimethylformamide as solvent was used, allowing access to new heterocyclic compounds with a good yield. Furthermore, 1,5-benzodaizepine-2-thione obtained after sulfurization of N-alkyl-4-phenyl-1,5-benzodiazepin-2-one can be used as a precursor for the synthesis of other heterocyclic via condensation reactions with hydroxylamine hydrochloride. All the synthesized compounds were identified based on the spectral data of ^{1}H, ^{13}C NMR and were confirmed for certain compounds by a crystallography study.

Experimental part

I- Chemical analysis:

The melting point was set using open capillary tubes, and the result was uncorrected. The ^{1}H and ^{13}C NMR data were obtained at 300 and 500 MHz using $CDCl_3$ as the solvent and tetramethylsilane (TMS) as an internal standard. The chemical shifts are reported in ppm, while the downfield coupling constants (J) are in Hz. The following abbreviations are used to describe peak patterns, where appropriate: s, pointing to a singlet; d, pointing to a doublet; dd, pointing to a double doublet; t, pointing to a triplet; q, pointing to a quartet; dt, pointing to a double triplet; m, pointing to a multiplet.

II- Preparation of 4-phenyl-1,5-benzodiazepin-2-one:

In a 250 ml flask containing 100 ml of xylene, 10g (0.092mol) of *o*-phenylenediamine was poured; then 20 ml (0.0919mol) of ethyl benzoyl-acetate was added and refluxed for 1 to 3 hours. The reaction was followed to completion and left at room temperature for 24 hours. The precipitate was washed with xylene, collected, and re-crystallized from ethanol to give a pale yellow powder.

4-phenyl-1,5-benzodiazepin-2-one: 58

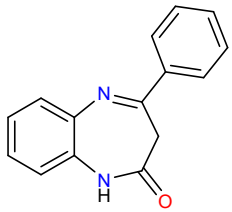

[M= 236.09 g/mol]

Yield = 73%**; F (°C)** = 198-200

^{1}H NMR (300MHz, $CDCl_3$) δ ppm: 3.40 (s, 2H, CH_2), 7.20-7.90 (m, 9H, H ar), 9, 37 (1H, s, NH).**^{13}CNMR (75 MHz, $CDCl_3$) δ ppm**: 39.79 (CH_2); 129.14-121.82 (CHar); 158.64 (C=N); 167.80 (C=O).

Mass spectrum (EI): m/z = 236.23

III- Preparation N-alkyl of 4-phenyl-1,5-benzodiazepin-2-one with alkyl halides.

Alkylation procedures:

In a 250 ml flask containing 100 ml of a solution of 0.02 mol of 4-phenyl-1,5-benzodiazepin-2-one in 60 ml of dimethylformamide, 0.04 mol of an alkylating agent, 0.04 mol of K_2CO_3, and 0.001 mol of tetra-butylammonium bromide were added. Dimethylformamide was filtered and evaporated under reduced pressure. Then, the resulting product was purified by chromatography on a silica column (eluent: ethyl acetate/hexane 10:90).

1-ethyl-4-phenyl-1,5-benzodiazepin-2-one [81]: 116

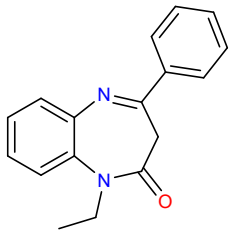

[M= 264.13 g/mol]

Yield = 73%, **F(°C)** = 93-95

1-butyl-4-phenyl-1.5-benzodiazepin-2-one 117

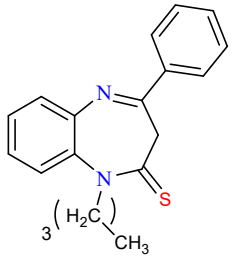

[M= 293.16 g/mol]

Yield = 90%; **F (°C)** = 70-72

^{1}H NMR (500 MHz, $CDCl_3$) δ ppm: 0.76 (t, 3H, CH_3), 1.08-1.50 (m, 4H, CH_2), 3.62 (t, 2H, NCH_2), 4.08-4.10 (q, 2H, CH_2-CO), 7.25-8.12 (m, 9H, CHar).

^{13}C NMR (125 MHz, $CDCl_3$) δ ppm: 13.69 (CH_3), 19.46 (CH_2), 30.10 (CH_2), 40.14 (CH_2), 47.04 (CH_2), 122.47-131.10 (CHar), 161.67 (CN).165.84 (C=O).

Mass spectrum (ESI): m/z = 293.17 $[M + H]^+$

1-hexyl-4-phenyl-1.5-benzodiazepin-2-one 118

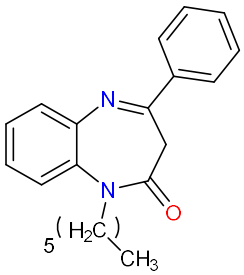

[M= 320.19 g/mol]

Yield = 85 %; **F (°C)** = 75-77

^{1}H NMR (500 MHz, $CDCl_3$) δ ppm: 0.73 (t, 3H, CH_3), 1.08-1.50 (m, 8H, CH_2), 3.01 (t, 2H, NCH_2), 4.24-4.26 (q, 2H, CH_2-CO), 7.25-8.12 (m, 9H, CHar).

^{13}C NMR (125 MHz, $CDCl_3$) δ ppm: 13.92 (CH_3), 22.47 (CH_2), 26.22 (CH_2), 27.96 (CH_2), 31.25 (CH_2), 40.11 (CH_2), 47.21 (CH_2), 122.49-131.10 (CHar), 161.59 (CN).165.96 (C=O).

Mass spectrum (ESI): m/z: 321.19 $[M + H]^+$

1-decyl-4-phenyl-1.5-benzodiazepin-2-one [91 114

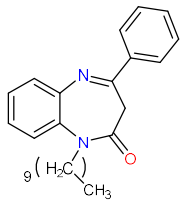

[M= 376.25 g/mol]

Yield = 82 %**; Oil**, yellow

1-dodecyl-4-phenyl-1.5-benzodiazepin-2-one [91 115

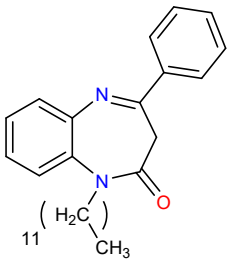

[M= 404.28 g/mol]

Yield = 75 %**; Oil**, yellow

1-octadecyl-4-phenyl-1.5-benzodiazepin-2-one 121

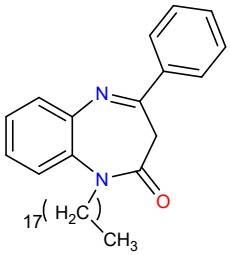

[M= 488.38 g/mol]

Yield = 67%**; Oil**, pale yellow

^{1}H NMR (300 MHz, $CDCl_3$) δ ppm: 0.81 (t, 3H, CH_3), 1.03-1.57 (m, 32H, CH_2), 3.61 (t, 2H, NCH_2), 4.14-4.23 (q, 2H, CH_2-CO), 7.19-8.07 (m, 9H, CHar).

^{13}C NMR (75 MHz, $CDCl_3$) δ ppm: 14.16 (CH_3), 22.73-47.12 (CH_2), 122.44-131.05(CHar), 161.53 (C=N), 165.80 (C=O).

1-benzyl-4-phenyl-1,5-benzodiazepin-2-one [81] 79

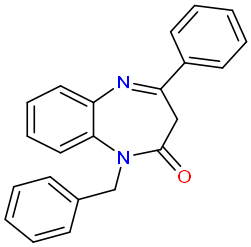

[M= 326.14 g/mol]

Yield = 83%**; F (°C)** = 128-130

IV-Preparation of alkyl of 4-phenyl-1,5-benzodiazepine-2-thione (123-132):

Thionation procedures in general:

To a solution of 1-alkyl of 4-phenyl-1,5-benzodiazepin-2-one (0.02 mmol), phosphorus pentasulfide (0.03 mol) was added to 20 ml of pyridine. The mixture refluxed for 72 hours, after which the solvent evaporated under reduced pressure. The precipitate formed was washed with hot water. The result obtained was crystallized from ethanol to afford a compound in the form of crystals.

1-ethyl-4-phenyl-1,5-benzodiazepine-2-thione [92] **123**

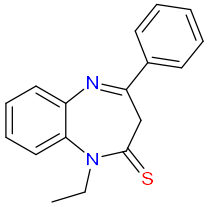

[M= 280.140 g/mol]

Yield = 81%; **F (°C)** = 72-74

1-butyl-4-phenyl-1.5-benzodiazepine-2-thione: 124

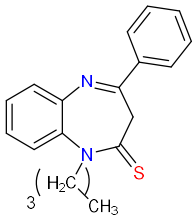

[M= 308.14 g/mol]

Yield = 92%; **F (°C)** = 85-87

^{1}H NMR (500 MHz, $CDCl_3$) δ ppm: 0.79 (t, 3H, CH_3), 1.12-1.63 (m, 4H, CH_2), 3.28-3.31 (q, 2H, -CH_2-C=S), 4.80 (t, 2H, NCH_2), 7.24-8.34 (m, 9H, CH ar).

^{13}C NMR (125 MHz, $CDCl_3$) δ ppm: 13.73 (CH_3), 19.90(CH_2), 28.93(CH_2), 48.73(CH_2), 55.10(CH_2), 122-131.42 (CH_{ar}), 163.16 (CN), 194.10 (C=S).

Mass spectrum (ESI): m/z: 309.14

1-octyl-4-phenyl-1.5-benzodiazepine-2-thione: 126

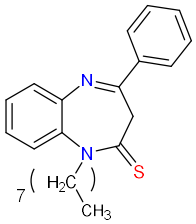

[M= 364.20 g/mol]

Yield = 83%, Oil, yellow

^{1}H NMR (500 MHz, $CDCl_3$) δ ppm: 0.81 (t, 3H, CH_3), 1.12-1.65 (m, 12H, CH_2), 3.28-3.30 (q, 2H, -CH_2-C=S), 4.78(t, 2H, NCH_2), 7.23-8.34 (m, 9H, CHar).

^{13}C NMR (125 MHz, $CDCl_3$) δ ppm: 13.90 (CH_3), 22.53-55.24(CH_2), 122.39 -131.42 (CH_{ar}), 162.89 (CN), 194.12 (C=S).

Mass spectrum (ESI): m/z: 365.20

1-decyl-4-phenyl-1.5-benzodiazepine-2-thione: 127

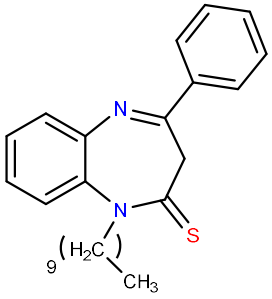

[M= 392.23 g/mol]

Yield = 77%**,** Oil, yellow

^{1}H NMR (300 MHz, $CDCl_3$) δ ppm: 0.90 (t, 3H, CH_3), 1.18-1.72 (m, 16H, CH_2), 3.31-3.35 (q, 2H, -CH_2-C=S), 4.81 (t, 2H, NCH_2), 7.29-8.40 (m, 9H, CH ar).

^{13}C NMR (75 MHz, $CDCl_3$) δ ppm: 14.13 (CH_3). 22.60-55.14 (CH_2), 122.35-131.32 (CH_{ar}), 162.97 (CN), 194.07 (C=S).

Mass spectrum (ESI): m/z = 393.23

1-dodecyl-4-phenyl-1.5-benzodiazepine-2-thione: 128

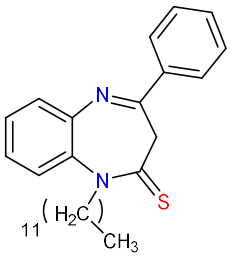

[M= 420.26 g/mol]

Yield = 88%**; F (°C)** = 85 -87

^{1}H NMR (300 MHz, $CDCl_3$) δ ppm: 0.87(t, 3H, CH_3), 1.14-1.63 (m, 20H, CH_2), 3.28-3.32 (q, 2H, CH_2-C=S), 4.82 (t, 2H, NCH_2), 7.23-8.35 (m, 9H, CHar).

^{13}C NMR (75 MHz, $CDCl_3$) δ ppm: 14.13 (CH_3). 22.70-55.27 (CH_2), 122.35-131.33 (CH_{ar}), 163.01 (CN), 194.08 (C=S).

Mass spectrum (ESI): m/z: 421.26

1-tetradecyl-4-phenyl-1.5-benzodiazepin-2-thione: 129

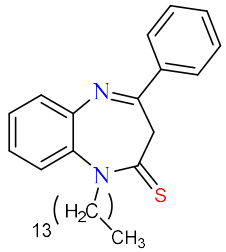

[M= 447.28 g/mol]

Yield = 82%**,** Oil, yellow

^{1}H NMR (300 MHz, $CDCl_3$) δ ppm: 0.91 (t, 3H, CH_3), 1.18-1.64(m, 24H, CH_2), 3.32-3.36 (q, 2H, NCH_2), 4.91 (t, 2H, NCH_2), 7.28-8.39 (m, 9H, CH_{ar}).

^{13}C NMR (75 MHz, $CDCl_3$) δ ppm: 14.26 (CH_3). 22.87-55.35 (CH_2), 122.35-131.33 (CH_{ar}), 163.23 (CN), 193.86 (C=S).

1-hexadecyl-4-phenyl-1.5-benzodiazepine-2-thione: 130

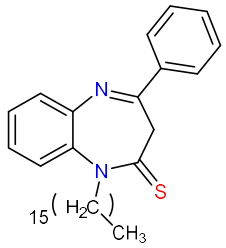

[M= 476.32 g/mol]

Yield = 90%**; F (°C)** = 75-77

^{1}H NMR (300 MHz, $CDCl_3$) δ ppm: 0.88 (t, 3H, CH_3), 1.13-1.60 (m, 28H, CH_2), 3.29-3.99 (q, 2H, NCH_2), 4.92 (t, 2H, NCH_2), 7.27-8.35 (m, 9H, CHar).

^{13}C NMR (75 MHz, $CDCl_3$) δ ppm: 14.17 (CH_3). 22.73-55.21 (CH_2), 122.36-131.36 (CH_{ar}), 163.23 (CN), 194.04 (C=S).

1-octadecyl-4-phenyl-1.5-benzodiazepine-2-thione 131

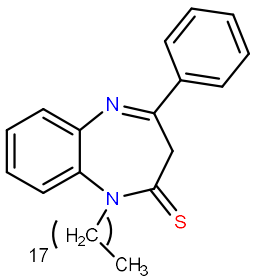

[M= 504.35 g/mol]

Yield = 87%**; F (°C)** = 68-70

^{1}H NMR (300 MHz, $CDCl_3$) δ ppm: 0.89 (t, 3H, CH_3); 1.17-1.63(m, 32H, CH_2), 3.32-3.36 (q, 2H, NCH_2), 4.85 (t, 2H, NCH2), 7.27-8.39 (m, 9H, CHar).

^{13}C NMR (75 MHz, $CDCl_3$) δ ppm: 14.17 (CH_3). 22.73-55.21 (CH_2), 122.36-131.36 (CH_{ar}), 163.23 (CN), 194.03 (C=S).

1-benzyl-4-phenyl-1,5-benzodiazepine-2-thione [93] 132

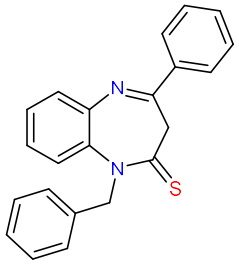

[M= 342.12 g/mol]

Yield = 87%**; F (°C)** = 126-128

Chapter III:

Novel pathways for the synthesis of benzimidazole derivatives from 4-phenyl-N alkyl-1,5-benzodiazepin-2-thiones

I-Introduction

Benzimidazole derivatives constitute a class of compounds of remarkable biological interest. They are known for their interesting and varied pharmacological activities. They are used as antimicrobial [94], antifungal activity against [95], anticancer [96], antiviral [97], and anticonvulsant activity agents [98].

For these different reasons, we are interested in the development of new heterocyclic compounds derived from benzimidazole by the rearrangement of 4-phenyl-1,5-benzodiazepine-2-thiones in the presence of hydroxylamine hydrochloride acting as a bi-nucleophilic reagent.

II- Synthesis of benzimidazole

A review of the literature shows that benzimidazole derivatives have been prepared using different synthesis methods:

II. 1. From *o*-phenylenediamine and its derivatives

Phillips *et al*. [99] studied the condensation reaction of *o*- phenylenediamine **3** with carboxylic acid **133** in hydrochloric acid (4N). They obtained the 2-alkylbenzimidazoles **134** (scheme47)

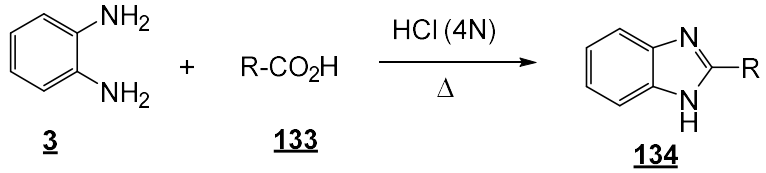

3 **133** **134**

- Scheme 47-

Alam *et al.*[100] reported the synthesis of new 2-substituted benzimidazole **136** derivatives in good yield by refluxing an equimolar ratio of *o*-phenylenediamine **3** and *p*-aminobenzoic acid **135** in xylene and polyphosphoric acid (PPA) for 6 h (Scheme48).

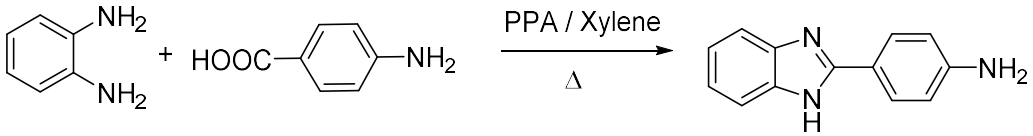

3 **135** **136**

- Scheme 48 -

In our laboratory, Lamkaddem [101] using the same operating conditions as Phillips studied the action of *o*-phenylenediamine **3** with malonic acid **137** in hydrochloric acid at reflux for 2h30 and isolated a 1,5-benzodiazepine compound **138** next to benzimidazole **139** (Scheme 49).

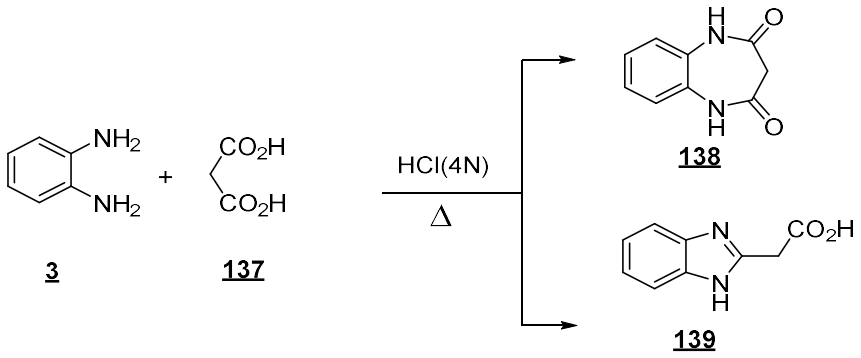

- Scheme 49 -

Bahrami *et al.*[102] synthesized a series of substituted benzimidazoles **141**, by condensing the 4-substituted derivatives of *o*-phenylenediamine **3** with the aromatic aldehydes **140** in the presence of H_2O_2 and HCl in acetonitrile. The reaction proceeds rapidly at room temperature and provides the products **141** in good yields (Scheme 50).

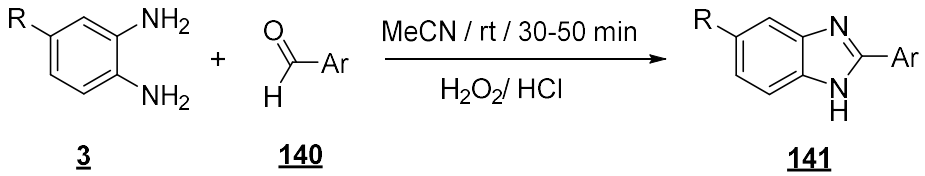

- Scheme 50 -

II. 2. From benzodiazepine derivatives

The 1,5-benzodiazepin-2-one derivatives are excellent precursors of various heterocyclic systems such as isoxazole, pyrazole, and benzimidazole. Indeed, these compounds having several reactive centers undergo rearrangements under the influence of bi-nucleophilic agents (hydrazine, hydroxylamine) to lead to products of smaller size, such as benzimidazoles.

Thus, Israel *et al.*[103] have shown that 4-methyl-1,5-benzodiazepine **63** is thermally transposed to α-methylvinylbenzimidazole **142** according to a 1,3-sigmatropic rearrangement (Scheme 51).

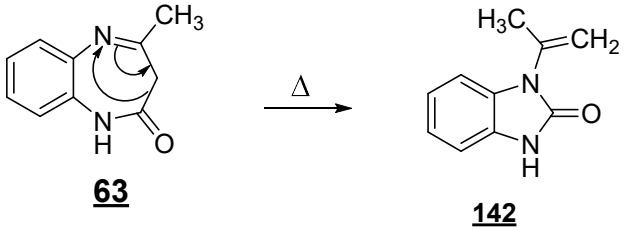

- Scheme 51 -

The action of hydrazine hydrate on 4-phenyl-1,5-benzodiazepine-2-thione-**143** leads to 5-(*o*-aminophenyl)amino-3-phenyl-pyrazole **144.** The condensation of the latter orthoesters in

xylene, cyanogen bromide in ethanol, carbon sulfide or ethyl chloroformate in the presence of pyridine results in 1-pyrazolylbenzimidazoles **145-148** according to [104] (Scheme 52).

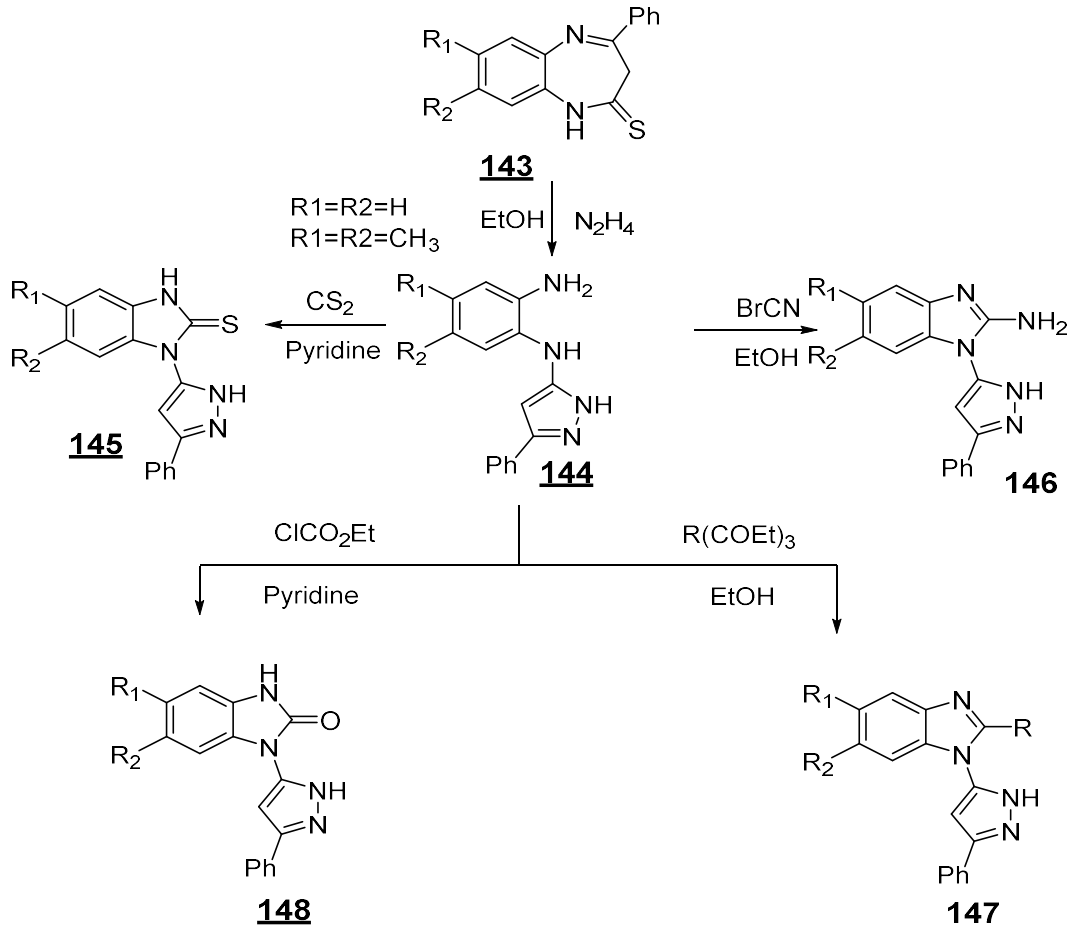

- Scheme 52 -

Recently, Chkirate *et al*. [90] in studied the reaction of semicarbazide hydrochloride **149** with 1,5-benzodiazepine **51b** in an aqueous ethanoic solution. The results observed show that the reaction is sensitive to the amount of semicarbazide. So, when the binucleophilic reagent is used in a steochiometric amount in ethanol, at reflux, only a derivative of pyrazolic structure **150** is obtained. The use of an excess of semicarbazide allowed to obtain the exclusive synthesis of compound **151** (Scheme 53).

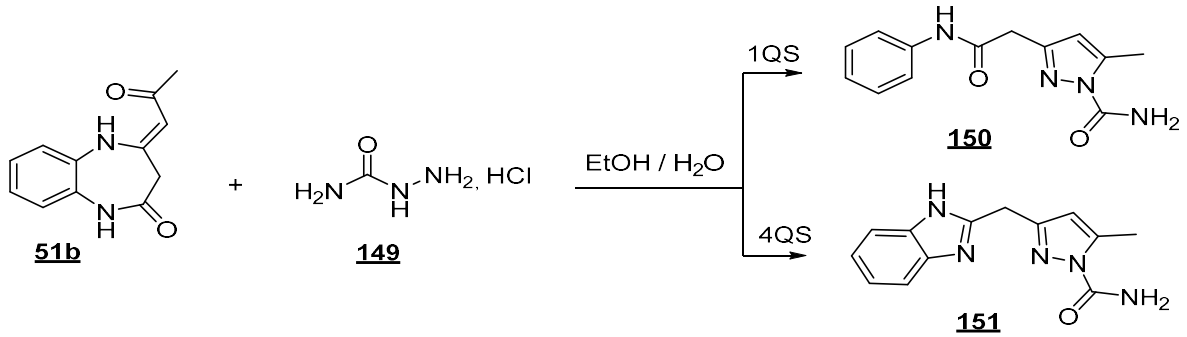

- Scheme 53 -

The reaction of hydroxylamine hydrochloride with 4-amino-1,5-benzodiazepine-3-carbonitrile **152** in water leads directly to a benzimidazole derivative **154** [105]. When the reaction is carried out in a basic medium, an oxime of type intermediate **153** is isolated. The latter is treated with 10% hydrochloric acid and gives benzimidazoline **154** (Scheme 54).

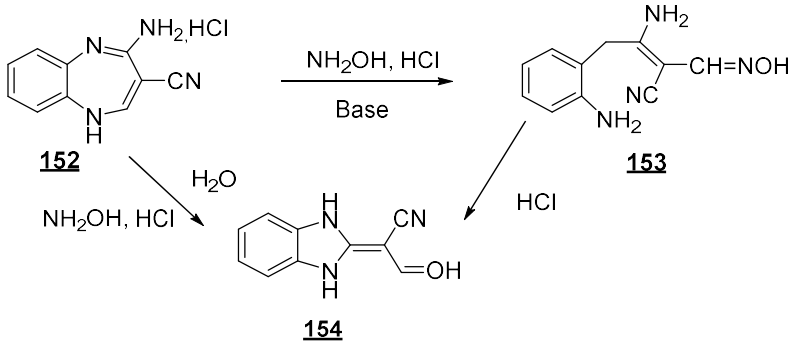

- Scheme 54 -

The same authors [105] isolate isoxazolic compound **156** by the action of hydroxylamine hydrochloride on 4-amino-1,5-benzodiazepin-3-carbonitriles **155** (Scheme 55).

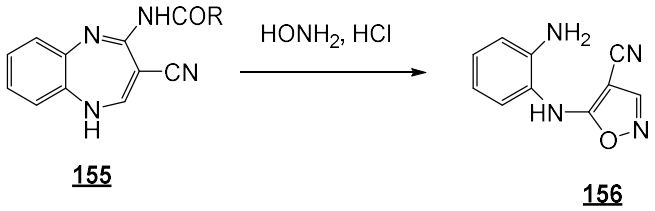

- Scheme 55 -

The action of hydroxylamine hydrochloride on 4-phenyl-1,5-benzodiazepin-2-one has also been described. in our laboratory, Essassi *et al.*[58] in chpter1 obtained 5-(aminophenyl)amino-3-phenyl isoxazole **157**, by the action of an excess of hydroxylamine on benzodiazepine **58** On the other hand, the use of a stoichiometric amount of hydroxylamine hydrochloride led to the oxime of benzodiazepine **158** (Scheme 56).

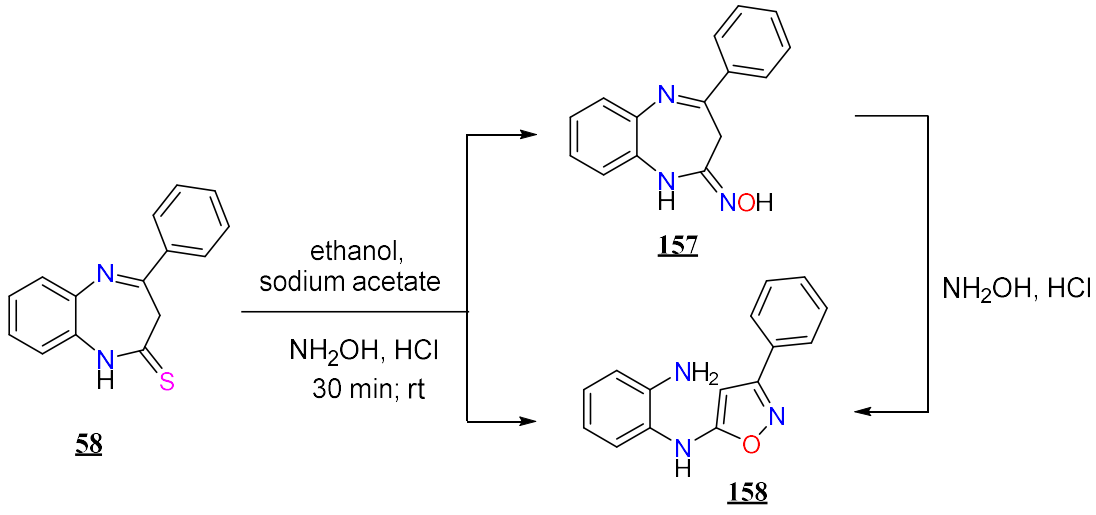

- Scheme 56 -

It should be noted that when the same reaction is carried out on 1-alkyl-4-phenyl-1,5-benziodiazepin-2-thiones, the authors [58] were able to isolate a single compound of isoxazolone structure **160**-**161** (Scheme 57).

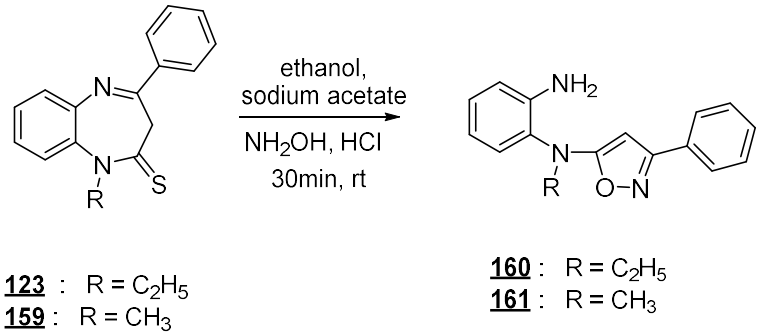

- Scheme 57 -

In 2017, Essaghouani *et al*. [106] reported the synthesis of 3-phenylisoxazolin-5-one **162** using the condensation of 4-phenyl-1,5-benzodiazepin-2-one **58** and hydroxylamine hydrochloride in ethanol at room temperature for 24 h (Scheme 58)

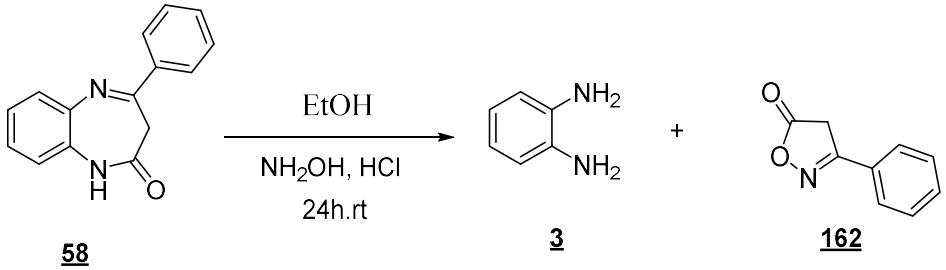

- Scheme 58 -

The structure of compound **162** has been confirmed by a single crystal X-ray diffraction (figure 21).

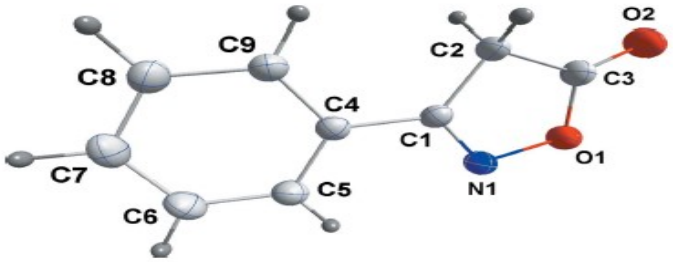

Figure 21. ORTEP representation of the structure of **162**

A study of the action of hydroxylamine hydrochloride on 4-(2-oxopropylidene)-2,3,4,5-tetrahydro-1,5-benzodiazepin-2-ones **51b** was carried out by El Azzaoui *et al.*[107].

They showed that the reaction is insensitive to the quantity of the reagent used in stoichiometric quantity or in excess, at room temperature or under reflux of methanol, the

observed result is always the same; the benzimidazole derivatives **163** and **164** were obtained exclusively. (Scheme 59)

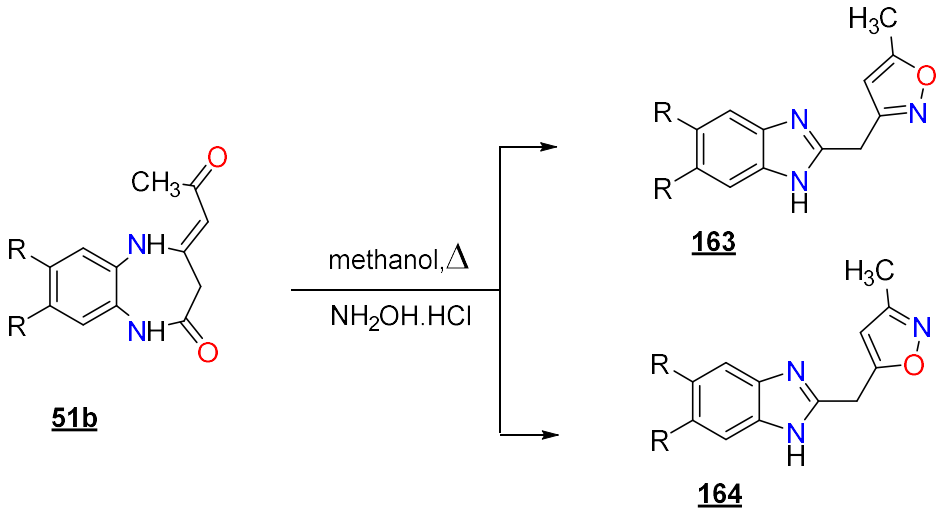

- Scheme 59 -

In order to prepare benzimidazole derivatives linked to other heterocycles, such as1,2,3-triazoles, isoxazoles and pyrazoles, Sebhaoui [108] showed that the formed cycloadducts **165**, **166**, **167** undergo a ring transformation of the diazpepine of the benzodiazepines into benzimidazoles under the action of hydroxylamine hydrochloride in refluxing ethanol for one hour (Scheme 60-62).

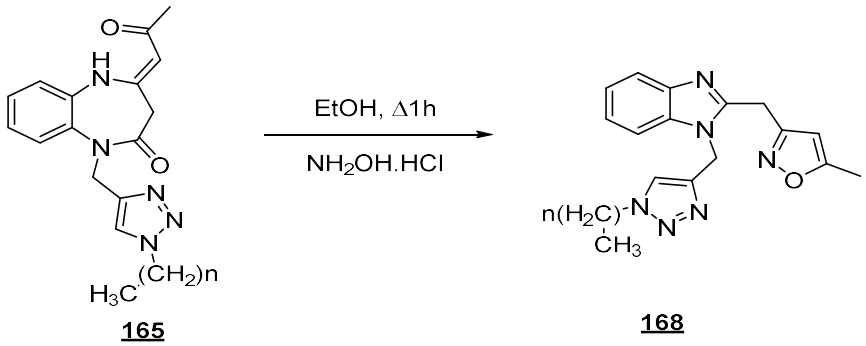

- Scheme 60 -

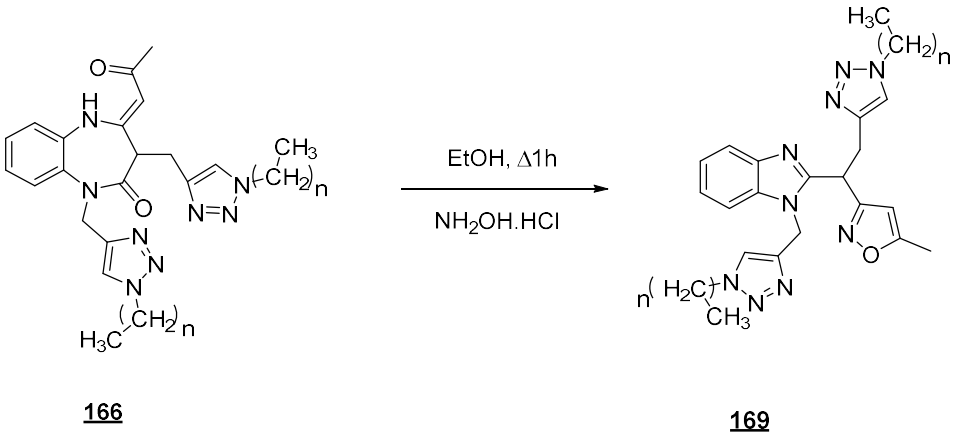

- Scheme 61 –

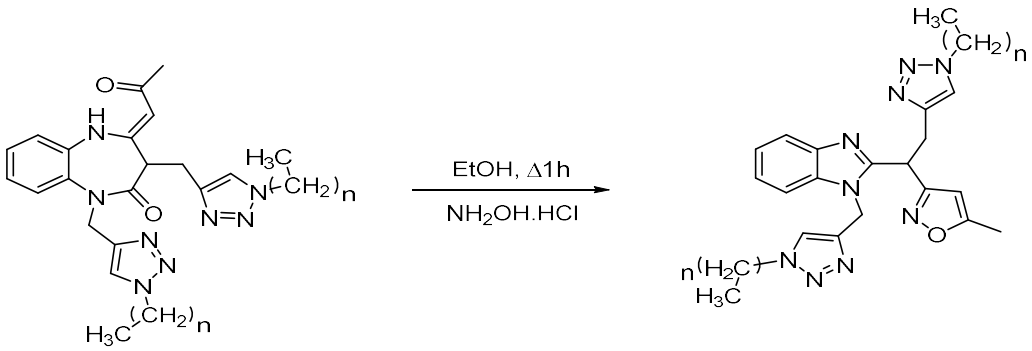

167 **170**

- Scheme 62 -

Recently, Idrissi, A. *et al.* [109] studied the condensation of 4-(Z)-7-Methyl-(2-oxopropylidene)-1,5-benzodiazepin-2-one **171** with hydroxylamine hydrochloride under reflux in methanol for 2h. The authors have isolated 5,6-diméthyl-2-[(5-méthyl-1,2-oxazol-3-yl) methyl]-1-(prop-2-en-1-yl)-benzimidazole **172** in good yield (Scheme 63).

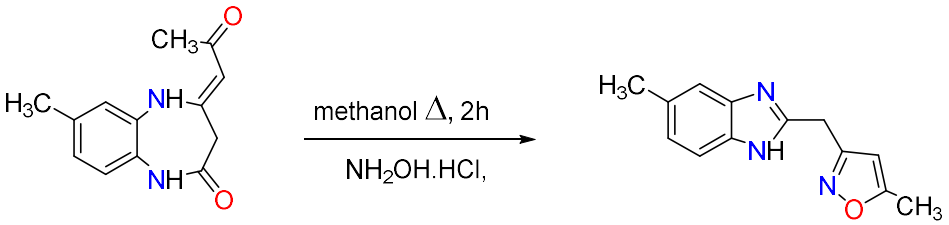

171 172

- Scheme 63 -

The structure of compound **172** has been confirmed by a single crystal X-ray diffraction (figure 22).

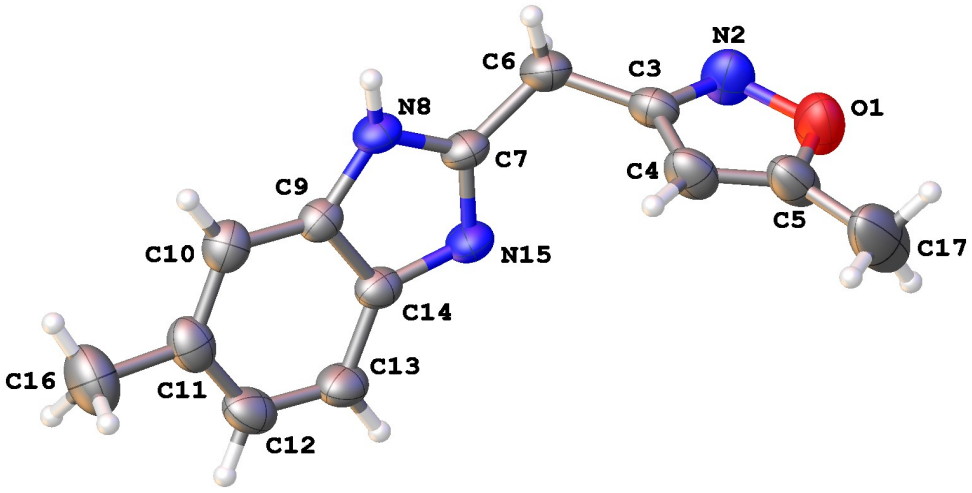

Figure22: ORTEP representation of the structure of **172**

III- Action of hydroxylamine hydrochloride with 1,5-benzodiazepine-2-thione derivatives:

III .1 Synthesis of (E)-2-(1-ethyl-1H-benzimidazol-2-yl)-1-phenylethanone oxime 173

The synthesis of this compound **173** consists of condensation between two equivalents of hydroxylamine **hydrochloride** and one equivalent of 1-ethyl-1,5-benzodiazepine-2-thione **123** in refluxing ethanol for 24 h. By thin layer chromatography (CCM) the reaction is monitored and shows the formation of a single product and the disappearance of the starting reagent after 24 h (Scheme 64).

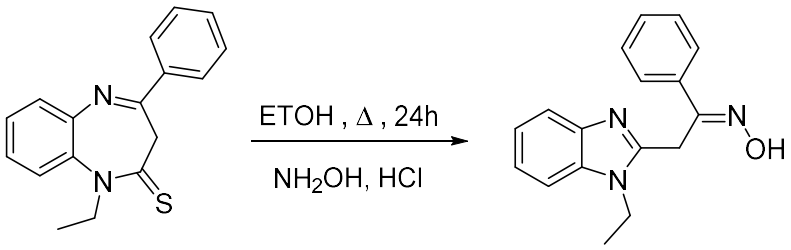

123 **173**

- Scheme 64 -

The structure of compound **173** was identified by the spectral data (^{1}H NMR, ^{13}C NMR and mass spectroscopy).

The analysis of the spectral data on the ^{1}HNMR spectrum of product **173** (figure 23) taken in Dimethyl sulfoxide (DMSO-d_6) shows, the presence of a triplet at about 1.32 ppm due to the three CH_3 protons coupled to the two adjacent protons of the CH_2 group, which appears in the form of a quadruplet at about 4.32 ppm. The signal located at about 4.42 ppm is attributed to the two CH_2. There is also a signal at 11.70 ppm integrating a proton, characteristic of the oxime O-H group.

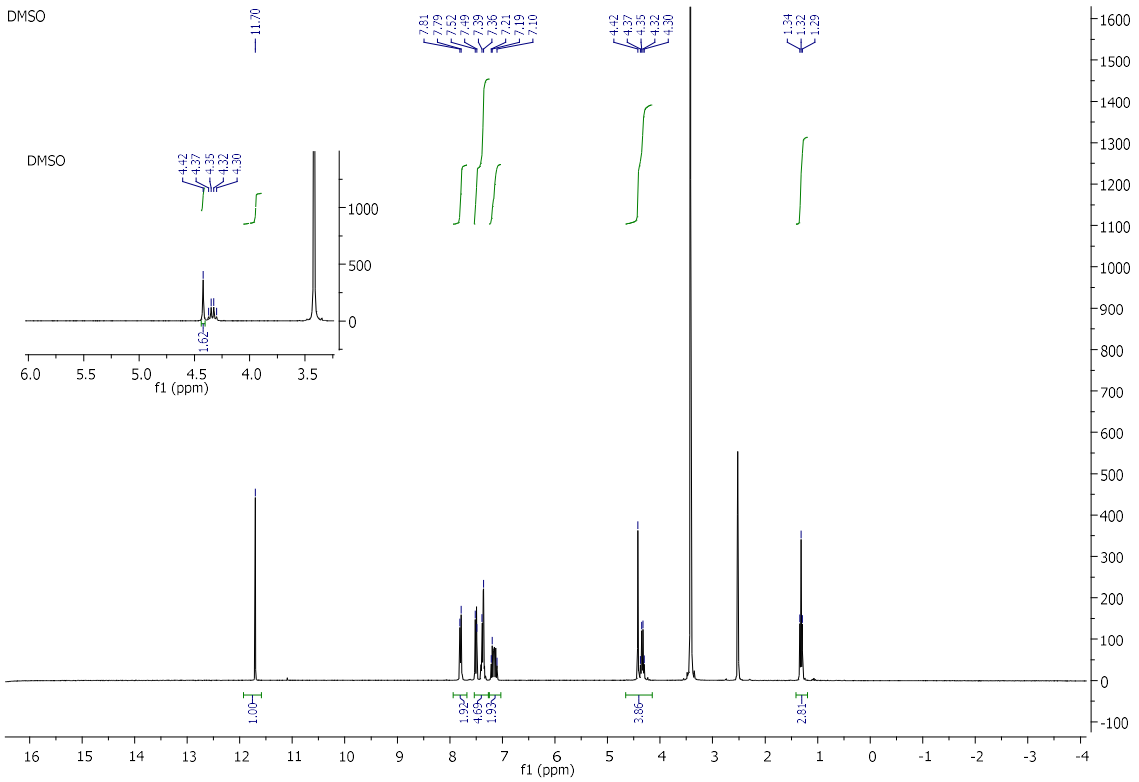

Figure 23: ^{1}H NMR spectrum of compound **173** (DMSO-d_6, 300 MHz)

On the ^{13}C NMR spectrum of product **173** taken in DMSO-d_6 (figure 24), we note the presence of a signal at 14.69 ppm assigned to the CH_3 group carbon, two signals at 23.90 and 37.82 ppm related to the two carbon CH_2 groups. The signals of the benzene carbons appear between 125.87 and 130.72 ppm.

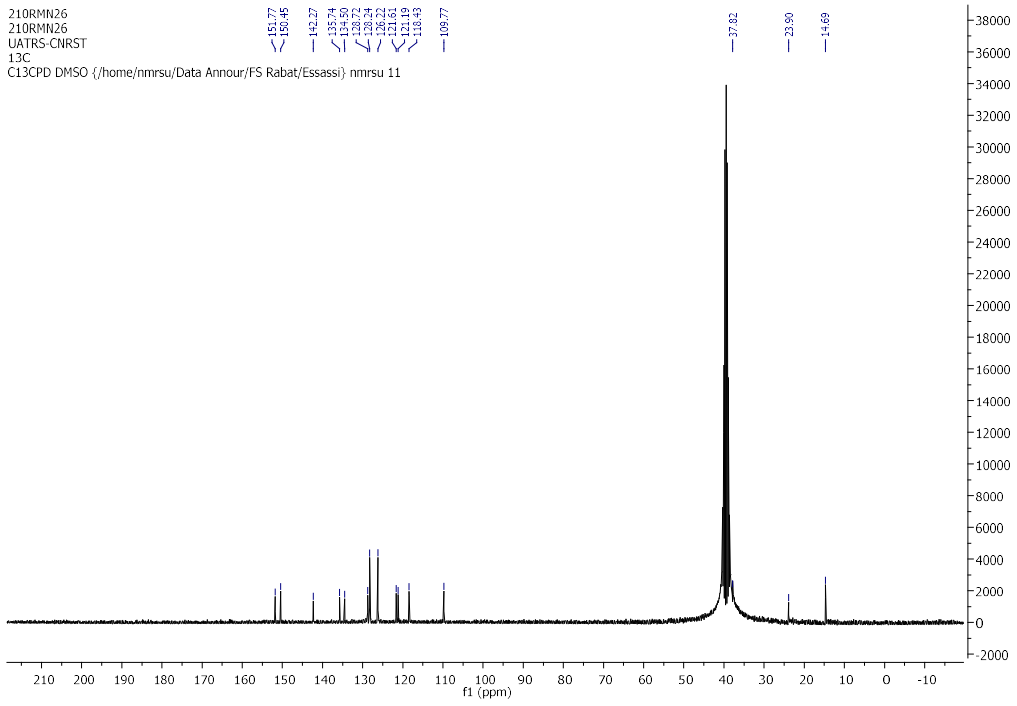

Figure 24: ^{13}C NMR spectrum of compound **173** (DMSO-d_6, 75 MHz)

The mass spectrum (ESI) in (figure 25) analysis of compound **173** gave the protonated molecular ion $(M+H)^+$ at m/z 280.14.

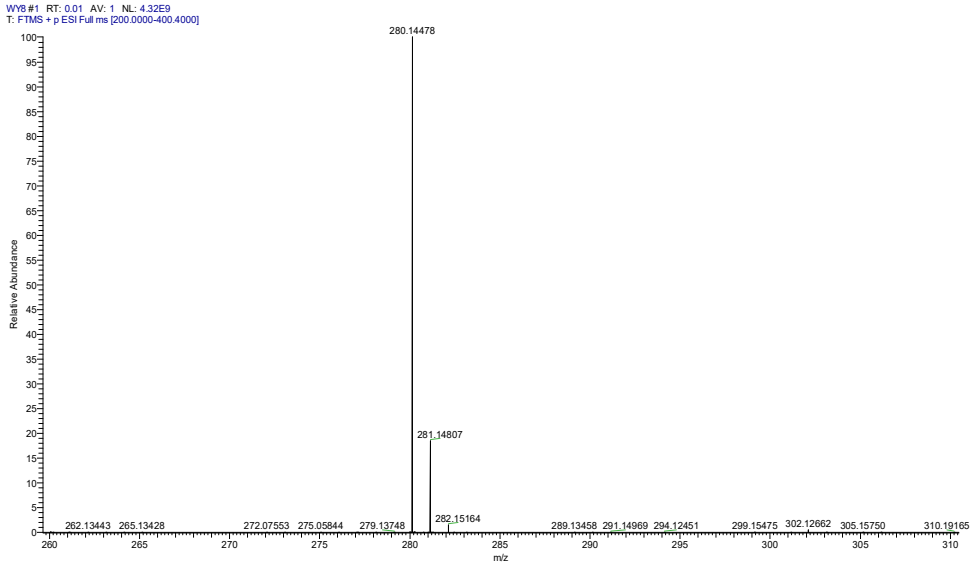

Figure.25. mass spectrum of product **173**

III.2. Synthesis of E-2-(1-benzyl-1H-benzimidazol-2-yl)-1-phenylethanone oxime 174

To confirm the previous result, we studied the condensation reaction between 1-benzyl-4-phenyl-1,5-benzodiazepine-2-thione **132** and hydroxylamine hydrochloride under the same reaction conditions. We obtained (E)-2-(1-benzyl-1H-benzimidazol-2-yl)-1-phenylethanone **174** in good yield after heating in reflux for 24 hours (scheme 65).

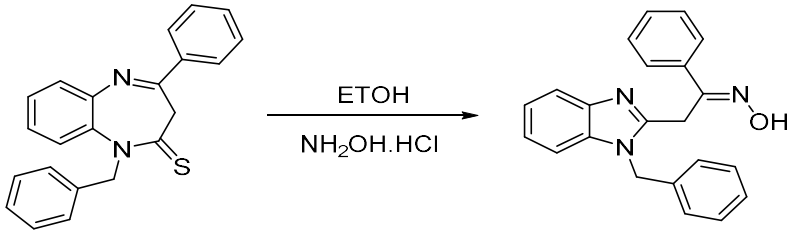

132 **174**

- Scheme 65 -

The structure of compound **174** was identified by the spectral data from ^{1}H NMR, ^{13}C, and mass spectrometry. Thus, the spectrum of ^{1}H NMR of compound **174** (figure 26) taken in DMSO-$_{d6}$ showed a multiplet centered at 6.96–7.63 ppm corresponding to the protons of the benzene ring, a singlet signal at 5.54 ppm due to the protons of the methylene group linked to the benzimidazolic nitrogen atom a signal at 4.36 ppm related to the methylene group oximic, and a singlet at 11.61 ppm due to proton of OH.

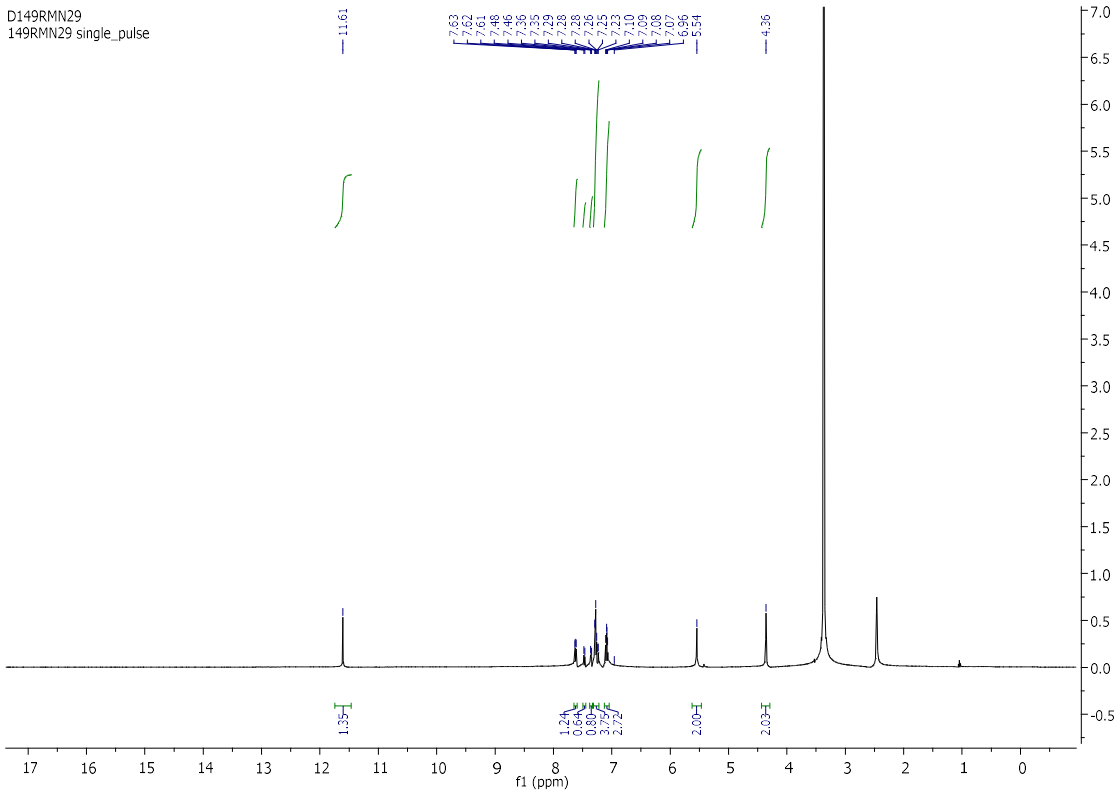

Figure 26: ^{1}H NMR spectrum of compound **174** (DMSO-d_6 500 MHz)

In the ^{13}CNMR spectrum (125 MHz) taken in DMSO-d_6 (figure 27) of product **174,** we observed in particular the presence of two signals at 24.62 and 46.78 corresponding to the carbons of CH_2 groups.

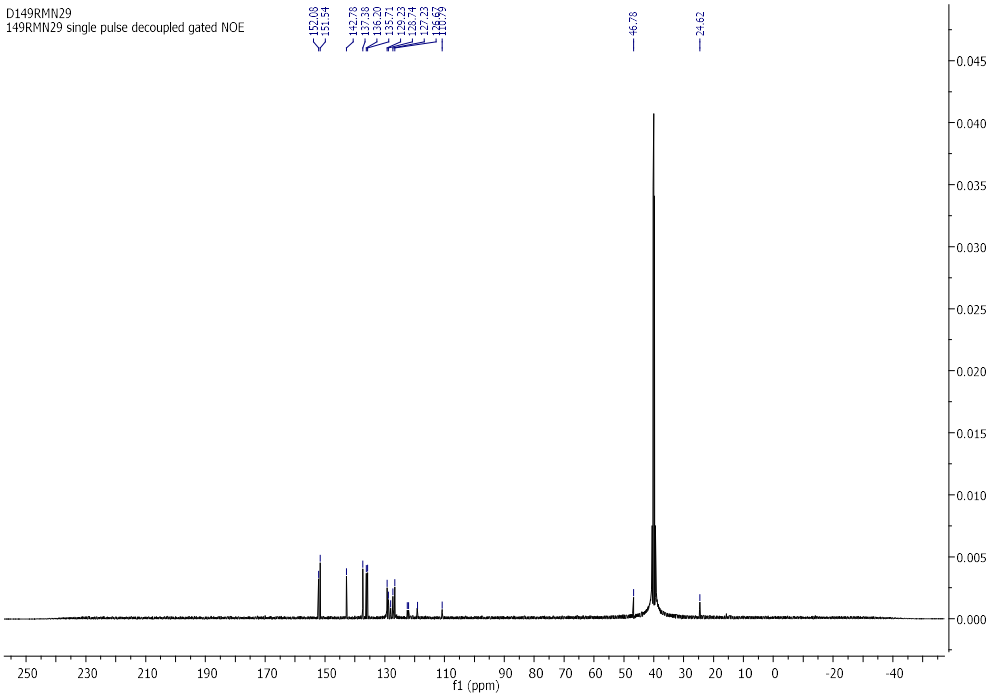

Figure 27: ^{13}C NMR spectrum of compound **174** (DMSO-d_6 125 MHz)

The mass spectrum (ESI) of compound **174** shows the protonated molecular ion $(M+H)^+$ at m/z (342.16) assigned to a molecular ion $C_{22}H_{19}N_3O$ (figure 28).

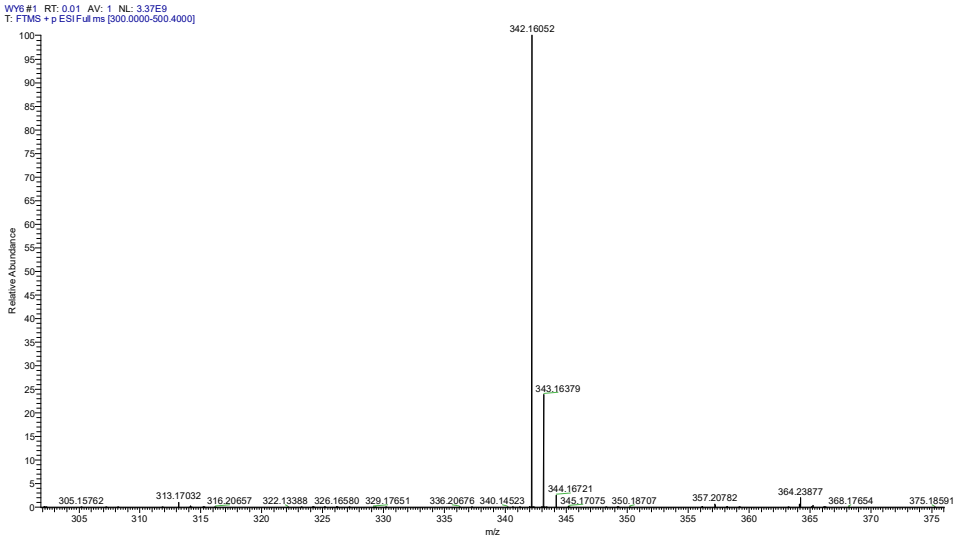

Figure 28: mass spectrum of product **174.**

III.3. Synthesis of benzimidazole derivatives with the long-carbon chains 175-181

In order to prepare the long carbon chains benzimidazole derivatives, the products **124**–**131** undergo a transformation of the seven-membered ring of the benzodiazepines into benzimidazoles under the action of hydroxylamine hydrochloride in refluxing ethanol for 24 h, leading to the benzimidazole derivatives **175**–**181** with good yields (Scheme66).

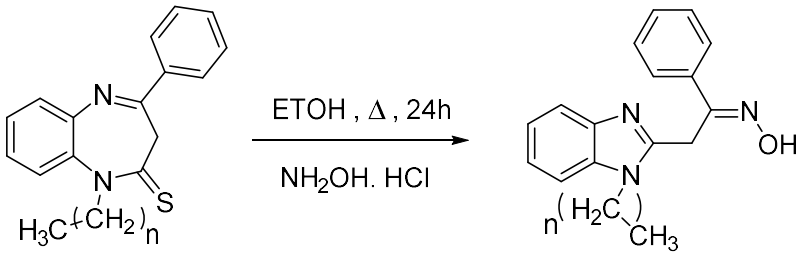

n = 3: 124
n = 5: 125
n = 7: 126
n = 9: 127
n =11: 128
n =15: 129
n =17: 130

n = 3: 175
n = 5: 176
n = 7: 177
n = 9: 178
n =11: 179
n =15: 180
n =17: 181

- Scheme 66 -

The structures of the synthesized compounds were established by spectroscopic data (^{1}H NMR. ^{13}C NMR., MS and IR) as well as by X-ray crystallographic study.

Figure29 illustrates the ^{1}H NMR. spectrum taken in the DMSO-d_6 of product **177**, The analysis of the spectral data shows in particular the multiple signals located in the zone [1.23-1.75 ppm] corresponding to the CH_2 protons of the long carbon chain, a triplet signal centered at 4.25 ppm due to the protons of the methylene groups linked to the benzimidazolic nitrogen

atom a well as the singlet signal observed at about 11.73 ppm is associated to the proton of the OH group.

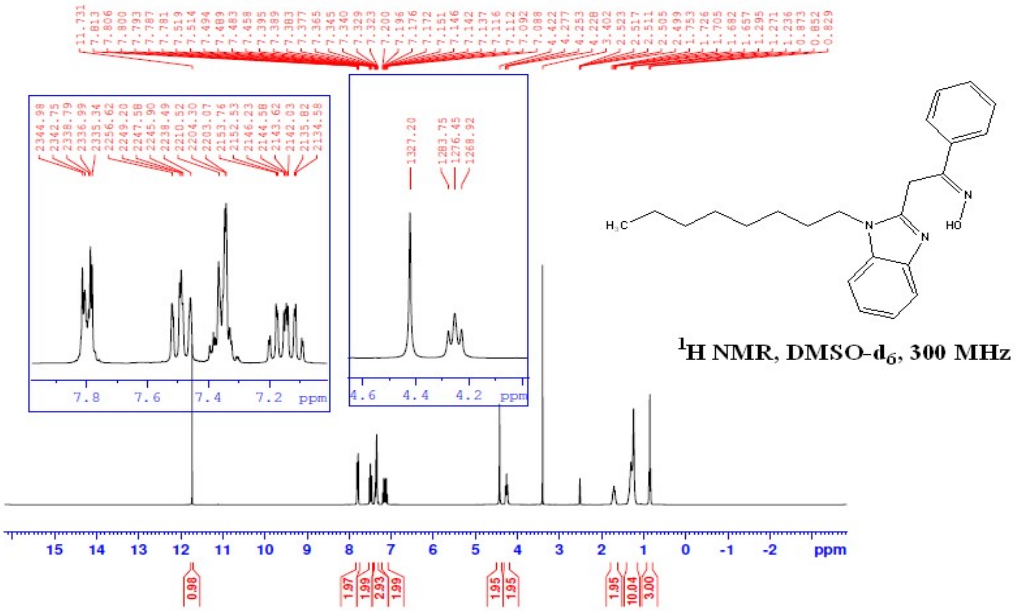

Figure 29: ^{1}H NMR spectrum of compound **177** (DMSO-d$_6$ 500 MHz)

By analyzing the ^{13}C NMR spectrums of the same product **177** (figure 30), we observed a signal at 14.40 ppm due to the CH_3 group, the set of signals observed from 22.55 ppm up to 40.82 ppm corresponding to the CH_2 carbons of the long-carbon chain, a signal at 43.46 ppm related to the oxime methylene group.

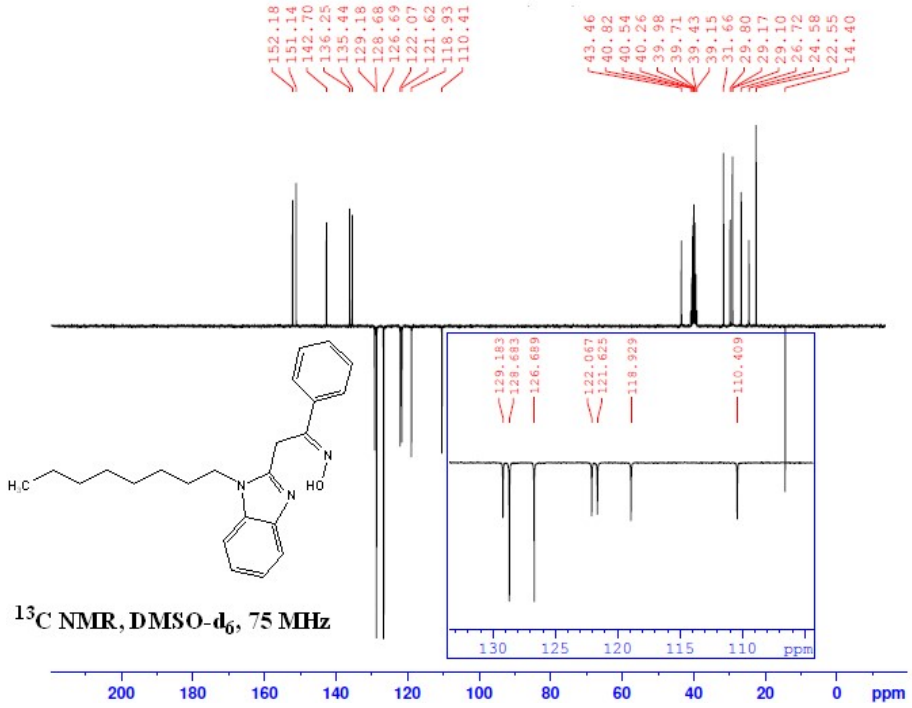

Figure 30: ^{13}C NMR spectrum of compound **177** (DMSO-d$_6$ 75 MHz)

The mass spectrum (ESI) (figure 31) of compound **177** shows the protonated molecular ion $(MH)^+$ at m/z (364.23)

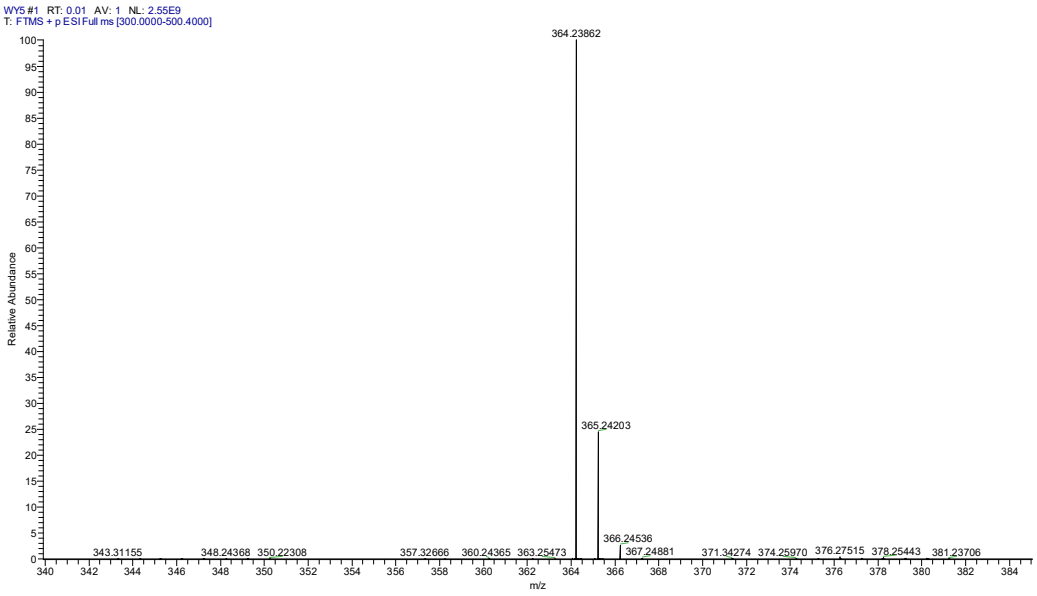

Figure 31: mass spectrum of compound **177**

Figure 32 represents the Infrared spectrum of compound **177**, the OH group appeared as a band around 3100-3300 cm^{-1}, the CH_2 group of the long carbon chain appeared around 2856 and 2973 cm-1.

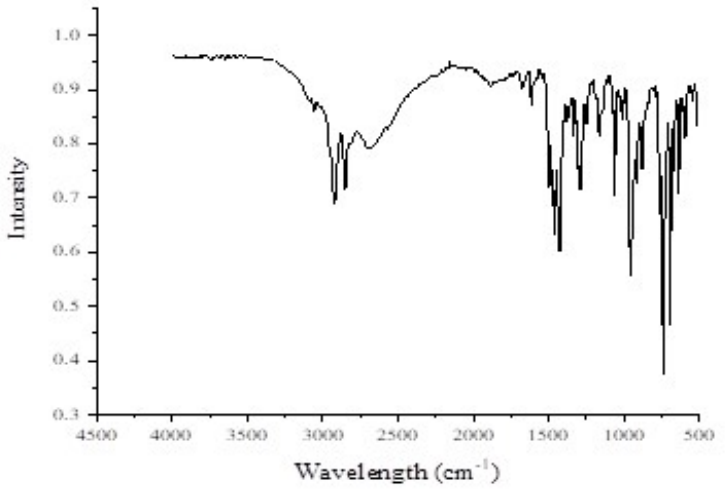

Figure 32: IR spectrum of compound **177**

A plausible mechanism has been proposed for the formation of compounds **173-181** (Scheme 67**)**.

Thus, the attack of the amino group of hydroxylamine on the carbon atom in position 4 of the seven membered rings gives the intermediates **A,** which undergo a ring opening

reaction after the cleavage- of the C4-N bond affording the compounds **B**. These latter, after an intramolecular cyclization involving the amino and thiocarbonyl groups, give the unstable benzimidazolines **C** which after the loss of a hydrogen sulfide molecule lead to the isolated compounds **173**-**181**,

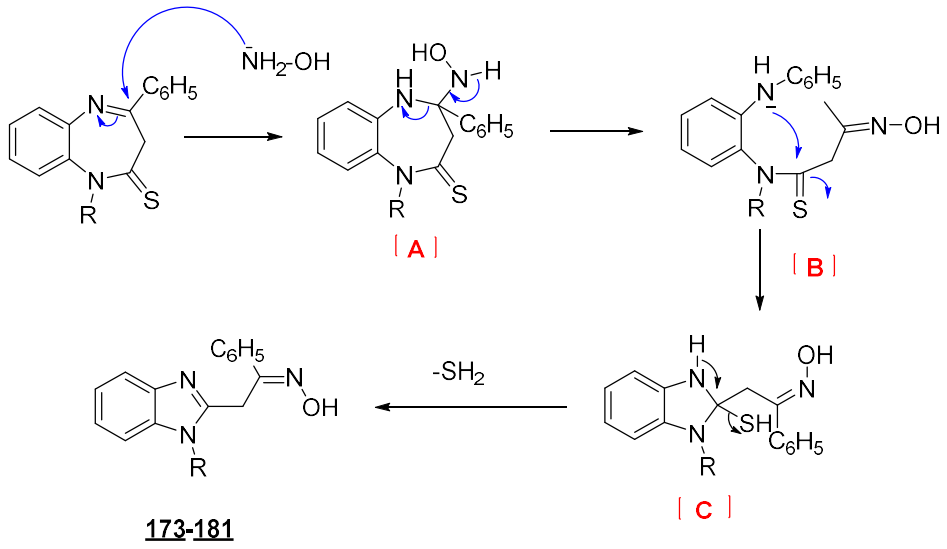

- Scheme 67 -

IV-Crystallography study

IV.1. Crystallographic study of compound 173

An X-ray crystallographic study was used to accurately determine the structure of the product. This crystallographic analysis clearly confirms the proposed structure from the spectral analyzes of NMR, and mass spectroscopy and shows that the oxime function adopts E configuration E.

The determination and refinement of the structure is carried out in space group *Monoclinic* P1 21/c1. The molecular structure of compound **173** is shown in figure 33. Crystallographic data and recording conditions are shown in table 5.

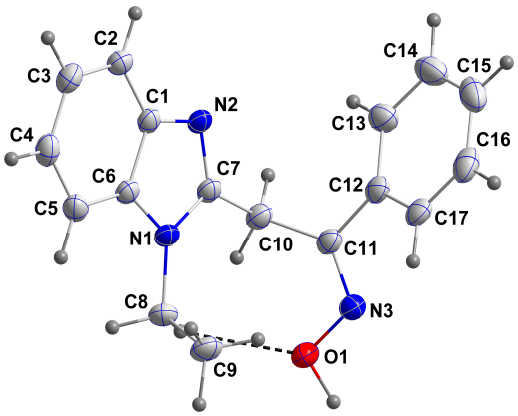

Figure 33: ORTEP representation of the structure **173**

The benzimidazole unit is planar and the conformations of the substituent are partially determined by an intermolecular C—H···O hydrogen bond. In the crystal, O—H···N hydrogen bonds form helical chains extending along the *b*-axis direction which are formed into a 3-D network by a combination of O—H···N hydrogen bonds and C—H···π(ring) and π-stacking interactions.

Table 5: Crystallographic data of the product **173**

Chemical formula	$C_{17}H_{17}N_3O$
Mr	279.33 g/mol
Crystal system, space group	Monoclinic, P1 21/c1
Temperature (K)	120
a, b, c (Å)	7.7281 (15), 12.684 (3), 15.425 (3)
β (°)	100.463 (2)
V (Å^3)	1486.9(5) Å^3
Z	4
Radiation type	Mo Kα
μ (mm^{-1})	0.08
Crystal size (mm)	0.094 x 0.281 x 0.325 mm
Data collection	
Diffractometer	Bruker Smart APEX CCD
Absorption correction	Multi-scan
Tmin, Tmax	0.78, 0.99
Refinement program	SHELXL-2018/1 (Sheldrick, 2018)
R.M.S. deviation from mean	0.041
Refinement	
R[F2 > 2σ(F2)], wR(F2), S	0.043, 0.112, 1.06
Reflections collected	13250
Independent reflections	3728 [R(int) = 0.0410]
Data / restraints / parameters	3728 / 0 / 255
Goodness-of-fit on F^2	1.058

IV.2. Crystallographic study of compound 174

The crystals used for the crystallographic study were obtained by evaporation of a solution of compound **174** in ethanol at room temperature, which is obtained in the form of colorless needles.

The RX diffraction analysis of a single crystal allowed us to determine the complete structure of this benzimidazole derivative. It crystallizes in the monoclinic system. The determination and refinement of the structure is carried out in space group Monoclinic, C12/*c*1.

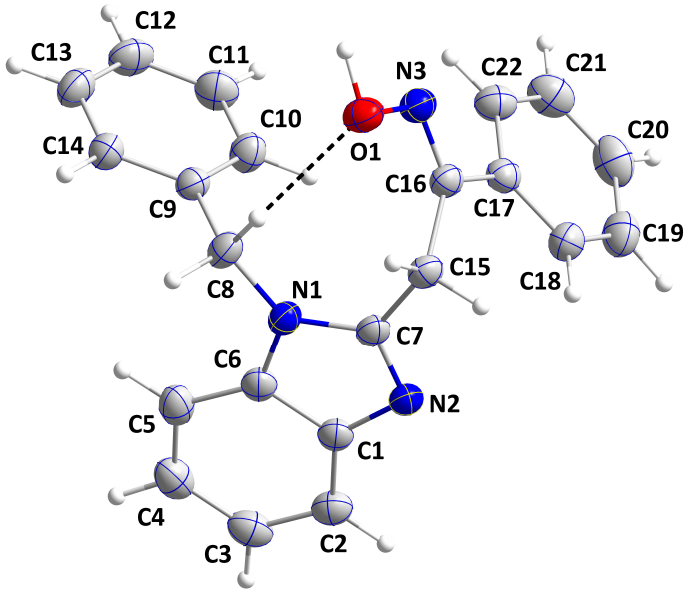

Figure 34: ORTEP representation of the structure **174**

The benzimidazole portion is not quite planar. The *L*-shaped molecular conformation is partially determined by an intermolecular C—H···O hydrogen bond.

In the crystal, N—H···O hydrogen bonds form helical chains extending along the *b*-axis direction while slipped π-stacking interactions between benzimidazole units link the chains into layers parallel to the *bc* plane.

Table 6: Crystallographic data of the product **174**

Chemical formula	$C_{22}H_{19}N_3O$
Mr	341.40 g/mol
Crystal system, space group	Monoclinic, C12/c1
Temperature (K)	150
a, b, c (Å)	19.4884 (5), 12.0291 (3), 15.5920 (4)
β (°)	97.360 (1)
V (Å3)	3625.08 (16)
Z	8
Radiation type	Cu Kα
Crystal size (mm)	0.136 x 0.235 x 0.262 mm
Data collection	
Diffractometer	Bruker D8 VENTURE PHOTON 100 CMOS
Absorption correction	Multi-scan
Tmin, Tmax	0.85, 0.92
Independent reflections	3530 [R(int) = 0.0338]
Final R indices	3058 data; I>2σ(I)
Absorption coefficient	0.621 mm^{-1}
Refinement	
Data / restraints / parameters	3530 / 0 / 312
Theta range for data collection	4.58 to 72.09°
R.M.S. deviation from mean	0.037 $eÅ^{-3}$

IV.3. Crystallographic study of compound **177**

The crystals used for the crystallographic study were obtained by evaporation of a solution of compound **177** in ethanol. The crystals used in this study are in the form of transparent needles (Figure 35).

The RX diffraction analysis of a single crystal allowed us to determine the complete structure of this compound. It crystallizes in the monoclinic system. The determination and refinement of the structure is carried out in space group Orthorhombic, *Pbca*.
Crystallographic data and structure recording conditions are shown in table 7.

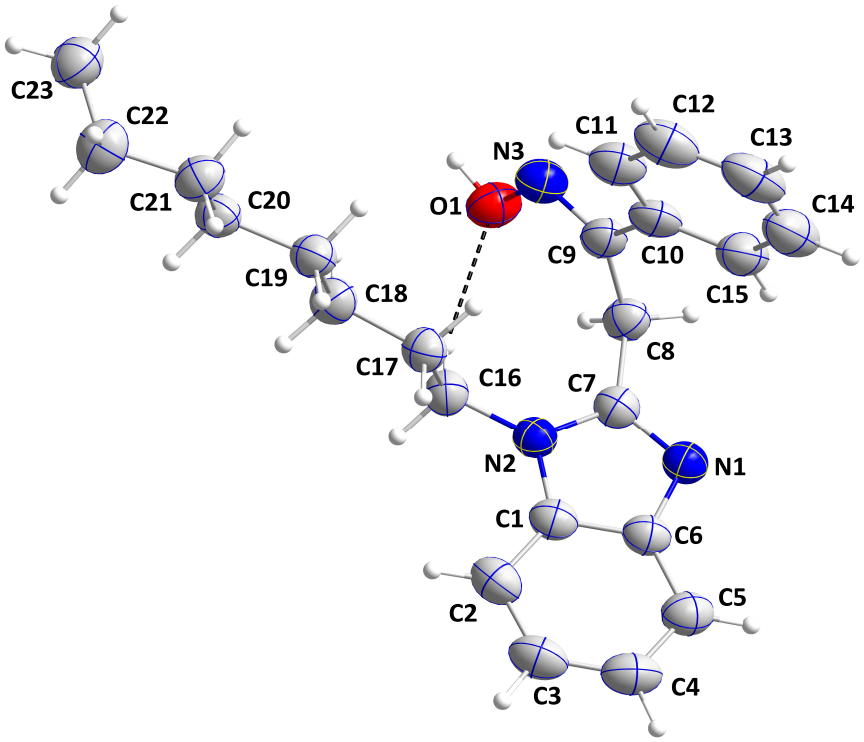

Figure 35: ORTEP representation of the structure **177**

The benzimidazole moiety is planar and together with the phenylethanone oxime unit adopts an "*L*"-shaped conformation with the *n*-octyl chain extending out to the side. In the crystal, helical chains of molecules extending along the *a*-axis direction are formed by O—H···N hydrogen bonds and are connected in pairs by slipped π-stacking interactions between imidazole rings. These pack with normal van der Waals contacts to generate alternating hydrophobic and hydrophilic regions.

Table 7: Crystallographic data of the product **177**

Chemical formula	$C_{23}H_{29}N_3O$
Mr	363.49g/mol
Crystal system, space group	Orthorhombic, Pbca
Temperature	150(2) K
a, b, c (Å)	12.8516 (9), 14.7241 (10), 22.7470 (16)
V (Å3)	4304.4 (5)
Z	8
Radiation type	Mo Kα
Crystal size (mm)	0.044 x 0.134 x 0.266 mm
Data collection	
Diffractometer	Bruker D8 QUEST PHOTON 3 diffractometer
Absorption correction	Multi-scan
Max. and min. transmission	0.9970 and 0.9820
Data / restraints / parameters	2597 / 0 / 245
Refinement program	SHELXL-2018/3 (Sheldrick, 2018)
Reflections collected	61836
Final R indices	1944 data; I>2σ(I)
Goodness-of-fit on F^2	1.097
R.M.S. deviation from mean	0.038 eÅ^{-3}

IV.4. Crystallographic study of compound 178

The crystals used for the crystallographic study were obtained by evaporation of a solution of compound **178** in ethanol at room temperature. They come in the form of colorless needles.

The RX diffraction analysis of a single crystal allowed us to determine the complete structure of this benzimidazole derivative. It crystallizes in the monoclinic system.

The determination and refinement of the structure is carried out in space group Monoclinic P 1 21/c 1.

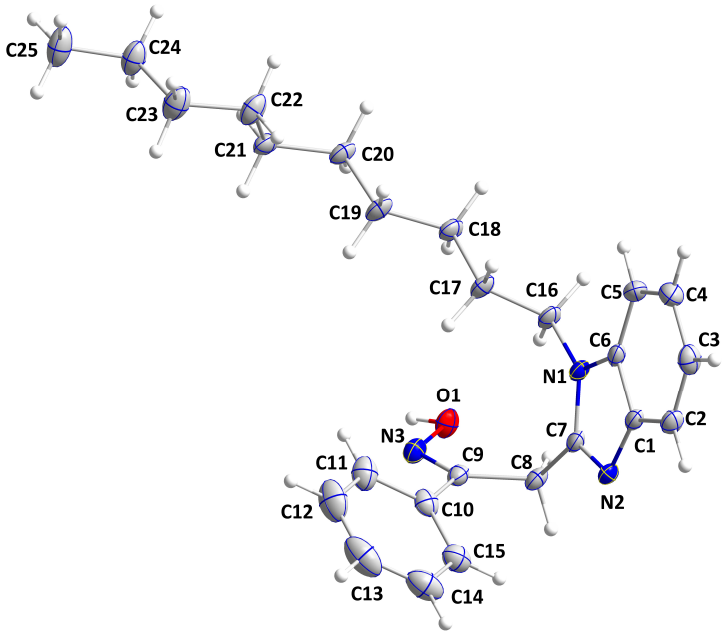

Figure 36: ORTEP representation of the structure **178**

The benzimidazole moiety is not quite planar and together with the phenylethanone oxime substituent adopts an "*L*"-shaped conformation. In the crystal, O—H···N hydrogen bonds form helical chains extending along the *b*-axis direction which are connected into layers parallel to the *bc* plane by slipped π-stacking interactions between imidazole rings.

Table 8: Crystallographic data of the product **178**

Chemical formula	$C_{25}H_{33}N_3O$
Mr	391.54 g/mol
Crystal system, space group	monoclinic P 1 21/c 1
Temperature (K)	150
a, b, c (Å)	12.4580 (8), 12.8188 (8), 15.1379 (9)
β (°)	112.573 (2)
V (Å3)	2232.3 (2)
Z	4
Radiation type	Mo Kα
Crystal size (mm)	0.096 x 0.329 x 0.352 mm
Data collection	
Diffractometer	Bruker D8 QUEST PHOTON 3 diffractometer
Absorption correction	Multi-scan
Tmax Tmin,	0.9930 and 0.9750
Refinement	
Data / restraints / parameters	12373 / 0 / 264
Goodness-of-fit on F^2	1.153
R.M.S. deviation from mean	0.105 $eÅ^{-3}$

V.5. Crystallographic study of compound 179

The crystal used for the crystallographic study was obtained by evaporation of a solution of compound **179** in ethanol at room temperature. They come in the form of colorless needles.

The RX diffraction analysis of a single crystal allowed us to determine the complete structure of this benzimidazole derivative. It crystallizes in the monoclinic system.

The determination and refinement of the structure is carried out in space group monoclinic P 1 21/c 1.

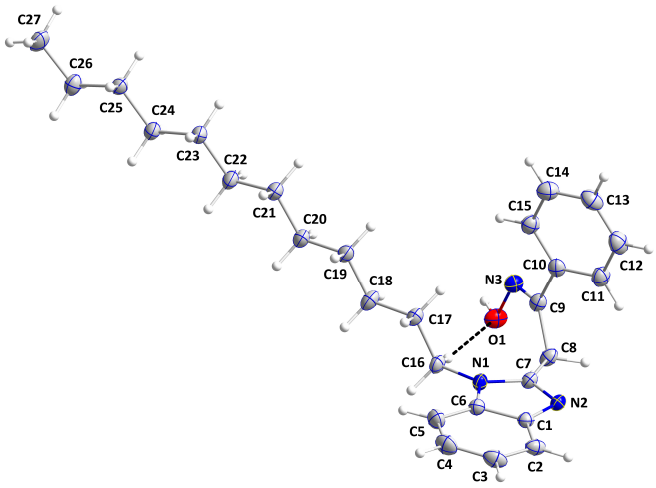

Figure 37: ORTEP representation of the structure **179**

The benzimidazole moiety is planar to within 0.0157 (7) Å and it and its attached phenylethanone oxime substituent adopt an "*L*"-shaped conformation with the dodecyl chain extending out from its side. In the crystal, helical chains of molecules extending along the *b*-axis direction are formed by O—H···N hydrogen bonds and C—H···π (ring) interactions.

The chains are connected into layers two molecules thick and parallel to the *bc* plane by π-stacking interactions between inversion-related imidazole rings while the layers pack along the *a*-axis direction with normal van der Waals contacts

Table 9: Crystallographic data of the product **179**

Chemical formula	$C_{27}H_{37}N_3O$
Mr	419.59 g/mol
Crystal system, espace group	Monoclinic P 1 21/c 1.
Temperature (K)	150
a, b, c (Å)	13.2228 (4), 12.6368 (4), 14.9154 (4)
β (°)	93.262 (2)
V (Å3)	2488.23 (13)
Z	4
Radiation type	Mo Kα
Crystal size (mm)	0.222 x 0.319 x 0.437 mm
Data collection	
Diffractometer	Bruker D8 QUEST PHOTON 3 diffractometer
Absorption correction	Numerical
Tmax ,Tmin,	0.9850 and 0.9710
Data / restraints / parameters	8322 / 1 / 285
Goodness-of-fit on F^2	1.058
Refinement	
Independent reflections	8322 [R(int) = 0.0340]
Final R indices	7270 data; I>2σ(I)
R.M.S. deviation from mean	0.042 $eÅ^{-3}$

IV.6. Crystallographic study of compound 180

The crystal used for the crystallographic study was obtained by evaporation of a solution of compound **180** in ethanol at room temperature. They come in the form of colorless needles.

The RX diffraction analysis of a single crystal allowed us to determine the complete structure of this benzimidazole derivative. It crystallizes in the monoclinic system. The determination and refinement of the structure is carried out in space group P 1 21/c 1

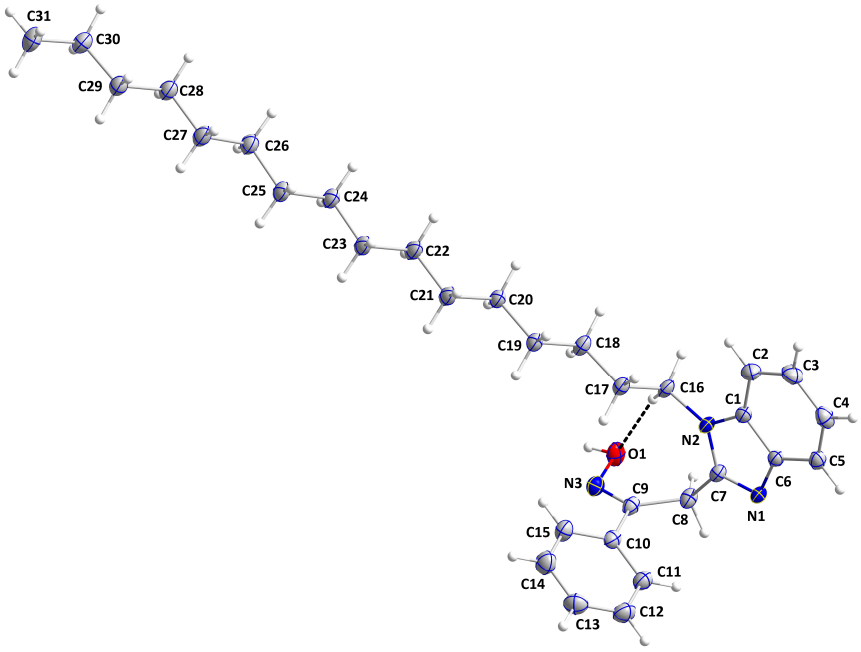

Figure 38: ORTEP representation of the structure **180**

The benzimidazole moiety is essentially planar and the alkyl chain extends out from its side. In the crystal, O—H···N hydrogen bonds and C—H···π(ring) interactions form helical chains extending along the *b*-axis direction. These are connected by slipped π-stacking interactions between imidazole rings to form a network structure with alternating hydrophobic and hydrophilic regions.

Table 10: Crystallographic data of the product **180**

Chemical formula	$C_{31}H_{45}N_3O$
Mr	475.70 g/mol
Crystal system, space group	Monoclinic P 1 21/c 1
Temperature (K)	150
a, b, c (Å)	17.1306 (5), 12.2648 (3), 14.8800 (4)
β (°)	112.419 (1)
V (Å3)	2890.05 (14)
Z	4
Radiation type	Mo Kα
Crystal size (mm)	0.066 x 0.274 x 0.352 mm
Data collection	
Diffractometer	Bruker D8 QUEST PHOTON 3 diffractometer
Absorption correction	Numerical
Tmax, Tmin,	0.9960 and 0.9770
Independent reflections	8872 [R(int) = 0.0387]
Reflections collected	147075
Refinement	
Data / restraints / parameters	8872 / 0 / 317
Goodness-of-fit on F^2	1.101
Final R indices	7616 data; I>2σ(I)
R.M.S. deviation from mean	0.040 eÅ^{-3}

IV.7. Crystallographic study of compound **181**

The crystal used for the crystallographic study was obtained by evaporation of a solution of compound **181** in ethanol at room temperature. They come in the form of colorless needles.

The RX diffraction analysis of a single crystal allowed us to determine the complete structure of this benzimidazole derivative. It crystallizes in the monoclinic system. The determination and refinement of the structure is carried out in space group Orthorhombic, *Pbca.*

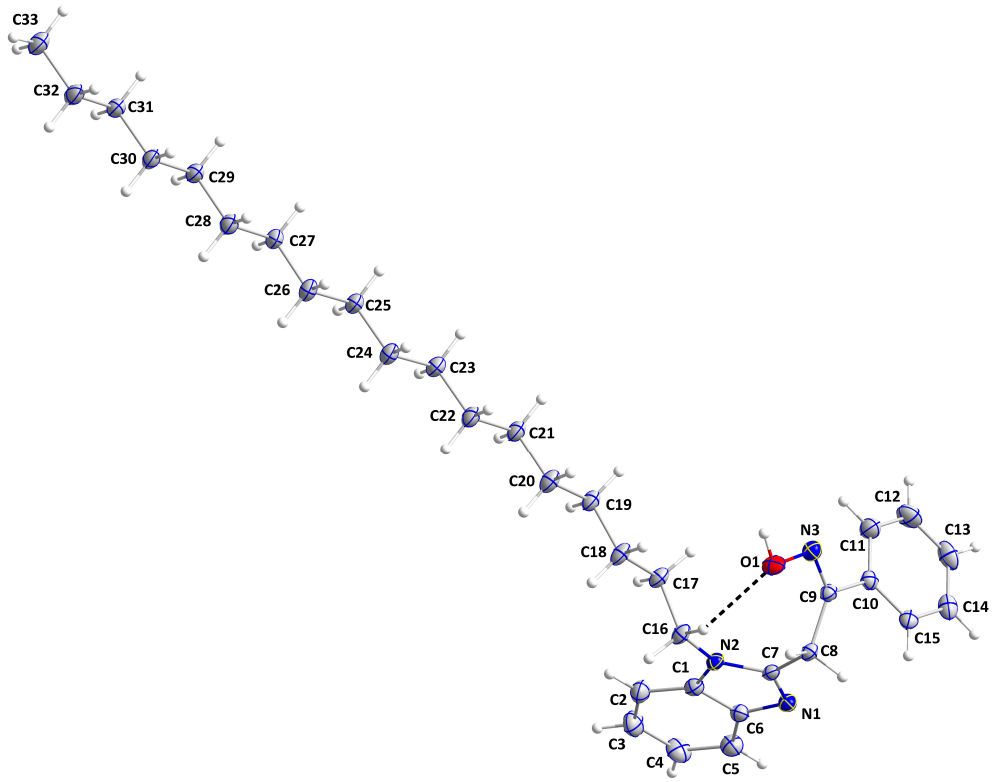

Figure 39: ORTEP representation of the structure **181**

The polar portion of the title molecule, $C_{33}H_{49}N_3O$, adopts an "*L*"-shaped conformation with the octadecyl chain in a "fully extended" orientation. In the crystal, O—H···N hydrogen bonds and C—H···π(ring) interactions form chains of molecules extending along the *b*-axis direction.

These are connected along the *a*-axis direction into layers by additional C—H···π(ring) interactions. The octadecyl chains in adjacent layers intercalate with the resulting micelle-like regions being connected by more C—H···π(ring) interactions.

Table 11: Crystallographic data of the product **181**

Chemical formula	$C_{33}H_{49}N_3O$
Mr	503.75 g/mol
Crystal system, space group	Orthorhombic, Pbca
Temperature (K)	150
a, b, c (Å)	9.4729 (17), 13.515 (2), 47.817 (8)
V (Å3)	6121.9 (19)
Z	8
Radiation type	Mo Kα
Crystal size (mm)	0.132 x 0.256 x 0.327 mm
Data collection	
Diffractometer	Bruker D8 QUEST PHOTON 3 diffractometer
Absorption correction	Multi-scan
Tmax Tmin,	0.9910 and 0.9790
Reflections collected	24664
Independent reflections	7991 [R(int) = 0.0485]
Refinement	
Data / restraints / parameters	7991 / 0 / 335
Goodness-of-fit on F^2	1.178
Final R indices	6670 data; I>2σ(I)
R.M.S. deviation from mean	0.052 $eÅ^{-3}$

V- Virtual screening study: Docking

V.1 .Docking principle:

In general, molecular docking is achieved through two steps. The first step is docking, which consists in searching for the appropriate ligand capable of improving interactions with the receptor using search algorithms that take into account the number of degrees of freedom, translation, and rotation of the ligand. Algorithms can be divided into three types: combinatorial or systematic search algorithms, stochastic or random search algorithms, and deterministic or simulation search algorithms [110-111].

The second is called "scoring," which is a mathematical method for giving a score or a numerical value to the degree of interaction of a ligand in a given pose (conformation) to its receptor based on calculations that take into account geometric complementarity, intermolecular distance, the number of hydrogen bonds established, electrostatic interactions, Van der Waals or even solvent energies [112].

These methods are used to estimate the interaction power and binding affinity of a ligand to its receptor in order to evaluate and differentiate, by a rapid calculation of the energy of the interaction, the correct conformations from the incorrect ones. In its broadest sense, the score functions approximate the free binding energy (ΔG_{bind}) resulting from the transition from the free form of the protein and ligand to the complex association. This energy is determined by calculating the free energies of ligand (G_{ligand}) protein ($G_{protein}$) and complex ($G_{complex}$) separately before making the difference according to the thermodynamic principle below [113-114].

$$\Delta G_{bind} = G_{complexe} - G_{ligand} - G_{protein}$$

At constant pressure and temperature, the free binding energy can also be calculated by the enthalpy (ΔH) and entropy (ΔS) variations of the Gibbs-Helmholtz equation system:

$$\Delta G_{bind} = \Delta H - T\Delta S$$

Docking can be interpreted qualitatively by observing the ligand entity in the protein cavity, but also quantitatively by processing data from scoring functions.

V.2. Results and discussion:

For docking studies, it is an important tool for virtual screening procedures and contains a library of compounds. The main objective of docking studies is to predict the activity of molecules before being tested experimentally or even before being synthesized and to obtain a fast method that is able to discover the novel lead compound (in virtual screening) or reproduce experimental conformation (for validation with experimental data) at the highest accuracy as possible. In our current work, due to the synthetic and biological tests were conducted before the theoretical study, but this does not prevent us from carrying out this study in order to find out if there is an interaction with the target and to test to understand the mechanism of action of the most active molecules.

The molecular docking of **173**, **174** and **177** ligands with protein topoisomerase II (PDB: 1JIJ) were studied with the help of the AutoDock Vina program [115] in this section. The receptor was selected from molecular docking studies of new benzimidazole derivatives study[116] and the 3D receptor structure were taken from protein data bank [117].

Here, the heteroatoms within the PDB: 1JIJ were cleared and polar hydrogens were inserted by using Discover Studio Visualizer 4.0 (DSV 4.0) [118] Additionally, the active residues of the PDB: 1JIJ were assigned as ASN199, GLN196, ASP195, GLY193, ASP177, GLN174, TYR170, ASP80, LEU70, HIS50, GLY49, ASP40, ALA39, GLY38, TYR36, then according to the active residue of protein, the grid parameters were identified as 68x62x50 $Å^3$ x, y, z dimensions, 0.375 Å space and -9.351, 14.724, 83.602 x, y, z centers. The next stage, over the

optimized structures of **173**, **174** and **177** ligands with DFT/B3LYP method and 6-311++G(d,p) basis level by utilizing torsion angles pdb and pdbqt forms were prepared, and docking computations were performed.

The obtained molecular docking scores were given in table 12. From the docking scores, the best binding energy was determined in the first mode as -9.1 kcal/mol energy, additionally, within table 12 the inhibition constants were presented as 0.213625 μM, 1.36759 μM and 1.1552 μM and the number of hydrogens bondings were found as 1, 1 and 0 for Compound **174**+1JIJ, Compound **173**+1JIJ and Compound **177**+1JIJ, respectively.

Here, inhibition constants were forum by using $K_i=\exp(\Delta G/RT)$ equation (ΔG is binding energy, $R=1.9872036\times10^{-3}$ kcal/mol and T=298.15 K).

Table 12: AutoDock Vina results of the binding affinity and RMSD values of different poses in topoisomerase II (PDB: 1JIJ) inhibitor of the title compounds **173**, **174** and **177**.

Mode	Compound **173**			Compound **174**			**Compound 177**		
	Affinity (kcal/mol)	rmsdl.b.	rmsdl.b.	Affinity (kcal/mol)	rmsdl.b.	rmsdl.b.	Affinity (kcal/mol)	rmsdl.b.	rmsdl.b.
1	-8.0	0.000	0.000	-9.1	0.000	0.000	-8.1	0.000	0.000
2	-8.0	2.840	6.734	-8.8	2.081	2.883	-8.0	2.646	6.904
3	-7.2	7.150	11.600	-8.7	15.615	18.665	-7.6	2.527	7.405
4	-7.2	15.583	17.806	-8.6	1.806	6.720	-7.6	2.931	7.649
5	-7.2	21.326	22.527	-8.2	15.152	18.324	-7.5	1.691	2.241
6	-7.0	21.905	23.609	-8.2	15.037	17.901	-7.2	21.288	23.654
7	-7.0	23.824	25.657	-8.2	7.142	11.296	-7.1	15.940	18.991
8	-7.0	15.823	18.607	-8.1	4.592	6.944	-7.0	16.058	19.099
9	-6.8	23.994	25.804	-8.1	22.284	24.451	-7.0	2.173	7.416
10	-6.7	21.806	23.131	-8.0	1.849	7.035	-6.9	7.059	11.359
Inhibition constant: 1.36759 μM **Hydrogen bonding**: 1				**Inhibition constant**: 0.213625 μM **Hydrogen bonding**: 1			**Inhibition constant**: 1.1552 μM **Hydrogen bonding:** 0		

Furthermore, the docking situations within the protein were shown in **figure 40**.

Finally, the (**a**) 3D and (**b**) 2D molecular docking results, figures 41–43 depict the various types of interactions and possible bonding.

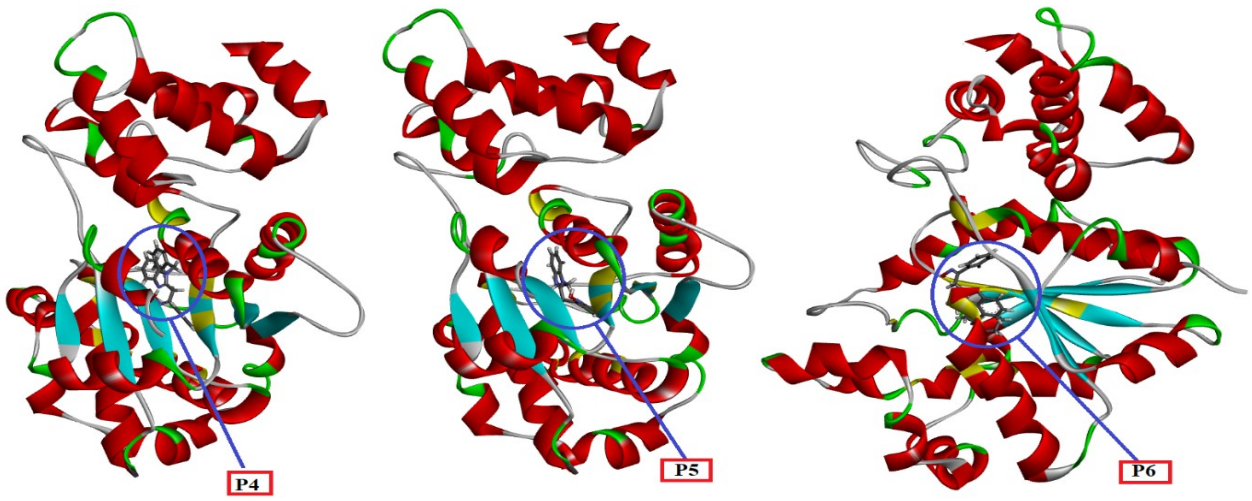

Figure 40. The three-dimensional structure of 1JIJ protein with the title molecules **174**, **173** and **177**

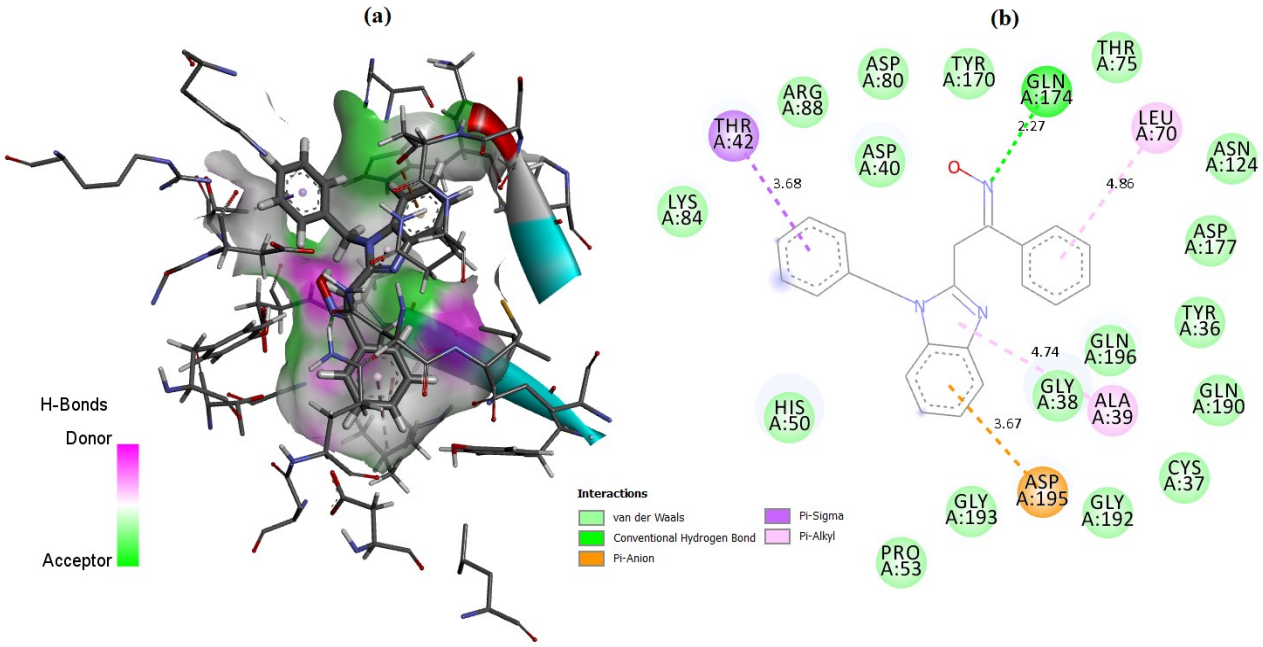

Figure 41. (a) 3D and (b) 2D molecular docking results of the 1JIJ+compound **174**

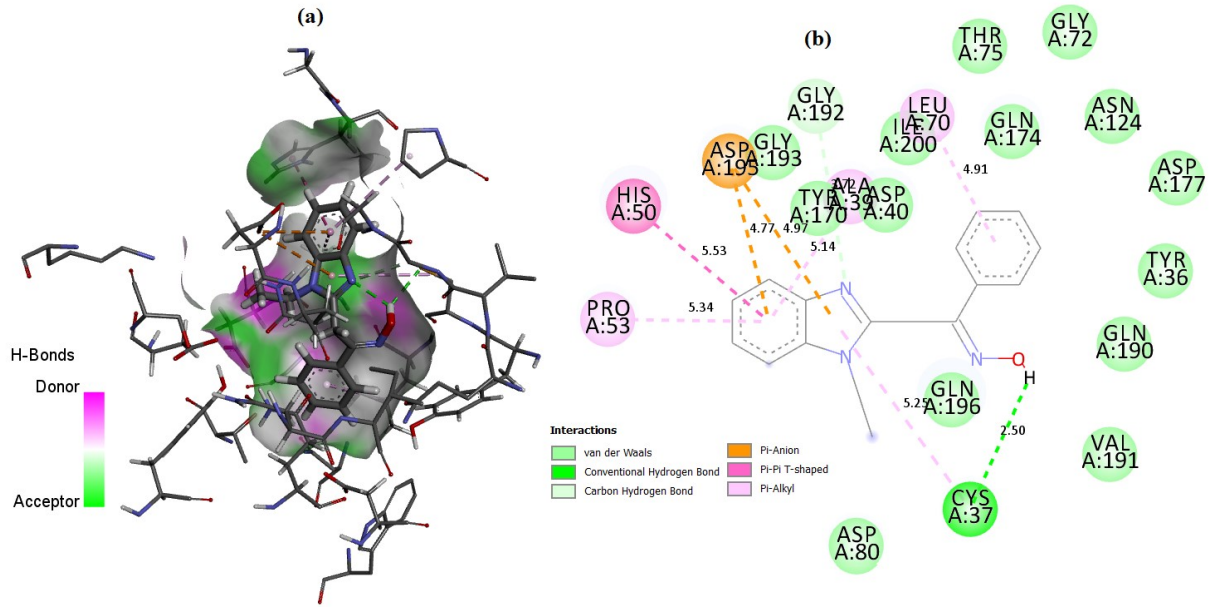

Figure 42. (a) 3D and (b) 2D molecular docking results of the 1JIJ+ compound **173**.

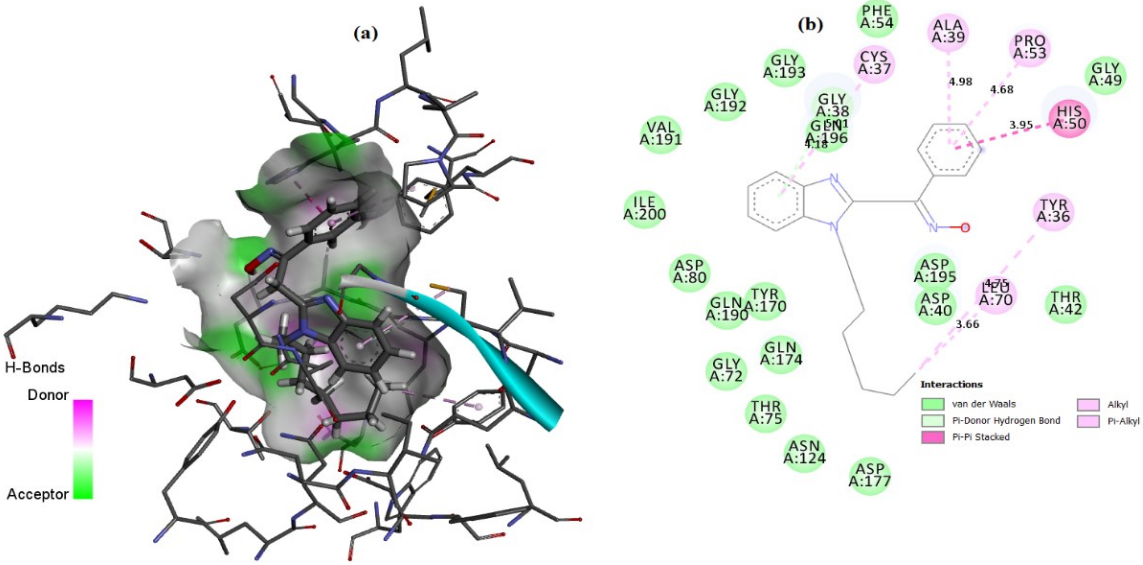

Figure 43. (a) 3D and (b) 2D molecular docking results of the 1JIJ+ compound **177**

Conclusion:

New heterocyclic benzimidazole derivatives have been successfully synthesized and characterized by single-crystal X-ray diffraction and selected spectroscopic techniques (^{1}H NMR and ^{13}C NMR).

Molecular docking studies, Hirschfield surface analysis, and electrostatic potential (ESP) plots show that the main intermolecular contact is between the hydrogen atoms in a heteroatom.

Experimental part

V.1. Chemical Analysis

The spectroscopic characterizations of the synthesized compounds **(173-181)** were achieved by recording NMR spectra: ^{1}H-NMR (300 MHz) and ^{13}C-NMR (75 MHz), respectively, which were measured on Bruker Avance DPX 300 instruments. Melting points of compounds **173**–**181** were determined in open capillaries. The chemical shifts (**δ**) were expressed in ppm and the coupling constants (J) in Hertz (Hz), downfield from TMS (tetramethylsilane, $Si(CH_3)_4$), which has been assigned a chemical shift of zero, using (TMS) as an internal reference.

V.2. Procedure of Synthesis compounds (173-181)

In a round flask (100 ml), a solution of N1-alkyl-4-phenyl-1,5-benzodiazepine-2-thiones (1-7) (4 mmol) in ethanol (40 ml) and 2 equivalents of hydroxylamine hydrochloride were added. A mixture was refluxed for 24 h with a magnetic stirrer. After cooling at room temperature, the precipitated compound was filtered and washed with 20 ml of cold ethanol.

(E)-2-(1-ethyl-1H-benzimidazol-2-yl)-1-phenylethanone oxime: 173

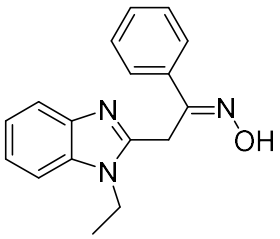

[M= 279.14 g/mol]

Yield = 85%**; F (°C)** = 110-112

^{1}HNMR (300 MHz, DMSO-d$_6$) δ ppm: 1.32 (t, 3H, C**H$_3$**, *J*= 6 Hz), 4.32 (q, 2H, C**H$_2$**-N, *J*= 6 Hz), 4.42 (s, 2H, C**H$_2$**), 7.10-7.81 (m, 9H, **H$_{ar}$**), 11.70 (s, 1H, O**H**).

^{13}CNMR (75 MHz, DMSO-d$_6$) δ ppm: 14.69 (**C**H_3), 23.90 (**C**H_2), 37.82 (**C**H_2), 109.77-128.72 (**C**Har), 135.74-155.77 (**Cq**).

(E)-2-(1-benzyl-1H-benzimidazol-2-yl)-1-phenylethanone oxime: 174

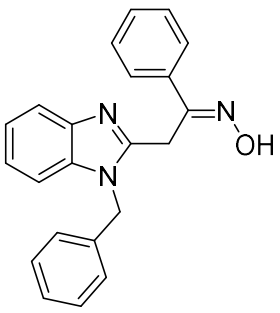

[M= 341.15 g/mol]

Yield = 88%**; F (°C)** = 102-104

^{1}HNMR ((CDCl$_3$ 500 MHz)) δ ppm: 4.36 (s, 2H, C**H$_2$**), 5.54 (s, 2H, C**H$_2$**), 6.96-7.63 (m, 14H, **H$_{Ar}$**), 11.61 (s, 1H, O**H**).

^{13}CNMR (CDCl$_3$ 125 MHz) δ ppm: 24.6 (**C**H$_2$), 46.8 (**C**H$_2$), 110.79-129.23(**C**Har), 135.71-152.08 (**C**q).

(E)-2-(1-octyl-1H-benzimidazol-2-yl)-1-phenylethanone oxime: 177

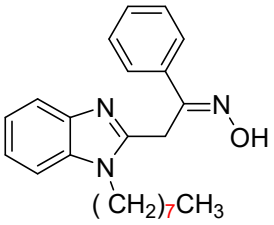

[M= 363.23 g/mol]

Yield = 80%**; F (°C)** = 115-117

^{1}HNMR (CDCl$_3$ 500 MHz) δ ppm: 0.85 (t, 3H, C**H$_3$**, J= 6.9 Hz), 1.23-1.75 (m, 12H, C**H$_2$**), 4.25 (t, 2H, C**H$_2$**-N, J= 7.2 Hz), 4.42 (s, 2H, C**H$_2$**), 7.08-7.81 (m, 9H, **H$_{Ar}$**), 11.73 (s, 1H, O**H**).

^{13}CNMR (CDCl$_3$ 125 MHz) δ ppm: 14.40 (**C**H$_3$),), 22.55-43.46 (**C**H$_2$), 110.44-129.18 (CHar), 135.44-152.18 (**Cq).**

(E)-2-(1-decyl-1H-benzimidazol-2-yl)-1-phenylethanone oxime: 178

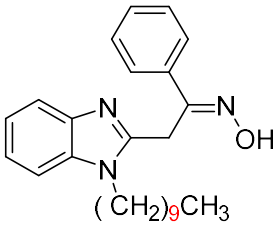

[M= 391.26 g/mol]

Yield = 79%**; F (°C)** = 96-98

^{1}HNMR (300 MHz, CDCl$_3$) δ ppm : 0.92 (t, 3H, C**H$_3$**, J= 6.9 Hz), 1.24-1.78 (m, 16H, C**H$_2$**), 4.23 (t, 2H, C**H$_2$**-N, J= 7.2 Hz), 4.77 (s, 2H, C**H$_2$**), 7.25-7.94 (m, 9H, **H$_{Ar}$**), 12.52 (s, 1H, O**H**).

^{13}CNMR **(75 MHz, CDCl$_3$)** δ ppm **:** 14.13 (**C**H$_3$),22.69-43.92 (**C**H$_2$), 109.59-129.05 (**C**Har), 135.06-152.71 (**Cq**).

(E)-2-(1-dodecyl-1H-benzimidazol-2-yl)-1-phenylethanone oxime: 179

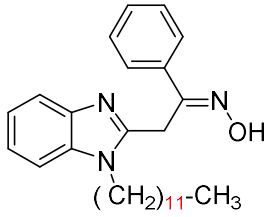

[M= 419.29 g/mol]

Yield = 87%**; F (°C)** = 108-110

^{1}HNMR (300 MHz, $CDCl_3$) δ ppm: 0.92 (t, 3H, C**H**$_3$, J= 6.9 Hz), 1.24-1.76 (m, 20H, C**H**$_2$), 4.19 (t, 2H, C**H**$_2$-N, J= 7.1 Hz), 4.70 (s, 2H, C**H**$_2$), 7.23-7.88 (m, 9H, **H**$_{Ar}$).

^{13}CNMR **(75 MHz, $CDCl_3$)** δ ppm **:** 14.13 (**C**H_3), 22.71-43.93 (**C**H_2), 109.57-129.10 (**C**Har), 134.95-152.33 (**C**q).

(E)-2-(1-octadecyl-1H-benzimidazol-2-yl)-1-phenylethanone oxime: 181

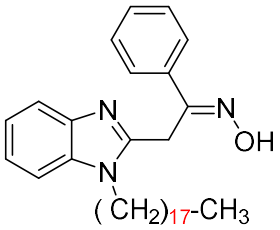

[M= 503.39 g/mol]

Yield = 95%**; F (°C)** = 96-98

^{1}HNMR (300 MHz, $CDCl_3$) δ ppm: 0.88 (t, 3H, C**H**$_3$, J= 6.9 Hz), 1.22-1.78 (m, 32H, C**H**$_2$), 4.15 (t, 2H, C**H**$_2$-N, J= 7.1 Hz), 4.61 (s, 2H, C**H**$_2$), 7.19-7.82 (m, 9H, **H**$_{Ar}$), 10.71 (s, 1H, O**H**).

^{13}CNMR (75 MHz, $CDCl_3$) δ ppm: 14.12 (**C**H_3), 22.70-43.91(**C**H_2), 109.47 - 129.21 (**C**H_{ar}), 135.08 - 152.95 (**Cq**).

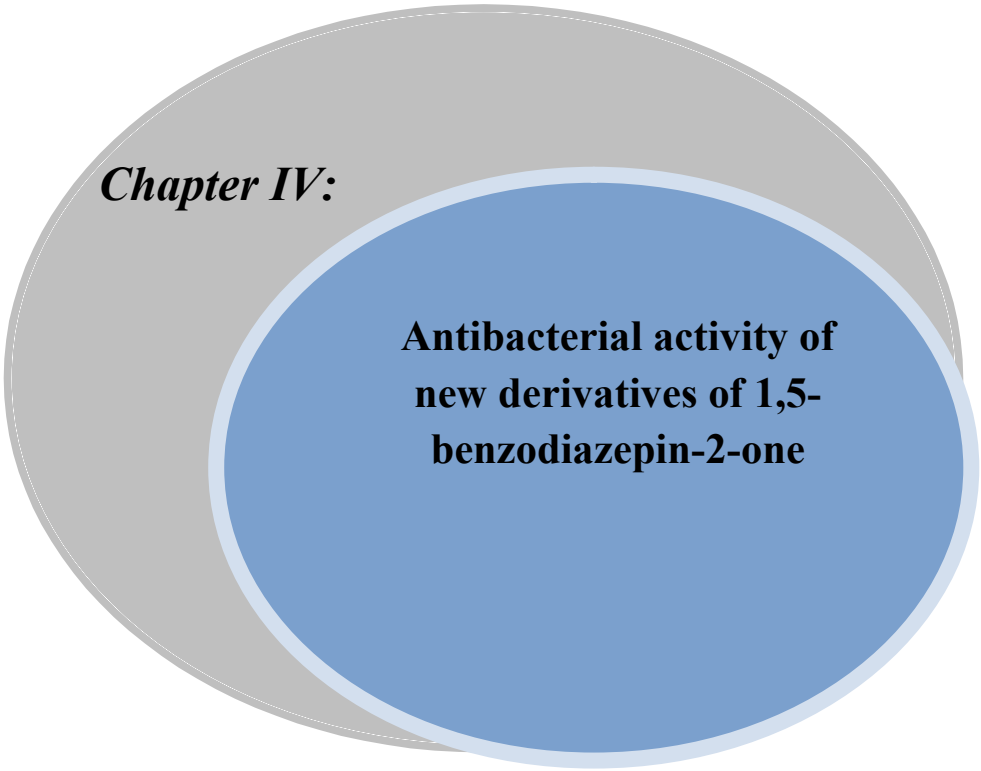
Chapter IV:
Antibacterial activity of new derivatives of 1,5-benzodiazepin-2-one

I- Introduction

Bacteria are microorganisms that are indispensable to humans and the environment as they play a vital role in almost all ecosystems through their participation in the biogeochemical cycles of matter. It can also be the cause of many infectious diseases. Therefore, some micro-organisms can be pathogenic and cause diseases in humans, plants, or animals. With the gradual emergence of pathogenic bacteria, antimicrobial resistant infections are becoming more frequent and increasingly difficult to treat, and as a result, antimicrobial resistance is now considered a growing health threat worldwide [119].

For this reason, the chemical synthesis of new molecules continues to produce new antibacterial agents that can contribute to the fight against the antibiotic crisis. And in order to valorize the 1,5-benzodiazepine and benzimidazole derivatives, which we have described in the previous chapters, the antibacterial evaluation of some synthesized 1,5-benzodiazepin-2-one **113, 114, 115, 116, 119, 120, 121**, 1,5-benzodiazepine-2-thione, **123, 126, 127, 128, 129, 130, 131** and benzimidazole **174, 177, 178, 179, 180, 181** derivatives towards different bacterial strains will be developed.

In vitro antibacterial evaluation against bacteria: *Escherichia coli ATCC 4157*, *Pseudomonas aeruginosa ATCC 27853*, *Staphylococcus aureus ATCC 25923*, *Streptococcus fasciens 29212* of some heterocyclic compounds derived from 1,5-benzodiazepine-2-one **113, 114, 115, 116, 119, 120, 121**, 1,5-benzodiazepine-2-thione, **123, 126, 127, 128, 129, 130, 131** and benzimidazole **174, 177, 178, 179, 180, 181** was carried out in the laboratory of Biochemistry and Immunology of the Faculty of Sciences of Rabat.

A brief overview of bacterial strains, antibiotics, and bacterial sensitivity techniques will be given, before presenting the results of this study.

II- Materials

II.1 Bacterial strains

Bacteria are microscopic organisms of various types. They have a chemically distinct cell wall, which gives them a particular shape: spherical, rod-shaped, or spiral. Bacteria multiply by cell division, a process that can occur every 20-30 minutes. Thus, a single bacterium that enters the body and multiplies at this rate can produce up to 30 billion or more new cells in 12 hours. Fortunately, most bacteria are harmless, and some are essential, such as those in the gut that aid digestion. A few of them, known as pathogens cause disease, and infectious diseases caused by pathogenic bacteria, are a public health problem that relies mainly on the use of antibiotics. In recent years, however, multi-drug resistant strains have emerged in several regions of the world.

4 reference strains:

√ *Escherichia coli ATCC*

- **Famille**: Enterobacteriaceae

- Gram bacille ⊖

- **Biochemical characteristics**: No deaminase
  Fermentation of glucose
  Fermentation of lactose, mannitol
  Production of indole from tryptophan
  No urease
  No H_2S.

√ *Pseudomonas aeroginosa ATCC*

- **Family**: Pseudomonaceae

- Gram bacille ⊖

- **Biochemical characteristics**: Strictly aerobic
  Oxidase positive
  Production of water soluble blue or pyocyanine pigment
  Fructose positive (methyl red)
  Lactose and H2S negative.

√ *Staphylococcus aureus ATCC*

- **Family**: *Staphylococcaceae*

- **Gram shells** ⊕

- **Biochemical characteristics**: Presence of catalase
  Absence of oxidase
  Fermentation of glucose
  Has coagulase
  Fibrinogen receptor

√ *Streptococcus fasciens ATCC*

- **Family**: *Streptococcaceae*

- **Gram shells** ⊕

- **Biochemical characteristics**: Esculin positive
  Resistance 30 minutes at 60°C
  Grow in broth with 40% bile
  Bile-esculin medium of choice

II.2. Tested products:

The tested products are 1,5-benzodiazepin-2-one **113**, **114**, **115**, **116**, **119**, **120**, **121** (figure44), **123**, **126**, **127**, **128**, **129**, **130**, **131** (figure 45) and benzimidazole **174**, **177**, **178**, **179**, **180**, **181** (figure46) derivatives synthesized in the Heterocyclic Organic Chemistry Laboratory of the Faculty of Sciences-Rabat, (figure 44, 45 and 46).

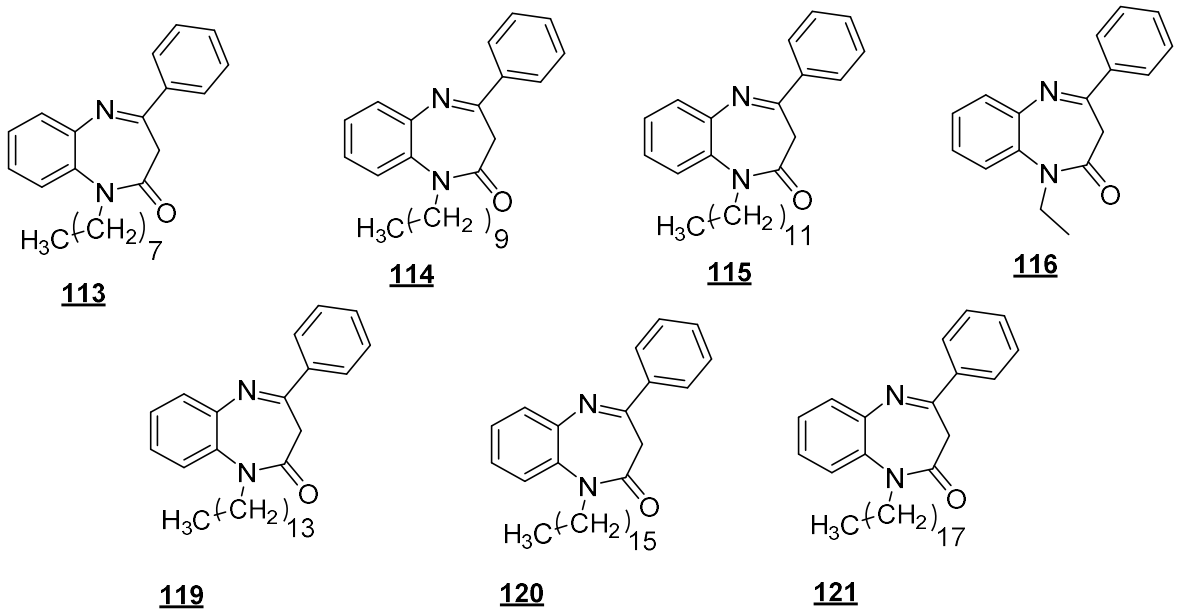

Figure 44: *Structure of the tested molecules 1,5-benzodiazepine*-2-àne **113**, **114**, **115**, **116**, **119**, **120**, **121**

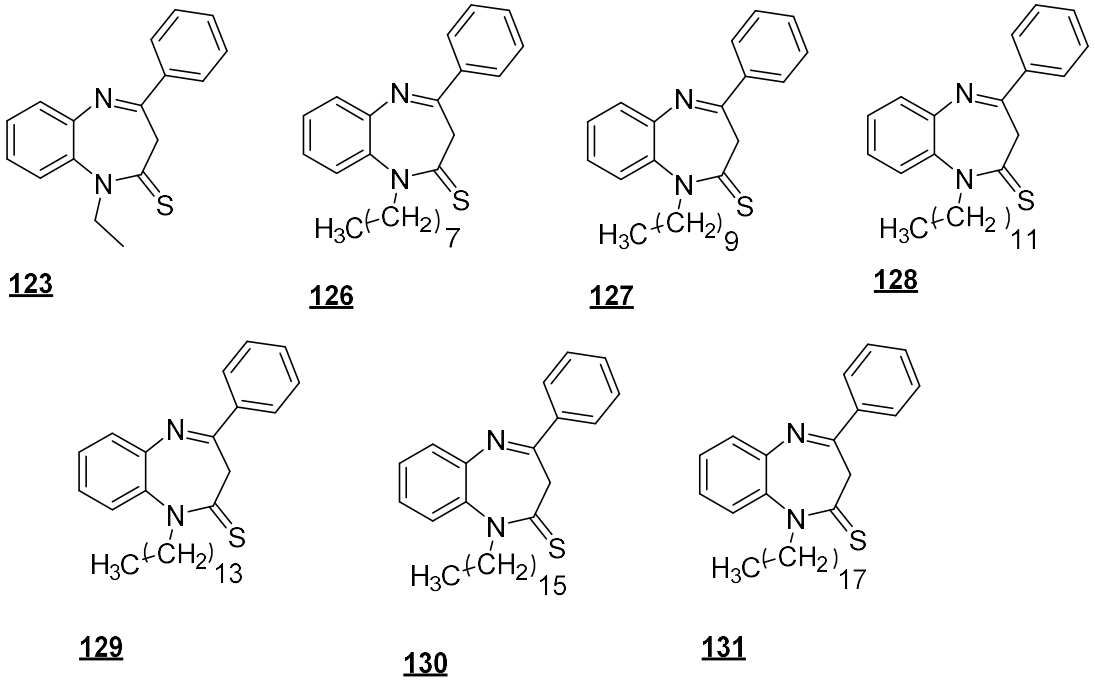

Figure 45: *Structure of the tested molecules 1,5-benzodiazepine*-2-thione **123**, **126**, **127**, **128**, **129**, **130**, **131**

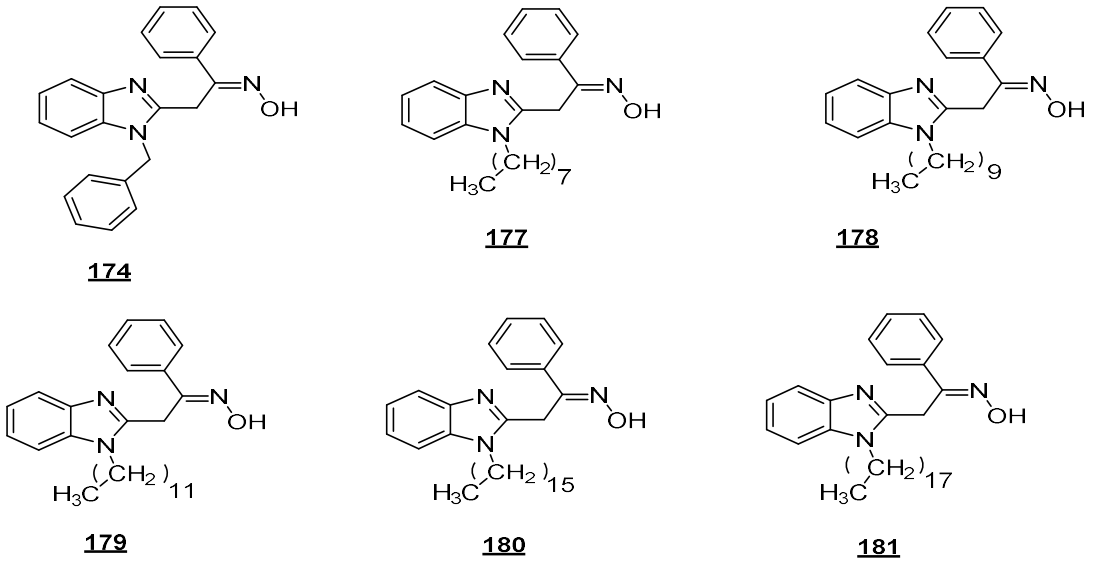

Figure 46*: Structure of the tested molecules* benzimidazole **174, 177, 178, 179, 180, 181**

III. Method for studying bacterial sensitivity to antibiotics:

The study of the sensitivity of a bacterial strain to antibiotics consists of putting the bacteria in the presence of antibiotics and observing the consequences on the development and survival of the bacterial culture.

The two methods commonly used to determine the sensitivity of the bacterial strain to antibiotics are [120-121]:

- The liquid dilution method (MIC).
- The agar diffusion method (antibiogram).

III.1 Liquid dilution method:

In this method, a series of hemolytic tubes are prepared in which the same quantity of nutrient broth inoculated with the germ to be studied is distributed, and then an increasing quantity of the molecule to be tested is distributed into each tube, except first tube, it will serve as a control, and produce a range of concentration in geometric progression of reason 2.

These tubes are placed in an oven at 37°C, then, after 24 hours of incubation, they are observed macroscopically, where the first tube in which there is no visible culture indicates the minimum inhibitory concentration.

III.2 Agar diffusion method (antibiogram):

It consists of inoculating the surface of a solid medium by flooding with the strain to be tested, then placing blotting paper discs containing an antibiotic at a certain concentration.

A gradient of antibiotic concentration is established in the agar around each disc. After 24 hours of incubation at 37°C, the discs appear surrounded by a zone of inhibition, the diameter of which is measured in mm; it will be possible to calculate the MIC of the antibiotic for the

strain examined by plotting this diameter on the concordance curve previously established with strains of different susceptibilities.

Susceptibility testing may be recommended in the following situations:

- Epidemiological study in reference laboratories to obtain data on the sensitivity of germs and to monitor trends in drug resistance.
- STI laboratories with a large number of tests to perform as part of monitoring the clinical efficacy of the treatment protocol.
- Investigation of new antimicrobial agents.
- Informing the clinician in case of treatment failure.

In our work, we used the solid dilution method for MIC determination; the strain was inoculated by spot.

The present part of the work is devoted to the evaluation of the sensitivity of bacteria to 1,5-benzodiazepine-2-one derivatives **113, 114, 115, 116, 119, 120, 121** (figure 44), 1,5-benzodiazepine-2-thione derivatives **123, 126, 127, 128, 129, 130, 131** (figure45) and benzimidazole **174, 177, 178, 179, 180, 181** (figure 46). This family of compounds is one of the heterocycles that have received the most attention, due to their multiple applications in a wide range of fields, including medicine.

Culture media and solvents:

The media used for the maintenance of the strains and the study of bacterial sensitivity to the products tested are Brain Heart Infusion (BHI) medium and Mueller Hinton Agar (MHA) medium, which are standardized by the World Health Organization (WHO) for the determination of the sensitivity of bacteria to antibiotics.

Composition of the culture media

Mueller Hinton Agar medium:

Infusion of 300 g beef (dehydrated)
Casein hydrolysate 17.5 g
Starch 1.5 g
Agar 10 g
Distilled water 1000 ml
Final pH 7.4

Brain Heart Infusion:

Proteose peptone 10 g
Veal brain infusion 125 g
Beef heart infusion 5 g

Sodium chloride 5 g

Sodium phosphate 2.5 g

Glucose 2 g

Distilled water 1000 ml

Final pH 7.4

Solvents used for the reconstitution of the products used:

-Dimethyl sulfoxide (DMSO)

-Physiological water 9 g/1000 ml

-Distilled water

III.3. Determination of the diameters of the zone of inhibition:

Sensitivity to 1,5-benzodiazepine-2-one derivatives **113, 114, 115, 116, 119, 120, 121** (figure44), 1,5-benzodiazepine-2-thione derivatives **123, 126, 127, 128, 129, 130, 131** (figure 45) and benzimidazole **174, 177, 178, 179, 180, 181** (figure46) derivatives was studied by the solid-state diffusion method (disc method), which allows the sensitivity of fast-growing bacteria to a range of antibiotics to be determined.

It is based on the diffusion of test substances along a concentration gradient, different dilutions of the test molecules were prepared in 1% DMSO: 500, 250, 125, 62.5, 31.2, and 15.6 µg/ml.

Preparation of the inoculums:

From a pure 24 h culture on isolation medium a bacterial suspension in sterile physiological water (0.9%) was prepared, and its opacity must be equivalent to an optical density of 0.08 to 0.10 at 625 nm. For solid-state diffusion methods, the bacterial suspension is diluted to 1/100.

Preparation of stock solutions of the products:

Stock solutions are prepared by dissolving the equivalent weight of 22 mg of active ingredient in the minimum volume of the appropriate solvent (0.44 ml), the final volume is adjusted to 44 ml with distilled water.

These stock solutions contain the test agent at the concentration of 500 µg / ml, which allows the preparation of the working solutions.

Seeding:

Inoculation is done by the Kirbey-Baur method, by swabbing.

- Dip a sterile swab into a bacterial suspension and allow it to soak.
- Remove it from the tube by gently wiping it on the wall.

- Inoculate the Muller-Hinton plate with a 4 mm thick agar by rubbing the swab on its surface and turning the plate 3 times by 60° to ensure a good distribution of the inoculum.
- Allow the plates to dry for 15-20 min

Incubate:

The plates in an oven at 37°C for 24 hours

Reading:

For each strain, and for each antibiotic: Measure with precision in millimeters the diameter of the zone of inhibition, the results of the antibiogram indicate whether the bacterium is Susceptible (S), Intermediate (I) or Resistant (R) to the antibiotic.

Antibacterial activity is considered positive from a diameter greater than 6 mm. It is generally assessed as follows: Very High activity: diameter ≥20 mm; Good activity: diameter between 16-19 mm; Medium activity: diameter between 11-15 mm; Low activity: diameter ≤10 mm.

III.4. Determination of the Minimum Inhibitory Concentration (MIC):

Experimental protocol:

The antibacterial tests of our products were carried out by the gel diffusion method.

- Set up a series of sterile tubes for each strain, each containing 9 ml of nutrient broth.
- Prepare a bacterial suspension with an optical density of 0.08 to 0.01 at 625 nm.
- Dispense 9 ml of this seeded medium into the individual tubes.
- Add 1 ml of each dilution of the antibiotic to the different tubes, tube number "1" receives no antibiotics and serves as a control.
- After 24 hours of incubation at 37°C, the presence of cloudiness in the control tube validates the test.
- The reading is taken by eye and the Minimum Inhibitory Concentration (MIC) is the lowest concentration of antibiotic that inhibits any visible growth of a bacterial strain after 24 hours incubation at 37°C. The MIC is indicated by the tube containing the lowest concentration of antibiotic where no growth is visible.

IV. Results and interpretation

Table13 and figure47 show the diameters of the inhibition zones of the tested synthetics against different gram negative and gram-positive bacteria.

Table13: show the diameters of the inhibition zones of the tested synthetics against different gram negative and gram-positive bacteria

Products	*Escherichia coli*	*Pseudomonas aeruginosa*	*Staphylococcus aureus*	*Streptococcus fasciens*
113	**19.25**	**15.3**	**13.7**	**11.75**
114	**14.6**	**11.3**	**13.8**	**23.1**
115	**13.25**	**19.05**	**14.7**	**10.55**
116	**12.7**	**11.5**	**12.15**	**10.7**
119	**13.8**	**17.25**	**19.05**	**11.25**
120	**18.95**	**15.2**	**18.75**	**14.75**
121	**15.05**	**18.85**	**23.85**	**13.85**
123	**15.75**	**17.5**	**19.95**	**10.8**
126	**23.75**	**10.05**	**21.05**	**15**
127	**22.4**	**14.3**	**13.7**	**15.1**
128	**9.7**	**13.1**	**17.25**	**19.2**
129	**11.75**	**12.4**	**19.2**	**17.7**
130	**14.3**	**14.8**	**20.4**	**24.85**
174	**12**	**12.9**	**13.2**	**10.45**
177	**11.75**	**14.2**	**14.3**	**15.75**
178	**9.65**	**10.75**	**13.5**	**23.8**
179	**13.75**	**11.3**	**14.75**	**14.8**
180	**11.85**	**12.25**	**10.75**	**11.7**
181	**11.85**	**13.75**	**16.15**	**16.4**
DMSO 1%	**0**	**0**	**0**	**0**
Amp	**11.55**	**10.2**	**11.15**	**11.15**
Chlor	**24.15**	**20**	**19.85**	**25.7**

Chlor= Chloramphenicol (30µg/mL), **DMSO=** Dimethylsulfoxide (1%), **Amp=** Ampicillin

The results are presented in the form of antibiograms below for 1,5-benzodiazepin-2-one derivatives **113**, **114**, **115**, **116**, **119**, **120**, **121** (figure 44),1,5-benzodiazepine-2-thion derivatives **123**, **126**, **127**, **128**, **129**, **130**, **131** (figure 45) and benzimidazole **174**, **177**, **178**, **179**, **180**, **181** (figure 46):

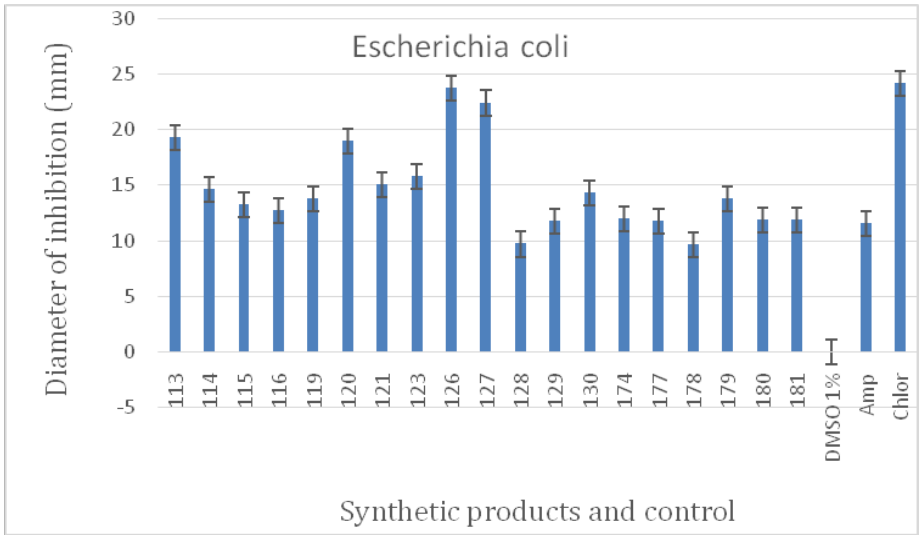
Escherichia coli
Diameter of inhibition (mm)
30
25
20
15
10
5
0
-5
113
114
115
116
119
120
121
123
126
127
128
129
130
174
177
178
179
180
181
DMSO 1%
Amp
Chlor
Synthetic products and control

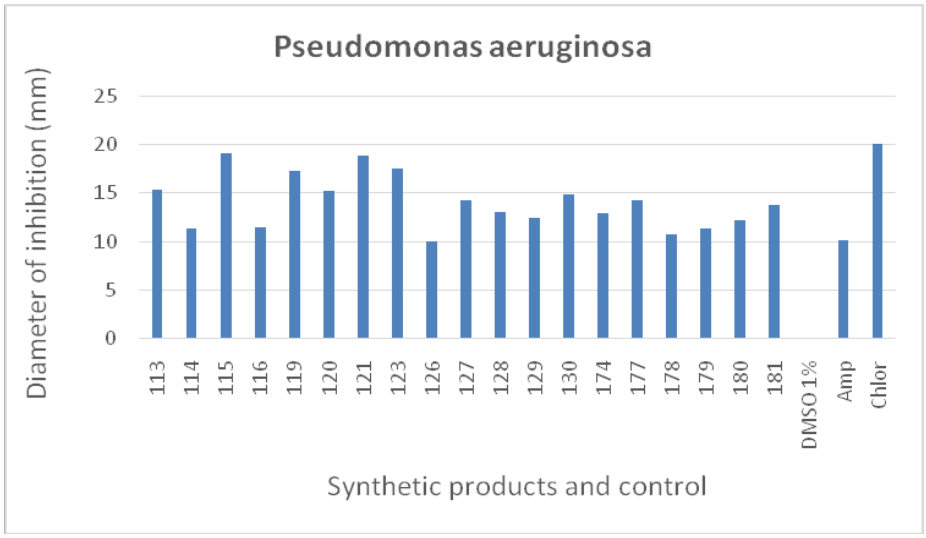
Pseudomonas aeruginosa
Diameter of inhibition (mm)
25
20
15
10
5
0
113
114
115
116
119
120
121
123
126
127
128
129
130
174
177
178
179
180
181
DMSO 1%
Amp
Chlor
Synthetic products and control

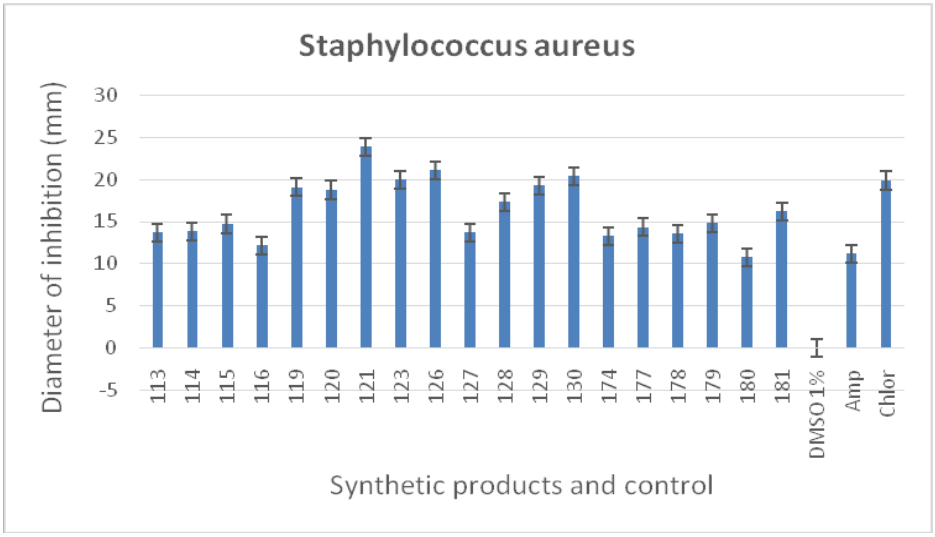
Staphylococcus aureus
Diameter of inhibition (mm)
30
25
20
15
10
5
0
-5
113
114
115
116
119
120
121
123
126
127
128
129
130
174
177
178
179
180
181
DMSO 1%
Amp
Chlor
Synthetic products and control

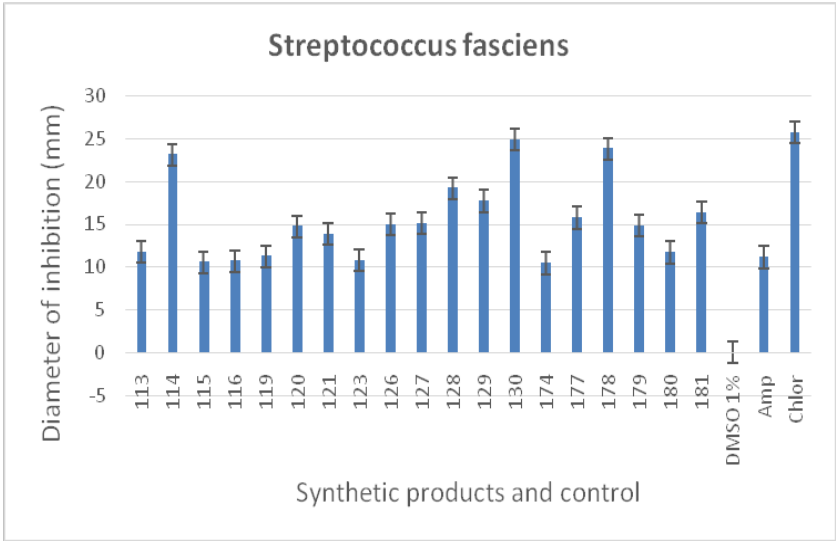

Figure 47: shows the diameters of the inhibition zones of the tested synthetics against different gram negative and gram-positive bacteria

The results of the antibacterial activity for the synthesis 1,5-benzodiazepine derivatives against the tested bacteria (*Escherichia coli ATCC 4157, Pseudomonas aeruginosa ATCC 27853, Staphylococcus aureus ATCC 25923, Streptococcus fasciens 29212*) are summarized in the figure above.

According to the results obtained, the products tested seem to have an inhibitory activity on certain classes of micro-organisms tested. Among the products that showed a Very High activity:

√ Molecule **126** shows a Very High activity towards the bacterial strain *Escherichia coli* with an inhibition zone diameter of 23.75 mm.

√ Molecule **121** showed Very High activity against the bacterial strain *Staphylococcus aureus* with an inhibition zone diameter of 23.85 mm.

√ Molecule **130** shows a Very High activity against the bacterial strain *Streptococcus fasciens* with an inhibition zone diameter of 23.85 mm (table 13).

√Molecule **178 and 114** shows a Very High activity against the bacterial strain *Streptococcus fasciens* with an inhibition zone diameter of: 23.8 mm,23.1mm

The MIC study was carried out by the solid-state dilution method against different bacterial strains. The results of the three series tested are shown in table 14.

Table 14: shows minimum inhibition concentration (µg/ml) of molecules synthesized against different bacterial strains.

	MIC (mg/ml)			
	E. coli	***P. aeruginosa***	***S.aueus***	***S. fasciens***
113	**5**	**10**	**5**	**10**
114	**10**	**5**	**5**	**10**
115	**10**	**5**	**5**	**20**
116	**10**	**5**	**10**	**20**
119	**10**	**10**	**10**	**5**
120	**5**	**10**	**10**	**20**
121	**10**	**10**	**10**	**20**
123	**10**	**5**	**5**	**5**
126	**10**	**20**	**10**	**5**
127	**10**	**10**	**5**	**5**
128	**20**	**10**	**5**	**5**
129	**5**	**10**	**10**	**10**
130	**5**	**10**	**5**	**10**
131	**10**	**20**	**10**	**5**
174	**20**	**20**	**20**	**20**
177	**20**	**20**	**20**	**20**
178	**10**	**20**	**10**	**10**
179	**10**	**10**	**10**	**10**
180	**10**	**20**	**10**	**5**
181	**10**	**10**	**10**	**10**
DMSO	**0**	**0**	**0**	**0**
Chlo	**6.25**	**6.25**	**12.5**	**12.5**

Antibacterial activity of 1,5-benzodiazepine derivatives **113**, **114**, **115**, **116**, **119**, **120**, **121** and **123**, **126**, **127**, **128**, **129**, **130**, **131** and benzimidazole **174**, **177**, **178**, **179**, **180**, **181**, represented in minimum inhibitory concentration [MIC (µg/mL)].

In vitro antibacterial evaluation against the bacteria *Escherichia coli ATCC 4157, Pseudomonas aeruginosa ATCC 27853, Staphylococcus aureus ATCC 25923, Streptococcus*

fasciens 29212 of this study determined the minimum inhibitory concentration (MIC) of certain synthesized derivatives of 1,5-benzodiazepine derivatives **113, 114, 115, 116, 119, 120, 121, 123, 126, 127, 128, 129, 130, 131 ,** and benzimidazole **174, 177, 178, 179, 180, 181.** (table14).

The results of the antibacterial activity of the tested products **113 , 120, 129, and 130** showed good activity against *E. coli* at MIC = 5 µg / ml, and on the other hand the compounds (**114**, **115**, **116**, and**123**), which is essentially observed, exhibits good growth inhibiting activity in the bacterial strain tested: *P. aeruginosa* at MIC = 5 µg / ml.

Likewise for the seven products (**113**, **114**, **115**, **123**, **127**, **128**, and **130**) against the *S. aureus* strain, finally for the compounds (**119**,**123**, **126**, **127**, **128**, **131**, and **180**) against the bacterial strain *S. fasciens* at MIC = 5 µg / ml.

In general, the molecular specifications of 1,5-benzodiazepine and benzimidazole derivatives are an important class of heterocycles widely used in pharmaceutical and therapeutic fields such as insecticides, antibacterial, antibiotics, antitumor, antioxidant and antifungal, anti-tuberculosis drugs, and ulcerogenic [122-128].

Conclusion:

In this chapter, we showed the evaluation of the antibacterial activity of some synthetic 1,5-benzodiazepin-2-one derivatives **113, 114, 115, 116, 119, 120, 121 and 123, 126, 127, 128, 129, 130, 131** and benzimidazole **174, 177, 178, 179, 180, 181.**

The antibacterial activity was evaluated in vitro against different gram-positive and gram-negative strains.

In fact, the best activity was recorded against the bacteria: *Streptococcus fasciens* 29212 and *Staphylococcus aureus ATCC 25923* at a minimum inhibitory concentration of 5µg/ml with the compounds **119**, **123**, **126**, **127**, **128**, **131**, and **180**, also **113**, **114**, **115**, **123**, **127**, **128**, and **130** compared to that of chloramphenicol as a reference standard to evaluate the effectiveness of these synthetic compounds.

I- Introduction

Organic chemistry is a very large field of chemistry and is divided into several families. It allows the synthesis of new substances that have biological activities that are used in the pharmaceutical industry. 1.5-benzodiazepine and its derivatives constitute an important class of these heterocyclic compounds, possessing a wide range of biological properties [129-132]. Syntheses of new heterocyclic compounds still continue because they have important applications in the pharmaceutical industry [133], as well as the agrochemical industry. Derivatives of 1.5-benzodiazepine have been exploited in agrochemistry [134, 135], in biology, and in medicinal chemistry, and several methods for their synthesis have been described [6,136-139].

The review of literature data indicates little work on the synthesis of 1,5-benzodiazepin-2-one derivatives from the condensation of 1,2-diamino-cyclohexane and 1,3-dicarbonyl compounds.

Thus, Babu *et al.* [140–141] prepared the 5-benzyl-4-aryl-octahydro-1*H*-1,5-benzodiazepin-2-one derivatives **184a-d** via a selective Beckmann rearrangement of the intermediate oximes **183 a-d** with thionyl chloride in dry ether, as described (scheme 68).

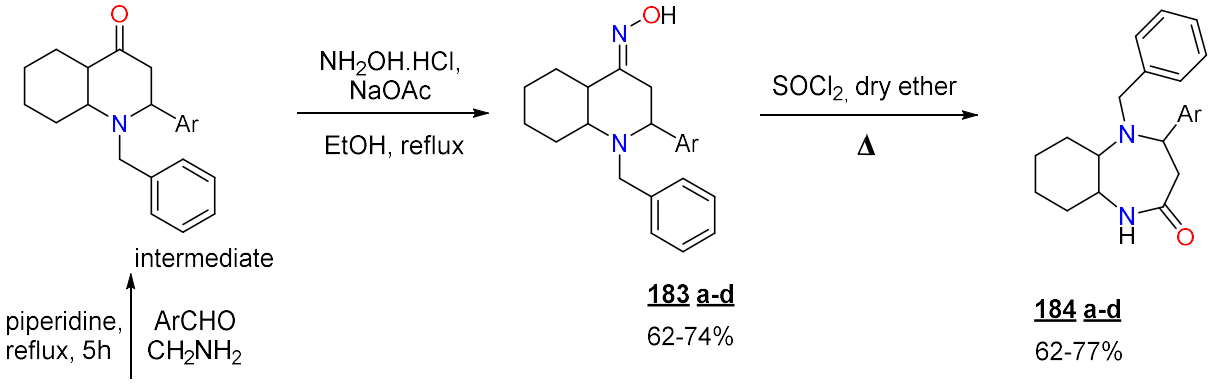

- Scheme 68 –

Dalai *et* al. [142] developed a simple and convenient one-pot method for the reductive *N*-alkylation of (R,R)-trans-1,2-diaminocyclohexane by prochiral ketones using the $Ti(OiPr_4)/NaBH_4$ system to obtain the corresponding alkyl amine derivative **188** under conditions described in scheme 69.

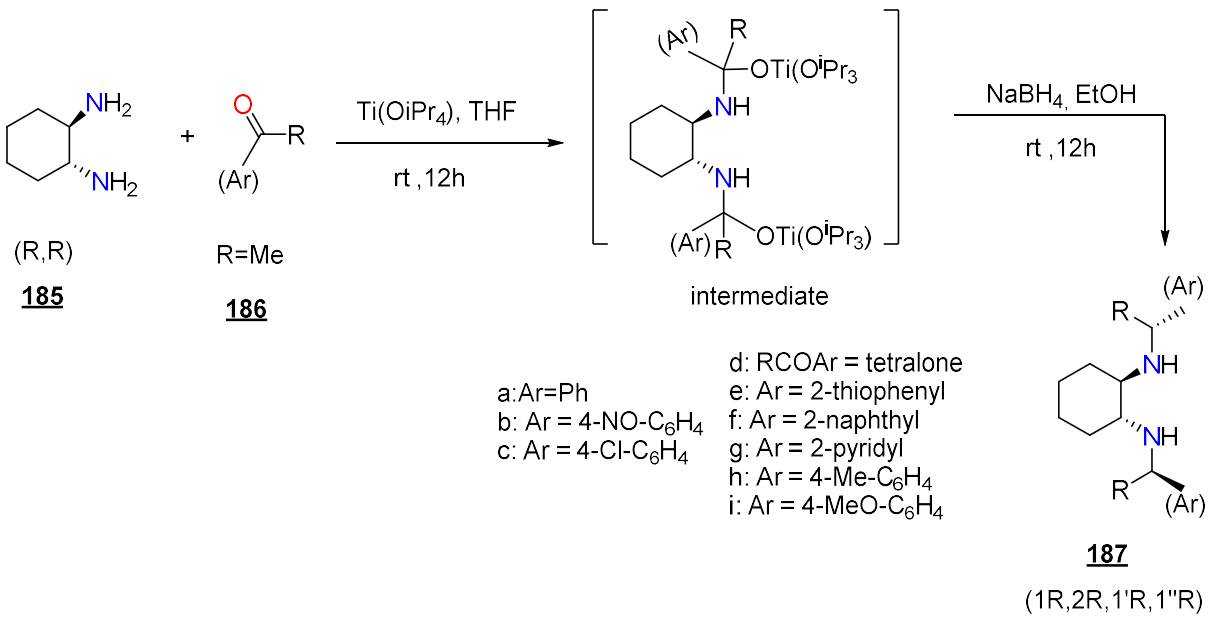

- Scheme 69 –

Sotoca *et al.* [143] prepared 1,5-benzodiazepines **190** in one pot using a solvent- and catalyst-free three-component reaction with trans-cyclohexane-1,2-diamine **185**, -ketoamides **188**, and aromatic aldehydes **189** as(scheme 70).

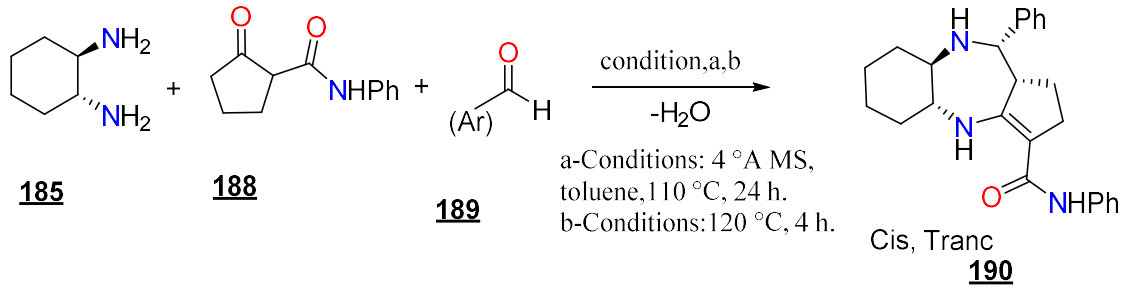

- Scheme 70 -

Mehranpour *et al.* [144] describe the synthesis of novel diazepinium salts **192** in good yields, by reactions of 1,2-diamines with 3-aryl and 3-heteroaryl-1,5-diazapentadienium salts (scheme 71).

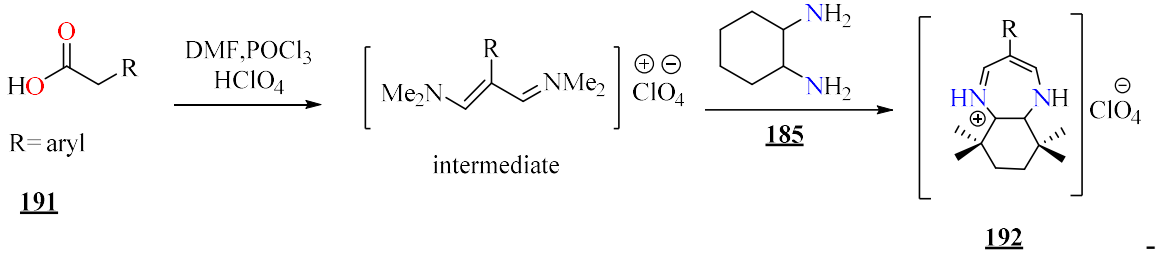

Scheme 75 -

Periasamy *et al.* [145] prepared various chiral amines and macrocycles **194** using methanolic ammonia, ethanol amine, *exo*-(–)-bornylamine, ethylene diamine, propylene

diamine, and *trans*-(*R*,*R*)-1,2-diaminocyclohexane, upon reduction using sodium borohydride in methanol (scheme 72).

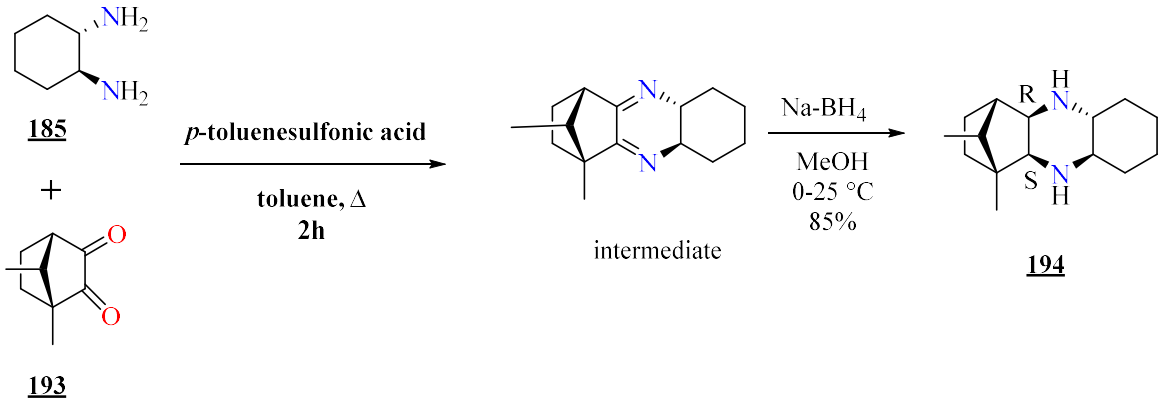

- Scheme 72 –

Zaleska *et al.*[146] developed an efficient synthesis method in one-pot to prepare a variety of pyrrolo[3,4-b]hexahydro-1*H*-1,5-benzodiazepine derivatives **197 a-c** from thiophene-2,3-dione **195** or **196** as well as pyrrolidinetrione derivatives and *trans*-(±)-1,2-diaminocyclohexane **185** as in scheme 73.

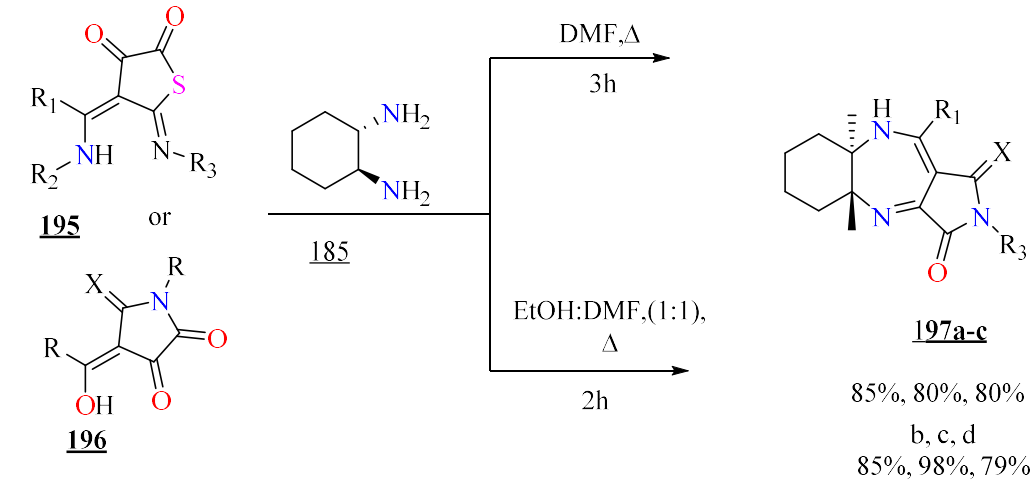

R_1	R_2	R_3
a-p-C_6H_4Cl,	C_6H_5,	C_6H_5
b-C_6H_5	C_6H_5	C_6H_5
c-p-$C_6H_4CH_3$,	C_6H_5,	C_6H_5
d-p-C_6H_4Br,	C_6H_5,	C_6H_5

- Scheme 73 -

Zaleska *et al.* [147] reported a novel methodology for the synthesis of hexahydroquinoxaline **199** and perhydrobenzimidazole **200** from trans 1,2-diaminocyclohexane **185** and 2-anilino-2-ethoxy-3-oxothiobutyric acid anilides **198**. They showed that the synthesis of the desired products depends on the polarity of the solvent (scheme 74).

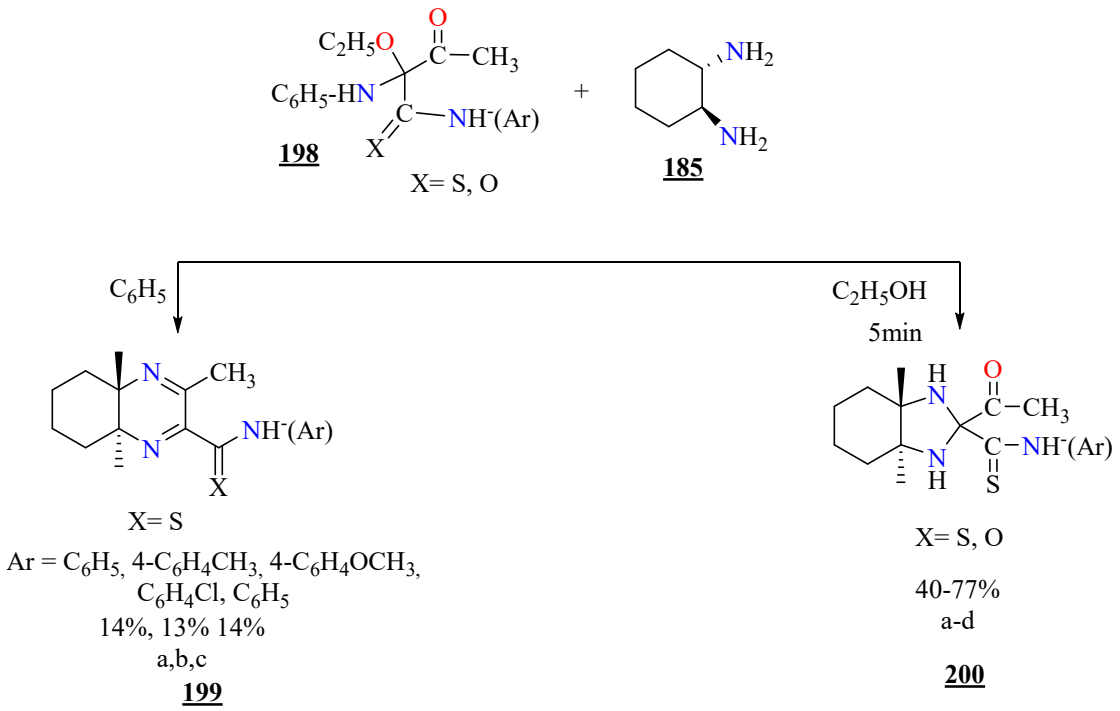

- Scheme 74 -

McCann *et* al. [148] prepared the bisoxoenamine **202,** and (5aR, 9aR) -2,4-dimethyl-5a, 6,7,8,9,9a-hexahydro-1*H*- 1,5-benzodiazepine **203** by condensation of 1,2-diaminocyclohexane **185** with acetyl acetone **201** at reflux of ethanol (scheme 75).

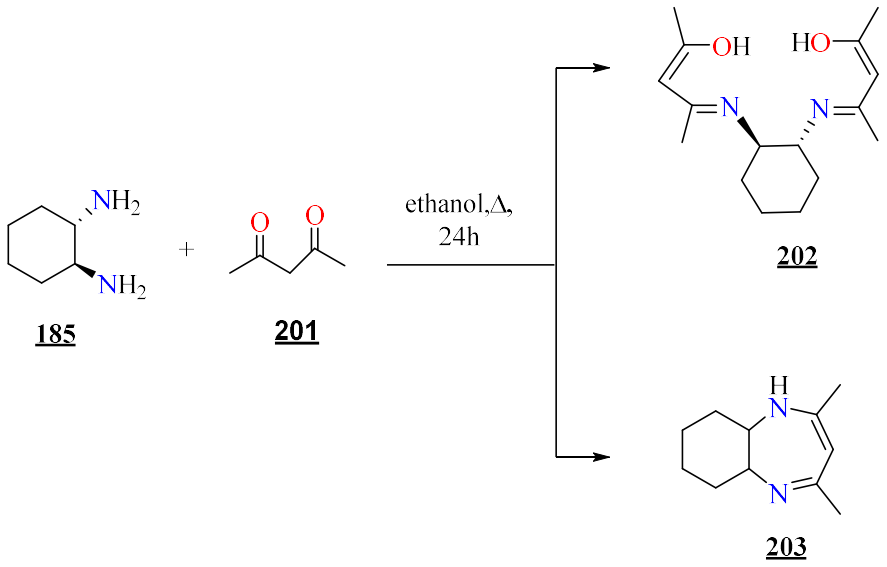

- Scheme 75-

In our laboratory, Chammache *et al*. [149] examined the reaction of ethyl benzoyl acetate with 1,2-diaminocyclohexane in refluxed xylene. The products that formed **204a** and **204b** were confirmed by spectroscopic data (^{1} H NMR, ^{13}C NMR, mass and IR) (scheme 76).

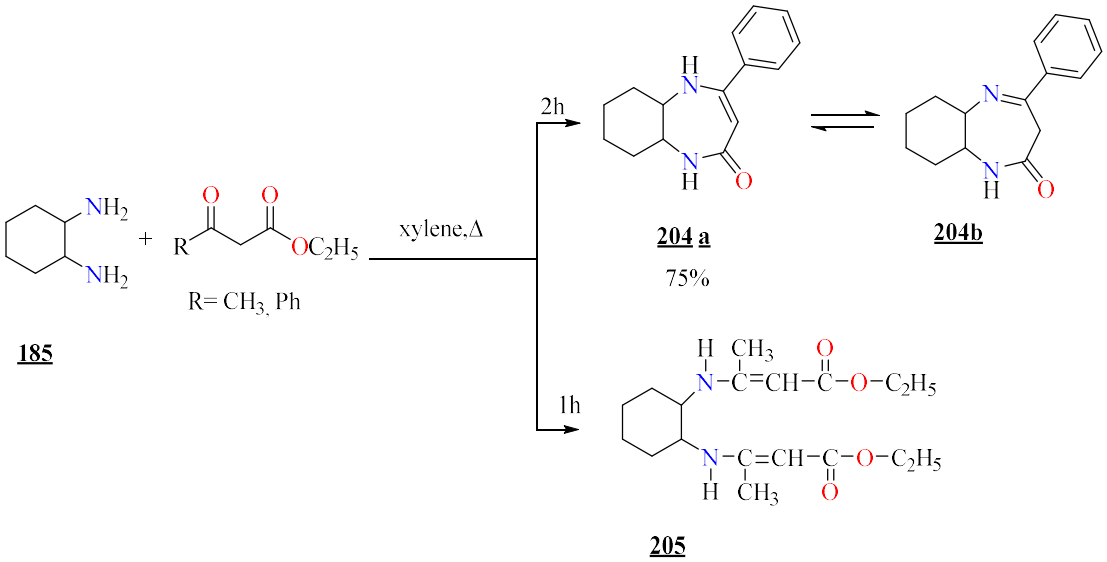

- Scheme 76-

I- Synthesis of 1.5- benzodiazepin-2-one from 1,2-diaminocyclohexane:

We synthesized 4-phenyl-5a, 6, 7, 8, 9,9a-hexahydro-1H-1,5-benzodiazepin- 2(5H)-one **204a** using the method described in the literature [149], which consists of carrying out the condensation of ethyl benzoylacetate **54** with 1,2-diaminocyclohexane **185** in xylene at reflux for 2h scheme 77.

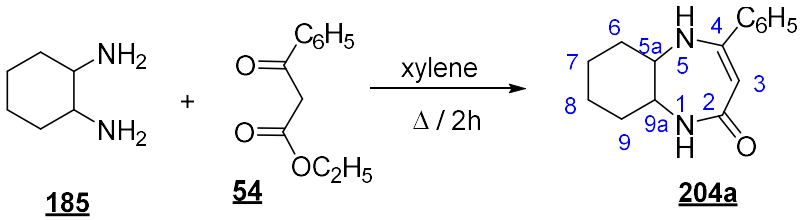

- Scheme 77-

The structure of compound **204a** has been elucidated on the basis of spectral data (^{1}H NMR, ^{13}CNMR, mass and IR).

Thus, the ^{1}H NMR spectrum of compound **204a** taken in DMSO-d6 shows, a multiplet at [1.19-2.18] ppm due to the protons in position 6,7, 8, and 9 of the cyclohexane ring, a massive at 3.07 ppm due to the proton of junction 5a, a signal at 4.42 ppm, which is attributed to the vinyl proton, the two signals at 6.67 and 6.37 ppm due to the two NH protons, and a multiple between 7.41-7.52 attributable to the aromatic protons.

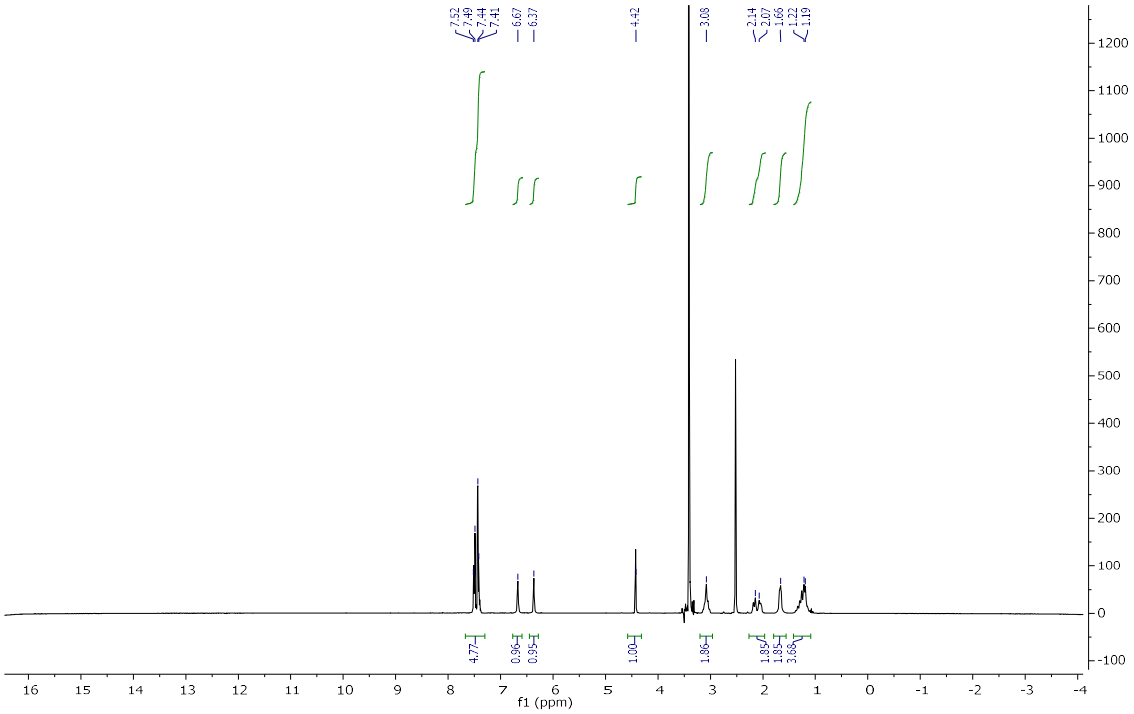

Figure 48: ^{1}H NMR spectrum of product **<u>204a</u>** 300 MHz, DMSO-d_6

In the ^{13}C NMR spectrum of the same compound, we note, in particular, the presence of a signal at 90.93 ppm attributable to the vinylic carbon in position 3. The signals related to the methine groups of the junctions appear at 54.21 and 59.79 ppm. The signals observed around 23.27, 23.43, 31.50 and 31.62 ppm are associated with the carbons of CH_2 groups. The most deshielded signal at 168.97 ppm is due to the carbonyl group.

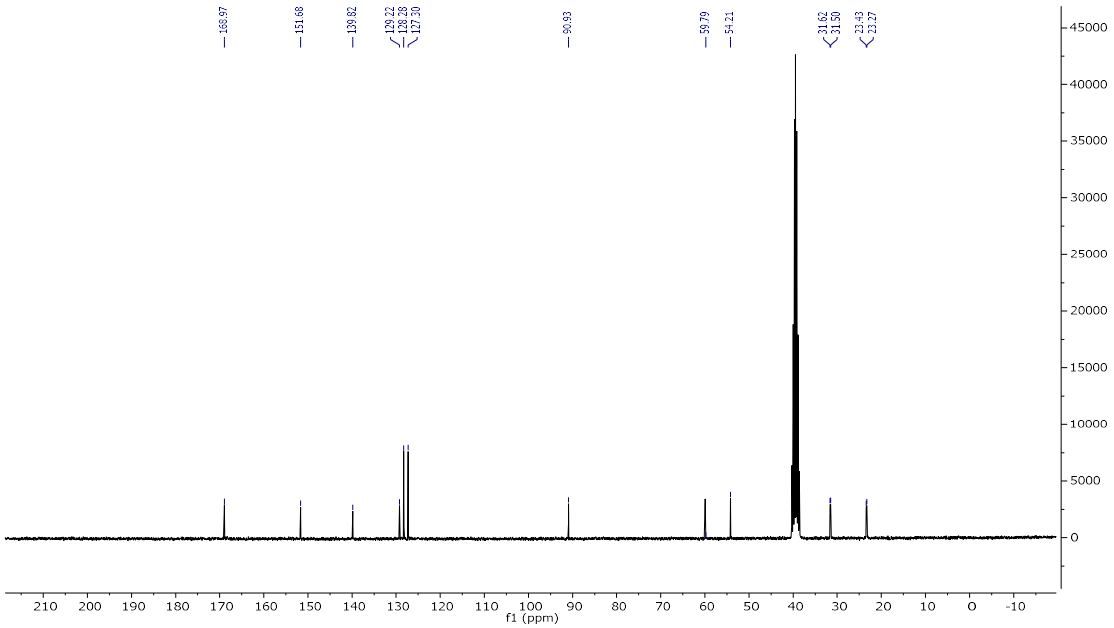

Figure 49: ^{13}C NMR spectrum of product **<u>204a</u>** 75 MHz, DMSO-d_6

In order to properly attribute the ^{13}C NMR spectral data the DEPT spectrum was recorded always taken in the same solvent DMSO-d6 (figure 50): the spectrum clearly shows and confirms the positions of the secondary carbons at the bottom (CH_2) and the ternary carbons at the top (CH).

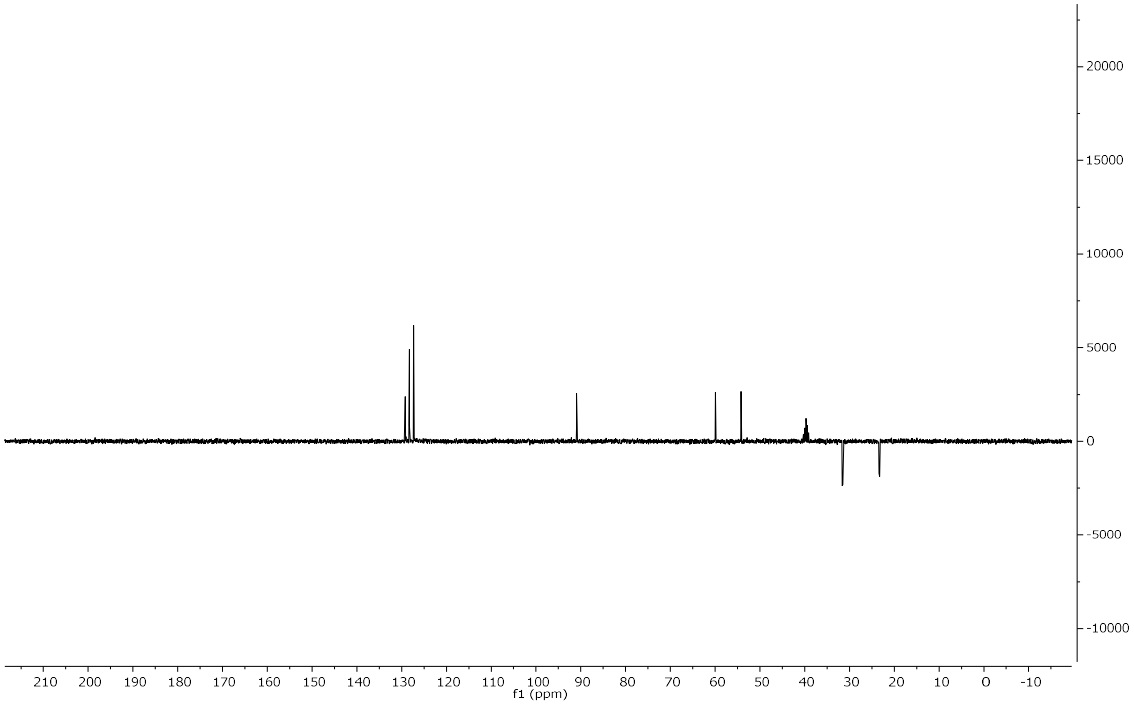

Figure50: DEPT-135 spectrum of compound **<u>204a</u>** 75 MHz, DMSO-$_{d6}$

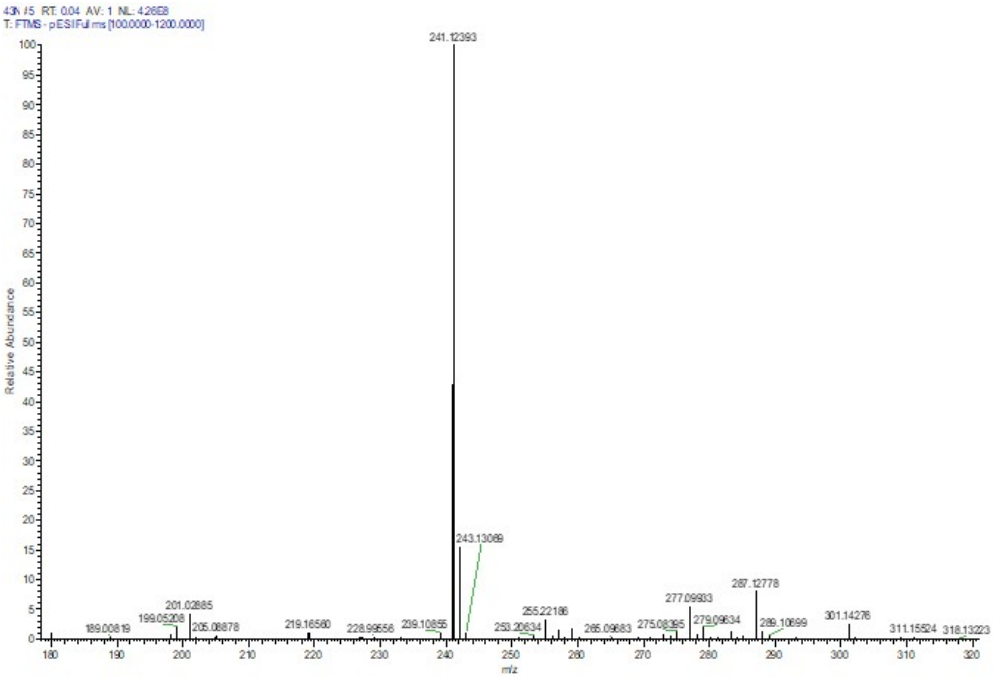

Figure 51: spectrum mass of compound **<u>204a</u>**

In the IR (figure52) spectrum, we observed a band in the region of 1665–1667 cm-1 characteristic of the lactamic C=O group and a band in the region of 3094–3281 cm-1 assigned to the (N-H) group.

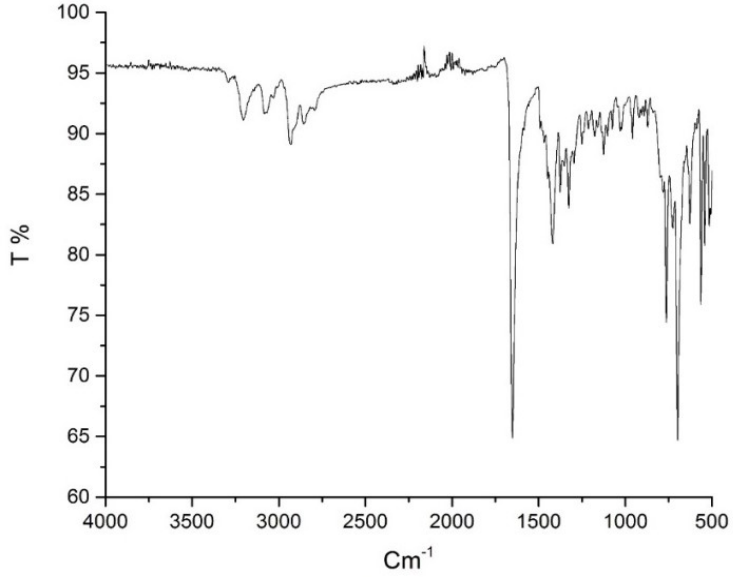

Figure 52: IR spectrum of compound **<u>204a</u>**

In order to confirm the structure of the isolated product, we used x-ray diffraction. As we expected, the studies performed confirmed the initially proposed structure (figure 53). It crystallizes in the monoclinic system.

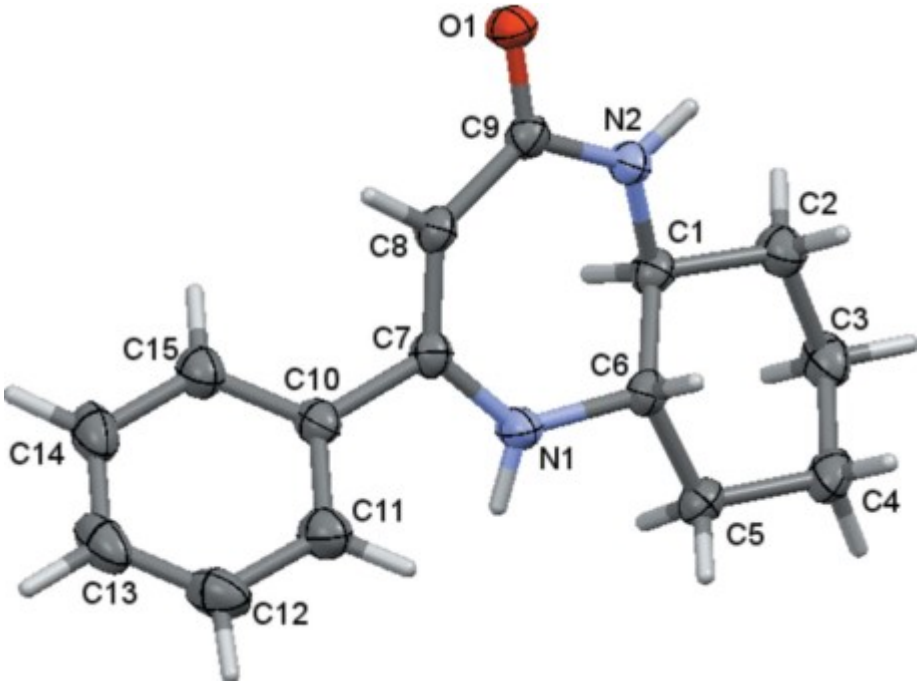

Figure 53: ORTEP representation of the compound **<u>204a</u>**

Crystallographic data and the recording conditions of the structure are shown in table15.

Table 15: crystallographic data of compound **204a**

Chemical formula	$C_{15}H_{18}N_2O$
M_r	242.31
Crystal system, space group	Monoclinic, $P2_1/c$
Temperature (K)	100
a, *b*, *c* (Å)	11.4283 (18), 9.2294 (15), 12.3632 (19)
β (°)	96.890 (2)
V (Å^3)	1294.6 (4)
Z	4
Radiation type	Mo *K*α
μ (mm−1)	0.08
Crystal size (mm)	0.30 × 0.27 × 0.19
Data collection	
Diffractometer	Bruker Smart *APEX* CCD
Absorption correction	Multi-scan *TWINABS* (Sheldrick, 2009)
T_{min}, T_{max}	0.98, 0.99
No. of measured, independent and observed [I > 2σ(I)] reflections	44744, 44744, 25002
Rint	0.046
(sin θ/λ)max (Å−1)	0.686
Refinement	
R[F2 > 2σ(F2)], wR(F2), S	0.054, 0.152, 0.93
No. of reflections	44744
No. of parameters	207
No. of restraints	18
H-atom treatment	H atoms treated by a mixture of independent and constrained refinement
Δρmax, Δρmin (e Å^{-3})	0.32, −0.24

III- Sulfurization of 1,5-benzodiazepine 205a

Several sulfurization methods are reported in the literature, the agents used are phosphorus pentasulfide [150] Lawson's reagent [151-152].

For our part, we prepared 1,5-benzodiazepine-2-thione **205a** according to the method described in the literature [149]. Indeed, the action of phosphorus pentasulfide on 1,5-benzodiazepin-2-one **204a** in pyridine leads to 1,5-benzodiazepine-2-thione **205a** in 80% yield (scheme 78).

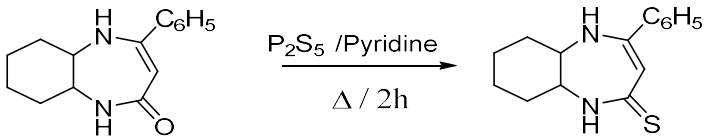

204a **205a**

- Scheme 78-

The structure of compound **205a** was characterized:

- In ^{1}H NMR taken in DMSO-d6, by the presence of a signal at 5.29 ppm due to the vinyl proton.

- In ^{13}C NMR spectrum also taken in, DMSO-$_{d6}$ by the presence of a signal at 191.68 ppm corresponding to the quaternary carbon of the thiolactam function.

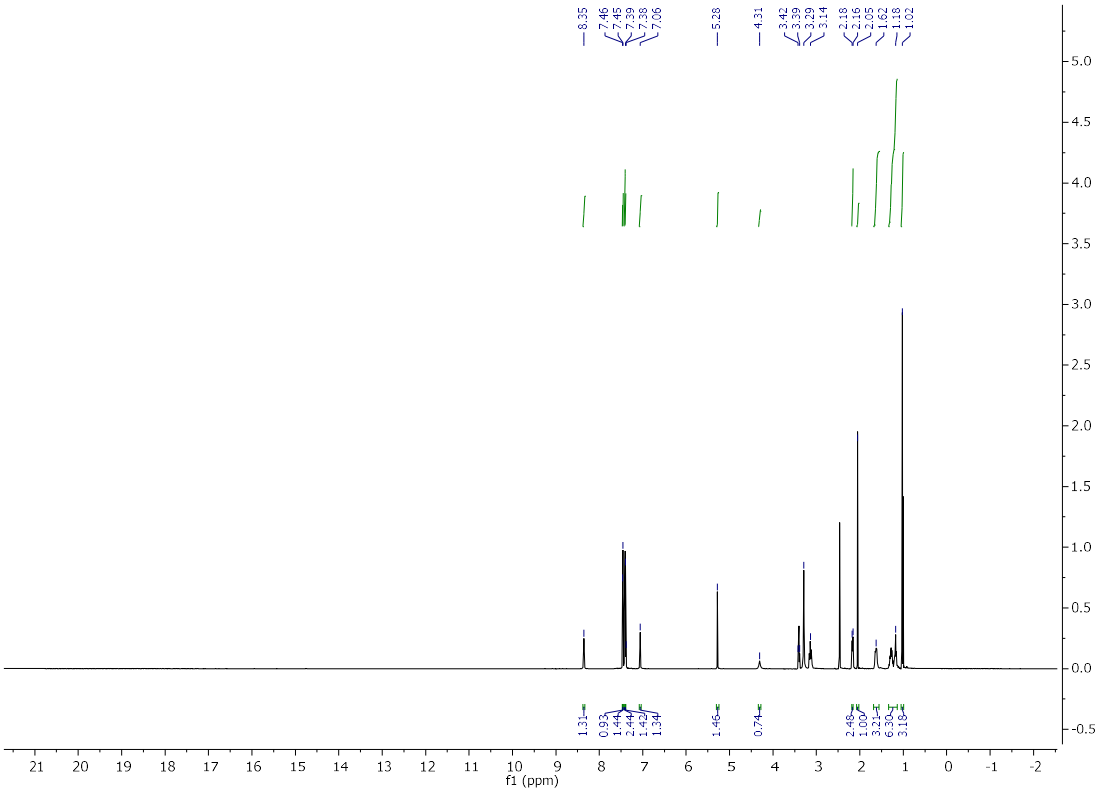

Figure 53: ^{1}H NMR spectrum of product **<u>205a</u>** (600 MHz, DMSO-$_{D6}$)

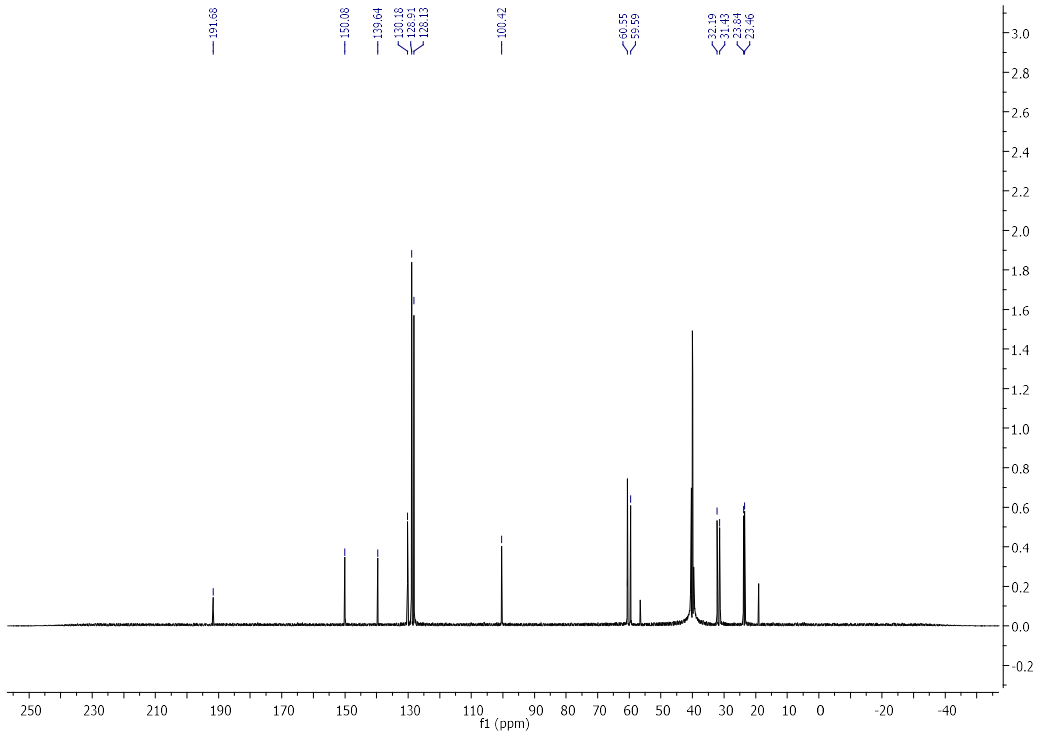

Figure 54: ^{13}C NMR spectrum of product **<u>205a</u>** (151 MHz, DMSO-d_6)

In addition to the spectroscopic analysis, the crystallographic analysis by x-ray diffraction of compound **205a**, allowed to establish with accuracy the structure of the molecule (figure 55).

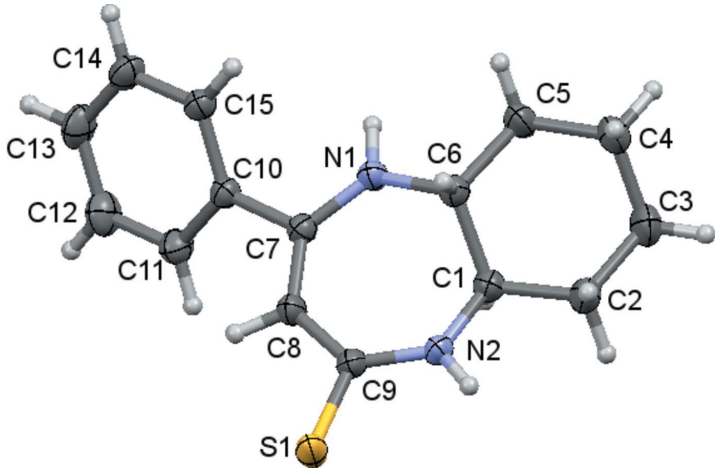

Figure 55: ORTEP representation of the compound

In the title compound the 7-membered ring has a twisted envelope conformation and the saturated 6-membered ring a chair conformation.

In this crystal, each molecule is connected to an ethanol solvent molecule by an N1-H1A-O1 hydrogen bond and these units are formed into helical chains extending along the b-axis direction by O1—H1*B*. . .S1 hydrogen bonds and C6—H6. . .Cg2 interactions **Table 16.**

D—H ⋯ A	**D—H**	**H ⋯ A**	**D⋯ A**	**D—H . . . A**
N1 — H1A. ..O1	0.91	2.13	3.030 (2)	173
N2 — H2. ..S1^{i}	0.91	2.53	3.4312 (15)	171
O1—H1*B*. . .S1^{ii}	0.87	2.42	3.2886 (18)	173
C6—H6…Cg2^{ii}	0.98	2.54	3.516 (2)	177

Part of one chain viewed along the c-axis direction. N—H . . . O and O—H . . . S hydrogen bonds and the C—H . . . (ring) interactions are shown, respectively, by blue, orange and green dashed lines figure 56:

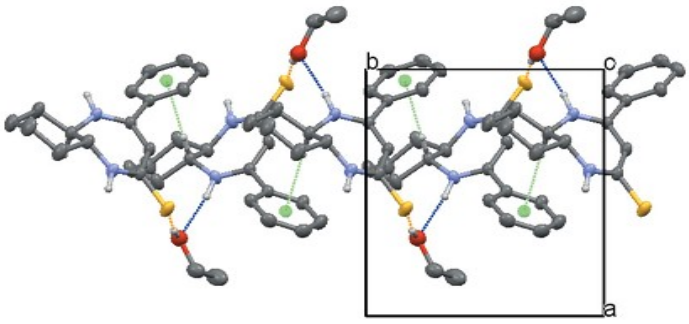

Figure 56

We reported in the table below of the crystallographic data of the product **205a**.

Table 17: Crystallographic data of compound 205a

Chemical formula	$C_{15}H_{18}N_2S{\cdot}C_2H_6O$
Mr	304.44
Crystal system, espace group	Monoclinic, P21/n
Temperature (K)	298
a, b, c (Å)	12.0255 (2), 8.9303 (2), 15.8822 (3)
β (°)	95.813 (1)
V (Å3)	1696.84 (6)
Z	4
Radiation type	Cu Kα
Crystal size (mm)	0.22 × 0.13 × 0.04
Data collection	
Diffractometer	Bruker D8 VENTURE PHOTON 100 CMOS
Absorption correction	Multi-scan SADABS (Krause *et al.*, 2015)
Tmin, Tmax	0.71, 0.93
No. of measured, independent and observed [I > 2σ(I)] reflections	12459, 3209, 2613
R[F2 > 2σ(F2)], wR(F2), S	0.044, 0.125, 1.07
No. of reflections	3209
No. of parameters	199
No. of restraints	26
H-atom treatment	H-atom parameters constrained
Δρmax, Δρmin (e Å−3)	0.30, −0.18

IV- Hydrogenation of 4-Phenyl-5a, 6, 7, 8, 9,9a-hexahydro-1H-1,5-benzodiazepin- 2(5H)-one:

The hydrogenated benzodiazepine derivatives, such as tetrahydro-1H-benzodiazepines, including chiral examples, represent a new, actively developed class of biologically active compounds displaying anxiety, anti-asthmatic, and anti-diabetic activities [153-155].

In continuation of our studies on functionalized heterocycles and our previous works on 1,5-benzodiazepine derivatives, we report the synthesis, crystal structure and Hirshfeld surface of 4-phenyl-decahydro-1H-1,5-benzodiazepin-2-one **206** obtained by hydrogenation of 4-phenyl- 5a,6,7,8,9,9a-hexahydro-1H-1,5-benzodiazepin-2(5H)-one **205a** in the presence of palladium on activated charcoal in anhydrous ethanol scheme 79.

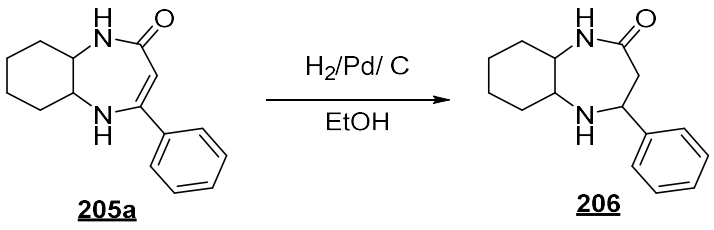

205a **206**

- Scheme 79-

The structure of compound **206** has been elucidated on the basis of spectral data (^{1}H NMR, ^{13}CNMR, mass and IR).

In ^{1}H NMR, we observed the absence of the signal of the vinyl proton and the presence of signals related to the methylene group in α of the carbonyl group.

In the ^{13}C NMR spectrums, we note in particular the presence of 3 signals at 57.15, 58.68, and 62.47 ppm corresponding to the 3 methine group (the 2 C-H of the junction and the ph-C-H).

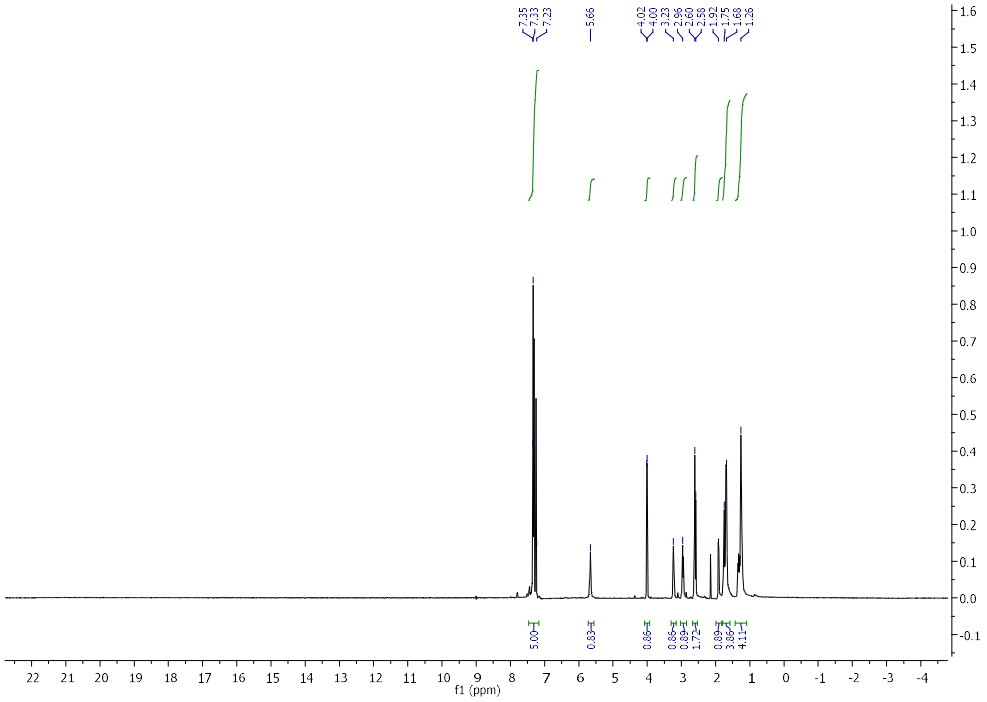

Figure 57 ^{1}H NMR spectrum of compound **206** ($CDCl_3$, 600 MHz)

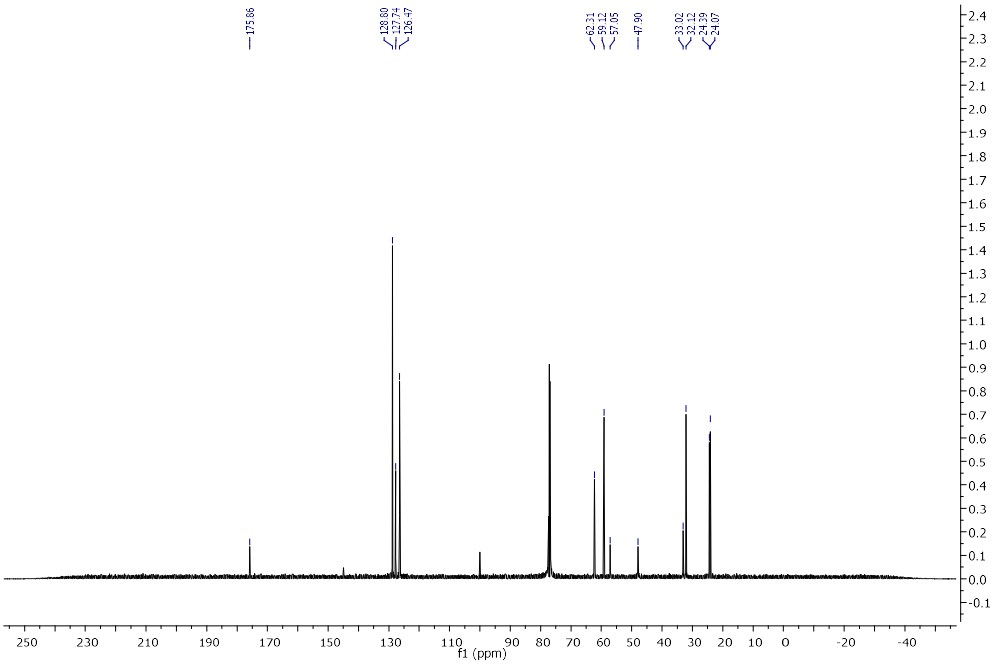

Figure 58: ^{13}C NMR spectrum of compound **206** ($CDCl_3$, 151 MHz)

The analysis of the mass spectrum (EI) (figure 59) shows the presence of in particular of the pic relative to the molecular ion $M^{\bullet+}$ = 244.

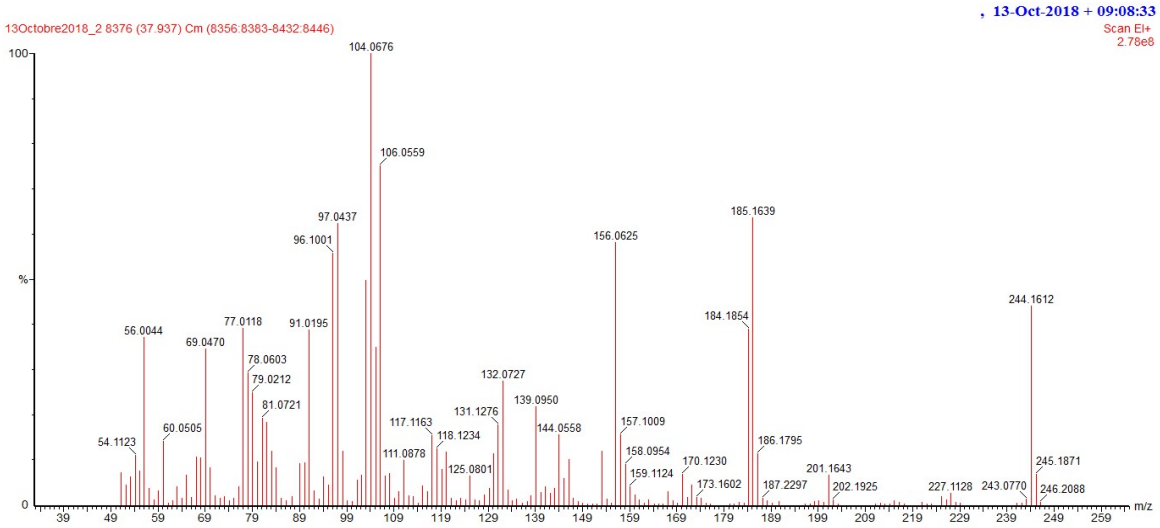

Figure 59: Mass Spectrum (EI) of compound **206**

Compound **206** is also characterized by x-ray diffraction. The ORTEP representation below confirms its structure.

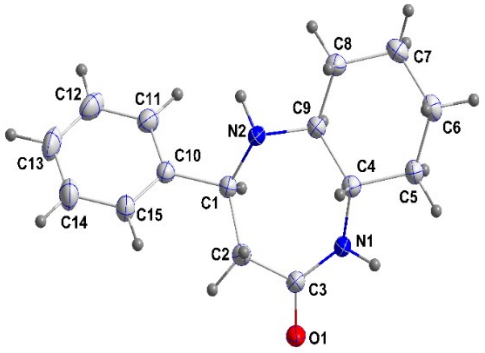

Figure 60: ORTEP representation of compound **206**

The conformation of the 6-membered ring is essentially the chair form while the 7-membered ring adopts a "twist boat" conformation with a total puckering amplitude of 0.7598(16) Å.

In the crystal, the molecules form inversion dimers through N1—H1A•••O1 hydrogen bonds (table 18 and figure 61) which pack with no unusually short intermolecular contacts.

Table 1. Hydrogen-bond geometry (Å, °)				
D—H···A	D—H	H···A	D···A	D—H···A
N1—H1A···O1[a]	0.91(2)	1.99(2)	2.8876(17)	172.0(18)
Symmetry code: [a] −x+1, −y, −z+1.				

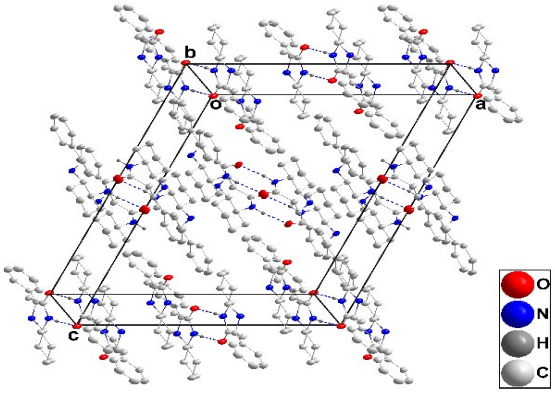

Figure 61 packing projected onto (111) with N—H···O hydrogen bonds shown as dashed lines.

Table 18. Crystal data and structure refinement details	
Chemical formula	$C_{15}H_{20}N_2O$
M_r	244.33
Crystal system, space group	Monoclinic, C2/c
Temperature (K)	150
a, b, c (Å)	18.9508 (11), 6.5145 (4), 22.1146 (13)
β (°)	108.914 (2)
V (Å^3)	2582.7 (3)
Z	8
Radiation type	Cu K_α
Crystal size (mm^3)	0.24 × 0.15 × 0.12
Data collection	
Diffractometer	Bruker D8 VENTURE PHOTON 100 CMOS
Absorption correction	Multi-scan
T_{min}, T_{max}	0.84, 0.93
Refinement	
No. of reflections	2500
No. of parameters	243
H-atom treatment	All H-atom parameters refined

VI- Theoretical study

VI-1 - Hirshfeld surface studies

Hirshfeld surface analysis is a quantitative way to study the intermolecular interactions of the molecules in a crystal structure. Moreover, it gives details of their crystal packing behaviour. Hirshfeld surfaces and Fingerprint Plots were Mappe using the Software Crystal Explorer 3.1.

In figure 62, the standard resolution molecular Hirshfeld surface (d_{norm}) of product **106** is depicted, and the surface appears transparent so the molecular moiety can be visualized in a similar orientation to all the structures around which it was calculated [156]. The 3D rnorm surface can be used to identify very close interactions between molecules. The value of dnorm is negative or (positive) when intermolecular contacts are shorter (l_{onger}) than the van der Waals radii, and the d_{norm} value is mapped onto the Hirshfeld surface by the red, white, or blue colors. The red regions represent closer contacts with a negative d_{norm} value, while the blue regions represent longer contacts with a positive d_{norm} value. Moreover, the white regions represent contacts equal to the van der Waals separation and have a d_{norm} value of zero. As depicted in figure 62, the important interactions in **106** may be H···O hydrogen bonds. In order to understand the importance of H···O hydrogen bonds and why no H···N hydrogen bonds are generated, we generated 2D fingerprint plots for **106**.

Front Back

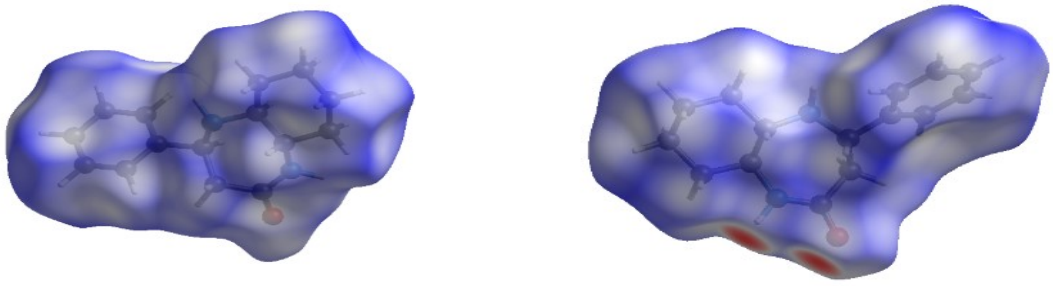

Figure 62: The d_{norm} Hirshfeld surface of **206** (red: negative, white: zero, blue: positive; scale: -0.5585 to 1.2364 a.u.).

The 2D fingerprint plots highlight particular atom pair contacts and enable the separation of contributions from different interaction types that overlap in the full fingerprint. Using the standard (0.6 - 2.6) view with the d_e and d_i distance scales displayed on the graph axes and including the reciprocal contacts, we found the most important interaction involving hydrogen

in **206** was the H···H contact (figure 63). The contributions of the H···O, H···N, and H···H contacts are 12.5 %, 2.5 %, and 68.5 %, respectively.

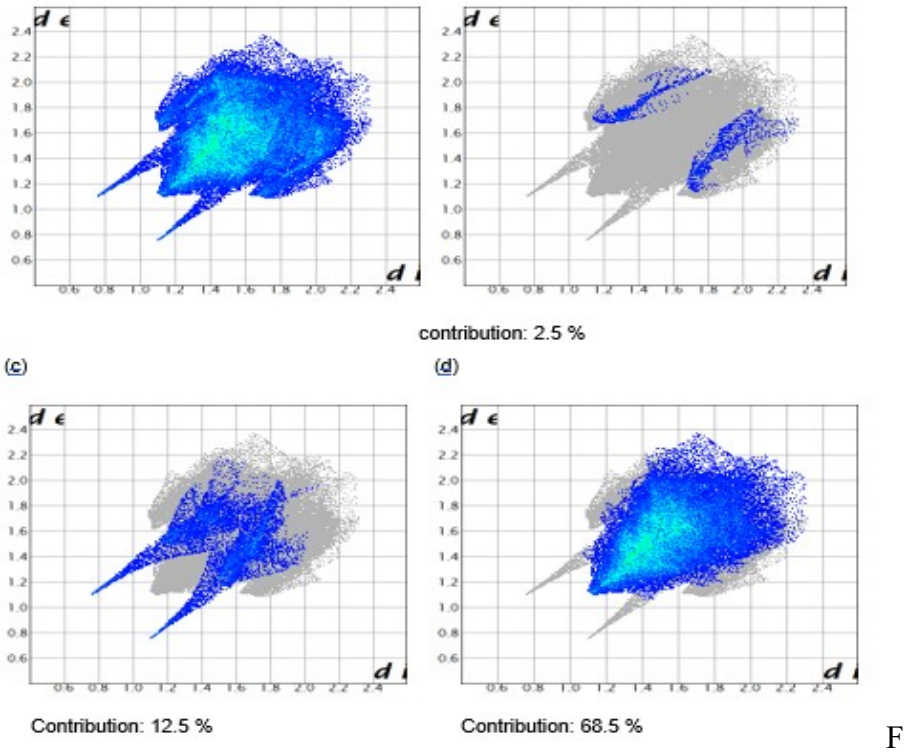

F

Figure 63: The 2D fingerprint plots for **206** (a) full, (b) resolved by the H···N contacts, (c) resolved by the H···O contacts, (d) resolved by the H···H contacts.

VI-2 - Infrared spectroscopy

A comparison was made between the experimental IR spectrum of **206** and the simulated one (figure 64) using a scaling factor of 1.0044 and a full width at half maximum of 10 cm^{-1}. [156]. Clearly, the theoretical infrared spectrum (Fig. 64(b)) is very similar to the experimental one (figure 64(a)) except that there is one more peak above 3500 cm^{-1} in the theoretical IR spectrum. Based on the analysis, this additional signal in the theoretical IR spectrum was associated with the stretching of the N-H bond in the amide group. The disappearance of this signal in the experimental spectrum may be due to the fact that the N-H bond in the amide group is involved in an intermolecular hydrogen bond.

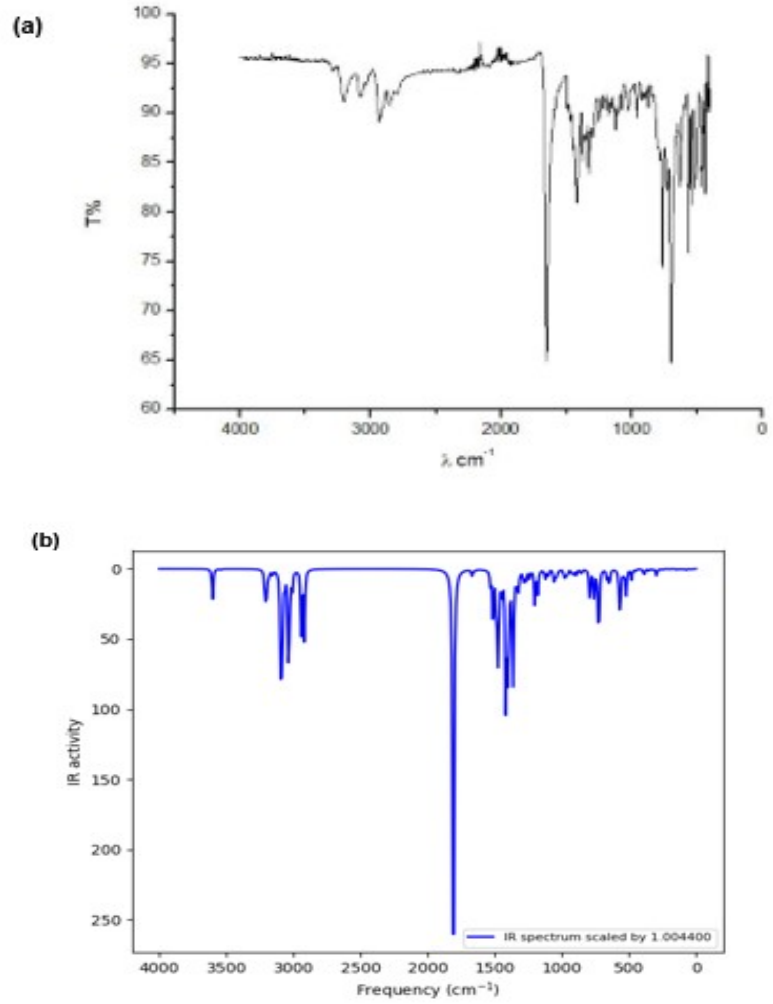

Figure 64: Experimental (a) and simulated (b) FT-IR spectrum of compound **206**

VI-3 Molecular docking

Molecular docking aims to determine the interaction mode of a complex formed by two or more molecules by looking for orientations in space and favorable conformations for the binding of a ligand to a receptor. A docking simulation essentially consists of two steps: the docking itself and the scoring. Thus, we examined the binding mode between 4-phenyl-decahydro-1H-1,5-benzodiazepin-2-one **206** and the μ-opioid receptor to better understand the in vitro activity by highlighting the interaction modes and the molecule studied, and the proposed receptor.

Thus, docking studies between **206** and mu-opioid receptor were performed to understand the interaction mechanism between small molecules and macromolecules. Figure 65 shows the best binding pose of **206** and the binding energy was (-165.4 kJ/mol) for the complex. Figure 65a shows the interacting active residues of the mu-opioid receptor for forming the 206-mu-opioid receptor complex. From Fig. 65(c), we see that there is one hydrogen bonding

and one p-stacking interaction between the HIS 297 residue and one negatively charged residue (ASP 206), one positively charged residue (LYS 233), and several residues of hydrophobic nature within the active range around the docked molecule.

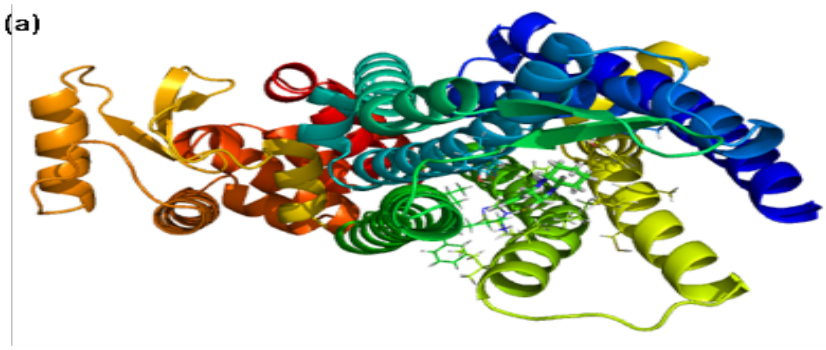

Figure 65 (a) The best binding poses of mu-opioid receptor with **206**, (b) The inset of mu-opioid receptor with **206**, (c) Ligand interaction diagram of mu-opioid receptor complex with **206**.

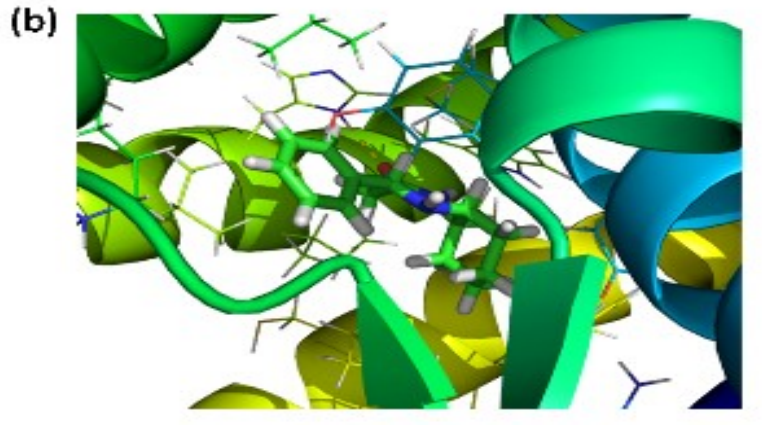

Figure 65 (b) The inset of mu-opioid receptor with **206**, (c) Ligand interaction diagram of mu-opioid receptor complex with **206**.

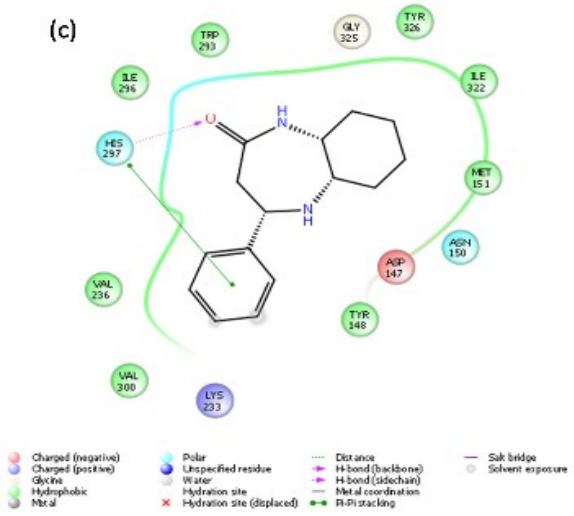

Figure 65 (c) Ligand interaction diagram of mu-opioid receptor complex with compound **206**.

The Root Mean Square Deviation (RMSD) and Root Mean Square Fluctuation (RMSF) of the mu-opioid receptor-206 complex, which can give information on the interaction stability of **206** in the mu-opioid receptor binding environment, are shown in figure 66. From figure 66a, the RMSD plot indicates that the mu-opioid receptor-**206** complex belongs to a large conformation due to the system convergence at above 3 Å. Figure 66b (the RMSF plot) shows that fluctuations of residues of the mu-opioid receptor-**206** complex during the 50 ns simulation and the complex system were stable. Moreover, the mu-opioid receptor active site residues which contact **206** are shown in green in figure 66(b).

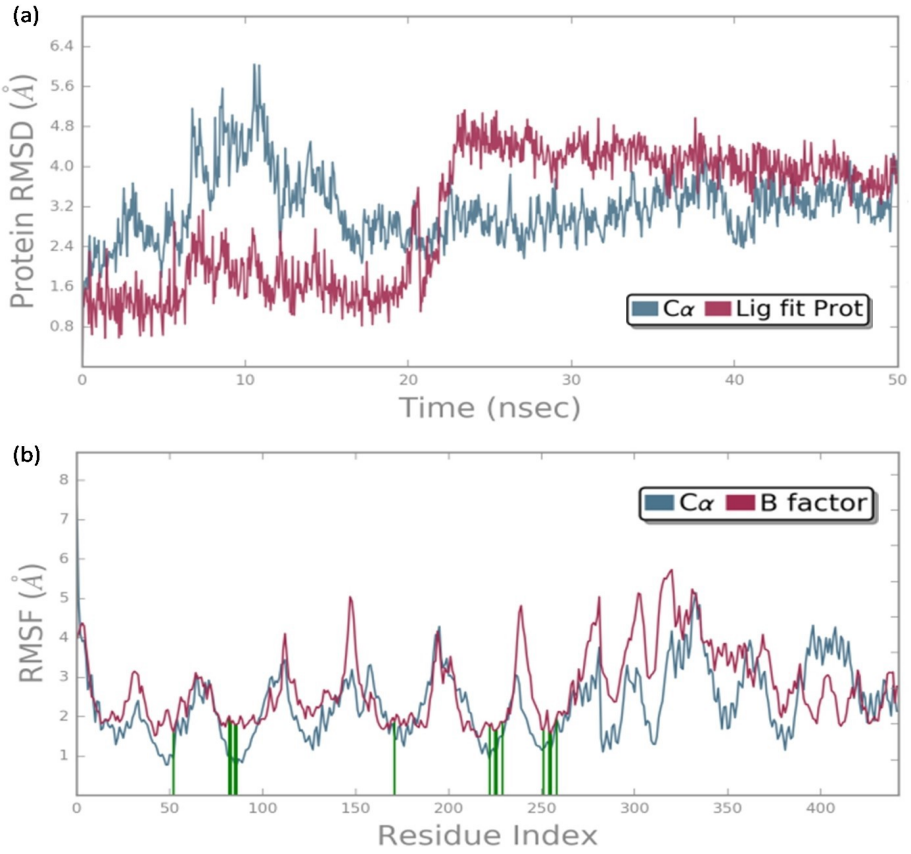

Figure 66: The (a) RMSD and (b) RMSF plot of mu-opioid receptor-**206** complex.

The interaction fraction of the mu-opioid receptor-206 complex is depicted in figure 67 where the TRP 293 residue shows 100% contact during the simulation and SER 329 has 40% of hydrogen bonding contribution with **206**

The final molecular dynamics output interaction plot (figure 67) shows more information about the interacting residues of mu-opioid receptor with **206** after the 50 ns simulation. The π-cation contact for TRP 293 is around 99%, while HIS 297 shows 15% and TYR 326 shows 22% contact with the NH2 group of **206**. In addition, HIS 297 (27%) and TYR 148 (11%) form π-π contacts with the benzene ring of **206** while SER 329 (32%) and HIS 297 (30%) have polar contacts with the NH2 group of **206** together with negatively-charged ASP **206**.

The final molecular dynamics results show that **206** were stable during the 50 ns simulation in mu-opioid receptor complex system.

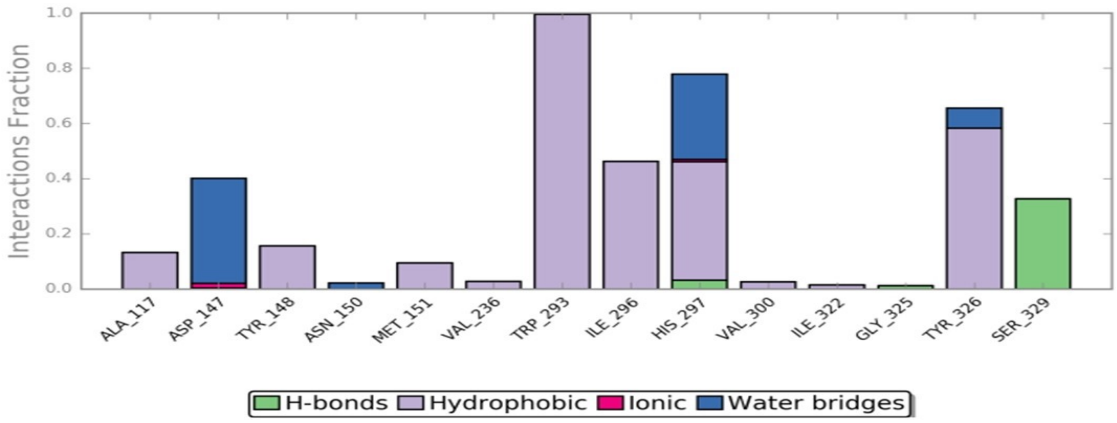

Figure 67: The protein-ligand interaction fraction of mu-opioid receptor-**206** complex.

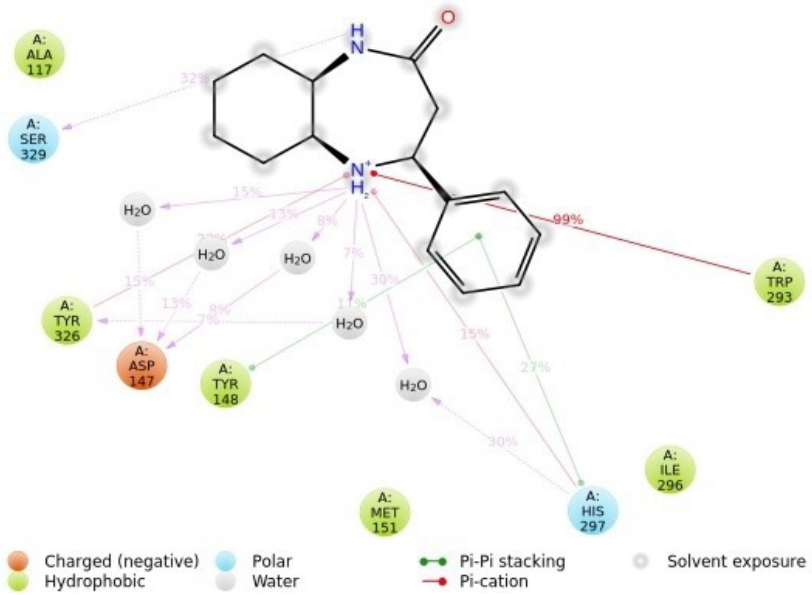

Figure 68: The detailed schematic interaction plot of the mu-opioid receptor-**206** complex

Conclusion

In this chapter, by catalytic hydrogenation, we have reported the synthesis of the 4-phenyl-decahydro-1H-1,5-benzodiazepin-2-one. The molecular structure was characterized by FT-IR, NMR (1H and ^{13}C) and confirmed by x-ray crystallography. Based on the DFT@B3LYP calculation, the title compound showed a different geometry in the gas phase concerning the solid phase. Moreover, the Hirshfeld surface analysis indicated that the H···H contact is the most important interaction for the studied compound. The molecular docking and molecular dynamics analysis indicate that compound **206** has a good binding affinity with the mu-opioid receptor and has good binding stability during a 50 ns simulation.

Experimental part:

Melting points were taken on samples in capillary tubes and are uncorrected. The ^{1}H and ^{13}C NMR data were obtained on a Bruker Avance 300, 600 MHz NMR in DMSO-d6, Chloroform-d, Mass spectra (CNRST). The x-ray diffraction was made on Bruker SMART APEX CCD difarctormter.

I-Procedures for preparation 204a:

4-phenyl-5a, 6, 7, 8, 9,9a-hexahydro-benzodiazepin-2-one 204a:

To a solution of 0.1 mol (11.4 g) of 1,2-diaminocyclohexane in 60 ml of *p*-xylene, 0.12 mol (23.06 g) of ethyl benzoyl acetate in 10 ml of *p*-xylene was added dropwise and refluxed for 2 h. The precipitated solid was collected by filtration and re-crystallized from the dry ethanol solution to give colorless blocks.

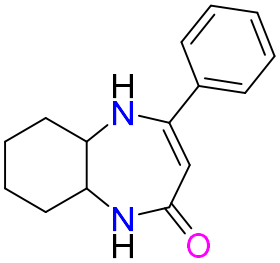

[M= 242.14 g/mol]

Yield = 52%**; F (°C)** = 230-232

^{1}H NMR (300 MHz, DMSO-d6) δ ppm: 1.02-2.14 (m, 8CH_2, cyclohexane), 3.08 (m, 2H, CH); 4.42 (t, 1H –C=H); 6.37(s, 1H, NH); 6.67(s, 1H, NH); 7.41-7.52(m, 5H, CHar).

^{13}C NMR (75 MHz, DMSO-d6) δ ppm: 23.27; 23.43; 31.50; 31.62 (CH_2); 54.21(CH); 59.79(CH); 90.93 (=CH); 127.30-129.22(CHar); 168.97(C=O).

II-Procedures for preparation 205a:

In a flask of 250 ml, a mixture of phosphorus pentasulfide (5.55 g, 0.025 mol) and 4-phenyl-5a,6,7,8,9,9a-hexahydro-1H-1,5-benzodiazepin-2(5H)-one (4.84 g, 0.02 mol) was added to 100 ml of pyridine. The mixture was refluxed for 3 h, and then the solvent was evaporated under reduced pressure. The precipitate that formed was washed with hot water. The result was recrystallized from ethanol to give a colorless compound**.**

4-phenyl--hexahydro-benzodiazepine-2-thione <u>205a</u>:

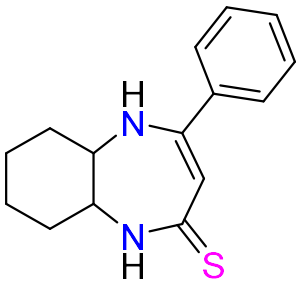

[M= 258.12 g/mol]

Yield = 84%; **F (°C)** = 75-77

^{1}HNMR (600 MHz, DMSO-d$_6$) δppm: 1.02-2.18 (m, 8H, CH_2cyclohexane), 3.14-3.29 (m, 1H, CH), 3.30-3.42 (m; 1H, CH), 5.29 (s, 1H, =CH), 7.06 (s, 1H, NH), 7.38-7.46 (m, 5H, CHar), 8.35(s, 1H, NH).

^{13}C NMR (151 MHz, DMSO-d$_6$) δppm: 23.46, 23.84, 31.43, 32.19 (CH_2), 59.59 (CH), 60.55(CH), 100.42(=CH), 128.13-130.18(CHar), 191.68(C=S).

4-phenyl--hexahydro-benzodiazepin-2-one <u>206</u>:

To 2 grams of 4-phenyl-5a, 6, 7, 8, 9, 9a-hexahydro-1H-1, 5-benzodiazepin-2-one were dissolved in 80 ml of ethanol, then was added a small quantity of activated carbon H_2, Pd/C. The reaction mixture was stirred at room temperature. The mixture was followed by CCM until completion. Then, it was filtered and evaporated; the result was recrystallized from acetone to obtain the compound as colorless crystals.

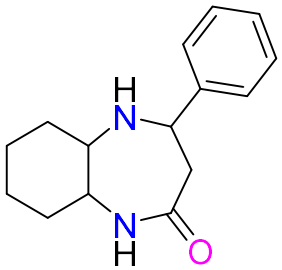

[M= 244.16 g/mol]

Yield = 82%; **F (°C)** = 75-77

^{1}H NMR (600 MHz, $CDCl_3$) δ ppm: 1.26-1.92(m, 8H, CH_2, cyclohexane), 2.58-2.96 (m, 2H, CH_2-C=O), 3.23- (m, 1H, CH), 4.00-4.02(m, 1H), 5.66(m, 1H, CH-ph) 7.23-7.35(m, 5H, CHar).

^{13}C NMR (151 MHz, $CDCl_3$) δ ppm: 24.07, 24.39, 32.12, 33.12, 47.90 (CH_2), 57.05 (CH), 59.12(CH), 62.31(CH), 126.47-128.30(CHar), 175 (C=O).

Mass spectrum (EI): $M^{+\cdot}$ (m/z = 244)

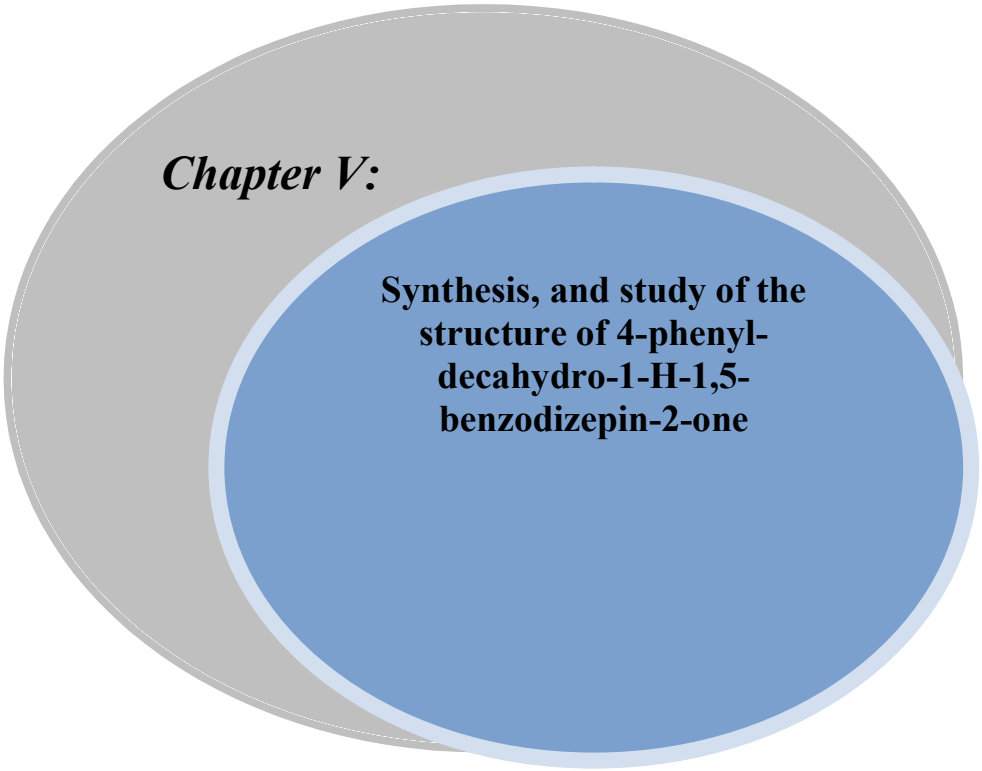
Chapter V:
Synthesis, and study of the structure of 4-phenyl-decahydro-1-H-1,5-benzodizepin-2-one

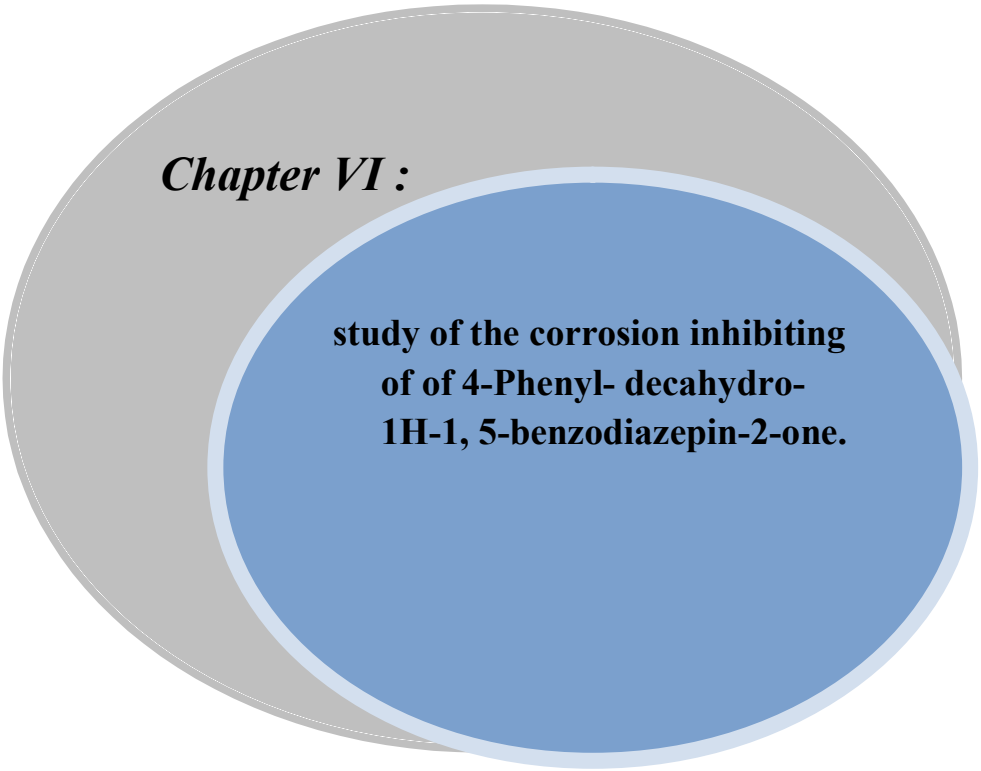
Chapter VI :
study of the corrosion inhibiting
of of 4-Phenyl- decahydro-
1H-1, 5-benzodiazepin-2-one.

I-Introduction

In our daily life, we encounter many undesirable phenomena, among them corrosion, which is the result of the chemical and/or physical action of a metal or alloy on its environment. Consequences are important in various fields, in particular in industry, where production stoppages, replacement of corroded parts, serious accidents, and risks of pollution are frequent events with sometimes heavy economic impact. Industrial installations and equipment that are susceptible to corrosion can be designed and constructed, taking into account the available anti-corrosion treatments. Various corrosion treatments are known and applicable to existing installations. The use of several metals (ferrous and non-ferrous) and the prohibition of toxic inhibitors (chromate, nitrite, etc.) complicate the implementation of effective anti-corrosion treatments and therefore justify the search for new means of protection.

In terms of protection, many organic compounds can be used as corrosion inhibitors. From a "mother" molecule with certain efficiency, it is always possible to achieve effectiveness. It is always possible to synthesize compounds or complexes with the aim of either improving the inhibiting efficiency or controlling the corrosion of the material in its environment. Indeed, organic inhibitors can play this role in a corrosive environment. The latter, when added in small quantities to the medium, can decrease the corrosion rate or even stop the corrosion of materials. They can be used either for permanent protection of the part (installation requires careful attention and scrupulous attention) or for temporary protection, especially when the part is particularly sensitive to corrosion or when it is exposed to a very aggressive environment.

Corrosion processes in these environments depend on many numbers of factors (the nature and composition of the material, the environment and its chemical characteristics, its temperature, etc.), which do not intervene individually, but in a more or less complex relationship with each other. As a result, corrosion has been still the subject of numerous studies because the corrosion phenomena encountered on a daily basis are complex and often specific.

It is a natural phenomenon that tends to return metals and alloys to their original state of oxide, sulfide, carbonate or other more stable salts in the surrounding environment [157].

Corrosion phenomena are classified into two broad categories [158]:

- √ High-temperature corrosion (or dry corrosion).
- √ Electrochemical corrosion (or wet corrosion).

I.1 Dry corrosion

At room temperature, most metals have a very thin layer of oxide as a result of the reaction of the metal with atmospheric oxygen. In some cases, metals subjected to heating show a thicker layer that is easily removed. Indeed, hot rolled brass has a complex oxide layer that is physically unstable but retains a protective value as long as the brass remains in the air and as long as the layer remains a continuous layer [159].

I.2 Wet corrosion or electrochemical corrosion

Wet corrosion is the set of reactions that take place when a metal comes into contact with a conductive medium containing oxidizing agents. Electrochemical corrosion processes are characterized by the fact that the corroding metal behaves like a poly-electrode, i.e. the two half-reactions of the overall redox process are observed simultaneously and at the same speed on different points of the metal surface. As a result, a set of micro-batteries, consisting of local micro-cathodes and micro-anodes, coexist on the metal surface in closed circuits due to the movement of anions and cations in the electrolyte [160].

II. Types of corrosion

II.1. Definition

Corrosion is defined as a natural process that causes the transformation of pure metals into undesirable substances resulting changes in the properties of the metal and often in functional degradation of the metal itself, as the physical-chemical interaction between a metal and its environment. Furthermore, the definition adopted for corrosion is degradation because of oxidation, a chemical action that creates oxides that flake away from the base. Also, depending on the medium, corrosion is said to be dry when it occurs in gaseous environments and wet when it occurs in liquid electrolytes [161].

II.2. Uniform or generalized corrosion

Uniform corrosion is the consequence of the oxidation of all the atoms on the surface of a material at the same speed by the corrosive medium. This result, on a macroscopic scale in a regular decrease of the metal thickness, as opposed to localized corrosion:

$$M + n\,O_x^{z+} \longrightarrow z\,M^n + n\,Red$$

$$M \longrightarrow M^n + n\,e^-$$

Figure 69: Uniform corrosion

II.3. Localized corrosion

This phenomenon occurs when the material is brought into contact with an environment that shows selective behavior towards the alloy. This selectivity can have multiple origins both at the level of the material (heterophase alloy, presence of inclusions, locally defective surface protection, bimetallic material...) and at the level of the environment (local variation in composition, and pH or temperature) [162].

II.3.1 Galvanic corrosion

Galvanic corrosion is the result of a chemical reaction caused by the contact of two dissimilar metals in the presence of an electrolyte. The strength of the reaction and the extent of the corroded surface depend on several factors, including the conductivity of the electrolyte and the difference in electrical energy between the metals involved. The less resistant metal becomes anode and more vulnerable to corrosion, while the more resistant metal becomes cathode [163].

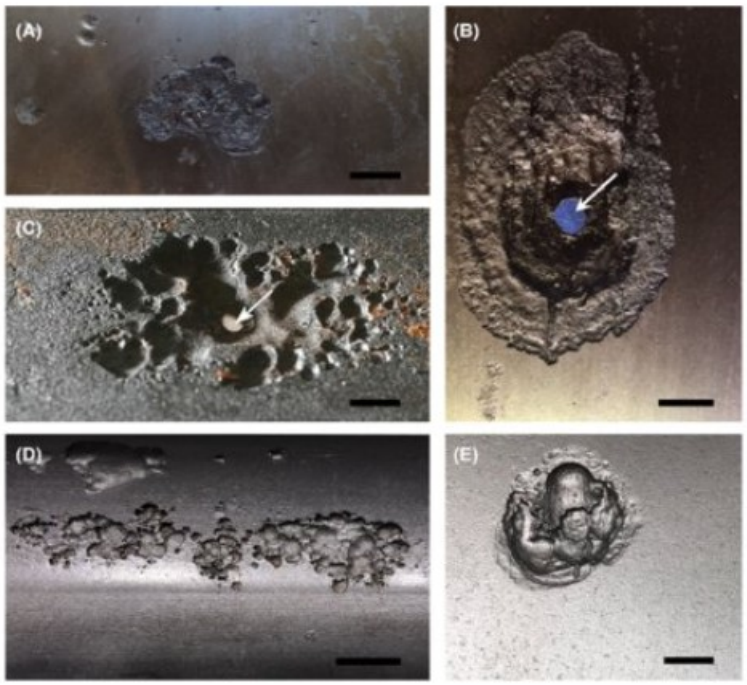

Figure 70 Galvanic corrosion

II.3.2. Pitting corrosion

Pitting corrosion is a very localized attack on the material resulting from specific local corrosion conditions. At this point, the anode is created, and the rest of the surface acts as a cathode. The small surface area of the anode and the large surface area of the cathode cause a high anode current and, thus, a high corrosion rate. The term "pitting corrosion" refers to the fact that the corrosion occurs mainly deep within the material and its depth is much greater than its diameter. This depth and the number of pits vary greatly, but pitting is one of the most serious forms of corrosion. In addition, pitting can be difficult to detect because these small holes can be masked by corrosion deposits [164].

Figure71 Pitting corrosion.

II.3.3. Crevice corrosion

Crevice is similar to pitting corrosion and occurs in crevices. With valves, crevice corrosion usually starts between the nuts and washers. It is more difficult for oxygen to diffuse into these crevices. This oxygen deficit leads to acidification, as a result of which the less noble metal becomes anodic and is dissolved. The alloying element Titanium reduces the susceptibility to pitting and crevice corrosion [165].

Figure 72 Crevice corrosion

II.3.4 Intergranular corrosion

This is a localized, more selective attack, generally caused by heat treatment of the metal, which develops at the junctions of the metal grains. Intergranular corrosion can take the form of sheet corrosion: metal sheets are formed on the metal surface. This corrosion is observed after mechanical treatment such as rolling [166].

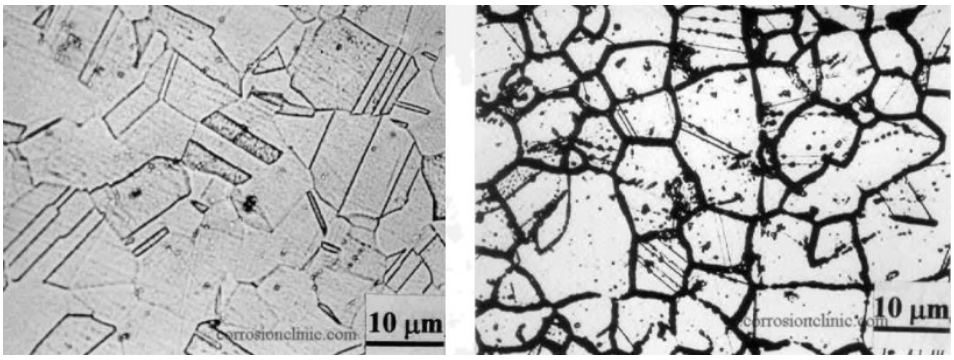

Figure 73 Intergranular corrosion

III. Classes of inhibitors

There are several possibilities for classifying inhibitors, which differ from each other in various ways [167]:

- Either on the basis of the nature of the products (organic or mineral inhibitors);
- Either on the basis of their electrochemical mechanism of action (cathodic, anodic or mixed inhibitors);
- Or from their interface mechanisms and principles of action (adsorption on the metal surface and/or formation of a protective film).
- Or from the field of application.

III.1 Nature of the inhibitor molecules

III.1.1. Organic inhibitors

Organic molecules are promised more than certain development in terms of corrosion inhibitor their use is currently preferred to that of inhibitors mainly inorganic for ecotoxicity reasons. Organic inhibitors are usually made from petroleum industry by-products [168-169]. They have at least an active center capable of exchanging electrons with the metal, such as nitrogen, oxygen, phosphorus, or sulfur. The usual functional groups, allowing their attachment to the metal are the following (-NH2, -SH, -OH, -COOH…).

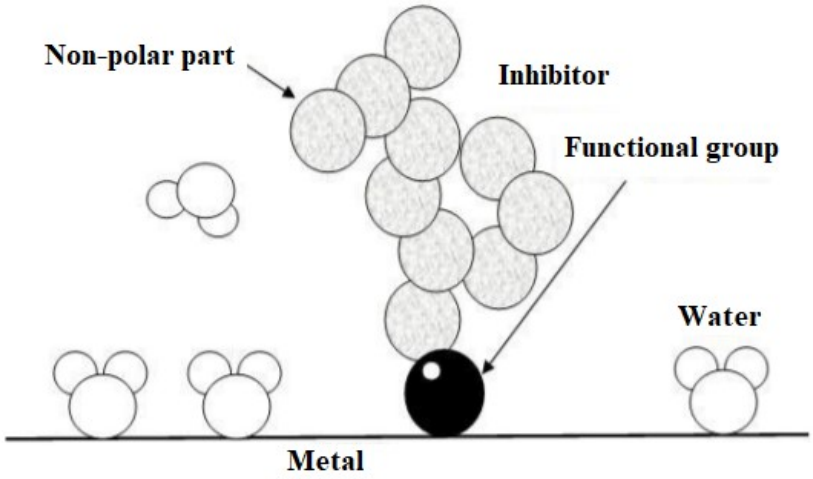

Figure 74: Adsorption of organic inhibitor in aqueous medium

III.1.2. Mineral inhibitors

These inhibitors are often used in near-neutral or even alkaline media and more rarely in acidic media alkaline medium, and more rarely in acidic medium. The products dissociate in solution and it is their dissociation products that ensure the inhibition phenomena (anions or cations). The main inhibiting anions are the oxo-anions of the XO4n-type, such as chromates, molybdates, phosphates, silicates, and the cations are mainly Ca^{2+} and Zn^{2+} and those which form insoluble salts with certain anions such as the hydroxyl HO^{-}. The use of inorganic inhibitors is still limited, as most of the effective compounds have an adverse effect on the environment [170].

III.1.3. Mechanisms of electrochemical action

III.1.3.1 Anodic inhibitors

There are many anodic inhibitors. They are inorganic substances, such as orthophosphates, silicates and chromates. Their mode of action consists in raising the value of the corrosion potential of the material to a value for which a passive protective film is formed on the anode. Although anodic inhibitors are very effective and often used, they usually have an undesirable property: if the inhibitor content is/becomes progressively lowered, the metal surface is no longer fully covered, and it functions as an anode, thus obtaining a dangerous combination, a small anode and a large cathode leading to pitting corrosion. In this case, the inhibitor does more harm than good. This is why anodic inhibitors are often referred to as dangerous. The benzoate ion seems to be an exception because a very low concentration of the inhibitor only causes generalized corrosion [171].

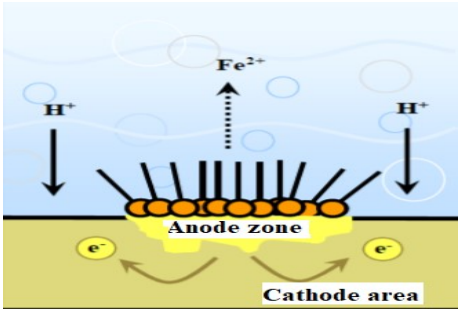

Figure 75: Formation of anodic barrier layers interfering with electrochemical reactions, in the case of a study in an acidic medium

III.1.3.2. Cathodic inhibitors

The action of these inhibitors results in a decrease in the speed of the cathodic reaction and reaction, and thus by a shift of the corrosion potential towards less noble values. They are generally cations that can migrate to the cathodic surface, where they precipitate as basic salts or hydroxides, forming adherent and compact films. Cathodic inhibitors include combinations of zinc, nickel, magnesium, alkaline phosphates and magnesium, alkaline phosphates [172].

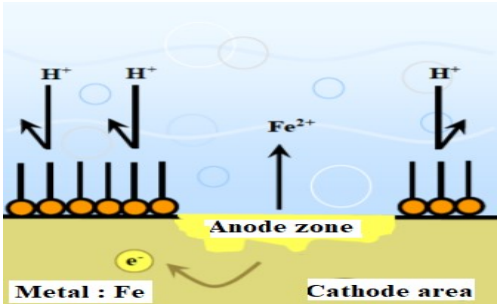

Figure 76: Formation of cathodic barrier layers interfering with electrochemical reactions in the case of a study in an acidic environment.

III.1.3.3. Mixed inhibitors

The simultaneous addition of two inhibitors can result in an increased inhibitory effect and can inhibitor effect and can also eliminate the risk of pitting corrosion at low concentrations. Pitting such an inhibitor often consists of a combination of an oxidizing agent, such as nitrate or nitrate or chromates and a non-oxidizing, but precipitating, orthophosphate or silicate. Examples of such inhibitors are the nitrate + benzoate mixture, which is the most common and effective inhibitor for automotive radiators and another example is an orthophosphate + chromate is orthophosphate + chromate, which is very effective even in salt water. In other cases, the mixed inhibitor is a mixture between a cathodic and an anodic inhibitor, such as polyphosphates [173].

III.1.3.4. Corrosion Factors

Corrosion phenomena depend on a large number of factors, the main ones being the following are the main ones. Factors of the corrosive medium: concentration of the reagent, oxygen content, and pH of the medium.

➢ Metallurgical factors alloy composition, heat and mechanical treatment.

➢ Factors defining the conditions of use: surface condition, shape of parts, type of inhibitor and assembly processes.

➢ Time dependent factors: mechanical stress, and modification of protective coatings [174, 175].

IV. Corrosion inhibition in acidic media

In acidic environments, the most frequently used inhibitors are organic molecules of organic type. These inhibitors act initially by adsorption on the surface of metals, even before intervening in the corrosion reaction processes to reduce the corrosion rate. In aqueous solutions, due to their polar nature, water molecules adsorb to the metal surface. Organic inhibitors must therefore displace the adsorbed water molecules [176], the adsorption of an organic substance on the metal surface can be described by the surface of the metal can be described by the following reaction:

$$\mathbf{Org_{(s)} + n\ H_2O_{ads} \rightarrow Org_{ads} + n\ H_2O_{(s)}}$$

Where **n** is the number of water molecules displaced from the surface for each organic molecule adsorbed, the number **n** is independent of the coverage and charge of the metal, but depends on the geometric area of the organic molecule relative to that of the metal. But it depends on the geometric area of the organic molecule relative to that of the water. Adsorption of an organic molecule occurs when the interaction energy between the metal surface and the molecule is greater than the interaction energy between the metal and the molecule. The interaction energy between the metal surface and the molecule is greater than the interaction energy between the metal and water molecules.

Corrosion inhibition by organic compounds is usually the result of their adsorption to the metal surface. The phenomenon can be demonstrated by:

➢ Study of adsorption isotherms

➢ Examination of the surface by means of specific techniques: scanning electron microscopy (SEM) and photoelectron spectroscopy (XPS).

Knowledge of the factors that influence the phenomenon of inhibitor adsorption phenomenon is essential for a better understanding of the inhibition mechanism of these substances

IV.1. Type of adsorption

Adsorption of organic compounds can be described by two main types of interaction: physical adsorption and chemical adsorption. These two types of adsorption are influenced by the nature and charge of the metal, the chemical structure of the metal, and the type of electrolyte [177].

IV.1. 1 physical Adsorption

Physical adsorption results from an electrostatic interaction between the ions or dipoles of organic molecules and the electrically charged metal surface. The charge of the metal is defined by the position of the corrosion potential of the metal relative to its zero-charge potential (E_0). When the corrosion potential of this metal has a value lower than E_0, the adsorption of cations is favored. Anions are readily adsorbed when the corrosion potential of the metal is in the region of positive potential compared to E_0.

The phenomenon of synergy observed in the inhibition of iron corrosion in a sulphuric acid medium by quaternary ammonium cations in the presence of chloride ions is interpreted by the position of E_0. In this case, the inhibition is greater in the presence of adsorbed anions and cations than in the case where only cations are adsorbed. At the corrosion potential of iron in sulphuric acid medium, the charge of the metal is positive and only a very small amount of the inhibitor cations adsorb. If chloride ions are added to the acid solution, they adsorb onto the iron surface and shift E0 to more positive values. Thus, the Cl anion facilitates the adsorption of the inhibitor cations. This result explains the higher inhibitory efficiency of several organic cations of iron corrosion in hydrochloric acid medium compared to that obtained in sulphuric acid medium [178-179].

IV.1. 2 Chemical adsorption

Chemical adsorption (chemisorption) is the most important type of interaction between the inhibitor and the metal. In this case, the adsorbed species come into direct contact with the metal surface. The chemical adsorption process involves electron transfer or sharing between the inhibitor molecules and the vacant "**d**" orbitals on the metal surface. This allows coordination bonds to be formed. In the case of an organic inhibitor, electron transfer occurs via orbitals with weakly bound electrons. This situation can occur with multiple bonds or aromatic rings with π-electrons. The transfer is, moreover, favored by the presence of heteroatoms with free pairs of electrons [180].

V- Corrosion Evaluation Methods:

The use of electrochemical methods is essential to approach the phenomenon of corrosion and recognize its mechanisms. However, the gravimetric method, which is easy to implement and has the advantage of allowing direct measurement, remains a basic method. Indeed, it is essential to complete the gravimetric tests with electrochemical measurements in order to ensure the validity of the results obtained.

V- 1. Electrochemical Methods:

Electrochemical methods allow the characterization of the metal/electrolyte interface. These methods can be classified into two main categories: stationary and transient methods.

Stationary methods (polarization curves):

This method allows access to the kinetics governing the metal-solution interfacial process. The polarization curves of the metal solution interface are a fundamental feature of the electrochemical kinetics and account for only the slowest stage of the overall process at the metal-solution interface

These curves allow the electro-chemical parameters of the metal-solution to be determined accurately; among the characteristics of these curves, we cite

- The instantaneous corrosion rate (Icorr);
- The corrosion potential (Ecorr);
- Tafel slopes (b);
- And the diffusion limits currents.

This method gives rapid measurements and is relatively simple to implement.

The determination of the corrosion rate from the polarization curves allows the kinetics governing the interfacial electrochemical process to be determined.

There are three main types of kinetics:

* Pure activation kinetics,
* Pure diffusion kinetics,
* Mixed kinetics (activation-diffusion).

Conclusion:

In this part of work, we were interested in the evaluation of the anticorrosive activity on mild steel (CS) in hydrochloric acid a medium (1M) in the absence and presence of 4-phenyl-octahydro-1,5-benzodiazepin-2(3H)-one **206** (inhibitor) at different concentrations studied at 303 °K. This study was performed using two methods: electrochemical impedance spectroscopy and the electrochemical method. This study was carried out at the Laboratory of Materials, Nanotechnology, and Environment, Faculty of Sciences, Mohammed V University of Rabat.

Experimental part

VI- Results and discussion

Here, we presented results relating to the influence of the concentration of the product **206** on the effect of temperature on steel (CS) protection in 1M hydrochloric acid medium.

Our study was carried out by electrochemical methods. To determine the mode of action of this organic inhibitor, we determined and analyzed a good number of thermodynamic values of the activation and adsorption process (ΔG, ΔH and ΔS).

VI.1. Preparation of Metal (steel)

The studies are carried out on mild steel plates whose dimensions are taken 1.5 x 1.5 x 0.05 cm^3 having the following chemical composition (%) (Table 19):

Table 19: Chemical composition of metal in steel plate (mass %)

Elements	Fe	C	Si	Mn	Ni	S	Mo	Cr
Mass %	98.5	0.382	0.243	0.654	0.078	0.041	0.021	0.010

Before each measurement, the surface of the metal steel plate (CS) manually was polished under a stream of water with abrasive paper (emery papers) with 200, 400, 800, 1000 and 1200. It is then rinsed with distilled water, degreased in ethanol, and dried before use. The corrosive solution of 1 M hydrochloric acid was synthesized by diluting 37% hydrochloric acid with bi-distilled water.

VI .2 Inhibitor:

The choice of **206** was founded on molecular structure considerations, i.e., this is an eco-friendly organic compound with many adsorption centers. The molecular structure in figure 77 shows the organic compound tested (inhibitors) against corrosion of mild steel alloy in 1M hydrochloric acid medium.

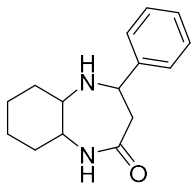

Figure 77:4-phenyl-octahydro-1,5-benzodiazepin-2-one **206** (W_3)

VI.3. Stationary electrochemical study

The cathodic and anodic polarization curves of steel in 1M hydrochloric acid medium without and with the addition of different concentrations of the inhibitor **206** are presented in

the figure below. It was obtained after 30 minutes of immersion in E_{corr} and at a temperature of 303 K.

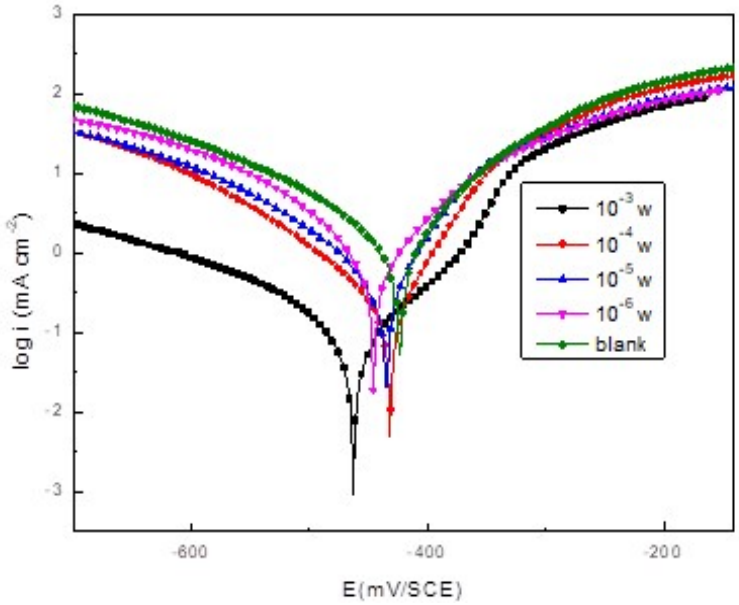

Figure 78: Potentiodynamic polarization curves for mild steel alloy (CS) in 1 M hydrochloric acid containing different concentrations of compound **206** at 303 K.

Table 20: shows the values associated with the electrochemical parameters determined from the polarization curves below.

Table 20: Electrochemical parameters of mild steel (CS) in 1M hydrochloric acid solution with or without addition of different concentrations of compound **206**

Medium	C (M)	$-E_{corr}$ (mV. SCE)	i_{corr} (µA. cm^{-2})	β_a (mV. dec^{-1})	$-\beta_c$ (mV. dec^{-1})	η_{TF} (%)
Reference	00	456.300	1104.10	112.8	155.4	-----
206	10^{-3}	461.880	99.57	107.8	131.9	90.98
	10^{-4}	429.650	155.08	84.0	114.5	85.95
	10^{-5}	432.159	198.74	87.1	127.9	81.99
	10^{-6}	442.834	296.92	92.5	140.4	73.11

The polarization curve obtained in the presence of the inhibitor is shown in the figure above. The molecule tested is a mixed inhibitor. We observe that the presence of the inhibitor significantly decreases the current densities (table 20). The previous figure clearly shows the shift of the corrosion potential towards the more cathodic potential. This observation can be

explained by the fact that the inhibitor reinforces the protective effect by forming a film on the surface of the metal.

The inhibitory efficiency of the inhibitor **206** increases with the concentration and reaches approximately 90.98 % at 10^{-3} mmol/L. This result shows the very good efficiency of our inhibitor for mild steel alloy (CS) in 1M hydrochloric acid.

VI.4. Transient electrochemical study

The Nyquist diagram of steel immersed in the acid solutions without or with the addition of different concentrations of compound **206** is given in the figure below. Measurements are made at corrosion potential after half an hour of immersion in the electrolyte at 303 K.

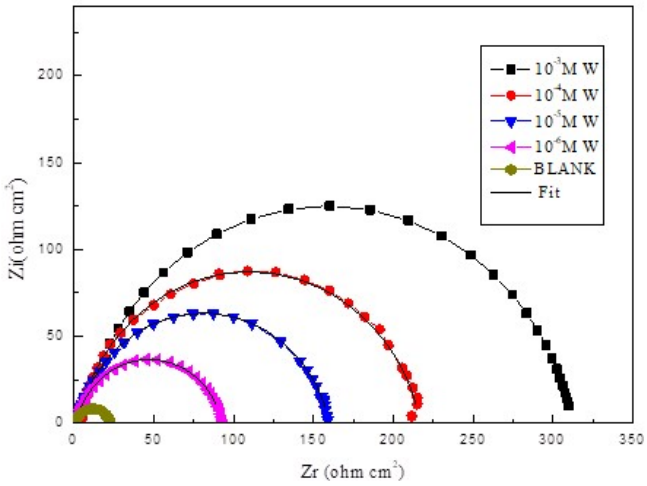

Figure 79: Nyquist diagrams for mild steel (CS) in 1M hydrochloric acid of different concentrations of compound **206** at 303 K.

Figure represents the electrochemical impedance diagram of steel in 1 M hydrochloric acid alone and in the presence of different concentrations of compound **206**.

In the Nyquist plane, the diagram consists of a main capacitive loop in the form of a semicircle with its center below the axis of the real one; this type of diagram is generally interpreted as a mechanism of charge transfer on a solid electrode with a heterogeneous and irregular surface [181], the value of *n* is linked to surface homogeneity and smoothness. Generally, surface smoothness increases with the increase in the *n* value. It can be observed that the values of *n* in presence of **206** are larger (0.870 for **206**) than that in their absence indicating that surface smoothness rises in presence of an inhibitor due to the adsorption of **206** on the CS surface.

The results from this diagram, such as the frequency (fmax), the double-layer capacitance Cdl, the charge transfer resistance (Rt), as well as those of the inhibitory efficiency are reported in the following table 3.

Table 21: Electrochemical impedance spectroscopy parametres for CS in the 1 M hydrochloric acid and compound **206** in different concentrations at 303K:

	C (M)	R_s (Ω cm^2)	R_p (Ω cm^2)	$10^6 \times Q$ ($\Omega s^{n-1} cm^{-2}$)	n	C_{dl} (μF cm^{-2})	$\chi 2$	η_{EI} (%)
Reference	00	0.83	21.57	293.9	0.845	116.2	0.002	---
206	10^{-3}	5.24	308.4	58.69	0.87	32.22	0.002	93.0
	10^{-4}	2.34	209.4	73.8	0.87	39.57	0.001	89.6
	10^{-5}	1.54	159	134.1	0.86	71.67	0.002	86.4
	10^{-6}	1.20	92.4	160.6	0.85	76.39	0.006	76.6

The analysis of the electrochemical impedance diagram of the steel in hydrochloric acid interface confirms that the adsorption of the organic compound **206** on the steel surface leads to the formation of a protective layer which results in the increase of the charge transfer resistance R_t and the decrease of the double layer capacity C_{dl}. The surface coverage increases with increasing concentration of each inhibitor. The E_{Rt} values (%) are in good agreement with those obtained from polarization measurements (table 21).

VI-5- Effect of temperature

The study of the effect of temperature provides information on the nature of the mechanism of action of the inhibitor (chemisorption or physisorption) [182], the same is true for the activation energies of the corrosion process in the absence or presence of the inhibitor. We have carried out tests at different temperatures (303 K, 313 K, 323 K, and 333 K) to test the importance of this factor on the inhibiting power.

Table 22 below shows the values of the corrosion rate of mild steel in 1M hydrochloric acid medium without and with the addition of **206** at a concentration of 1 g/L. It reveals that the i_{corr} diminishes with augmenting temperature. This kind of conduct can be explained on the basis that augments in temperature cause a displacement in the equilibrium position of the adsorption/ desorption phenomenon towards the desorption of **206** molecules on the CS surface. The values of the inhibitory efficiency of our compound are also reported in this table 22.

Table 22: The electrochemical variants for CS in 1M HCl only and with **206** at several temperatures

	T (K)	$-E_{corr}$ (mV. ECS)	i_{corr} (µA/cm²)	β_a (mV dec^{-1})	$-\beta_c$ (mV dec^{-1})	η_{TF} (%)
1M HCl	303	456.3	1104.1	112.8	155.4	-------
	313	423.5	1477.4	91.3	131.3	--------
	323	436.3	2254	91.4	117.8	--------
	333	433.3	3944.9	103.9	134.6	-------
10^{-3}M of **206**	303	461.880	99.57	107.8	131.9	90.98
	313	447.252	219.81	66.1	95.8	85.1
	323	470.492	415.98	80.4	84.6	80.9
	333	468.465	870.64	50.7	47.3	77.9

Examination of these results leads to the following findings:

➢ Variation of the electrolyte temperature from 303 K to 333 K causes an increase in the corrosion rate in the presence of the compound **206**:

➢ Efficiency increases with temperature to reach 90.98 % at 303 K.

A. kinetic parameters of Activation (Ea, ΔH°a, ΔS°a)

The figure below represents the variation of the logarithm of the corrosion rate of mild steel in 1M hydrochloric acid as a function of 1/T in the absence and presence of the **206** compound.

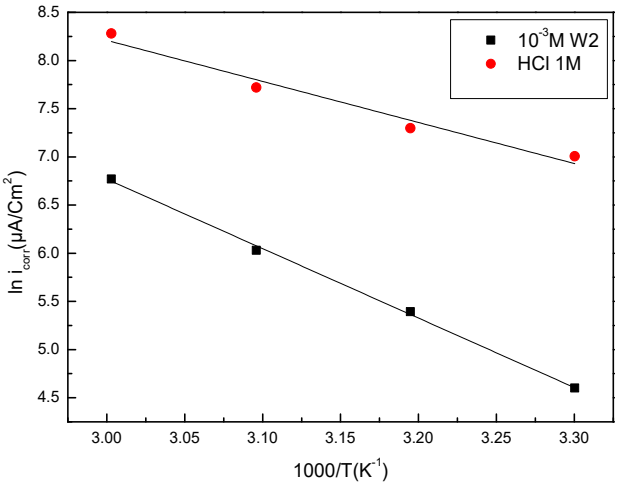

Figure 80: Arrhenius plots for corrosion of mild steel in 1 M hydrochloric acid in the absence and presence of **206**.

The obtained values of Ea, ΔH°a, and ΔS°a in the different solutions without or with addition of compound **206** are showed in table 23.

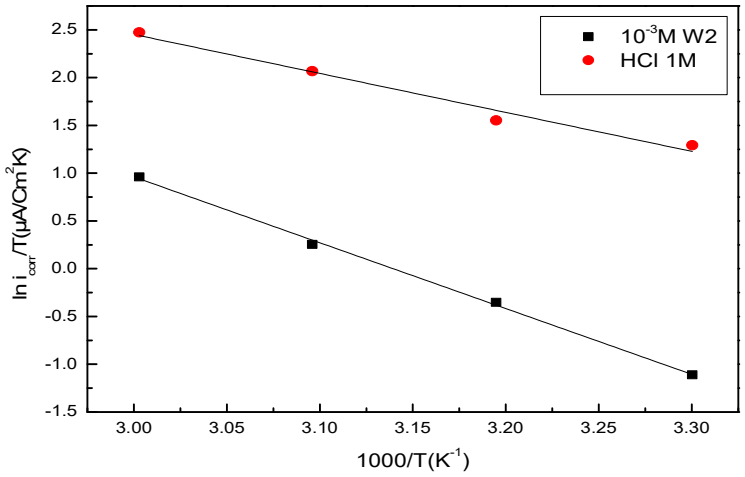

Figure 81: Variation of ln (icorr/T) =f (1/T) of mild steel in 1 M hydrochloric acid medium without or with addition of **206** to 10^{-3}M.

Table 23: corrosion activation parameters of mild steel in 1M hydrochloric acid medium without or with 10^{-3} M of **206** additions

	E_a (kJ/mol)	ΔH_a (kJ/mol)	ΔS_a (J/mol.K)
Blanc 1M	35.4	32.76	-79.19
206 10^{-3}	59.91	57.33	17.74

The values in table 23 show that the activation energy is lower in absence of the inhibitor than in the presence. This decrease is in favor of the strong bond adsorption of this compound on the steel surface. The positive enthalpy signal reflects the endothermic nature of the steel dissolution process. This process is a difficult reaction in 1M hydrochloric acid medium in the presence of the inhibitor. The high and negative value of the entropy ΔS°a implies that there is a decrease in disorder during the transformation of the reactants into the activated complex [183].

Adsorption isotherms and thermodynamic parameters

The corrosion inhibition of steel by **206** is due to the adsorption susceptibility of this compound on the metal surface. The variation of Cinh/ratio as a function of concentration (C) shows that the adsorption of **206** follows the Langmuir adsorption model.

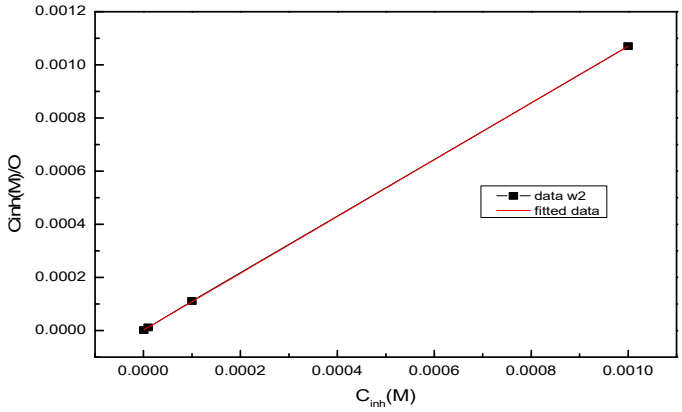

Figure 82: Langmuir adsorption isotherm diagram for the adsorption of corrosion of **206** on mild steel (CS) in hydrochloric acid.

Tableau 24: Adsorption parameters **206** for the concentration effect on mild steel in 1M hydrochloric acid at 303K

Inhibitor	K_{ads} (L mol^{-1})	*Slope*	R^2	ΔG°_{ads} (KJ.mol^{-1})
206 (10^{-3}M)	5.970.10^5	1.02	1	-43.60

The negative value of ΔG_{ads} indicates the spontaneity of the adsorption process and the stability of the adsorbed layer on the metal surface. The calculated value of ΔG°_{ads} is close to (-40 kJ. mol^{-1}) and suggest that the chemical process of adsorption was chemisorption [184].

Part II

Chapter I :

Synthesis, X-ray, spectroscopic characterization, Hirshfeld surface analysis, DFT calculation and molecular docking investigations of a novel 7-phenyl-2,3,4,5-tetrahydro-1H-1,4-diazepin-5-one derivative

Introduction:

1,4-diazepine and its derivatives containing heterocyclic ring systems possess a wide range of therapeutic applications, and details have contributed to advances in understanding the basic principles and activities of this structure.

These derivative scaffolds are present in a number of drugs that have been used for anxiolytic, sedative [185-188], anti-HIV [189], as potential fungicidal, insecticidal, and herbicidal agents [190], anticancer and anti-inflammatory activity [191].

Therefore, the development of new strategies is one reason why the synthesis of 1,4-diazepin-2-ones is ever evolving, and the diazepine ring is reported in the literature to be prepared from linear precursors by intermolecular reductive amination [192-194], lactam formation [195], and transamination [196].

In this chapter, we focused on the synthesis, Hirshfeld surface analysis, and molecular docking study of 7-phenyl-1,4-diazepin-5-one. But before describing our results, we will report on previous works in the literature.

I-Synthesis of 7-phenyl -1,4- diazepin-5-one and its derivative:

Hofmann *et al*. [197], by examining condensation between β-cetoesters **54**, **62**, and ethylenediamine **207** were able to isolate the products **208**-**209**. Indeed, when the cyclization agent was ethyl benzoylacetate **54,** the reaction led to the product 7-phenyl-1,4-diazepin-5-one **210**, which can exist in the two tautomeric forms **210a** and **210b** (scheme 80).

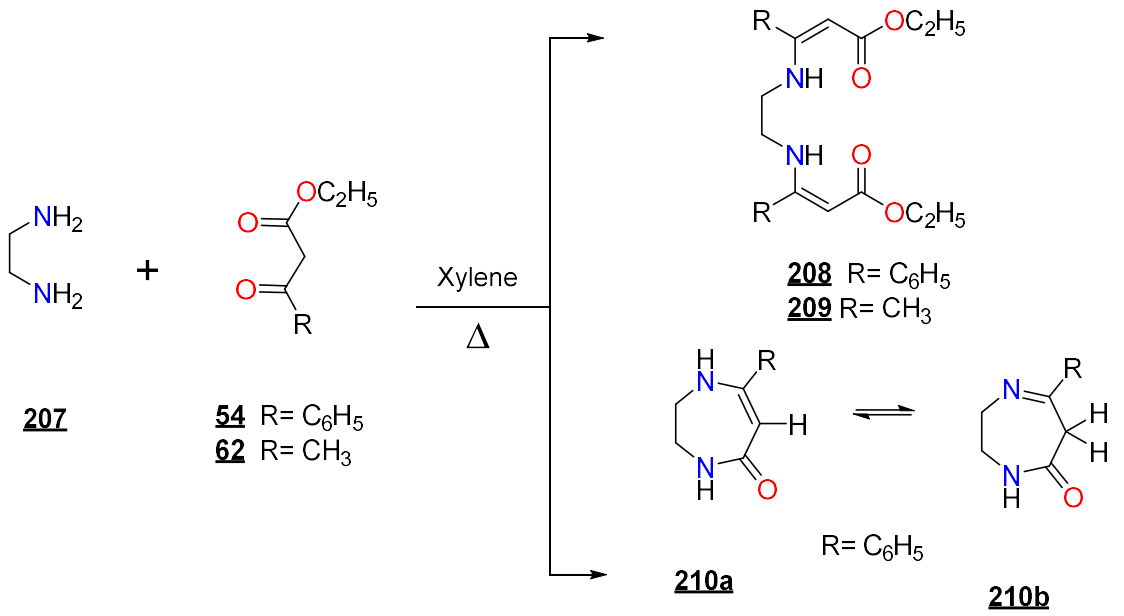

- Scheme 80-

Begland *et al.* [198], described the synthesis of 5,7-dimethyl-6H-1,4-diazepine-2,3-dicarbonitrile **212** by condensation of 2.3-diaminomaleonitrile **211** with acetylacetone in the presence of oxalic acid (scheme 81).

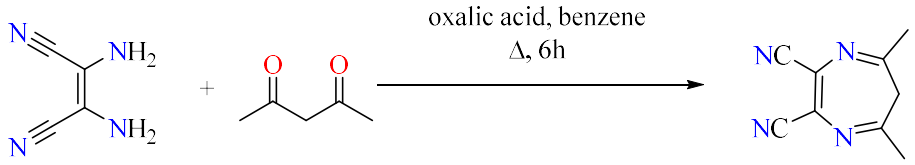

211 **212** (98%)

- Scheme 81-

In our laboratory, Chammach *et al.* [199] prepared 7-phenyl-l,4-diazepin-5-one **213** by condensation of ethylenediamine **207** with ethyl benzoylacetate **54** in xylene in good yield according to [197], and have shown, by a study based on ^{1}HMR spectral data, and electron impact fragmentations, that the compound should preferentially adopt the enaminic form **212a** (scheme 82).

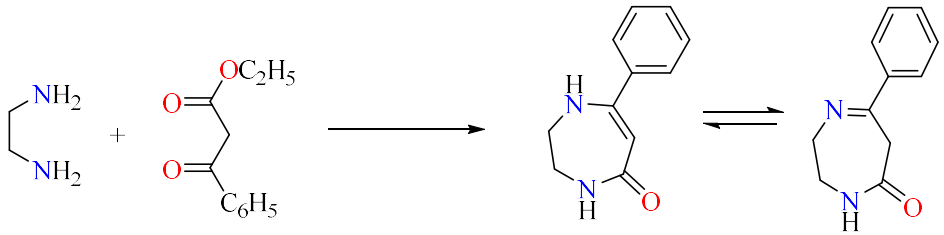

207 **54** **213a** **213b**

- Scheme 82-

The structure of compound **213a** has been confirmed by a crystallography study (figure 83) [200].

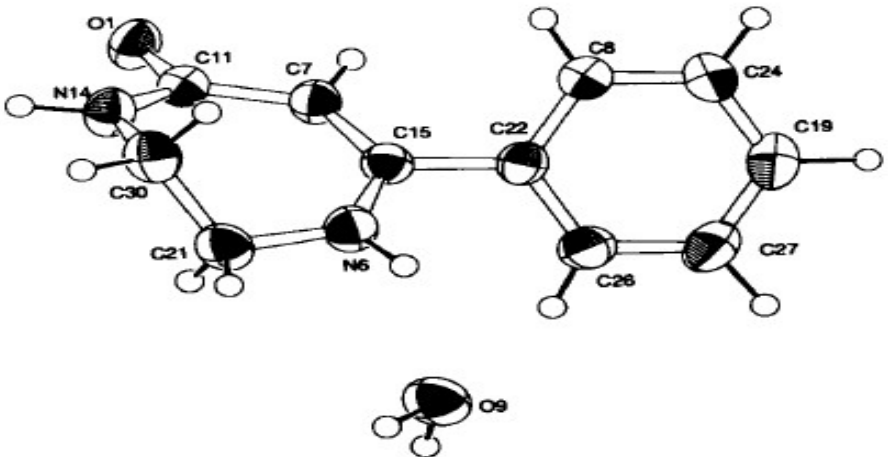

Figure 83

Banfi *et al*. [201] describe a synthesis for the preparing of the aliphatic 1-sulfonyl 1,4-diazepan-5-ones **214** by multicomponent reactions followed; by Mitsunobu cyclization as shown in scheme 83.

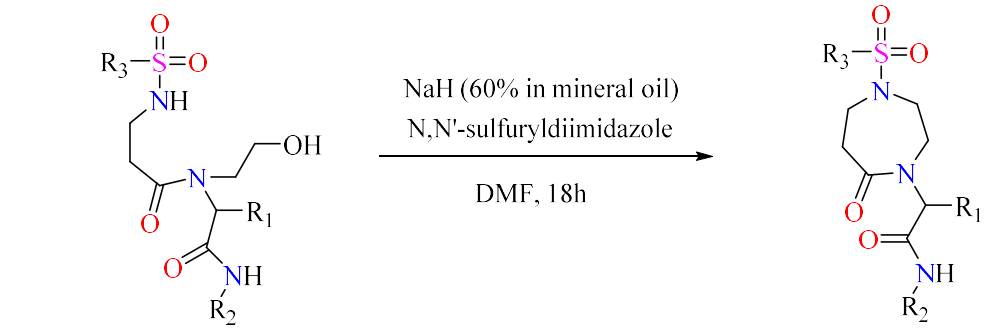

214

R_3= *p*-Tol, R_2 = cychex, R_1= iP

215

68%

- Scheme 83-

Wlodarczyk *et al*. [202] were interested in the concept of organic synthesis assisted under microwave, they were able to obtain 7-substitute- 1,4-diazepine-5-ones **216** from the condensation of *β*-ketoester with 1.2-ethylenediamine (scheme 84).

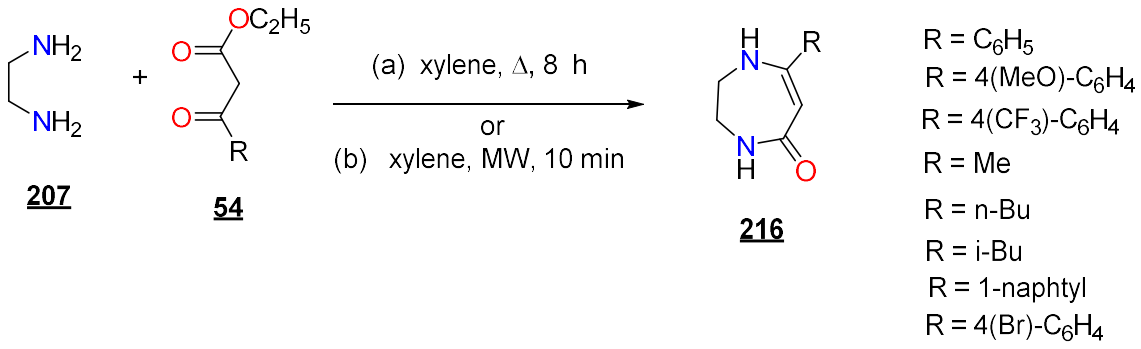

207

54

216

- Scheme 84-

A multicomponent reaction of 1,2-diamines **207** with 1,3-dicarbonyls **217** and aromatic aldehydes **218** is described by Sotoca *et al*. [143] for the direct stereoselective synthesis of 1,4-diazepane derivatives **219** (scheme 85).

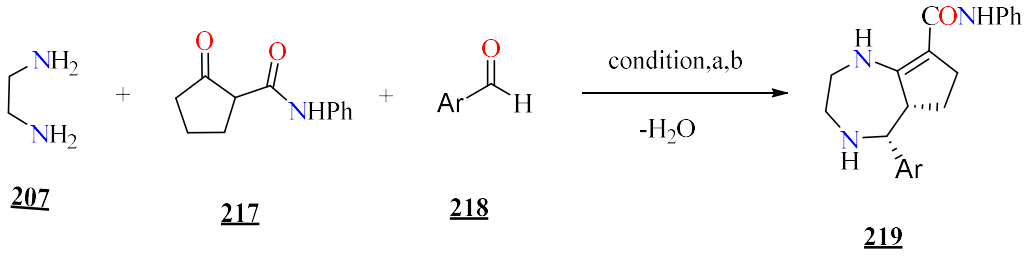

207

217

218

219

a-Conditions: 4 °A MS, toluene,110 °C, 24 h.
b-Conditions:120 °C, 4 h.

- Scheme 85-

Sethuvasana *et al.* [203] describe the synthesis of a new series of 2,7-diaryldiazepan-5-ones **224a-i** from their corresponding piperidin-4-ones **223** using Schmidt rearrangement. Earlier, the Schmidt rearrangement of piperidin-4-ones was carried out in two steps, i.e., converting piperidin-4-ones into hydrochlorides and subjecting them to Schmidt rearrangement after isolation (scheme 86).

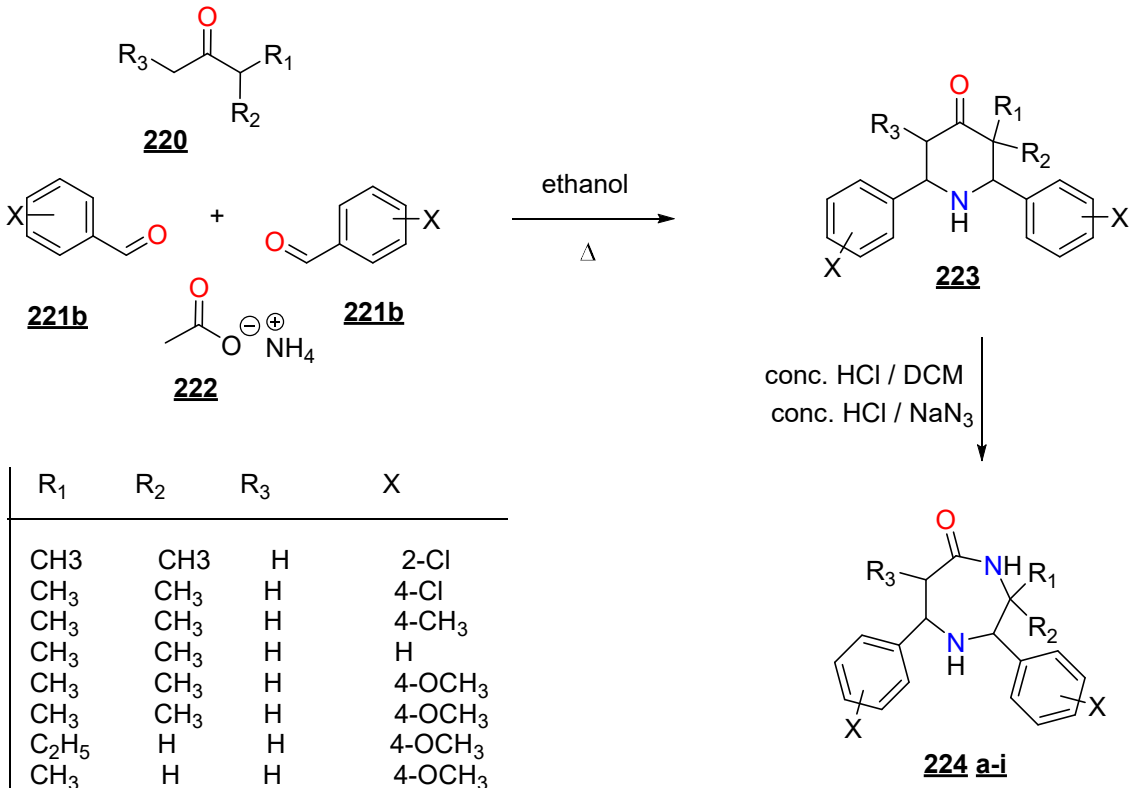

R_1	R_2	R_3	X
CH3	CH3	H	2-Cl
CH_3	CH_3	H	4-Cl
CH_3	CH_3	H	4-CH_3
CH_3	CH_3	H	H
CH_3	CH_3	H	4-OCH_3
CH_3	CH_3	H	4-OCH_3
C_2H_5	H	H	4-OCH_3
CH_3	H	H	4-OCH_3

- Scheme 86-

Ahumada *et al.* [204] reported a facile way to the formation in one-pot of 7-(thiophene-2-yl)-5-(trifluoromethyl)-2,3-dihydro-1H-1,4-diazepine derivatives **227** by condensation 2-thenoyltrifluoroacetone with 1.2-ethylendiamine **207**. In addition the known N, N'-ethylene-bis(trifluoroacetamide) **226** was isolated as a by-product (scheme87).

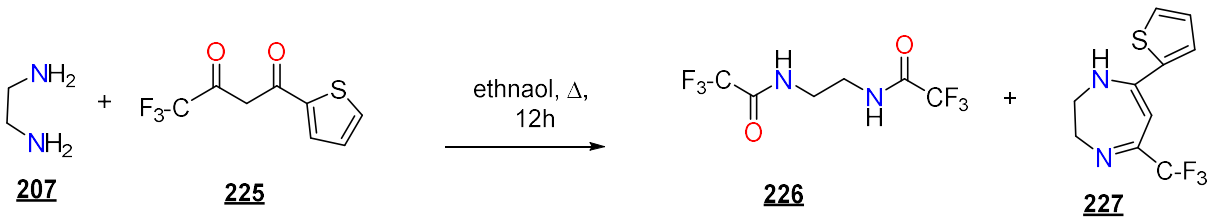

- Scheme 87-

Mehranpour *et al.* [144] described the synthesis of 1,4-diazepinium salts **229a** and **229b** from the condensation of the intermediate salts (generated through the action of DMF/$POCl_3$

on aryl-acetic in the presence of perchlolonic acid) with 1,2-ethylenediamine and its derivatives.. The compounds are obtained in good yield (scheme88).

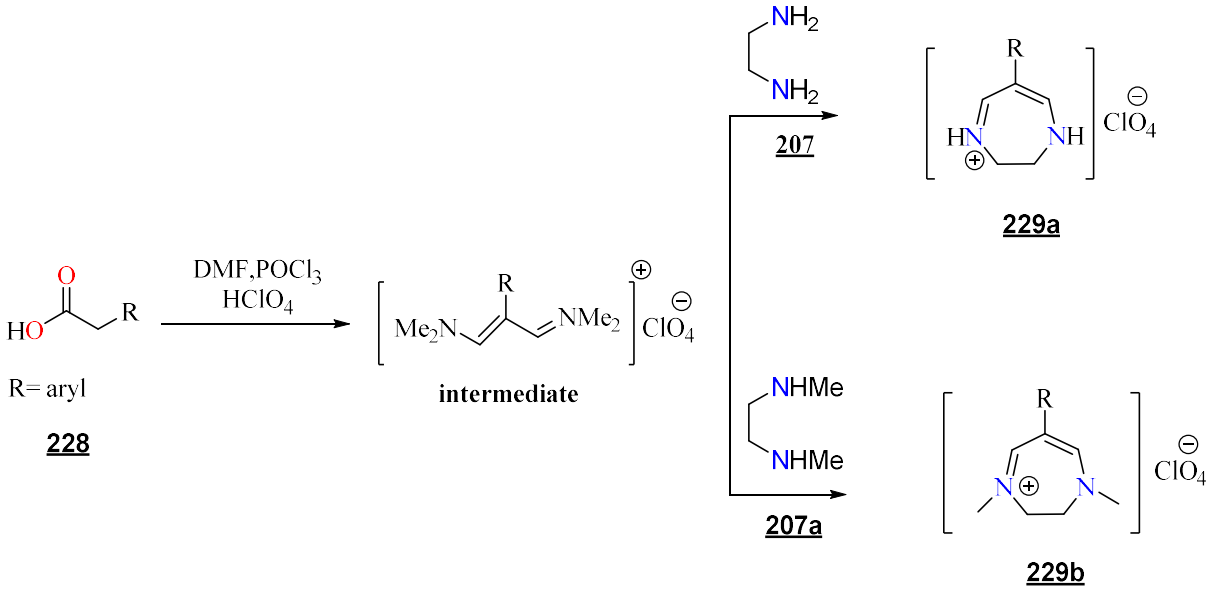

- Scheme 88-

Zia *et al*. [205] synthesized in two steps the 1,4-diazepine derivative **232**. The first one corresponds to the heating of *β*-diketone **230** in glacial acetic acid for 2 hours leading to the flavonoid compound **231**. In the second step, the compound **231** reacted with a large excess of 1.2-ethylenediamine **207** in refluxing ethanol for 2 h to give 1,4-diazepinic **232** (scheme 89).

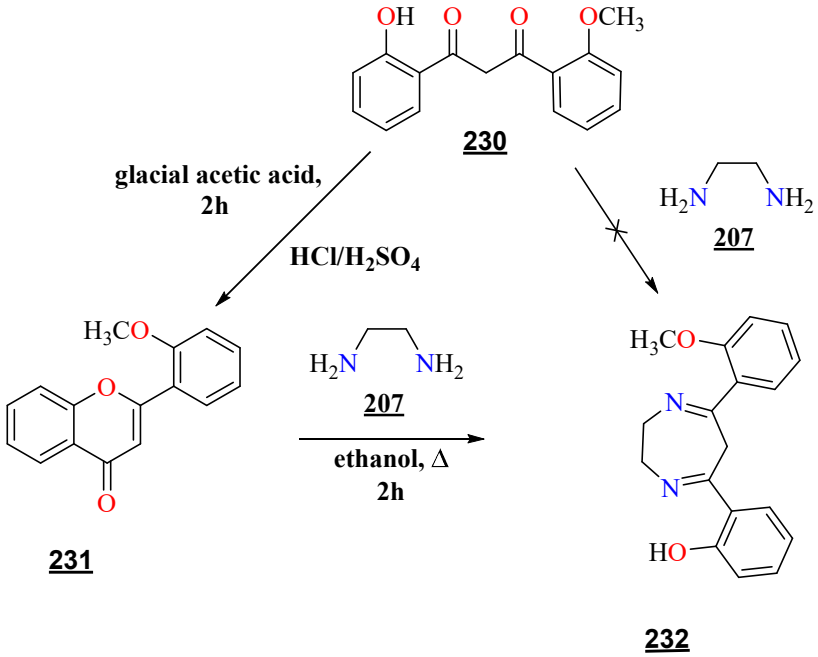

- Scheme 89-

Taking into account the data in the literature, we have re-synthesized compound **210a** according to the method described by Hoffman [197] in order to test a theoretical study and test it as an anticorrosion compound.

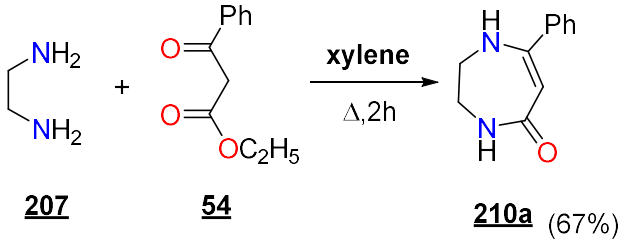

207 **54** **210a** (67%)

Scheme 90

The compound was identified using spectroscopy data (^{1}H and^{13}C NMR, Mass), and the structure was confirmed by x-ray diffraction.

In^{1}HNMR spectrum of compound **210a** taken in deuterated dimethyl sulfoxide (DMSO-d6), we observed the signals due to aromatic protons resonating between 7.36 -7.46 ppm, a multiplet at 4.47 ppm assigned to the methine protons and a multiplet betewn 3.19-3.39 ppm corresponding to methylene protons.

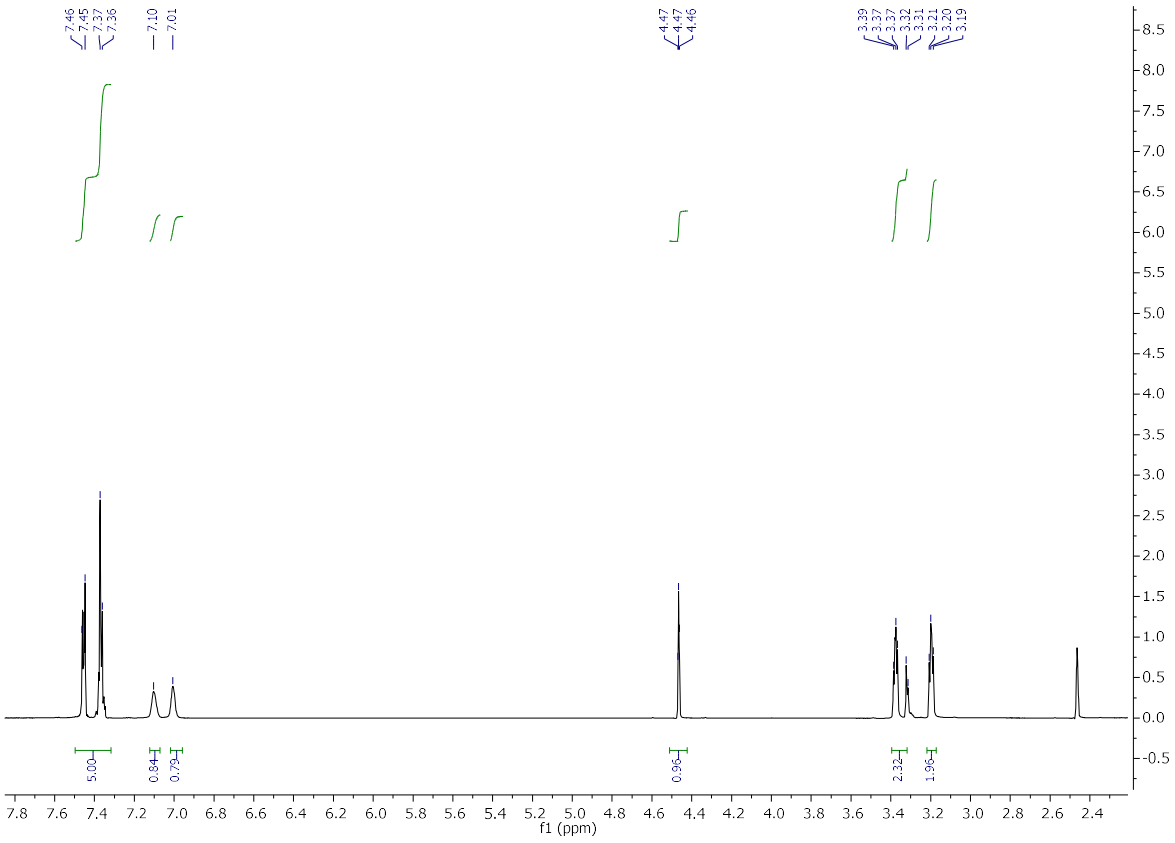

Figure 83: ^{1}H NMR spectrum of compound **210a** (600 MHz, DMSO-d6)

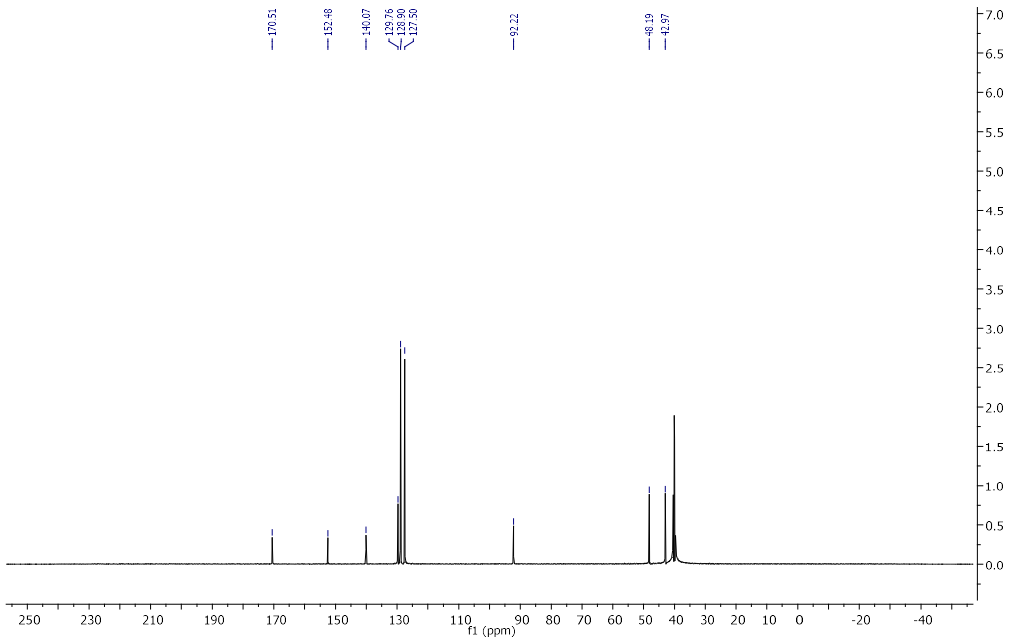

Figure 84: ^{13}C NMR spectrum of compound **212a** (151 MHz, DMSO-d_6))

Similarly, the ^{13}C NMR spectrum, in particular, showed a signal at 42.97 and 48.19 ppm associated with the carbon of methylene groups and a signal at 92.22 ppm due to vinlyic in position 6 of the diazepine ring.

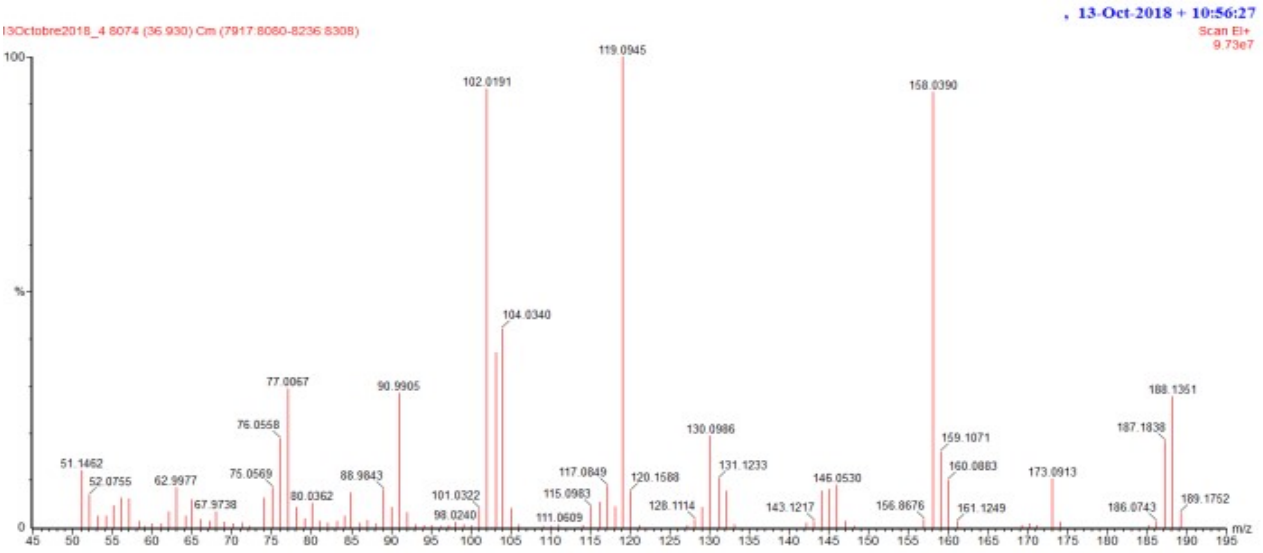

Figure 85: Mass spectrum of compound **210a**

In order to determine the exact structure of the product obtained, we used a crystallographic study by x-ray diffraction. This crystallographic analysis confirms the structure proposed by the NMR and mass spectroscopy analyses.

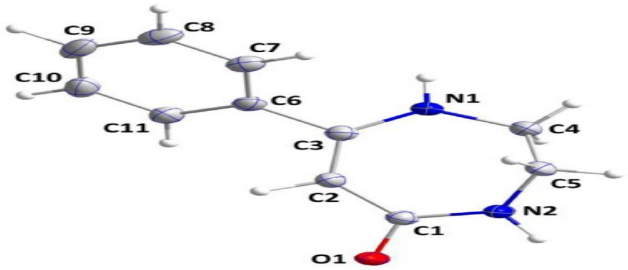

Figure 86: ORTEP representation of the structure of **210a**

The tetrahydrodiazepine ring adopts a twisted envelope conformation. The benzene ring is inclined to the mean plane defined by N1/C1 C4 (deviation from mean plane: −0.0220 (5) ˚A (C1); 0.0300(8) ˚A (C2); r.m.s. deviation 0.0213) by 43.55(4)°, whereas the inclination to the mean plane of the full diazepine ring is 41.46(6)°. In the crystal, N2—H2A . . .O1 hydrogen bonds (Table 18) form inversion dimers which are linked into corrugated sheets parallel to the bc plane by N1 –H1 . . .O1 hydrogen bonds and C5—H5A . . .Cg 1 and C5—H5B . . .Cg1 interactions (table 25 and figure 87).

Table 25: **Hydrogen-bond geometry (Å,°)**

D—H ···A	**D—H**	**H···A**	**D··· A**	**D—H···A**
N1—H1*A*. . .O1^{i}	0.947(16)	1.913(16)	2.8591(12)	177.0(13)
N2—H2. . .O1^{ii}	0.905(16)	1.924(16)	2.7937(12)	160.4(14)
C5 –H5A –Cg1 ^{iii}	0.996(13)	2.755(14)	3.6160(13)	145.0(12)
C5 –H5B –Cg1 ^{iv}	1.019(14)	2.970(15)	3.7285(15)	131.9(10)

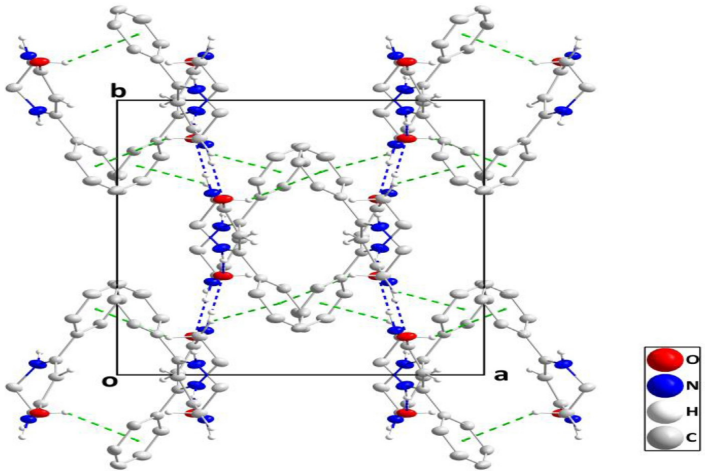

Figure 88: Packing viewed along the *c* -axis direction with N –H . . .O hydrogen bonds shown by blue dashed lines. The C –H . . . π (ring) interactions are shown by green dashed lines.

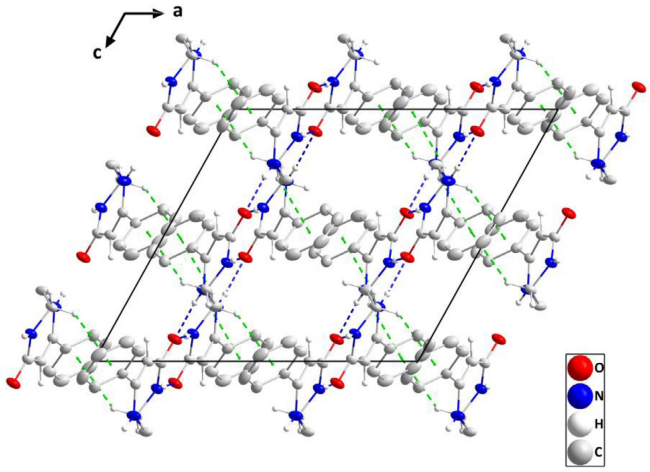

Figure 89: Packing viewed along the b -axis direction with intermolecular interactions depicted as in figure 89

Table 26: Experimental Details of compound **<u>210a</u>**

Chemical formula	C $_{11}$ H $_{12}$ N $_{2}$ O
Formula weight	188.23 g/mol
Temperature	150(2) K
Wavelength	1.54178 ˚A
1.54178 ˚A Crystal size	0.181 × 0.197 × 0.260 mm 3
Crystal system	Monoclinic
Space group C 1 2/c 1	C 1 2/c 1
Unit cell dimensions (A˚)	a = 13.6868(6) , b = 13.8189(6), c = 12.1418(5)
Volume	2005.29(15) ˚A 3
Z	8
Absorption coefficient	0.657 mm −1
F(000)	800

II-Theoretical study of the compound:

II.1. Hirshfeld analysis of the compound <u>210a</u>:

The nature of intermolecular interactions in compound **<u>210a</u>** was clarified using three-dimensional Hirshfeld surface analysis. As depicted in figure 90, the important interactions in the compound may be H . . . O and H . . . N hydrogen bonds.

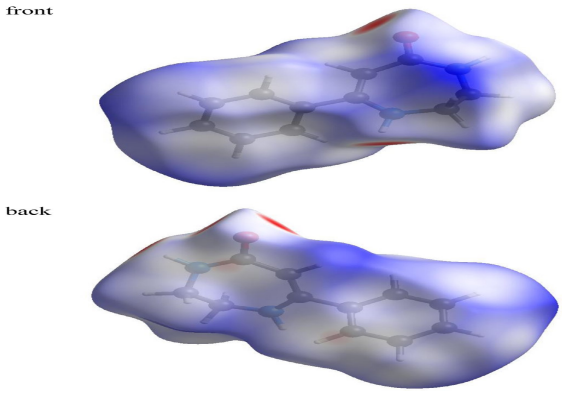

Figure 90: The d_{norm} Hirshfeld surface of the title compound (red: negative, white: zero, blue: positive; scale: −0.6042 to 1.9277 a.u.).

In order to understand the relative importance of H . . . O hydrogen bonds over H . . . N hydrogen bonds, we calculated the 2D fingerprint plots for the title compound.

The 2D fingerprint plots (figure34) highlight particular atom pair contacts and enable the separation of contributions from different interaction types that overlap in the full fingerprint. Using the standard 0.6–2.6 a.u. view with the distance scales displayed on the graph axes and including the reciprocal contacts, we found the most important interaction involving hydrogen in the compound was the H . . . H contact. The contribution of the H . . . O, H . . . N, and H . . . H contacts are 14.8%, 1.6%, and 57.8%, respectively.

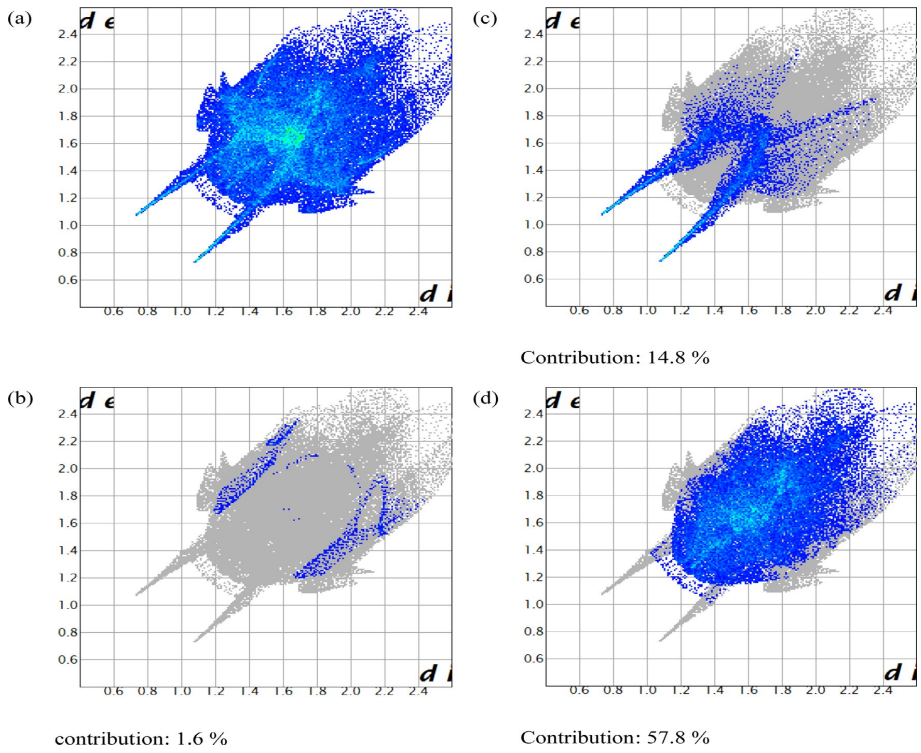

Figure 91: The 2D fingerprint plot of the title compound (a) full, (b) resolved by the H . . . O contacts, (c) resolved by the H . . . N contacts, (d) resolved by the H . . . H contacts.

II.2. Molecular docking analysis of <u>210a</u>:

Based on the biological activity of the 1,4-diazepine-5-one derivative and the continuity of the work in our laboratory, we are interested in the development of a checkpoint kinase **<u>210a</u>** (Chk1) inhibitor. To carry out this work, a first study of molecular modeling (docking) was carried out. The antitumor activity of tetrahydrodiazepine derivatives is invigorated using molecular docking studies. The Checkpoint Kinase Chk1/SB218078 was chosen as a target enzyme (pdb code 1NVS). The ability of the novel tetrahydrodiazepine derivative to inhibit Checkpoint Kinase Chk1/SB218078 is estimated by predicting the binding energy of the stable complex compound-Checkpoint Kinase and the number of conventional intermolecular hydrogen bonds established between the synthesized compound and active site residues of Checkpoint Kinase Chk1/SB218078. Indeed, the formed complex displayed a negative binding energy of (−4.67 kcal/mol), which is a signpost that the inhibition of Checkpoint Kinase Chk1/SB218078 is thermodynamically favorable. Docking results reveal that the binding interactions are mainly of π-type (figure92). Indeed, three π-alkyl interactions are formed between the aromatic ring of tetrahydrodiazepine derivative and Leu-A137, Al A36, and Cys-A87 and π- σ interaction between sigma bonds of the aromatic ring and Leu-A15 (figure 92). Further, a carbon hydrogen bond is formed between the methane of Gly16 and the keto group of the seven-member ring of tetrahydrodiazepine derivative at a distance of 3.05 ˚A (figure 92).

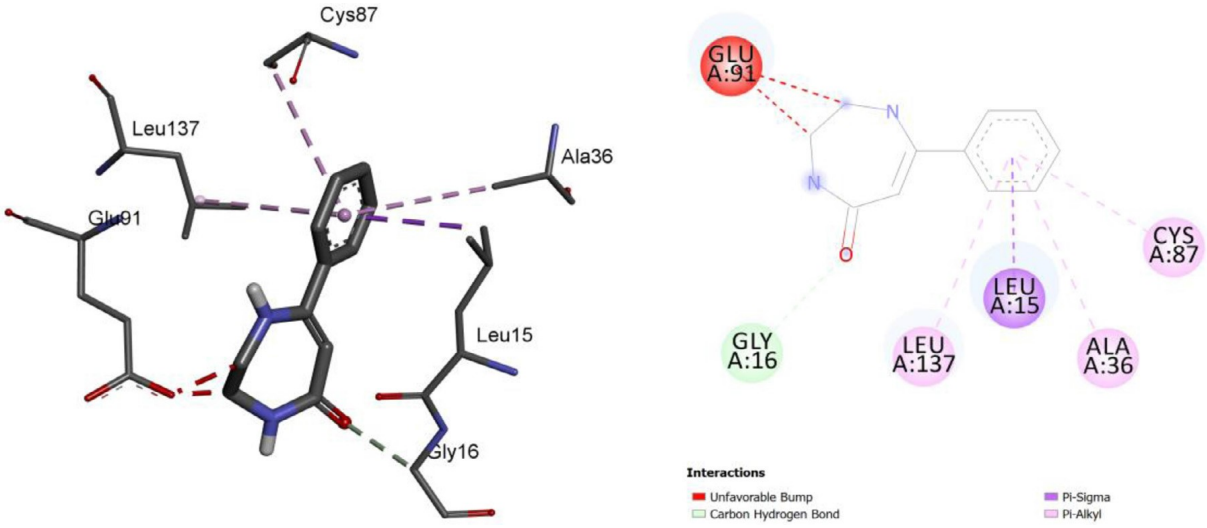

Figure 92: 3D (left) and 2D (left) intermolecular interactions of name of compound and active amino acids of Checkpoint Kinase Chk1/SB218078.

Conclusion

In this chapter, we have presented some bibliographic data on 1,4-diazepin-5-one derivatives, their different synthetic methods, and their applications described in the literature. The compound was further investigated by X-ray crystallography and Hirshfeld surface analysis studies.

Experimental part

Procedures for preparing 7-phenyl-1.4-diazepan-5-one 210a:

A solution (0.1 mol) of ethyl benzoyl acetate and 10 mL of xylene were added drop-wise over 40 min. of refluxing into 0.1 mol of 1.2-ethylenediamine and 100 ml of xylene. After the reaction was completed, it was left for 24 hours at room temperature. On cooling, the oil solidified into a hard mass. The xylene layer was decanted and discarded. The solid was suspended in about 100 mL of chloroform, and the mixture was filtered after extraction. It was re-crystallized to obtain a solid compound in the form of colorless crystals.

The physical and chemical properties of the product <u>210a</u>:

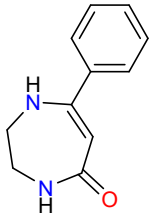

White, solid

F(^{0}C): 212-214 , Yield: 67%

^{1}HNMR (600 MHz, DMSO-d$_6$) δ ppm: 3.19-3.21(m,2H), 3.31-3.39(m,2H),4.46-4.47(t,1H,CH),7.01(s,1H,NH),7.10(s,1H,NH),7.36- 7.46 (m,5H,CHar).

^{13}C NMR (151 MHz, DMSO-d$_6$) δ ppm: 42.97(CH_2), 48.19(CH_2), 92.22 (=CH), 127.50-129.76 (Carom), 170.51 (C=O).

Mass spectrum (EI): m/z = 188

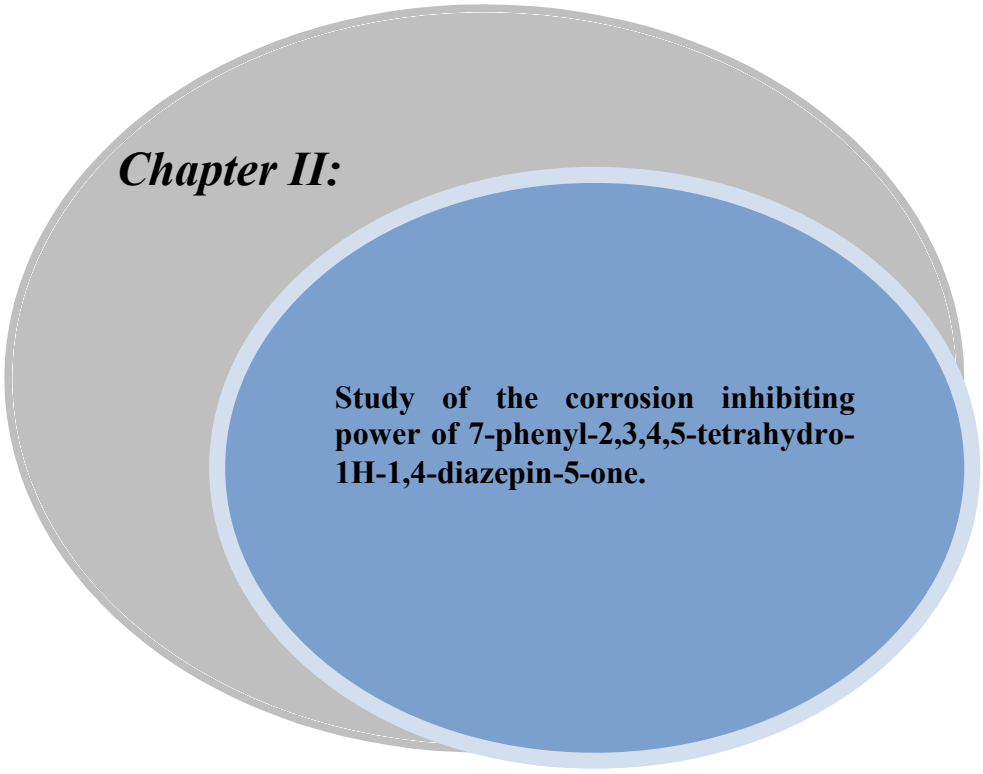
Chapter II:
Study of the corrosion inhibiting power of 7-phenyl-2,3,4,5-tetrahydro-1H-1,4-diazepin-5-one.

I- Introduction

Corrosion inhibitor is a chemical substance that involves the formation of a layer, often a passivation layer that prevents access of the corrosive substance to the metal when added in a low concentration to the corrosive medium, as well as damage of metals and alloys through chemical or electrochemical interaction with their surrounding environment [206]. A corrosion inhibitor must attenuate the corrosion rate of the metal while maintaining its physicochemical properties. It must not only be stable in the presence of the other constituents of the medium but also not affect the stability of the species contained in the medium. An inhibitor is definitely recognized, such as if it is stable at the temperature of use, effective at low concentrations, compatible with the standards of non-toxicity, and inexpensive. The literature mentions a large number of inhibitors. It can be classified based on several criteria [207], including their application, formulation (organic inhibitors, mineral inhibitors), the electrochemical reaction inhibited (cathodic inhibitor, anodic inhibitor, or mixed), or the reaction mechanism involved, adsorption and/or film formation [208]. On the other hand, synthetic organic compounds containing unsaturated bonds and/or polar atoms such as oxygen, nitrogen, and sulfur are often good inhibitors of iron corrosion in hydrochloric acid. We use oxadiazoles [209], triazoles [210], benzotriazoles [211], imidazole, benzimidazole [212], and 1,5-benzodiazepines [213] as examples.

The objective is to search for new effective inhibitors to prevent or reduce corrosion. Therefore, we examined the corrosion inhibitory potency of 7-phenyl-2,3,4,5-tetrahydro-1 H-1,4-diazepin-5-one (figure 93). The techniques used in this work were potentiodynamic polarization and electrochemical impedance spectroscopy.

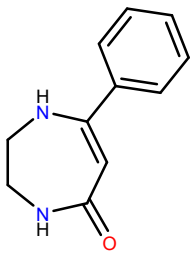

Figure 93: 7-phenyl-2,3,4,5-tetrahydro-1 H -1,4- diazepin-5-one **<u>210a</u>**

II. Preparation Metal (steel)

The studies are carried out on mild steel plates whose dimensions are taken 1.5 x 1.5 x 0.05 cm^3 having the following chemical composition (%) (table27).

Table 27: Chemical composition of metal (steel) (mass %)

Elements	Fe	C	Si	P	Mn	Al	S
Mass %	99.21	0.21	0.38	0.09	0.05	0.01	0.05

Before each measurement, the surface of the metal plates was manually polished under a stream of water with abrasive paper (emery paper) at 180, 400, 800, 1000, and 1200. It is then rinsed with distilled water, degreased in ethanol and dried before use.

III- Results and discussion

We present the results relating to the influence of the concentration of the product **210a** and the effect of the temperature on the protection of steel in 1M hydrochloric acid medium. Our study was carried out by electrochemical methods. To determine the mode of action of this organic inhibitor, we determined and analyzed a large number of thermodynamic values of the activation and adsorption processes (ΔG, ΔH and ΔS).

III-1 Stationary methods (polarization curves)

Table 28 summarizes corrosion kinetic parameters such as corrosion current density values (Icorr), corrosion potential (Ecorr), cathodic and anodic Tafel slopes (βa and βc), and inhibitory efficiency (EI%) obtained from potentiodynamic polarization curves of carbon steel in 1M hydrochloric acid medium containing various concentrations of 210a at 303 K.

Table 28**:** Electrochemical parameters in the presence of different concentrations of **210a**

C (M)	E_{corr} (mV)	I_{corr} (μA)	$-\beta_c$ (mV)	β_a (mV)	E%
10^{-3}	-453.836	115.68	68.8	66.9	89.5
10^{-4}	-443.516	154.61	79.1.3	60.6	85.5
10^{-5}	-449.184	216.4	88.7	64.9	80.4
10^{-6}	-448.554	265.937	64.7.6	67.4	75.9

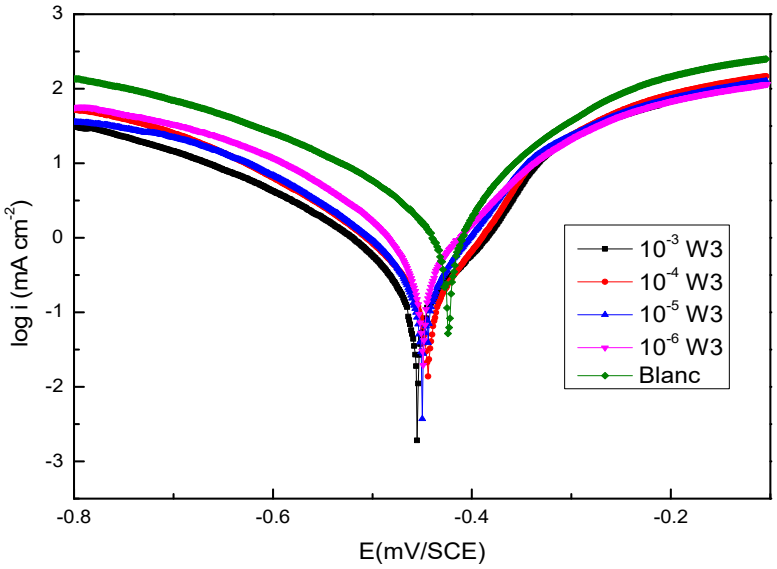

Figure 94: Potentiodynamic polarization curves for mild steel in 1M hydrochloric acid containing different concentrations of **210a** at 303 K.

Figure 94 shows the polarization curves of carbon steel in 1M hydrochloric acid medium, without and with the addition of different concentrations of **210a** inhibitor. We can see that the addition of **210a** causes a shift in the corrosion potential towards more cathodic values.

This shift is accompanied by a clear decrease in the cathodic current density. This decrease is all the more marked as the concentration of **210a** added to the hydrochloric acid solution is high. The cathodic curves show a wide range of linearity, indicating that Tafel's law is well verified. Tafel's law is well verified.

The discharge of the proton is then done according to pure activation kinetic activation kinetics. The anodic branches are slightly affected in the presence of this inhibitor.

The presence of compound **210a** causes a decrease in the oxidation current density. These observations confirm the mixed character of the inhibitor and clearly show that the inhibitor reduces the anodic dissolution rate of the steel and the proton reduction rate of protons.

III-2 Transient methods (Electrochemical impedance spectroscopy)

The values of the charge transfer resistance (R_t) are calculated from the difference impedance between the lower and higher frequencies, as suggested by Tsuru *et al.* [214]. Equation determines the double layer capacitance (C_{dl}) and the frequency at which the imaginary component of the impedance is maximum (-Zmax).

$$C_{dl} = \frac{1}{\omega \times R_t}$$

$$ou\ \omega = 2\ \pi . f_{max}$$

In figure 95 Nyquist diagrams of steel immersed in the acid solution with and without the addition of different concentrations of compound **<u>210a</u>** are shown, where these diagrams show a single capacitive loop whose size increases with the concentration of inhibitor, indicating the formation of a protective film on the steel surface.

This behavior is primarily due to the charge transfer process taking place at the solution/electrode interface. It is also clear that these impedance diagrams are not perfect semicircles, and this is due to the frequency dispersion of the interfacial impedance [216].

The values of electrochemical parameters, charge transfer resistance (Rt), double-layer capacitance (Cdl), (fmax), and inhibitory efficiency (ERt%) for different concentrations of 210a are gathered in table 29.

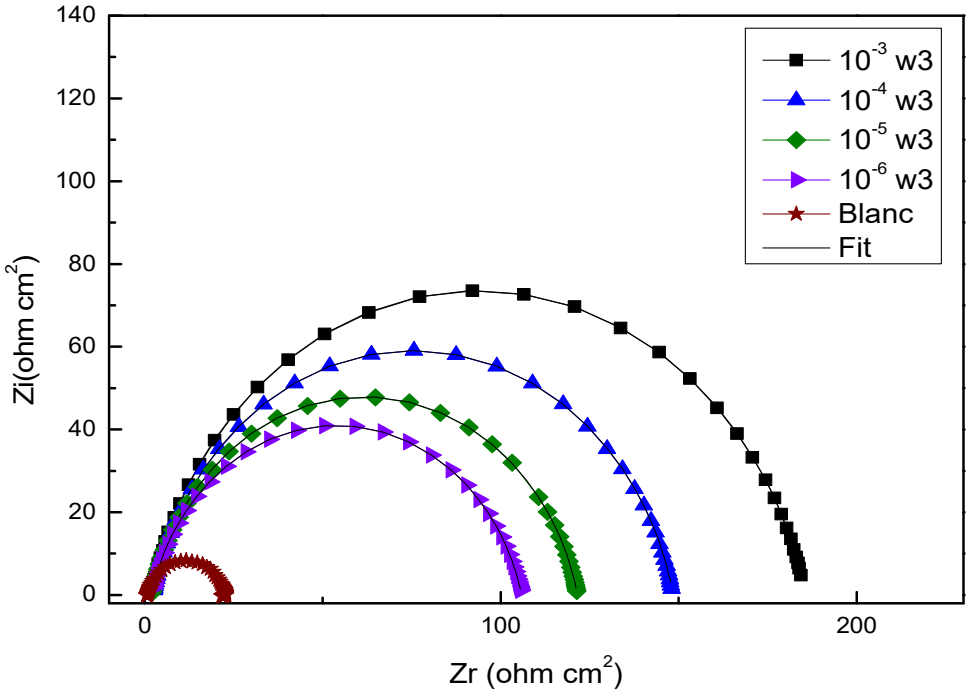

Figure 95: Nyquist diagrams for mild steel in 1M hydrochloric acid of different concentrations of compound **<u>210a</u>** at 303 K.

Table 30: Electrochemical impedance parameters in the presence of different concentrations of **210a**

Conc. (M)	R_s (Ω cm^2)	R_p (Ω cm^2)	$10^6 \times A$ (Ω s^{n-1} cm^{-2})	n	C_{dl} (μF cm^{-2})	$\chi 2$	E(%)
1M	0.83	21.57	293.9	0.845	116.2	0.002	---
10^{-3}	1.81	184.1	129.95	0.86	70.77	0.006	88.2
10^{-4}	2.3	144.2	145	0.866	79.7	0.004	85
10^{-5}	1.86	121	161.1	0.85	80.40	0.005	82.1
10^{-6}	1.82	105.4	182.4	0.84	85.92	0.005	79.5

From the analysis of the results reported in table 30, we can see that:

➢ Value of charge transfer resistance (Rp) increases significantly with increasing 210a concentration, and consequently, the inhibitory efficiency increases to 88.2% at 10^{-3} M 210a. This result indicates that the corrosion of carbon steel in acidic solutions is primarily controlled by a charge transfer process.

➢ Capacity of the double-layer decreases with the addition of 210a, it decreases (from 116.2 µF. cm2) for the reference (to 70.77 µF. cm2 for 10^{-3} M). This decrease in C_{dl} value is associated with the adsorption of **210a** on the metal surface which induces the formation of the corrosion inhibiting film on this surface. Indeed, the more the inhibitor adsorbs, the more the thickness of the deposit of its molecules increases and the more the capacity of the double layer decreases [217].

IV- Thermodynamic study:

The study of the effect of temperature provides information on the nature of the mechanism of action of the inhibitor (chemisorption or physisorption) [218]. The same is true for the activation energies of the corrosion process in the absence and presence of the inhibitor.

Given the importance of this factor on the inhibitory power, we performed mass loss tests at different temperatures (303 K, 313 K, 323 K, and 333 K).

The values of the corrosion rate and the corresponding inhibitory efficiency are collected in table 31:

Table31: Thermodynamic parameters for **210a** adsorption onto the activated carbon at different temperatures.

210a	E_{corr} (mV)	I_{corr} (µA)	$-\beta_c$ (mV)	β_a (mV)	E%
T=303	-453.836	115.68	68.8	66.9	89.5
T=313	-450.093	219.54	76.2	65.9	85.4
T=323	-471.336	402.16	37.6	41.9	82.1
T=333	-458.538	944.10	80.9	73.9	76.1

The effect of temperature, studied in the range of 303–333 K, reveals a decrease in efficiency with increasing temperature. The decrease in inhibitory efficiency seems to be attributed to the increase in the dissolution rate of the steel related to the partial desorption of **210a** from the metal surface.

Other authors have already observed this behavior in their tests on the inhibitory action of some heterocyclic organic compounds on steel corrosion in acidic media. However, other studies have shown the opposite trend [219].The decrease in E (%) with increasing temperature is evidence of the physical adsorption of **210a** on the electrode surface. This results from a physical interaction of the Van Der Waals type that is very sensitive to thermal agitation [220].

IV-1- Activation kinetic parameters (Ea, ΔH°a, ΔS°a)

The values of the thermodynamic parameters of adsorption can provide information on the mechanism of corrosion inhibition. Indeed, an endothermic adsorption process (ΔH°ads > 0) is attributed to chemisorption [221], an exothermic adsorption process (ΔH° < 0) can involve physisorption and/or chemisorption.

The Arrhenius equation allowed us to calculate the activation energy value of the corrosion process at different temperatures in the absence and presence of **210a**.

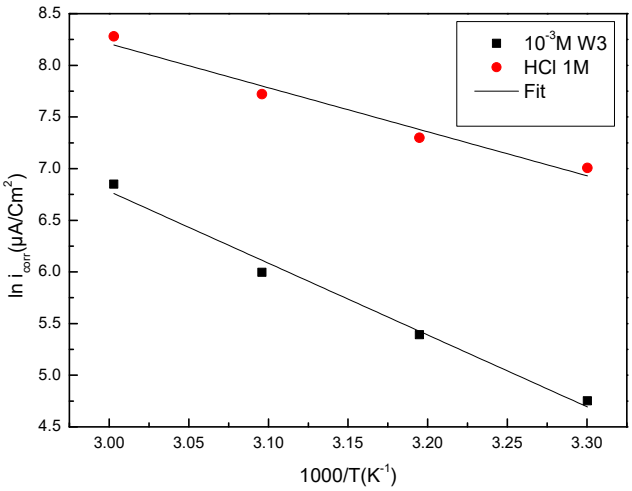

Figure 96: Arrhenius plots for corrosion of mild steel in 1 M hydrochloric acid in the absence and presence of **210a**

Figure 97 shows the variation of Ln (I/T) as a function of inverse temperature in the absence and presence of different concentrations of **210a** in 1 M hydrochloric acid medium. The lines obtained have slope (-ΔH°a / R) and an intercept equal to [Ln (R/Nh) + (ΔS°a /R)]. The exploitation of these two equations allowed us to calculate the different values of ΔH°a and ΔS°a (table 32).

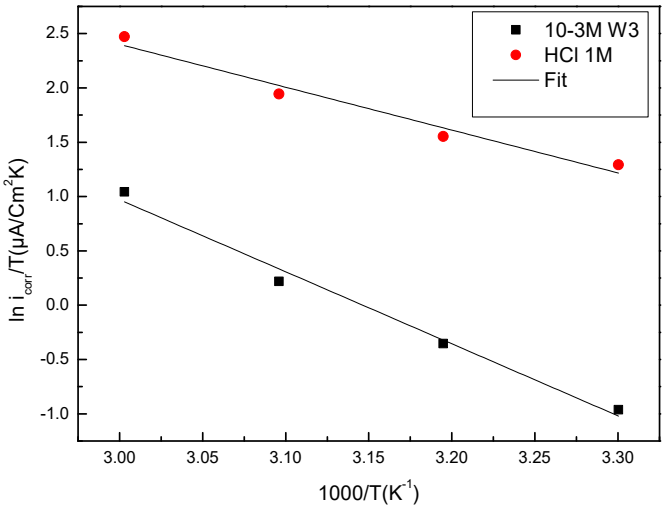

Figure 97: Variation of ln (icorr/T) =f (1/T) of mild steel in 1 M hydrochloric acid medium without and with addition of **210a** to 10^{-3}M.

Table 32: Corrosion activation parameters of mild steel in 1M hydrochloric acid medium without and with addition of 10^{-3}M **<u>210a</u>**

	E_a (kJ/mol)	ΔH_a (J/mol)	ΔS_a (J/mol.K)
Blanc 1M	35.4	32.76	-79.19
<u>210a</u>	57.74	55.10	24.07

We observed that the ΔHa and ΔSa values for the steel dissolution reaction in hydrochloric acid medium in the presence of **<u>210a</u>** are higher than those of 1M hydrochloric acid solution. The positive sign of the enthalpy ΔHa indicates that our inhibitor is chemisorbed on the steel surface.

IV- 2- Adsorption isotherms and thermodynamic parameters

The corrosion inhibition of steel by **<u>210a</u>** is due to the adsorption susceptibility of this compound on the metal surface. The variation of Cinh/ratio as a function of concentration (C) shows that the adsorption of **<u>210a</u>** follows the Langmuir adsorption model.

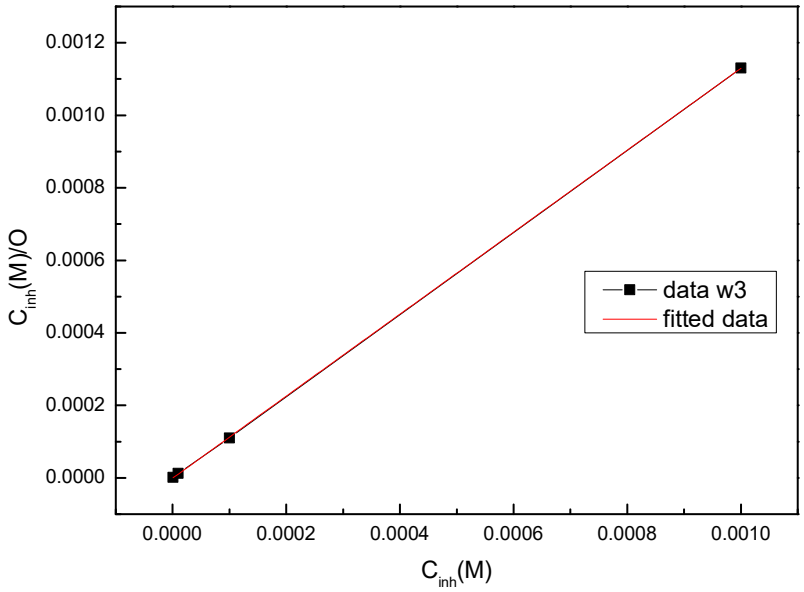

Figure 98: Langmuir adsorption isotherm diagram for the adsorption of corrosion of **<u>210a</u>** on mild steel in 1M hydrochloric acid

Table 33: Adsorption parameters for the concentration effect of mild steel in hydrochloric acid 1M at 303K

Inhibitor	K_{ads} (L mol^{-1})	ΔG_{ads} (KJ.mol^{-1})	R^2
210a (10^{-3}M)	$1.67.10^6$	-49.40	1

Negative value of ΔG_{ads} indicates the spontaneity of the adsorption process, and the stability of the adsorbed layer on the metal surface. The calculated value of ΔG_{ads} is close to (40 kJ. mol^{-1}) indicating that adsorption is the most likely chemical process.

Conclusion:

In this chapter, all results of the study of corrosion inhibition of the carbon steel plate for the compound **210a** in 1 M hydrochloric acid medium were collected.

Based on the result obtained, it can be concluded that the studied product is a good inhibitor, and its efficiency reaches its maximum value at 10^{-3}M.

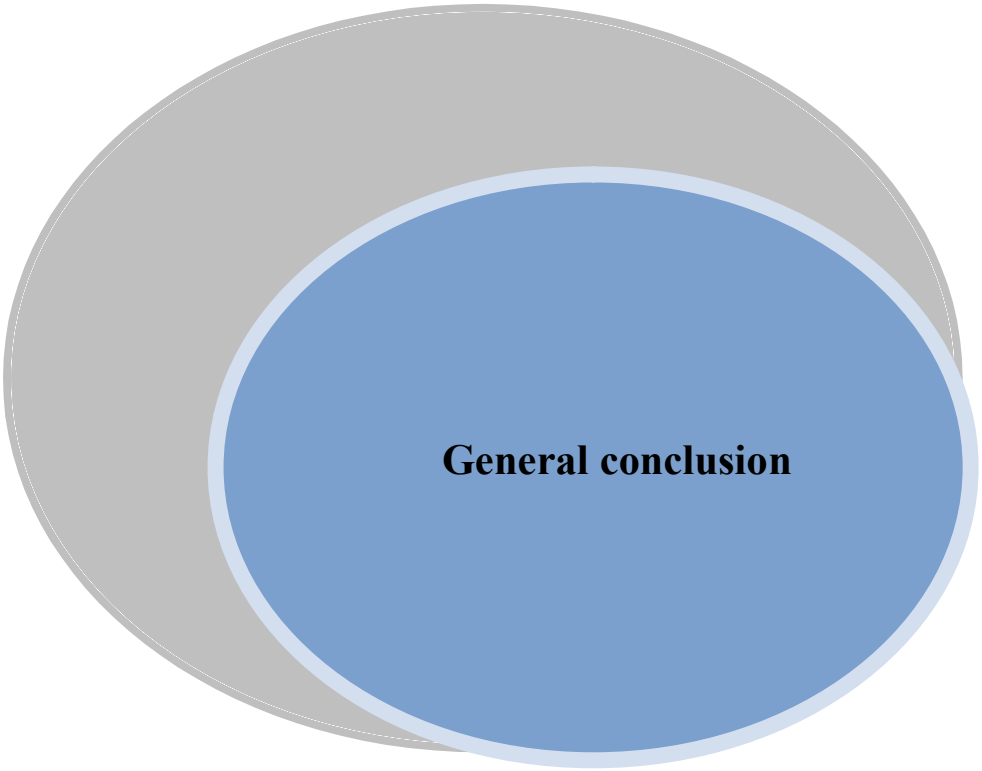
General conclusion

General conclusion

The research work conducted during this thesis is part of our laboratory's strategy to search for new heterocyclic molecules likely to exhibit biological properties.

We have chosen for us the theme of the synthesis of new heterocyclic compounds containing the motifs of 1,5-benzodiazepin-2-one benzimidazole or 1,4-diazepin-2-one and the study of their electrochemical and biological properties.

This work consists of two parts. The first is devoted to the synthesis, reactivity, physicochemical, antibacterial, and corrosion inhibiting properties of 1,5-benzodiazepin-2-one and its derivatives, while the second is determined for the research in the 1,4-diazepine series.

The first chapter of Part I represents a bibliographic overview of the synthesis and reactivity of 4-phenyl-1,5-benzodiazepin-2-one derivatives.

In the second chapter, we prepared, in a first step, new N-alkyl-4-phenyl-1,5-benzodiazepin-2-one derivatives via alkylation reactions under the conditions of liquid-solid phase transfer catalysis with different alkylating agents. In a second step, new derivatives of N-alkyl-4-phenyl-1,5-benzodiazepine-2-thione via sulfurisation reactions

Original results were obtained by the action of hydroxylamine hydrochloride on N-alkyl-4-phenyl-1,5-benzodiazepine-2-thiones produced novel results, as the latter underwent an interesting rearrangement, yielding new benzimidazole derivatives. The structures of the synthesized compounds products were determined by the usual ^{1}H NMR and ^{13}C NMR spectroscopic methods and confirmed by X-ray crystallographic studies for seven products, showing in particular that the oxime function adopts the E configuration. Similarly, it was possible to propose a plausible mechanism to explain the formation of benzimidazole derivatives from 1,5-benzodiazepine-2-thiones by highlighting an original rearrangement of the seven-membered ring in the presence of hydroxylamine hydrochloride, which acts as a binucleophile reagent.

A preliminary study on the investigation of antibacterial activity of some prepared 1,5-benzodiazepin-2-one, 1,5-benzodiazepine-2-thione, and benzimidazole derivatives was performed and described in the fourth chapter.

The fifth chapter is reserved for the synthesis characterization and crystal structure study, as well as other theoretical studies of 4-phenyl-decahydro-1H-1- 5-benzodiazepin-2-one.

In the last chapter, we tested the inhibitory effect of 4-phenyl-decahydro-1H-1-5-benzodiazepin-2-one on the corrosion of mild steel in 1M hydrochloric acid solution via different experimental methods such as potentiodynamic polarization curves and electrochemical impedance spectroscopy. Our tested compound is a very good organic inhibitor in hydrochloric acid (1 M HCl), according to the results.

Finally, the second part, divided into two chapters, concerns the synthesis, Hirshfeld surface analysis, molecular docking study, and evaluation of the corrosion inhibiting power of 7-phenyl-2,3,4,5-tetrahydro-1 H-1,4-diazepin-5-one.

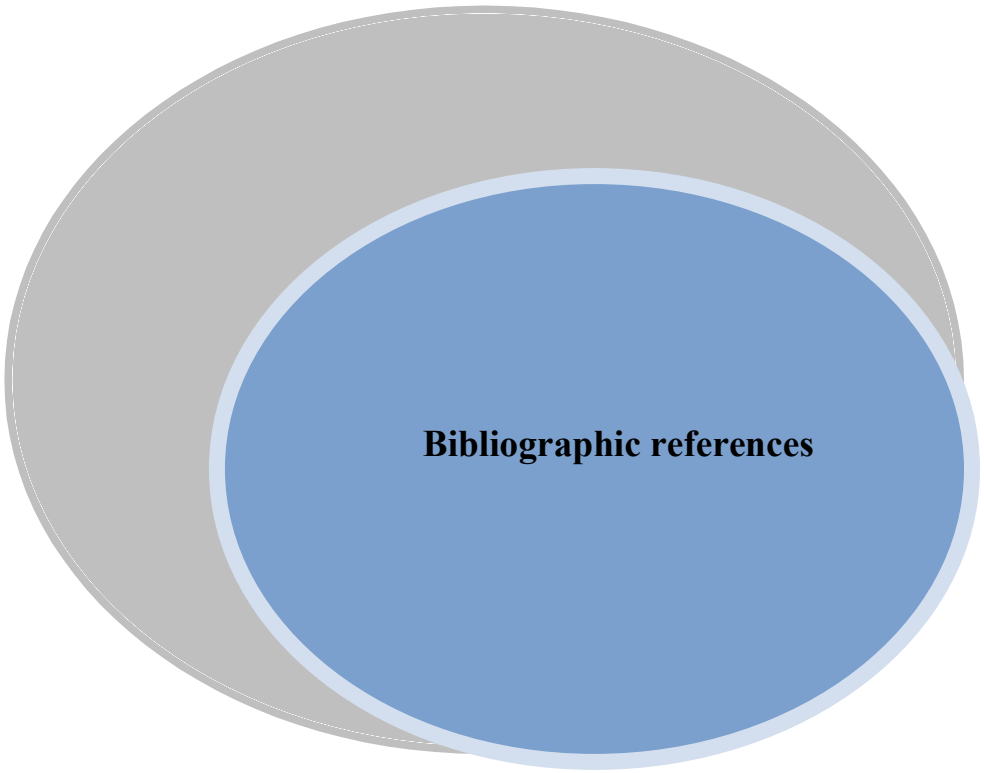
Bibliographic references

Bibliographic references:

1- Garattini, S., Caccia, S., Carli, M., & Mennini, T. (1981). Notes on kinetics and metabolism of benzodiazepines. In Recent Advances in Neuropsycho-Pharmacology (pp. 351-364). Pergamon.

2- Sucheta, K., & Rao, B. V. (2005). Microwave induced solvent-free synthesis of substituted 1, 5-benzodiazepine derivatives.

3- Gupta, S. S., Kumari, S., Kumar, I., & Sharma, U. (2020). Eco-friendly and sustainable synthetic approaches to biologically significant fused N-heterocyclic. Chemistry of Heterocyclic Compounds, 56(4), 433-444.

4- Hussenether, T., Hübner, H., Gmeiner, P., & Troschütz, R. (2004). Clozapine derived 2, 3-dihydro-1H-1, 4-and 1, 5-benzodiazepines with D4 receptor selectivity: synthesis and biological testing. Bioorganic & medicinal chemistry, 12(10), 2625-2637.

5- Fruscella, P., Sottocorno, M., Di Braccio, M., Diomede, L., Piccardi, N., Cagnotto, A. Grossi, G., Romano, M., Mennini, T., & Roma, G. (2001). 1,5-Benzodiazepine tricyclic derivatives exerting anti-inflammatory effects in mice by inhibiting interleukin-6 and prostaglandinE_2 production. Pharmacological Research, 43(5), 445-451.

6- Di Braccio, M., Grossi, G., Ceruti, M., Rocco, F., Loddo, R., Sanna, G., Busonera, B., Murreddu, M., & Marongiu, M. E. (2005). 1, 5-Benzodiazepines XIV. Synthesis of new substituted 9H-bis-[1, 2, 4] triazolo [4, 3-a: 3′, 4′-d][1, 5] benzodiazepines and relate compounds endowed with in vitro cytotoxic properties. Il Farmaco, 60(2), 113-125.

7- Padoley, K. V., Mudliar, S. N., & Pandey, R. A. (2008). Heterocyclic nitrogenous pollutants in the environment and their treatment options–an overview. Bioresource technology, 99(10), 4029-4043

8- Keita, A., Lazrak, F., Essassi, E. M., Alaoui, I. C., Rodi, Y. K., Bellan, J., & Pierrot, M. (2003). 2, 4-Dioxo (dimercapto)-1, 5-benzodiazepino-13-couronne-2, Nouveau Macrocycle Complexant de L'ion Ag+. Phosphorus, Sulfur, and Silicon and the Related Elements, 178(7), 1541-1548.

9- El Ghayati, L., Ramli, Y., Hökelek, T., Labd Taha, M., Mague, J. T., & Essassi, E. M. (2019). Crystal structure and Hirshfeld surface analysis of 3, 4-dihydro-2-(2, 4-dioxo-6-methylpyran-3-ylidene)-4-(4-pyridin-4-yl)-1, 5-benzodiazepine. Acta Crystallographica Section E: Crystallographic Communications, 75(1), 94-98.

10- Sebhaoui, J., El Bakri, Y., Essassi, E. M., & Mague, J. T. (2017). (4Z)-4-(2-Oxopropylidene)-2, 3, 4, 5-tetrahydro-1H-1, 5-benzodiazepin-2-one. IUCrData, 2(7), x171057.

11- Doumbia, M. L., Bouhfid, R., Essassi, E. M., & El Ammari, L. (2009). 5-Methyl-3-[1-(2-pyridylmethyl)-1H-benzimidazol-2-ylmethyl] isoxazole. Acta Crystallographica Section E: Structure Reports Online, 65(11), o2714-o2715.

12- Chkirate, K., Karrouchi, K., Dege, N., Sebbar, N. K., Ejjoummany, A., Radi, S., Adarsh, N. N., Talbaoui, A., Ferbinteanu, M., Essassi, El. M . & Garcia, Y. (2020). Co (II) and Zn (II) pyrazolyl-benzimidazole complexes with remarkable antibacterial activity. New Journal of Chemistry, 44(6), 2210-2221.

13- Herpin, T. F., Van Kirk, K. G., Salvino, J. M., Yu, S. T., & Labaudinière, R. F. (2000). Synthesis of a 10 000 member 1, 5-benzodiazepine-2-one library by the directed sorting method. Journal of Combinatorial Chemistry, 2(5), 513-521.

14- Rajarao, S. J. R., Platt, B., Sukoff, S. J., Lin, Q., Bender, C. N., Nieuwenhuijsen, B. W., Ring, R. H., Schechter, L. E., Rosenzweig-Lipson, S., & Beyer, C. E. (2007). Anxiolytic-like activity of the non-selective galanin receptor agonist, galnon. Neuropeptides, 41(5), 307-320.

15- Rishipathak, D. D., Patil, D., & Chikhale, H. U. (2022). Synthesis and Biological Evaluation of Some Newer 1h-Benzo [b][1, 5] diazepin-2 (3h)-One Derivatives as Potential Anticonvulsant Agents. Pharmaceutical Sciences

16- Myshkina, O. A., Balandina, S. Y., Makhmudov, R. R., Dmitriev, M. V., & Lisovenko, N. Y. (2021). Synthesis and antimicrobial and antinociceptive activity of 4-substituted 2-trichloromethyl-3H-1, 5-benzodiazepines. Russian Chemical Bulletin, 70(7), 1408-1414

17- Roma, G., Grossi, G. C., Di Braccio, M., Ghia, M., & Mattioli, F. (1991). 1, 5-Benzodiazepines IX. A new route to substituted 4H-[1, 2, 4] triazolo [4, 3-a][1, 5]

benzodiazepin-5-amines with analgesic and/or anti-inflammatory activities. European journal of medicinal chemistry, 26(5), 489-496

18- Werner, W., Baumgart, J., Burckhardt, G., Fleck, W. F., Geller, K., Gutsche, W., Hanschmann, H., Messerschmidt, A., Römer, W., Dieter Tresselt, D., & Löber, G. (1990). Physicochemical characterization of substituted chromeno [4, 3-b][1, 5] benzodiazepine stereoisomers designed as cell membrane active antitumor agents. Biophysical chemistry, 35(2-3), 271-285.

19- Sternbach, L. H. (1978). The benzodiazepine story. Progress in Drug Research/Fortschritte der Arzneimittelforschung/Progrès des recherches pharmaceutiques, 229-266.

20- Hamor, T. A., & Martin, I. L. (1983). 4 The Benzodiazepines. Progress in medicinal chemistry, 20, 157-223

21- Gatta, E., Cupello, A., Di Braccio, M., Grossi, G., Ferruzzi, R., Roma, G., & Robello, M. (2010). New 1, 5-benzodiazepine compounds: activity at native GABAA receptors. Neuroscience, 166(3), 917-923.

22- Zellou, A., Cherrah, Y., Hassar, M., & Essassi, E. M. (1998, January). Synthesis and pharmacologic s tudy of 1, 5-benzodiazepine-2, 4-diones and their alkyl derivatives. In Annals Pharmaceutiques Francaises (Vol. 56, No. 4, pp. 169-174).

23- Imran, M., Shah, F. A., Nadeem, H., Zeb, A., Faheem, M., Naz, S., Asma Bukhari, A., Ali, T., & Li, S. (2021). Synthesis and biological evaluation of benzimidazole derivatives as potential neuroprotective agents in an ethanol-induced rodent model. ACS Chemical Neuroscience, 12(3), 489-505.

24- Abdel-Motaal, M., Almohawes, K., & Tantawy, M. A. (2020). Antimicrobial evaluation and docking study of some new substituted benzimidazole-2yl derivatives. Bioorganic Chemistry, 101, 103972

25- Rashid, M. (2020). Design, synthesis and ADMET prediction of bis-benzimidazole as anticancer agent. Bioorganic chemistry, 96, 103576

26- Devivar, R. V., Kawashima, E., Revankar, G. R., Breitenbach, J. M., Kreske, E. D., Drach, J. C., & Townsend, L. B. (1994). Benzimidazole Ribonucleosides: Design, Synthesis, and Antiviral Activity of Certain 2-(Alkylthio)-and 2-(Benzylthio)-5, 6-dichloro-1-(. beta.-D-ribofuranosyl) benzimidazoles. Journal of Medicinal Chemistry, 37(18), 2942-2949.

27- Ateş-Alagöz, Z., Kuş, C., & Çoban, T. (2005). Synthesis and antioxidant properties of novel benzimidazoles containing substituted indole or 1, 1, 4, 4-tetramethyl-1, 2, 3, 4-tetrahydro-naphthalene fragments. Journal of enzyme inhibition and medicinal chemistry, 20(4), 325-331.

28- Palanisamy, P., Jenniefer, S. J., Muthiah, P. T., & Kumaresan, S. (2013). Synthesis, characterization, antimicrobial, anticancer, and antituberculosis activity of some new pyrazole, isoxazole, pyrimidine and benzodiazepine derivatives containing thiochromeno and benzothiepino moieties. RSC advances, 3(42), 19300-19310.

29- López-Muñoz, F., Álamo, C., & García-García, P. (2011). The discovery of chlordiazepoxide and the clinical introduction of benzodiazepines: half a century of anxiolytic drugs. Journal of anxiety disorders, 25(4), 554-562.

30- Williams, M. (1984). Molecular aspects of the action of benzodiazepine and nonbenzodiazepine anxiolytics: a hypothetical allosteric model of the benzodiazepine receptor complex. Progress in Neuro-Psychopharmacology and Biological Psychiatry, 8(2), 209-247.

31- Archer, G. A., & Sternbach, L. H. (1968). Chemistry of benzodiazepines. Chemical Reviews, 68(6), 747-784.

32- Müller, W. E., Groh, B., Bub, O., Hofmann, H. P., & Kreiskott, H. (1986). In vitro and in vivo studies of the mechanism of action of arfendazam, a novel 1, 5-benzodiazepine. Pharmacopsychiatry, 19(04), 314-315.

33- Huppertz, L. M., Bisel, P., Westphal, F., Franz, F., Auwärter, V., & Moosmann, B. (2015). Characterization of the four designer benzodiazepines clonazolam, deschloroetizolam, flubromazolam, and meclonazepam, and identification of their in vitro metabolites. Forensic Toxicology, 33(2), 388-395.

34- Verma, R., Bhatia, R., Singh, G., Kumar, B., Mehan, S., & Monga, V. (2020). Design, synthesis and neuropharmacological evaluation of new 2, 4-disubstituted-1, 5-benzodiazepines as CNS active agents. Bioorganic Chemistry, 101, 104010.

35- Bock, M. G., Freidinger, R. M., Freedman, S. B., & Matassa, V. G. (1995). Cholecystokinin (CCK) receptor antagonists. Curr Pharm Des, 1, 279-294.

36- Mansour, H., & El-Hendawy, M. M. (2020). Mechanistic perspectives on piperidine-catalyzed synthesis of 1, 5-benzodiazepin-2-ones. Molecular Catalysis, 484, 110774.

37- Obara, N., Watanabe, T., Asakawa, T., Kan, T., & Tanaka, T. (2019). Synthesis of 3-amino-1, 5-benzodiazepine-2-one derivatives from dehydroalanine derivatives. Synthesis, 51(10), 2198-2206.

38- Wu, H. T., & Wang, L. Z. (2020). Expedient green-chemistry approaches for a one-pot synthesis of two series of novel 1, 5-benzodiazepines via domino reactions. New Journal of Chemistry, 44(25), 10428-10440.

39- Qomi, H. R., & Habibi, A. (2017). Synthesis of a novel functionalized tricyclic pyrimidine-fused 1, 5-benzodiazepine library. Tetrahedron, 73(21), 2991-3001.

40- Lyubimov, S. E., Sokolovskaya, M. V., Mikhel, I. S., Birin, K. P., & Davankov, V. A. (2019). Asymmetric Ir-catalyzed hydrogenation of 4-R-1, 3-dihydro-2H-1, 5-benzodiazepin-2-ones using a novel phosphoramidite ligand. Russian Chemical Bulletin, 68(7), 1429-1434.

41- Jaafar, Z., Chniti, S., Sassi, A. B., Dziri, H., Marque, S., Lecouvey, M., Gharbi, R., & Msaddek, M. (2019). Design and microwave-assisted synthesis of dimers of 1, 5-benzodiazepine-1, 2, 3-triazole hybrids bearing alkyl/aryl spacers and their biological assessment. Journal of Molecular Structure, 1195, 689-701.

42- Chniti, S., Nsira, A., Khouaja, S., Mechria, A., Gharbi, R., Msaddek, M., & Lecouvey, M. (2018). Highly diastereoselective synthesis of rigid 3-enamino-1, 5-benzodiazepines. Organic Chemistry, (part v), 0-0.

43- Chander, S., Tang, C. R., Al-Maqtari, H. M., Jamalis, J., Penta, A., Hadda, T. B., Mohd Sirat, H., Zheng, Y., & Sankaranarayanan, M. (2017). Synthesis and study of anti-HIV-1 RT activity of 5-benzoyl-4-methyl-1, 3, 4, 5-tetrahydro-2H-1, 5-benzodiazepin-2-one derivatives. Bioorganic chemistry, 72, 74-79.

44- Naveen, S., Kumara, K., Al-Maqtari, H. M., Urs, M. D., Jamalis, J., Reddy, K. R., Lingegowda, N.S., & Lokanath, N. K. (2019). Synthesis, characterization crystal and molecular structure studies of 5-(3-Methylbenzoyl)-4-methyl-1, 3, 4, 5-tetrahydro-2H-1, 5-benzodiazepin-2-one: Hirshfeld surface analysis and DFT calculations. Chemical Data Collections, 24, 100292.

45- Castillo, J. C., Presset, M., Abonia, R., Coquerel, Y., & Rodriguez, J. (2012). Microwave-Assisted Domino Benzannulation of α-Oxo Ketenes: Preparation of 1, 3-Dihydro-2H-1, 5-benzodiazepin-2-ones. European Journal of Organic Chemistry, 2012(12), 2338-2345.

46- Rao, M. H., Reddy, A. P. R., & Veeranagaiah, V. (1992). Synthesis of 1H-1, 5-Benzodiazepin-2 (3H)-ones from 5 (4H)-Isoxazolone, a Heterocyclic Bifunctional C-3 Synthon. Synthesis, 1992(05), 446-448.

47- Misra, A., Dwivedi, J., Shukla, S., Kishore, D., & Sharma, S. (2020). Bacterial cell leakage potential of newly synthesized quinazoline derivatives of 1, 5-benzodiazepines analogue. Journal of Heterocyclic Chemistry, 57(4), 1545-1558.

48- Movassaghi, M., & Hill, M. D. (2006). Single-step synthesis of pyrimidine derivatives. Journal of the American Chemical Society, 128(44), 14254-14255.

49- Ahmad, O. K., Hill, M. D., & Movassaghi, M. (2009). Synthesis of densely substituted pyrimidine derivatives. The Journal of Organic Chemistry, 74(21), 8460-8463.

50- Fang, C., Cao, J., Sun, K., Zhu, J., Lu, T., & Du, D. (2018). Direct and Enantioselective Synthesis of N− H-Free 1, 5-Benzodiazepin-2-ones by an N-Heterocyclic Carbene Catalyzed [3+ 4] Annulation Reaction. Chemistry–A European Journal, 24(9), 2103-2108

51- Jiang, D., Dong, S., Tang, W., Lu, T., & Du, D. (2015). N-heterocyclic carbene-catalyzed formal [3+ 2] annulation of α-bromoenals with 3-aminooxindoles: A stereoselective synthesis of spirooxindole γ-butyrolactams. The Journal of Organic Chemistry, 80(22), 11593-11597.

52- (a) F.-G. Sun, L.-H. Sun, S. Ye, Adv. Synth. Catal. 353 (2011) 3134; (b) C. Yao, D. Wang, J. Lu, T. Li, W. Jiao, C. Yu, Chem. Eur. J. 18 (2012) 1914; (c) C.-L. Zhang, D.-L. Wang, K.-Q. Chen, S. Ye, Org. Biomol. Chem. 13(2015), 11255; (d) J. Xu, W. Zhang, Y. Liu, S. Zhu, M. Liu, X. Hua, S. Chen, T. Lu, D. Du, RSC Adv. 6 (2016)18601; (e) L. Yi, Y. Zhang, Z.-F. Zhang, D. Sun, S. Ye, Org. Lett. 19(2017)2286; (f) Q. Ni, X. Song, G. Raabe, D. Enders, Chem. Asian J. 9(2014)1535; (g) S. Mondal, S. R. Yetra, A. Patra, S. S. Kunte, R. Gonnade, A. Biju, Chem. Commun. 50(2014) 14539; (h) S. R. Yetra, T. Kaicharla, S. S. Kunte, R. G. Gonnade, A. T. Biju, Org. Lett. 15(2013)5202; (i) S. R. Yetra, T. Roy, A. Bhunia, D. Porwal, A. T. Biju, J. Org. Chem. 79(2014) 4245; (j) S. R. Yetra, A. Bhunia, A. Patra, M. V. Mane, K.Vanka, A. T. Biju, Adv. Synth. Catal. 355 (2013), 1089.

53- El Abbassi, M., Essassi, E. M., & Fifani, J. (1987). Nouvelle synthese des benzodiazepines-1, 5 a partir de la γ-pyrone. Tetrahedron letters, 28(13), 1389-1392.

54- Wang, Z. X., & Qin, H. L. (2005). Reaction of 1, 3-dicarbonyl compounds with o-phenylenediamine or 3, 3′-diaminobenzidine in water or under solvent-free conditions via microwave irradiation. Journal of heterocyclic chemistry, 42(5), 1001-1005.

55- Bougrin, K., Bennani, A. K., Tétouani, S. F., & Soufiaoui, M. (1994). An easy route to synthesize 1, 5-arylodiazepin-2-ones. Tetrahedron letters, 35(45), 8373-8376.

56- Saber, A., Zouihri, H., Essassi, E. M., & Ng, S. W. (2010). 4-Methyl-2, 3-dihydro-1H-1, 5-benzodiazepin-2-one monohydrate. Acta Crystallographica Section E: Structure Reports Online, 66(6), o1408-o1408.

57- Dioukhane, K., Aouine, Y., Faraj, H., Alami, A., Essassi, E. M., & Zouihri, H. (2018). 4-Methyl-1H-1, 5-benzodiazepin-2 (3H)-one. IUCrData, 3(12), x181718.

58- Essassi, E.M. (1994). THE USE OF 1, 5-BENZODIAZEPINES IN HETEROCYCLIC SYNTHESIS. Bulletin of Belgian chemical societies, 103(11), 679-686.https://doi.org/10.1002/bscb.19941031109

59- Achour, R., Cherkaoui, M. Z., Essassi, E. M., & Zniber, R. (1994). Synthesis of New Adamantylated Heterocycles. Synthetic communications, 24(20), 2899-2905.

60- Tabata, H., Tsuji, Y., Yoneda, T., Tasaka, T., Oshitari, T., Takahashi, H., & Natsugari, H. (2018). Atropisomerism in the 2, 3, 4, 5-Tetrahydro-1H-1, 5-benzodiazepine Nucleus: Effects of Central Chirality at C3 on the N-Mesylation Reaction. Synlett, 29(16), 2141-2146.

61- Kanyonga, P. M., Zellou, A., Cherrah, Y., & Essassi, E. M. (2009). Synthesis and pharmacological study of 4-phenyl-l, 5-benzodiazépin-2-one and its derivatives. Cameroon Journal of Experimental Biology, 5(2), 104-111

62- Nsira, A., Karoui, A., Gharbi, R., & Msaddek, M. (2012). Chemoselectivity of the 1, 3-dipolar cycloaddition of some diazoalkanes with 1, 5-benzodiazepine derivatives. Journal of Chemical Research, 36(3), 152-156.

63- (a) Rida, M., Meslouhi, H. E., Ahabchane, N. H., Garrigues, B., Es-Safi, N., & Essassi, E. M. (2008). A Convenient Method for the Synthesis of 1, 5-benzodiazepin-2-one. The Open Organic Chemistry Journal, 2(1). (b) M. Rida., Doctoral thesis, Faculty of Sciences Rabat.(2016).

64- Mtiraoui, H., Nsira, A., Msaddek, M., Renard, P. Y., & Sabot, C. (2017). Regioselective synthesis of o-triazolyl-1, 5-benzodiazepin-2-ones and o-isoxazolyl-1, 5-benzodiazepin-2-ones via copper-catalyzed 1, 3-dipolar cycloaddition reactions. Comptes Rendus Chimie, 20(7), 747-757.

65- El Foujji, L., Sebhaoui, J., El Bakri, Y., El Ghayati, L., Essassi, E. M., & Mague, J. T. (2018). (3R, 4Z)-1, 3-Diethyl-4-(2-oxopropylidene)-2, 3, 4, 5-tetrahydro-1H-1, 5-benzodiazepin-2-one. IUCrData, 3(4), x180515.

66- Sebhaoui, J., El Bakri, Y., Essassi, E. M., & Mague, J. T. (2016). (4Z)-1-Dodecyl-4-(2-oxopropylidene)-2, 3, 4, 5-tetrahydro-1H-1, 5-benzodiazepin-2-one. IUCrData, 1(11), x161696.

67- B. Daouda., doctoral thesis. Faculty of Sciences Rabat. (2013).

68- El Ghayati, L., Hamou Ahabchane, N., Lamine Doumbia, M., Sebbar, N. K., Essassi, E. M., & Mague, J. T. (2017). 1-Ethyl-4-phenyl-1, 5-benzodiazepine-2-thione. IUCrData, 2(1), x161998.

69- Alaoui, I. C., Rodi, Y. K., Keita, A., Sabir, S., Skalli, M. K., El Hadrami, E. M., & Essassi, E. M. (2008). Synthesis of new heterocyclic systems by 1, 3-dipolar cycloaddition from the 1, 5-benzodiazepine-2, 4-dione. Phys Chem News, 39, 98-103.

70- Ahabchane, N.H., Keïta, A., & Essassi, E.M. (1999). Synthesis of 1-pyrazolyl, isoxazolyl and 1, 2, 3-triazolylmethyl-1, 5-benzodiazepines by dipolar cycloaddition-1, 3. Proceedings of the Academy of Sciences-Series IIC-Chemistry, 2(9-10), 519-523.

71- (a) Solomko, Z. F., Gaponov, A. A., Avramenko, V. I., & Khmel, M. P. (1987). Synthesis of 4-styryl-2, 3-dihydro-1H-1, 5-benzodiazepin-2-ones. Chemistry of Heterocyclic Compounds, 23(11), 1252-1254. (b) K. Ei-Shafei, H. S. Ei-Kashef, and A. M. El-Khawage, Indian J. Chem., 21B (1982)655. (c) R.C. Harris and J. M. Straley, French Chem. Abstr., 73(1970) 100054. (d) A.A. Stolyarchuk, Yu. N. Furman, V. L. Pikalov, Z. F. Solomko, and V. S. Tkachenko, Khim.-Farm. Zh., Chemistry of Heterocyclic Compounds. 9 (1975)19. (e) N.N. Mushkalo, N. O. Markova, and L. K. Mushkalo, Vestn. Kazan. State Univ., 21(1980)31.

72- Abdel-Ghany, H., E1-Sayed, A. M., Sultan, A. A., & E1-Shafei, A. K. (1990). A Novel Syntheses of Pyrano (2, 3-c)(1, 5) Benzodiazepines. Synthetic Communications, 20(6), 893-900.

73- Avramenko, V. I., Sharbatyan, P. A., Solomko, Z. F., & Pribega, L. V. (1979). Bromination of 4-(p-methoxyphenyl)-2, 3-dihydro-1h-1, 5-benzodiazepin-2 one. Chemistry of Heterocyclic Compounds, 15(6), 691-694.

74- Bozhanov, V. I., & Ivonin, S. P. (2002). Synthesis of 4-Pyridyl-2, 3-dihydro-1H-1, 5-benzodiazepin-2-ones. Chemistry of Heterocyclic Compounds, 38(9), 1098-1103.

75- Abronin, I. A., Gorb, L. G., Dryuk, V. G., Sheremet, V. I., Solomko, Z. F., & Kremlev, M. M. (1981). Chlorination of 4-methyl-8-methoxy-2, 3-dihydro-1H, 1, 5-benzodiazepin-2-one. Chemistry of Heterocyclic Compounds, 17(9), 954-956.

76- El-Snyed, A. M., Abdel-Ghany, H., & El-Snghier, A. M. M. (1999). A Novel Synthesis of Pyrano (2, 3-c)-, 1, 3-Oxazino (2, 3 b)-, 1, 2, 4-Triazolo (3, 4-b)-, Oxazolo (2, 3-b)-, Furano (3, 2-c)-, and 3-Substituted-(1, 5) benzodiazepin-2-ones. Synthetic Communications, 29(20), 3561-3572.

77- Abdel-Ghany, H., El-Sayed, A. M., Khodairy, A., & Salah, H. (2001). Synthesis of new 3-substituted and spiro 1, 5-benzodiazepin-2-ones under phase-transfer catalysis conditions. Synthetic Communications, 31(16), 2523-2535.

78- Lyubimov, S. E., Ozolin, D. V., & Davankov, V. A. (2017). Asymmetric Ir-catalyzed hydrogenation of 1, 5-benzodiazepinones using mixtures of ligands. Russian Chemical Bulletin, 66(6), 1059-1061

79- Sokolovskaya, M. V., Lyubimov, S. E., Mikhel, I. S., Birin, K. P., & Davankov, V. A. (2018). Asymmetric Ir-catalyzed hydrogenation of 1, 3-dihydro-2H-1, 5-benzodiazepin-2-ones using phosphoramidites. Russian Chemical Bulletin, 67(2), 260-264.

80- Yang, Z., Ding, Z., Chen, F., He, Y. M., Yang, N., & Fan, Q. H. (2017). Asymmetric hydrogenation of cyclic imines of benzoazepines and benzodiazepines with chiral, cationic ruthenium–diamine catalysts. European Journal of Organic Chemistry, 2017(14), 1973-1977.

81- Essassi, E. M., Ghomsi, J. T., & Ahabchane, N. H. (2011). 4-Phenyl-1, 5-benzodiazepin-2-one Compound as a Precursor of Various New heterocyclic System with Potent pharmacological Properties. Frontiers in Science and Engineering, 1(1).

82- Nawrocka, W., Sztuba, B., Opolski, A., Wietrzyk, J., Kowalska, M. W., & Glowiak, T. (2001). Synthesis and Antiproliferative Activity in Vitro of Novel 1, 5-Benzodiazepines. Part II. Archiv der Pharmazie: An International Journal Pharmaceutical and Medicinal Chemistry, 334(1), 3-10.

83- El-Gaml, K. M. (2014). Application of chalcone in synthesis of new heterocycles containing 1, 5-benzodiazepine derivatives. American Journal of Organic Chemistry, 4(1), 14-19.

84- Ben-Cherif, W., Gharbi, R., Sebai, H., Dridi, D., Boughattas, N. A., & Ben-Attia, M. (2010). Neuropharmacological screening of two 1, 5-benzodiazepine compounds in mice. Comptes Rendus Biologies, 333(3), 214-219.

85- Neochoritis, C. G., Tsoleridis, C. A., Stephanidou-Stephanatou, J., Kontogiorgis, C. A., & Hadjipavlou-Litina, D. J. (2010). 1, 5-Benzoxazepines vs 1, 5-benzodiazepines. One-pot

microwave-assisted synthesis and evaluation for antioxidant activity and lipid peroxidation inhibition. Journal of medicinal chemistry, 53(23), 8409-8420.

86- Gouéth, P. Y., Ronco, G., & Villa, P. (1994). Synthesis of ether-linked di-and trisaccharide derivatives part I-synthesis of disaccharides from 5, 6-anhydro-d-glucose derivatives. Journal of Carbohydrate Chemistry, 13(5), 679-696.

87- Bouhlal, D., Godé, P., Goethals, G., Massoui, M., Villa, P., & Martin, P. (2000). Synthesis and amphiphilic properties of glycosyl-1, 4-benzodiazepin-2, 5 diones. Carbohydrate Research, 329(1), 207-214.

88- Makosza, M. (2000). Phase-transfer catalysis. A general green methodology in organic synthesis. Pure and applied chemistry, 72(7), 1399-1403.

89- Chebabe, D., Dermaj, A., El Abidine Ait Chikh, Z., Hajjaji, N., Rico-Lattes, I., & Lattes, A. (2004). Synthesis of New Surfactants Mono and Bipolar Derived from 1, 2, 4-Triazole-5-thione. Synthetic communications, 34(22), 4189-4198.

90- K. Chkirat, Doctoral thesis, Faculty of Sciences, Rabat (2019).

91- Nguema Ongone, T., Achour, R., El Ghoul, M., El Ouasif, L., El Jemli, M., Chemlal, L., Cherrah, Y., Alaoui, K., & Zellou, A. (2019). Analgesic and antioxidant activities of 4-phenyl-1, 5-benzodiazepin-2-one and its long carbon chains derivatives. Journal of Chemistry, 2019.

92- El Ghayati, L., Sert, Y., Sebbar, N. K., Ramli, Y., Ahabchane, N. H., Talbaoui, A., ... & Alsalme, A. (2021). Syntheses of novel 1, 5-benzodiazepine derivatives: Crystal structures, spectroscopic characterizations, Hirshfeld surface analyses, molecular docking studies, DFT calculations, corrosion inhibition anticipation, and antibacterial activities. Journal of Heterocyclic Chemistry, 58(1), 270-2.

93- L.M Doumbia. Doctoral thesis, Faculty of Sciences, Rabat (2008).

94- Liu, H. B., Gao, W. W., Tangadanchu, V. K. R., Zhou, C. H., & Geng, R. X. (2018). Novel aminopyrimidinyl benzimidazoles as potentially antimicrobial agents: Design, synthesis and biological evaluation. European journal of medicinal chemistry, 143, 66-84.

95- Morcoss, M. M., El Shimaa, M. N., Ibrahem, R. A., Abdel-Rahman, H. M., Abdel-Aziz, M., & Abou El-Ella, D. A. (2020). Design, synthesis, mechanistic studies and in silico ADME predictions of benzimidazole derivatives as novel antifungal agents. Bioorganic chemistry, 101, 103956.

96- Ren, Y., Wang, Y., Li, G., Zhang, Z., Ma, L., Cheng, B., & Chen, J. (2021). Discovery of novel benzimidazole and indazole analogues as tubulin polymerization inhibitors with potent anticancer activities. Journal of Medicinal Chemistry, 64(8), 4498-4515.

97- Devivar, R. V., Kawashima, E., Revankar, G. R., Breitenbach, J. M., Kreske, E. D., Drach, J. C., & Townsend, L. B. (1994). Benzimidazole Ribonucleosides: Design, Synthesis, and Antiviral Activity of Certain 2-(Alkylthio)-and 2-(Benzylthio)-5, 6-dichloro-1-(. beta.-D-ribofuranosyl) benzimidazoles. Journal of Medicinal Chemistry, 37(18), 2942-2949.

98- Bhrigu, B., Siddiqui, N., Pathak, D., Alam, M. S., Ali, R., & Azad, B. (2012). Anticonvulsant evaluation of some newer benzimidazole derivatives: Design and synthesis. Acta Pol. Pharm. Drug Res, 69(1), 53-62.

99- Phillips, M. A. (1928). CCCXVII.—The formation of 2-substituted benziminazoles. Journal of the Chemical Society (Resumed), 2393-2399.

100- Alam, S. A. M. F., Ahmad, T., Nazmuzzaman, M., Ray, S. K., Sharifuzzaman, M., Karim, M. R., Alam M. G. , Ajam M. M. , Maitra P. , Mandol D. , Uddin M. E. , & Ahammed, T. (2017). Synthesis of benzimidazole derivatives containing schiff base exhibiting antimicrobial activities. Int. J. Res. Stud. Biosci, 5, 18-24.

101- A. Lamkaddem, 3rd Cycle Specialty Diploma, Rabat (1987).

102- Bahrami, K., Khodaei, M. M., & Kavianinia, I. (2007). A simple and efficient one-pot synthesis of 2-substituted benzimidazoles. Synthesis, 2007(04), 547-550.

103- Israel, M., Jones, L. C., & Modest, E. J. (1968). Thermal rearrangement of condensed dihydrodiazepinones. Tetrahedron Letters, 9(46), 4811-4814.

104- Essassi, E.M., Salem, M., & Viallefont, P. (1994). Synthesis Of Pyrazolo [2, 3-a] Triazepino [3, 2-a] Benzimidazoles and Pyrazolo [3, 2-d][1, 3, 5] Thiadiazepino [3, 2-a] benzimidazoles from 1, 5-benzodiazepines. Bulletin of Belgian Chemical Societies, 103(2), 57-62.

105- Okamoto, Y., & Takagi, K. (1987). Chemistry of 4-amino-1H-1, 5-benzodiazepine-3-carbonitrile. Journal of heterocyclic chemistry, 24(4), 885-893.

106- Essaghouani, A., Boulhaoua, M., El Ouasif, L., Sebbar, N. K., Essassi, E. M., & Mague, J. T. (2017). 3-Phenylisoxazolin-5-one: a redetermination. IUCrData, 2(1), x170032.

107- El Azzaoui, B., Rachid, B., Doumbia, M. L., Essassi, E. M., Gornitzka, H., & Bellan, J. (2006). Unexpected opening of benzimidazole derivatives during 1, 3-dipolar cycloaddition. Tetrahedron letters, 47(50), 8807-8810.

108- J. Sebhaoui. doctoral thesis, Faculty of Sciences Rabat (2019).

109- Idrissi, A., Chkirate, K., Abad, N., Djerrari, B., Achour, R., Essassi, E. M., & Van Meervelt, L. (2021). Crystal structure, Hirshfeld surface analysis and density functional theory study of 6-methyl-2-[(5-methylisoxazol-3-yl) methyl]-1H-benzimidazole. Acta Crystallographica Section E: Crystallographic Communications, 77(4), 396-401.

110- Kitchen, D. B., Decornez, H., Furr, J. R., & Bajorath, J. (2004). Docking and scoring in virtual screening for drug discovery: methods and applications. Nature reviews Drug discovery, 3(11), 935-949.

111- Sousa, S. F., Fernandes, P. A., & Ramos, M. J. (2006). Protein–ligand docking: current status and future challenges. Proteins: Structure, Function, and Bioinformatics, 65(1), 15-26.

112- Dias, R., de Azevedo, J., & Walter, F. (2008). Molecular docking algorithms. Current drug targets, 9(12), 1040-1047. Kollman,

113- P. A., Massova, I., Reyes, C., Kuhn, B., Huo, S., Chong, L., ... & Cheatham, T. E. (2000). Calculating structures and free energies of complex molecules: combining molecular mechanics and continuum models. Accounts of chemical research, 33(12), 889-897.

114- Brooijmans, N., & Kuntz, I. D. (2003). Molecular recognition and docking algorithms. Annual review of biophysics and biomolecular structure, 32(1), 335-373.

115- Trott, O., & Olson, A. J. (2010). AutoDock Vina: improving the speed and accuracy of docking with a new scoring function, efficient optimization, and multithreading. Journal of computational chemistry, 31(2), 455-461.

116- Gullapelli, K., Brahmeshwari, G., Ravichander, M., & Kusuma, U. (2017). Synthesis, antibacterial and molecular docking studies of new benzimidazole derivatives. Egyptian journal of basic and applied sciences, 4(4), 303-309.

117- https://www.rcsb.org.

118- https://www.3dsbiovia.com.

119- World Health Organization. (2014). Consultation for Priority Actions on Antimicrobial Resistance in the Western Pacific Region, Manila, Philippines, 30 July to 1 August 2014.

120- Wiegand, I., Hilpert, K., & Hancock, R. E. (2008). Agar and broth dilution methods to determine the minimal inhibitory concentration (MIC) of antimicrobial substances. Nature protocols, 3(2), 163-175.

121- Bonev, B., Hooper, J., & Parisot, J. (2008). Principles of assessing bacterial susceptibility to antibiotics using the agar diffusion method. Journal of antimicrobial chemotherapy, 61(6), 1295-1301.

122- (a) Prakash, G. S., Vaghoo, H., Venkat, A., Panja, C., Chacko, S., Mathew, T., & Olah, G. A. (2009). Gallium (III) triflate-catalyzed synthesis of heterocycles: quinoxalines, 1, 5-benzodiazepines and their fluorinated derivatives. Future Medicinal Chemistry, 1(5), 909-920. (b) Bhati, S., Kumar, V., Singh, S., & Singh, J. (2020). Synthesis, characterization, antimicrobial, anti-tubercular, antioxidant activities and docking simulations of derivatives of 2-(pyridin-3-yl)-1Hbenzo [d] imidazole and 1, 3, 4-oxadiazole analogy. Letters in Drug Design & Discovery, 17(8), 1047-1059.

123- Elbouhi, M., Badaoui, H., Ouabane, M., Alaoui, M. A., Koubi, Y., Mokhlis, Y.,. ElKamel, K., & Lakhlifi, T. (2022). Anti-Tumor Activity of Novel Benzimidazole-Chalcone Hybrids as non-Intercalative Topoisomerase II Catalytic Inhibitors: 2D-QSAR study. RHAZES: Green and Applied Chemistry, 14, 62-75.

124- Caiana, E. C., Veras, B. O. D., Souza, A. L. D., & Queiroz, N. (2021). Synthesis of Hydroxybenzodiazepines with Potential Antioxidant and Antifungal Action. Journal of the Brazilian Chemical Society, 32, 626-637.

125- Navin, P., Sarvil, P., Amit, P., Divyesh, P., Dhansukh, R., Moo-Puc, R., & Rivera, G. (2017). Synthesis and biological evaluation of newer 1, 3, 4-oxadiazoles incorporated with benzothiazepine and benzodiazepine moieties. Zeitschrift für Naturforschung C, 72(3-4), 133-146.

126- Gawandi, S. J., Desai, V. G., Joshi, S., Shingade, S., & Pissurlenkar, R. R. (2021). Assessment of elementary derivatives of 1, 5-benzodiazepine as anticancer agents with synergy potential. Bioorganic Chemistry, 117, 105331.

127- Andrzejewska, M., Yepez-Mulia, L., Tapia, A., Cedillo-Rivera, R., Laudy, A. E., Starościak, B. J., & Kazimierczuk, Z. (2004). Synthesis and antiprotozoal and antibacterial activities of S-substituted 4, 6-dibromo-and 4, 6-dichloro-2-mercaptobenzimidazoles. European journal of pharmaceutical sciences, 21(2-3), 323-329

128- El-Sayed, A. A., Abu-Bakr, S. M., Swelam, S. A., Khaireldin, N. Y., Shoueir, K. R., & Khalil, A. M. (2021). Applying Nanotechnology in the Synthesis of Benzimidazole Derivatives: A Pharmacological Approach.

129- Koech, P. K., & Krische, M. J. (2006). Enantioselective total and formal syntheses of paroxetine (PAXIL) via phosphine-catalyzed enone α-arylation using arylbismuth (V) reagents: a regiochemical complement to Heck arylation. Tetrahedron, 62(45), 10594-10602.

130- Pejović, A., Denić, M. S., Stevanović, D., Damljanović, I., Vukićević, M., Kostova, K., Tavlinova-Kirilova, M., Randjelović, P., Stojanović, N. M., Bogdanović, G. A., Blagojević,P., D'hooghe, M., Radulović, N. S., & Vukićević, R. D. (2014). Discovery of anxiolytic 2-ferrocenyl-1, 3-thiazolidin-4-ones exerting GABAA receptor interaction via the benzodiazepine-binding site. European Journal of Medicinal Chemistry, 83, 57-73.

131- Hussenether, T., Hübner, H., Gmeiner, P., & Troschütz, R. (2004). Clozapine derived 2, 3-dihydro-1H-1, 4-and 1, 5-benzodiazepines with D4 receptor selectivity: synthesis and biological testing. Bioorganic & medicinal chemistry, 12(10), 2625-2637.

132- Malik, A. K., Aulakh, J. S., Fekete, A., & Schmitt-Kopplin, P. (2009). Separation of the phenoxy acid herbicides and their enantiomers by capillary zone electrophoresis in presence of highly sulphated cyclodextrins. Journal of the Chinese Chemical Society, 56(6), 1163-1167.

133- Baumann, M., Baxendale, I. R., Hornung, C. H., Ley, S. V., Rojo, M. V., & Roper, K. A. (2014). Synthesis of riboflavines, quinoxalinones and benzodiazepines through chemoselective flow based hydrogenations. Molecules, 19(7), 9736-9759.

134- Tazerouti, F., Yacine Badjah-Hadj-Ahmed, A., Youcef Meklati, B., Franco, P., & Minguillon, C. (2002). Enantiomeric separation of drugs and herbicides on a β-cyclodextrin-bonded stationary phase. Chirality, 14(1), 59-66.

135- Viets, V. L., & Miller, W. R. (1997). Treatment approaches for pathological gamblers. Clinical psychology review, 17(7), 689-702.

136- Sacerdote, P., Panerai, A. E., Frattola, L., & Ferrarese, C. (1999). Benzodiazepine-induced chemotaxis is impaired in monocytes from patients with generalized anxiety disorder. Psychoneuroendocrinology, 24(2), 243-249.

137- T. F. Herpin, K. G. V. Kirk, J. M. Salvino, S. T. Yu, R. F. Labaudinière, J. Comb. Chem. 2(2002)513–521.

138- Z. Y. Ding, F. Chen, J. Qin, Y. M. He, Q. H. Fan, Angew. Chem. Int. Ed. 2012, 51, 5706–5710; Angew. Chem. 124(2012)5804–5808.

139- J. Liu, A. C. Cheng, H. L. Tang, J. C. Medina, ACS Med. Chem. Lett. 2(2011)515–518

140- Babu, M., Pitchumani, K., & Ramesh, P. (2012). Isoxazoles incorporated N-substituted decahydroquinolines: A precursor to the next generation antimicrobial drug. European journal of medicinal chemistry, 47, 608-614

141- Babu, M., Pitchumani, K., & Ramesh, P. (2014). Synthesis of 5-benzyl-4-aryl-octahydro-1H-benzo [b][1, 5] diazepin-2-ones as potent antidepressant and antimicrobial agents. Medicinal Chemistry Research, 23(4), 2070-2079.

142- Dalai, M., & Periasamy, M. (2009). Diastereoselective reductive N-alkylation of (R, R)-trans-1, 2-diaminocyclohexane with prochiral ketones using the Ti (OiPr) 4/NaBH4 system. Tetrahedron: Asymmetry, 20(11), 1247-1253.

143- Sotoca, E., Constantieux, T., & Rodriguez, J. (2008). Solvent-and Catalyst-Free Three-Component Reaction with β-Ketoamides for the Stereoselective One-Pot Access to 1, 4-Diazepines. Synlett, 2008(09), 1313-1316.

144- Mehranpour, A. M., Hashemnia, S., & Shayan, Z. (2011). Synthesis and characterization of new derivatives of 1, 4-diazepinium salts. Synthetic Communications, 41(23), 3501-3511.

145- Periasamy, M., Sanjeevakumar, N., & Reddy, P. O. (2012). Convenient Methods to Access Chiral Camphanyl Amine Derivatives by Sodium Borohydride Reduction of d-(–)-Camphorquinone Imines. Synthesis, 44(20), 3185-3190.

146- Zaleska, B., Cież, D., & Lech, J. (2001). Efficient Synthesis of Pyrrolo [3, 4-b] hexahydro-1H-1, 5-benzodiazepine Derivatives. Synlett, 2001(12), 1953-1955.

147- Zaleska, B., & Socha, R. (2000). Synthesis of Enantiopure Chiral Perhydrobenzimidazole and Hexahydroquinoxaline Derivatives. Monatshefte für Chemie/Chemical Monthly, 131(10), 1061-1066.

148- McCann, M., Townsend, S., Devereux, M., McKee, V., & Walker, B. (2001). Mixtures obtained by reacting trans-(±)-1, 2-diaminocyclohexane with acetylacetone in the presence of simple cobalt (II) salts. Polyhedron, 20(22-23), 2799-2806.

149- M. Chammache, Doctoral thesis, Faculty of Sciences Rabat (2003).

150- Curphey, T. J. (2002). Thionation with the reagent combination of phosphorus pentasulfide and hexamethyldisiloxane. The Journal of organic chemistry, 67(18), 6461-6473.

151- Abdallah, W., Daami-Remadi, M., Znati, M., Jannet, H. B., & Gharbi, R. (2017). Design and synthesis of (3, 5-disubstituted isoxazole)-linked [1, 5]-benzodiazepine conjugates: evaluation of their antimicrobial and anti-tyrosinase activities. Journal of Chemical Research, 41(1), 12-17.

152- Khatoon, H., & Abdulmalek, E. (2021). A Focused Review of Synthetic Applications of Lawesson's Reagent in Organic Synthesis. Molecules, 26(22), 6937.

153- El Bakri, Y., Marmouzi, I., El Jemli, M., Karthikeyan, S., Harmaoui, A., Faouzi, M. E. A., Mague, J. T., & Essassi, E. M. (2019). Synthesis, biological activity and molecular modeling of a new series of condensed 1, 2, 4-triazoles. Bioorganic chemistry, 92, 103193.

154- Taylor, A. M., Côté, A., Hewitt, M. C., Pastor, R., Leblanc, Y., Nasveschuk, C. G., S. F. Bellon, S. F., Audia, J. E., Magnuson, S. R., & Albrecht, B. K. (2016). Fragment-based discovery of a selective and cell-active benzodiazepinone CBP/EP300 bromodomain inhibitor (CPI-637). ACS medicinal chemistry letters, 7(5), 531-536.

155- El Ghayati, L., Ramli, Y., Hökelek, T., Labd Taha, M., Mague, J. T., & Essassi, E. M. (2019). Crystal structure and Hirshfeld surface analysis of 3, 4-dihydro-2-(2, 4-dioxo-6-methylpyran-3-ylidene)-4-(4-pyridin-4-yl)-1, 5-benzodiazepine. Acta Crystallographica Section E: Crystallographic Communications, 75(1), 94-98.

156- Shifler, D. A. (2005). Understanding material interactions in marine environments to promote extended structural life. Corrosion Science, 47(10), 2335-2352.

157- Clerbois, L., Heitz, E., Ijsseling, F. P., Rowlands, J. C., & Simpson, J. P. (1985). Principles for scaling of corrosion tests: Report prepared by the European Federation of Corrosion Working Party on 'Physicochemical methods of corrosion testing–fundamentals and applications'. British Corrosion Journal, 20(3), 107-116.

158- El-Sherbini, E. F. (2006). Perchlorate pitting corrosion of tin in Na_2CO_3 solutions and effect of some inorganic inhibitors. Corrosion science, 48(5), 1093-1105.

159- Rosenfeld, I. L. (1981). New data on the mechanisms of metals protection with inhibitors. Corrosion (Houston);(United States), 37(7).

160- Bardal, E. (Ed.). (2004). Corrosion and protection. London: Springer London.

161- (a) Nestle, A., & Nathan, C. C. (1973). Corrosion inhibitors in petroleum production primary recovery. Corrosion Inhibitors, 61-75.(b) Parangusan, H., Bhadra, J., & Al-Thani, N. (2021). A review of passivity breakdown on metal surfaces: Influence of chloride-and sulfide-ion concentrations, temperature, and pH. Emergent Materials, 4(5), 1187-1203.

162- Koudelka, M., Sanchez, J., & Augustyński, J. (1982). On the nature of surface films formed on iron in aggressive and inhibiting polyphosphate solutions. Journal of the Electrochemical Society, 129(6), 1186.

163- Akpanyung, K. V., & Loto, R. T. (2019, December). Pitting corrosion evaluation: A review. In Journal of Physics: Conference Series (Vol. 1378, No. 2, p. 022088). IOP Publishing.

164- Li, H. B., Jiang, Z. H., Yang, Y., Cao, Y., & Zhang, Z. R. (2009). Pitting corrosion and crevice corrosion behaviors of high nitrogen austenitic stainless steels. International journal of minerals, metallurgy and materials, 16(5), 517-524.Arıkan, M. E., Arıkan, R., & Doruk, M. (2012). Determination of susceptibility to intergranular corrosion of UNS 31803 type duplex stainless steel by electrochemical reactivation method: A comparative study. International Journal of Corrosion, 2012.

165- Özcan, M., Dehri, İ. L. Y. A. S., & Erbil, M. (2004). Organic sulphur-containing compounds as corrosion inhibitors for mild steel in acidic media: correlation between inhibition efficiency and chemical structure. Applied surface science, 236(1-4), 155-164.

166- Wang, H., Brown, B., Nesic, S., & Pailleret, A. (2020, June). Investigation of Organic Inhibitor on Mild Steel using In Situ Atomic Force Microscopy and Electrochemical Measurement. In CORROSION 2020. OnePetro

167- Liu, Y., Ren, Y., Cao, Y., Huang, H., Wu, Q., Li, W., Wu, S., & Zhang, J. (2017). Discovery of a low toxicity O-GlcNAc transferase (OGT) inhibitor by structure-based virtual screening of natural products. Scientific reports, 7(1), 1-11.

168- Ngenge, T. A., Jabeen, A., Maurice, T. F., Baig, T. A., & Shaheen, F. (2019). Organic and mineral composition of seeds of Afrostyrax lepidophyllus Mildbr. and evaluation of ROS inhibition and cytotoxicity of isolated compounds. Chemistry Africa, 2(4), 615-624.

169- Raja, P. B., Ismail, M., Ghoreishiamiri, S., Mirza, J., Ismail, M. C., Kakooei, S., & Rahim, A. A. (2016). Reviews on corrosion inhibitors: a short view. Chemical Engineering Communications, 203(9), 1145-1156.

170- Nam, N. D., Van Hien, P., Hoai, N. T., & Thu, V. T. H. (2018). A study on the mixed corrosion inhibitor with a dominant cathodic inhibitor for mild steel in aqueous chloride solution. Journal of the Taiwan Institute of Chemical Engineers, 91, 556-569.

171- Akimov, G. V. (1959). Factors influencing corrosion. Corrosion, 15(9), 23-36.

172- Kuznetsov, Y. I. (2004). Physicochemical aspects of metal corrosion inhibition in aqueous solutions. Russian chemical reviews, 73(1), 75.

173- Bentiss, F., Lagrenee, M., Traisnel, M., & Hornez, J. C. (1999). The corrosion inhibition of mild steel in acidic media by a new triazole derivative. Corrosion Science, 41(4), 789-803.

174- Sing, K. S. (1998). Adsorption methods for the characterization of porous materials. Advances in colloid and interface science, 76, 3-11.

175- Sing, K. S. (1998). Adsorption methods for the characterization of porous materials. Advances in colloid and interface science, 76, 3-11.

176- Dadgarinezhad, A., & Baghaei, F. (2012). Electrochemical Investigation of the Inhibitive Effect of a New Synthetic Schiff-base on the Corrosion of Mild Steel in Acidic Media. Gazi University Journal of Science, 25(3), 593-600.

177- Bowden, F. P., & Moore, A. C. (1951). Physical and chemical adsorption of long chain compounds on radioactive metals. Transactions of the Faraday Society, 47, 900-908.

178- Fawzy, A., Abdallah, M., Zaafarany, I. A., Ahmed, S. A., & Althagafi, I. I. (2018). Thermodynamic, kinetic and mechanistic approach to the corrosion inhibition of carbon steel by new synthesized amino acids-based surfactants as green inhibitors in neutral and alkaline aqueous media. Journal of Molecular Liquids, 265, 276-291.

179- (a) Feliu, S., Galván, J. C., & Morcillo, M. (1990). The charge transfer reaction in Nyquist diagrams of painted steel. Corrosion Science, 30(10), 989-998. (b) Alamshany, Z. M., & Ganash, A. A. (2019). Synthesis, characterization, and anti-corrosion properties of an 8-hydroxyquinoline derivative. Heliyon, 5(11), e02895.(c) Gupta, N. K., Verma, C., Quraishi, M. A., & Mukherjee, A. K. (2016). Schiff's bases derived from l-lysine and aromatic aldehydes as green corrosion inhibitors for mild steel: experimental and theoretical studies. Journal of Molecular Liquids, 215, 47-57.

180- Zadeh, A. R. H., Danaee, I., & Maddahy, M. H. (2013). Thermodynamic and adsorption behaviour of medicinal nitramine as a corrosion inhibitor for AISI steel alloy in HCl solution. Journal of Materials Science & Technology, 29(9), 884-892.

181- Galai, M., El Faydy, M., El Kacimi, Y., Dahmani, K., Alaoui, K., Touir, R., Lakhrissi, B., & Ebn Touhami, M. (2017). Synthesis, characterization and anti-corrosion properties of novel

quinolinol on C-steel in a molar hydrochloric acid solution. Port Electrochim Acta, 35(4), 233-251.

182- Qiang, Y., Zhang, S., Tan, B., & Chen, S. (2018). Evaluation of Ginkgo leaf extract as an eco-friendly corrosion inhibitor of X70 steel in HCl solution. Corrosion Science, 133, 6-16.

183- Smith, S. G., Sanchez, R., & Zhou, M. M. (2014). Privileged diazepine compounds and their emergence as bromodomain inhibitors. Chemistry & biology, 21(5), 573-583.

184- Dubnick, B., Lippa, A. S., Klepner, C. A., Coupet, J., Greenblatt, E. N., & Beer, B. (1983). The separation of 3H-benzodiazepine binding sites in brain and of benzodiazepine pharmacological properties. Pharmacology Biochemistry and Behavior, 18(2), 311-318.

185- Olkkola, K. T., & Ahonen, J. (2008). Midazolam and other benzodiazepines. Modern anesthetics, 335-360.

186- Wang, Q., Han, Y., & Xue, H. (1999). Ligands of the GABAA receptor benzodiazepine binding site. CNS Drug Reviews, 5(2), 125-144

187- Fader, L. D., Bethell, R., Bonneau, P., Bös, M., Bousquet, Y., Cordingley, M. G., Guse, I., Hucke,O., Landry,S., Lemke, C. T., & Yoakim, C. (2011). Discovery of a 1, 5-dihydrobenzo [b][1, 4] diazepine-2, 4-dione series of inhibitors of HIV-1 capsid assembly. Bioorganic & medicinal chemistry letters, 21(1), 398-404.

188- Vicentini, C. B., Guarneri, M., Scatturin, A., Giori, P., & Heilman, W. (1996). 6-Alkyl and 6-arylcarbamoyloximino pyrazolo [3, 4-b][1, 4] diazepines as potential fungicidal, insecticidal and herbicidal agents. Farmaco (Societa Chimica Italiana: 1989), 51(8-9), 609-612.

189- Sandra, C. M., Cortes Eduardo, C., Simon, H. O., Apan Teresa, R., Camacho Antonio, N., V. Lijanova, I., & Marcos, M. G. (2012). Anticancer activity and anti-inflammatory studies of 5-aryl-1, 4-benzodiazepine derivatives. Anti Cancer Agents in Medicinal Chemistry, 12(6), 611.

190- Iden, H. S., & Lubell, W. D. (2006). 1, 4-Diazepinone and pyrrolodiazepinone syntheses via homoallylic ketones from cascade addition of vinyl grignard reagent to α-aminoacyl-β-amino esters. Organic Letters, 8(16), 3425-3428.

191- Iden, H. S., & Lubell, W. D. (2007). 1, 3, 5-Trisubstituted 1, 4-Diazepin-2-ones. The Journal of Organic Chemistry, 72(23), 8980-8983.

192- Iden, H. S., & Lubell, W. D. (2008). 1, 3, 5-Tri-and 1, 3, 4, 5-Tetra-Substituted 1, 4-Diazepin-2-one Solid-Phase Synthesis. Journal of Combinatorial Chemistry, 10(5), 691-699.

193- Balsells, J., Waters, M., Hansen, K., Kieczykowski, G. R., & Song, Z. J. (2007). A Short and Efficient Synthesis of 3-[2, 2, 2-Trifluoroethyl] hexahydro-2H-1, 4-diazepin-2-one. Synthesis, 2007(18), 2779-2781.

194- Alajarín, M., Vidal, A., & Tovar, F. (2005). The consecutive [2+ 2] cycloaddition-ring expansion route to diastereomeric 1, 4-diazepin-5-ones from imino-ketenimines. Alternative intramolecular transamidation of β-lactams. Tetrahedron, 61(6), 1531-1537.

195- Hofmann, C. M., & Safir, S. R. (1962). Synthesis and Structure of 7-Methyl-and 7-Phenyl-1, 2, 3, 4-tetrahydro-1, 4-diazepin-5-ones. The Journal of Organic Chemistry, 27(10), 3565-3568.

196- Begland, R. W., Hartter, D. R., Jones, F. N., Sam, D. J., Sheppard, W. A., Webster, O. W., & Weigert, F. J. (1974). Hydrogen cyanide chemistry. VIII. New chemistry of diaminomaleonitrile. Heterocyclic synthesis. The Journal of Organic Chemistry, 39(16), 2341-2350.

197- Chammache, M., Essassi, E.M., Salem, M., & Zniber, R. (1993). Study of the Reactivity of 7-Phenyl-1, 4-Diazepine-5-One. Bulletin of Belgian Chemical Societies, 102(2), 89-98.

198- Chammache, M., Essassi, E. M., & Pierrot, M. (2001). Crystal structure of 7-phenyl-1, 4-diazepin-5-one monohydrate, C11H12N2O· H2O. Zeitschrift für Kristallographie-New Crystal Structures, 216(1-4), 101-102.

199- Banfi, L., Basso, A., Guanti, G., Kielland, N., Repetto, C., & Riva, R. (2007). Ugi multicomponent reaction followed by an intramolecular nucleophilic substitution: convergent multicomponent synthesis of 1-sulfonyl 1, 4-diazepan-5-ones and of their benzo-fused derivatives. The Journal of organic chemistry, 72(6), 2151-2160.

200- Wlodarczyk, N., Gilleron, P., Millet, R., Houssin, R., & Hénichart, J. P. (2007). Synthesis of 1, 4-diazepin-5-ones under microwave irradiation and their reduction products. Tetrahedron letters, 48(14), 2583-2586.

201- Sethuvasan, S., Sugumar, P., Maheshwaran, V., Ponnuswamy, M. N., & Ponnuswamy, S. (2016). Synthesis, spectral characterization, crystal structure and molecular docking study of 2, 7-diaryl-1, 4-diazepan-5-ones. Journal of Molecular Structure, 1116, 188-199.

202- Ahumada, G., Carrillo, D., Manzur, C., Fuentealba, M., Roisnel, T., & Hamon, J. R. (2016). A facile access to new diazepines derivatives: Spectral characterization and crystal structures of 7-(thiophene-2-yl)-5-(trifluoromethyl)-2, 3-dihydro-1H-1, 4-diazepine and 2-thiophene-4-trifluoromethyl-1, 5-benzodiazepine. Journal of Molecular Structure, 1125, 781-787.

203- Zia, M., Khalid, M., Hameed, S., Irran, E., & Naseer, M. M. (2020). Synthesis and solid state self-assembly of a 1, 4-diazepine derivative: water cluster as molecular glue and conformational isomerism. Journal of Molecular Structure, 1207, 127811.

204- Masroor, S. (2021). Methods of Corrosion Monitoring. Organic Corrosion Inhibitors: Synthesis, Characterization, Mechanism, and Applications, 19-37.

205- Landolt, D. (2007). Corrosion and surface chemistry of metals. EPFL press.

206- Bradford, S. A., & Bringas, J. E. (1993). Corrosion control (Vol. 115). New York: Van Nostrand Reinhold.

207- Bentiss, F., Traisnel, M., & Lagrenee, M. (2001). Influence of 2, 5-bis (4-dimethylaminophenyl)-1, 3, 4-thiadiazole on corrosion inhibition of mild steel in acidic media. Journal of Applied Electrochemistry, 31(1), 41-48.

208- Wang, H. L., Fan, H. B., & Zheng, J. S. (2003). Corrosion inhibition of mild steel in hydrochloric acid solution by a mercapto-triazole compound. Materials Chemistry and Physics, 77(3), 655-661.

209- Khadom, A. A. (2015). Protection of steel corrosion reaction by benzotriazoles: A historical background. Journal of Failure Analysis and Prevention, 15(6), 794-802.

210- Gutiérrez, E., Rodríguez, J. A., Cruz-Borbolla, J., Alvarado-Rodríguez, J. G., & Thangarasu, P. (2016). Development of a predictive model for corrosion inhibition of carbon steel by imidazole and benzimidazole derivatives. Corrosion Science, 108, 23-35.

211- Sikine, M., Rodi, Y. K., Elmsellem, H., Krim, O., Steli, H., Ouzidan, Y., Rodi, A. K., FChahdi , F. O., Sebbar , N. K. & Essassi, E. M. (2016). Inhibition study of mild steel corrosion in hydrochloric acid by 1, 5-benzodiazepine-2, 4-dione. J. Mater. Environ. Sci, 7, 1386-1395.

212- Tsuru, T., & Haruyama, S. (1978). Corrosion Monitor Based on Impedance Method; Construction and its Application to Homogeneous Corrosion Corrosion Monitor Based on Impedance Method (Part 2). Corrosion Engineering, 27(11), 573-579.

213- Jüttner, K. (1990). Electrochemical impedance spectroscopy (EIS) of corrosion processes on inhomogeneous surfaces. Electrochimica Acta, 35(10), 1501-1508.

214- Bommersbach, P., Alemany-Dumont, C., Millet, J. P., & Normand, B. (2005). Formation and behaviour study of an environment-friendly corrosion inhibitor by electrochemical methods. Electrochimica Acta, 51(6), 1076-1084.

215- Volpe, M., & Cleri, F. (2003). Chemisorption of atomic hydrogen in graphite and carbon nanotubes. Surface science, 544(1), 24-34.

216- Behpour, M., Ghoreishi, S. M., Soltani, N., Salavati-Niasari, M., Hamadanian, M., & Gandomi, A. (2008). Electrochemical and theoretical investigation on the corrosion inhibition of mild steel by thiosalicylaldehyde derivatives in hydrochloric acid solution. Corrosion Science, 50(8), 2172-2181.

217- Ammar, I. A., & El Khorafi, F. M. (1973). Adsorbability of thiourea on iron cathodes. Materials and corrosion, 24(8), 702-707.

218- Durnie, W., De Marco, R., Jefferson, A., & Kinsella, B. (1999). Development of a structure-activity relationship for oil field corrosion inhibitors. Journal of the Electrochemical Society, 146(5), 1751.

219- Sahmoune, M. N. (2019). Evaluation of thermodynamic parameters for adsorption of heavy metals by green adsorbents. Environmental Chemistry Letters, 17(2), 697-704.

220- Sheng, G. D., Shao, D. D., Ren, X. M., Wang, X. Q., Li, J. X., Chen, Y. X., & Wang, X. K. (2010). Kinetics and thermodynamics of adsorption of ionizable aromatic compounds from aqueous solutions by as-prepared and oxidized multiwalled carbon nanotubes. Journal of hazardous materials, 178(1-3), 505-516.

221- Sheng, G. D., Shao, D. D., Ren, X. M., Wang, X. Q., Li, J. X., Chen, Y. X., & Wang, X. K. (2010). Kinetics and thermodynamics of adsorption of ionizable aromatic compounds from aqueous solutions by as-prepared and oxidized multiwalled carbon nanotubes. Journal of hazardous materials, 178(1-3), 505-516.